# M

## MAGNETOTACTIC BACTERIA

Mihály Pósfai
University of Pannonia, Veszprém, Hungary

### Definition

Magnetotactic bacteria (MTB) are a diverse group of Gram-negative, motile prokaryotes that align and migrate along the geomagnetic field. This magnetotactic behavior is based on intracellular organelles called magnetosomes, which are inorganic nanocrystals of either magnetite ($Fe_3O_4$) or greigite ($Fe_3S_4$), surrounded by a lipid bilayer membrane. The magnetosomes are typically arranged in one or more chains, conveying a magnetic dipole moment to the cell (Figure 1). Magnetotaxis is thought to be beneficial for the cell for finding its optimum position in vertical concentration gradients in aquatic habitats.

### History

Bacteria that responded to magnetic fields were discovered independently by Bellini (1963) and Blakemore (1975), who coined the term magnetotaxis and noted the presence of crystals in the cells. Intracellular magnetite was identified and the physics of magnetotaxis was described by Frankel et al. (1979). Iron sulfide-producing MTB were found in 1990 (Mann et al., 1990; Farina et al., 1990). The ecology of MTB and the structures and morphologies of the crystalline components of magnetosomes have been widely studied since the discovery of MTB. In the past decade, significant progress has been made in elucidating the molecular, biochemical, and genetic bases of magnetosome formation (Schüler, 2007).

### Ecophysiology

MTB are ubiquitous in both marine and freshwater aquatic habitats, where suboxic or anoxic conditions prevail, and dissolved iron is available. Because of their fastidious nature, only a few strains are available in pure culture. With one exception, all strains in pure culture have a respiratory form of metabolism. All known MTB are microaerophiles (they require a certain amount of oxygen for growth, but exhibit a negative tactic and/or growth response to atmospheric concentrations of oxygen) or anaerobes or facultatively anaerobic microaerophiles (Bazylinski and Frankel, 2004). The physiology of MTB appears to dictate their ecology: since MTB derive energy from the proximity of oxidants and reductants, magnetite producing organisms occur in largest numbers (up to $10^5$ cells/ml) in layers at or near the oxic–anoxic interfaces (OAI) of chemically stratified habitats. Iron sulfide-producing bacteria live below the OAI under anaerobic conditions (Simmons et al., 2004). Whereas magnetite-producing bacteria occur virtually in all types of water bodies, sulfide-producing organisms have been found in marine habitats only. Considering the large amount of iron concentrated in magnetosomes ($10^{-15}$ to $10^{-13}$ g Fe per cell) and the estimated population density of MTB at and below the OAI, MTB are likely to contribute significantly to the flux of reduced Fe to sediments in chemically stratified marine basins.

### Magneto-aerotaxis

Magnetotaxis means active motion guided by the magnetic field. MTB passively orient along the geomagnetic field and actively swim by means of flagella. A key element of magnetotaxis is that the cell should possess a large enough magnetic dipole moment to overcome the disorientating effects of thermal motions and be aligned parallel to the magnetic field. In the geomagnetic field, the magnetic energy of magnetotactic cells is typically ten times larger than thermal energy, which means that the cell can migrate along the field at 90% of its forward speed (Frankel et al., 1979).

Joachim Reitner & Volker Thiel (eds.), *Encyclopedia of Geobiology*, DOI 10.1007/978-1-4020-9212-1,

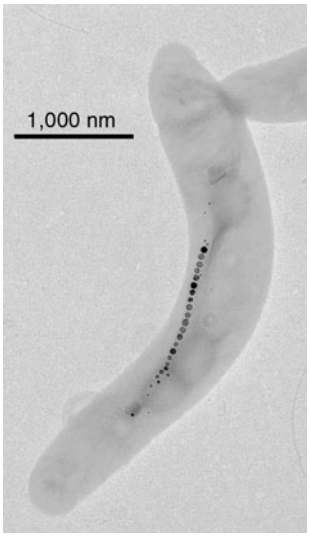


**Magnetotactic Bacteria, Figure 1** A cell of *Magnetospirillum gryphiswaldense* that contains a single chain of magnetite magnetosomes.

"Polar" and "axial" magnetotaxis are distinguished (Frankel et al., 1997). Polar magnetotaxis is displayed by MTB that swim persistently toward one of the poles of a bar magnet under oxic conditions. Those that swim toward the "south" pole of a magnet have North-seeking polarity, since they would swim northward in the geomagnetic field. MTB from the northern hemisphere are predominantly North-seekers, whereas those from the southern hemisphere are predominantly South-seekers (Bazylinski and Frankel, 2004).

The observation of polar magnetotaxis led to the idea that MTB are guided by the geomagnetic field to less oxygenated regions. Since the geomagnetic field is inclined downward from the horizontal in the northern hemisphere and upward in the southern hemisphere under oxic conditions the cells with polar magnetotaxis swim downward in both hemispheres (Bazylinski and Frankel, 2004). However, if the cell is in a reducing environment, it reverses the direction of flagellar rotation and migrates upward. Since the motion of the cell is determined by both the magnetic field and the oxygen tension, the term "magneto-aerotaxis" was introduced (Frankel et al., 1997).

Axial magnetotaxis means that the axis of motion is determined by the magnetic field but its direction is not. As the cell swims, it samples the oxygen concentration and compares it with that in the recent past. Cells moving toward the optimal habitat have a decreased probability of reversing the sense of flagellar rotation, whereas those that are moving away from the optimal oxygen concentration have an increased probability of reversing the sense of flagellar rotation and thus their swimming direction (Frankel et al., 1997). The magneto-aerotactic response provides an efficient mechanism for MTB to find the OAI in their chemically stratified habitats.

## Mineralogy and magnetism

Magnetotaxis relies on intracellular grains of iron oxide or sulfide minerals. Magnetite ($Fe_3O_4$) is the only iron oxide mineral that has been described to date from magnetotactic cells. The sulfide-producing cells use greigite ($Fe_3S_4$) for navigation, but they also may contain nonmagnetic mackinawite (FeS) that rapidly converts to greigite through a solid-state phase transition (Pósfai et al., 2007).

Magnetite produced by MTB is chemically pure $Fe_3O_4$, in contrast to grains from rocks that usually contain other transition metals besides iron. Structurally, the nanocrystals are either perfect or contain twin boundaries. The morphologies of magnetite magnetosomes are typically highly regulated, strain-specific, and in many cases, unusual for a mineral with cubic symmetry (Pósfai et al., 2007). Whereas magnetotactic spirilla contain cubooctahedral crystals, vibrio and cocci typically produce magnetite with prismatic habits (Figure 2a). Large, rod-shaped cells tend to contain arrowhead- or bullet-shaped magnetite crystals (Bazylinski and Frankel, 2004).

The sizes and shapes of magnetosomes are critical for magnetotaxis. Isolated, isometric magnetite crystals with diameters smaller than ~30 nm are superparamagnetic, i.e., they do not have a permanent magnetic moment. Crystals with diameters from ~30 to ~120 nm are magnetic single domains at room temperature, whereas grains larger than ~120 nm contain two or more magnetic domains, reducing the net magnetic moment of the crystal. Most magnetosomes are in the single-domain range, allowing the assembly of a highly efficient internal compass that consists of a chain (or chains) of single-domain magnets. Interactions between neighboring particles in chain configurations ensure that even those magnetite particles that are small enough to be superparamagnetic or large enough to contain two or more magnetic domains if they were isolated are also constrained to be single domains (Dunin-Borkowski et al., 2001). Since elongated particles are arranged with their axis of elongation (which typically coincides with their crystallographic easy magnetization axis) parallel to the chain of magnetosomes, shape anisotropy constrains the magnetic flux lines to be parallel to the axis of motility. Thus, in most magnetite-producing cells the effects of particle size, shape and magnetocrystalline anisotropy, and magnetostatic interactions among particles in chains combine to produce the possible largest magnetic moment (Figure 2b) (Pósfai et al., 2007).

The sizes, shapes, and orientations of iron sulfide magnetosomes are less distinct than those of magnetite magnetosomes. Greigite magnetosomes typically contain planar defects, as a result of an incomplete solid-phase transformation from mackinawite to greigite. The shapes and orientations of the crystals are random,

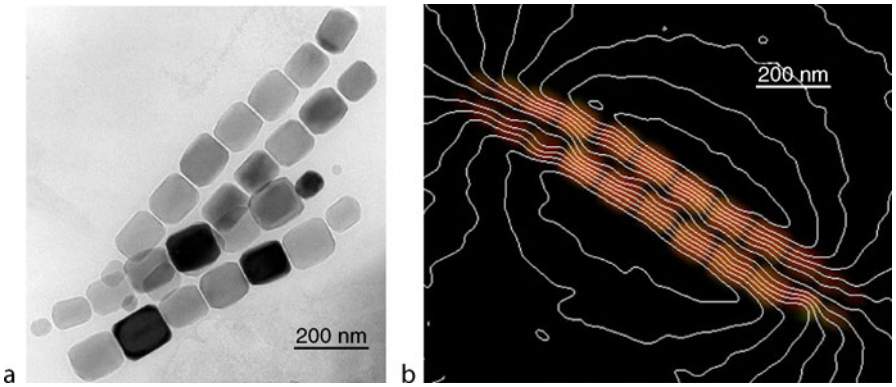


**Magnetotactic Bacteria, Figure 2** (**a**) Electron micrograph of two double chains of elongated magnetite magnetosomes from a freshwater magnetotactic coccus. (**b**) Magnetic induction map of a similar double chain of magnetite magnetosomes, obtained from electron holograms.

resulting in poorer confinement and greater variability in the directions of the magnetic induction lines in the cells than in magnetite-bearing bacteria. Remarkably, despite the different crystal structures, orientations, and arrangements of ferrimagnetic crystals, the magnetic moments of different cells are fairly constant (Pósfai et al., 2007), thereby satisfying the requirement for magnetotaxis.

## Cell biology and genomic analyses

Magnetic enrichments have shown great morphological and ultrastructural diversity of MTB from a wide variety of aquatic environments. Magnetite-producing morphotypes include spirilla, cocci, vibrios, and rods of various sizes, moving at speeds ranging from 40 to 1,000 μm/s. A unique, greigite-producing magnetotactic organism, the "multicellular magnetotactic prokaryote" (MMP) consists of 15–45 cells organized around an internal acellular compartment (Keim et al., 2004). The aggregated cells of the MMP move together as one unit, with the coordinated motion of flagella on the outside of the cells.

The highly controlled, strain-specific properties of magnetite magnetosomes and their chains indicate that biomineralization is under genetic control, executed by specific proteins in the magnetosome membrane. Many details of magnetosome formation have been elucidated by studies of the biochemistry of the magnetosome membrane and genomic analyses of MTB. Workable genetic systems have been developed for two *Magnetospirillum* strains: *M. magnetotacticum* AMB-1 and *M. gryphiswaldense* MSR-1 (Jogler and Schüler, 2007). By genetic manipulation, including the generation of mutants and the expression of magnetobacterial genes in other hosts, the major steps of magnetite biomineralization have been identified in these systems. Magnetite nucleation is preceded by the formation of vesicles, which are invaginations of the cytoplasmic membrane (Komeili et al., 2006). Dissolved ferrous or ferric iron is transported into the cell by an unknown uptake system. Magnetosome membrane proteins (MamB/MamM) are involved in the transport of ferrous iron from the cytoplasm into the magnetosome vesicle, and then magnetite formation is activated by another protein (MamA). Within the vesicle, iron is oxidized and magnetite nucleation is triggered by the Mms6 protein. The least known aspect of the biomineralization process is the control over the distinct crystal morphology. The vesicles containing fully developed magnetite crystals are anchored to a filamentous cytoskeletal structure by the MamJ protein, resulting in an ordered magnetosome chain (Scheffel et al., 2006). Genomic analyses revealed that the genes that encode the magnetosome proteins are clustered in a 130 kb region, representing a "magnetosome island." This genomic island appears to be conserved among different *Magnetospirillum* strains and, to a lesser degree, in a magnetotactic coccus (Jogler and Schüler, 2007), raising the question of whether the "magnetosome island" is a universal feature of MTB.

## Diversity

The term "magnetotactic bacteria" does not refer to a taxonomical unit. All known MTB belong to various groups within the domain Bacteria. Most magnetotactic microorganisms that are available in pure culture are affiliated with the *Alphaproteobacteria*, including *M. magnetotacticum* and *M. gryphiswaldense*, a marine vibrio (MV-1), and a coccus (MC-1). In addition to the cultivated strains, 16S rRNA analysis of magnetic enrichments from many freshwater and marine samples revealed that a variety of magnetite-producing morphotypes are likely affiliated with the *Alphaproteobacteria* (Amann et al., 2007). Two magnetite-producing candidate species, "*Magnetobacterium bavaricum*" and "*Magnetotacticum bremense*," are affiliated with the *Nitrospira* phylum.

Sulfide-producing MTB could not have been cultured to date, but a multicellular organism was found to be closely related to the dissimilatory sulfate-reducing

bacteria within the *Deltaproteobacteria*. Another sulfide-producing MTB was assigned to *Gammaproteobacteria*. These findings may suggest that magnetotaxis based on iron oxide and sulfide nanoparticles evolved independently; however, a magnetite-producing, sulfate-reducing organism (*Desulfovibrio magneticus* strain RS-1) is also affiliated with the *Deltaproteobacteria* (Amann et al., 2007).

The diversity of MTB indicates that magnetotaxis evolved independently in several phylogenetic groups. On the other hand, the discovery of a potentially mobil "magnetosome island" in the genome of magnetite-producing MTB could suggest that the trait of magnetotaxis was spread by lateral gene transfer among the various groups of MTB.

## Magnetofossils, paleomagnetism

After MTB die, their intracellular magnetite or greigite particles are deposited in the sediment. If diagenetic conditions are favorable, the magnetosome crystals can be preserved as magnetofossils. Magnetofossils have been identified on the basis of the special properties of magnetosome crystals, including a narrow crystal size distribution, characteristic morphologies, chemical purity and, in some cases, chain configurations. Ferrimagnetic nanocrystals presumably originating from MTB have been described from a variety of sedimentary rock types, including clays, carbonates, marls, and evaporites. The magnetofossil record extends from present-day marine and lake sediments to the Cretaceous and with lesser certainty to the late Archean (Kopp and Kirschvink, 2008).

MTB carry a primary remanent magnetization, since they are aligned with the geomagnetic field, presumably even after cell death and burial in the sediment. Because magnetofossils are single magnetic domains, they have an optimized magnetic stability and can be important carriers of paleomagnetic information. Magnetofossils can serve as environmental proxies because MTB live under specific redox conditions. They can also be markers of ancient life, albeit dubious ones, as illustrated by a lengthy debate over whether nanocrystalline magnetite particles in the Martian meteorite ALH84001 represent magnetofossils or had formed inorganically (Winklhofer and Petersen, 2007).

## Nanotechnological applications

Magnetic nanoparticles are widely used in technological applications, such as in spintronics, in magnetic inks, in high-density magnetic memory devices, and in medical applications (as contrast agents in magnetic resonance imaging and as magnetic carriers for drug targeting and delivery). Magnetite crystals produced by MTB have uniform sizes and shapes and can be separated from disrupted cells by magnetic methods with their magnetosome membrane intact. The membrane-bound bacterial nanoparticles have a large specific surface area and are well dispersed in aqueous solutions. Antibodies or proteins can be immobilized on the magnetosome membrane, producing functionalized magnetic nanoparticles (Matsunaga and Arakaki, 2007). Since bound and free analytes can be separated in a magnetic field, bacterial nanoparticles have been used for the rapid and sensitive detection of small molecules, including environmental pollutants, hormones, and toxic detergents. Immunomagnetic particles are also useful for sorting target cells from cell suspensions using a permanent magnet, and for using them in high-performance DNA/mRNA recovery and DNA discrimination analysis (Matsunaga and Arakaki, 2007).

## Summary

MTB provide a fascinating example of microbial biomineralization and motivate interdisciplinary research at the junctions of biology, mineralogy, geology, geochemistry, and physics. The molecular and genetic bases of magnetic nanocrystal formation by MTB are now beginning to be understood. The results of research on MTB will be useful for understanding biomineralization processes and magnetic sensing mechanisms in more complex organisms, and for designing nanotechnological applications of bacterial nanocrystals.

## Bibliography


Amann, R., Peplies, J., and Schüler, D., 2007. Diversity and taxonomy of magnetotactic bacteria. In Schüler, D. (ed.), *Magnetoreception and Magnetosomes in Bacteria*. Berlin: Springer, pp. 25–36.

Bazylinski, D. A., and Frankel, R. B., 2004. Magnetosome formation in prokaryotes. *Nature Reviews Microbiology*, **2**, 217–230.

Bellini, S., 1963. *Su di un particolare comportamento di batteri d'acqua dolce*. Instituto di Microbiologia dell'Universita di Pavia.

Blakemore, R. P., 1975. Magnetotactic bactaeria. *Science*, **190**, 377–379.

Dunin-Borkowski, R. E., McCartney, M. R., Pósfai, M., Frankel, R. B., Bazylinski, D. A., and Buseck, P. R., 2001. Off-axis electron holography of magnetotactic bacteria: magnetic microstructure of strains MV-1 and MS-1. *European Journal of Mineralogy*, **13**, 671–684.

Farina, M., Esquivel, D. M. S., and Lins de Barros, H. G. P., 1990. Magnetic iron-sulphur crystals from a magnetotactic microorganism. *Nature*, **343**, 256–258.

Frankel, R. B., Blakemore, R. P., and Wolfe, R. S., 1979. Magnetite in freshwater magnetotactic bacteria. *Science*, **203**, 1355–1356.

Frankel, R. B., Bazylinski, D. A., Johnson, M. S., and Taylor, B. L., 1997. Magneto-aerotaxis in marine coccoid bacteria. *Biophysical Journal*, **73**, 994–1000.

Jogler, C., and Schüler, D., 2007. Genetic analysis of magnetosome biomineralization. In Schüler, D. (ed.), *Magnetoreception and Magnetosomes in Bacteria*. Berlin: Springer, pp. 133–162.

Keim, C. N., Abreu, F., Lins, U., Lins de Barros, H. G. P., and Farina, M., 2004. Cell organization and ultrastructure of a magnetotactic multicellular organism. *Journal of Structural Biology*, **145**, 254–262.

Komeili, A., Li, Z., Newman, D. K., and Jensen, G. J., 2006. Magnetosomes are cell membrane invaginations organized by the actin-like protein Mamk. *Science*, **311**, 242–245.

Kopp, R. E., and Kirschvink, J. L., 2008. The identification and biogeochemical interpretation of fossil magnetotactic bacteria. *Earth-Science Reviews*, **86**, 42–61.

Mann, S., Sparks, N. H. C., Frankel, R. B., Bazylinski, D. A., and Jannasch, H. W., 1990. Biomineralization of ferrimagnetic greigite ($Fe_3S_4$) and iron pyrite ($FeS_2$) in a magnetotactic bacterium. *Nature*, **343**, 258–261.
Matsunaga, T., and Arakaki, A., 2007. Molecular bioengineering of bacterial magnetic particles for biotechnological applications. In Schüler, D. (ed.), *Magnetoreception and Magnetosomes in Bacteria*. Berlin: Springer, pp. 227–254.
Pósfai, M., Kasama, T., and Dunin-Borkowski, R. E., 2007. Characterization of bacterial magnetic nanostructures using high-resolution transmission electron microscopy and off-axis electron holography. In Schüler, D. (ed.), *Magnetoreception and Magnetosomes in Bacteria*. Berlin: Springer, pp. 175–226.
Scheffel, A., Gruska, M., Faivre, D., Linaroudis, A., Plitzko, J. M., and Schüler, D., 2006. An acidic protein aligns magnetosomes along a filamentous structure in magnetotactic bacteria. *Nature*, **440**, 110–114.
Schüler, D., 2007. *Magnetoreception and Magnetosomes in Bacteria*. Berlin: Springer, p. 319.
Simmons, S. L., Sievert, S. M., Frankel, R. B., Bazylinski, D. A., and Edwards, K. J., 2004. Spatiotemporal distribution of marine magnetotactic bacteria in a seasonally stratified coastal salt pond. *Applied and Environmental Microbiology*, **70**, 6230–6239.
Winklhofer, M., and Petersen, N., 2007. Paleomagnetism and magnetic bacteria. In Schüler, D. (ed.), *Magnetoreception and Magnetosomes in Bacteria*. Berlin: Springer, pp. 255–274.

## Cross-references

Bacteria
Biosignatures in Rocks
Iron Sulfide Formation
Microbial Biomineralization
Nanocrystals, Microbially Induced

# MANGANESE (SEDIMENTARY CARBONATES AND SULFIDES)

Michael E. Böttcher
Leibniz Institute for Baltic Sea Research, Warnemünde, Germany

## Synonyms

Alabandite; Authigenic manganese minerals; Inca rose; Rambergite; Rhodochrosite

## Definition

*Rhodochrosite*. Manganese(II) carbonate ($MnCO_3$; trigonal, calcite structure), named after the greek word for *"rose-colored."* It was named as the state mineral of Colorado (USA) in 2002. Complete solid solution formation with calcite occurs at low temperatures (Böttcher, 1998), the "Ca-rhodochrosites" or "pseudo-kutnahorites" (Mucci, 2004).
*Kutnahorite*. Manganese(II)-calcium carbonate ($CaMn(CO_3)_2$; trigonal; ordered dolomite structure), named after the location KutnoHora (Peacor et al., 1987). Although physicochemically stable at low temperatures with respect to equally composed solid-solutions (Mucci, 2004), it is not formed in sediments, and only known from high-temperature hydrothermal and metamorphic environments.
*Rambergite*. Manganese(II) sulfide (μ-MnS; hexagonal), named after the mineralogist Hans Ramberg, is found as authigenic product in anoxic sediments of the Baltic Sea (Böttcher and Huckriede, 1997; Burke and Kemp, 2002).
*Alabandite*. Manganese(II) sulfide (α-MnS, cubic), named after the location Alabanda, Turkey, is found in sediments as minor intergrowth with rambergite (Lepland and Stevens, 1998).

## Manganese carbonate formation in suboxic/anoxic sediments

Mixed manganese–calcium carbonates, with minor incorporation of magnesium and divalent iron, are formed in (brackish-marine) sediments as authigenic products of suboxic and anoxic early diagenesis, in the Baltic Sea deeps and the Panama Basin. Significant sedimentary Ca-rhodochrosite accumulation requires manganese(IV) dioxide pre-enrichment at the sediment–water interface by episodic water column oxidation, as shown for the temporarily euxinic deeps of the Baltic Sea (Huckriede and Meischner, 1996). The required dissolved carbonate species are formed in the pore water upon mineralization of organic matter, and aqueous $Mn^{2+}$ is derived from microbial or chemical reduction of manganese(III, IV) oxides as electron acceptors (e.g., Banfield and Nealson, 1997). The carbonates occur as kidney-shaped globules, as overgrowth on foraminifers, detrital carbonates, and microbial cells or as idiomorphic crystals, depending on the microenvironment. Experimental studies reveal that the composition of manganese-rich carbonates is controlled by the pore water composition, the abundance of carbonate surfaces, and the presence of inhibitors (Böttcher, 1998; Mucci, 2004). Under equilibrium conditions, natural anoxic pore waters are in the stability field of coexisting rhodochrosite and iron sulfides (Figure 1), and no manganese sulfide should be formed during typically zoned early diagenetic processes.

## Manganese sulfide formation in anoxic sediments

The only places worldwide where sedimentary manganese sulfides have been found sofar are the Baltic Sea anoxic deeps (e.g., Baron and Debyser, 1957). Idiomorphic MnS (Figure 2) is associated with organic matter, Ca-rhodochrosite, and iron sulfides (Böttcher and Huckriede, 1997; Lepland and Stevens, 1998). Although MnS has been obviously formed under slow diffusion-controlled conditions where rhodochrosite formation was chemically inhibited, the exact process is still under debate. Occurrence of Ca-rhodochrosite replacing hexagonal MnS (Burke and Kemp, 2002) indicates possible re-adaption of the metastable sedimentary system toward equilibrium conditions.

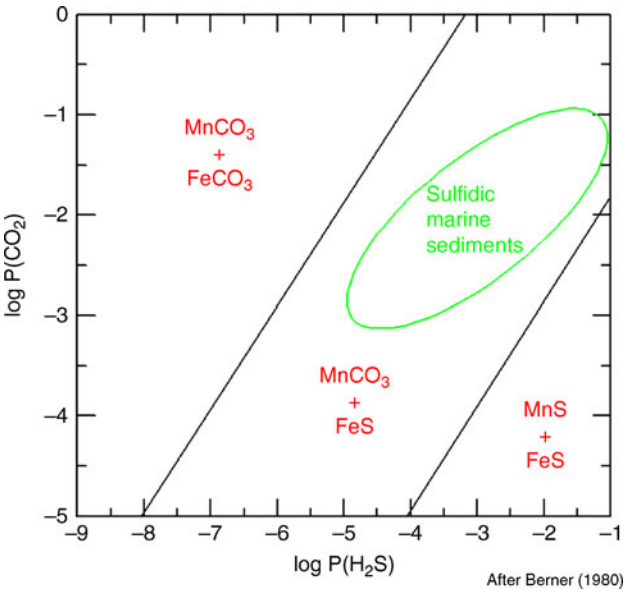


**Manganese (Sedimentary Carbonates and Sulfides), Figure 1** Low temperature equilibrium phase relationships of reduced iron- and manganese-bearing solids as a function of carbon dioxide and hydrogen sulfide partial pressures.

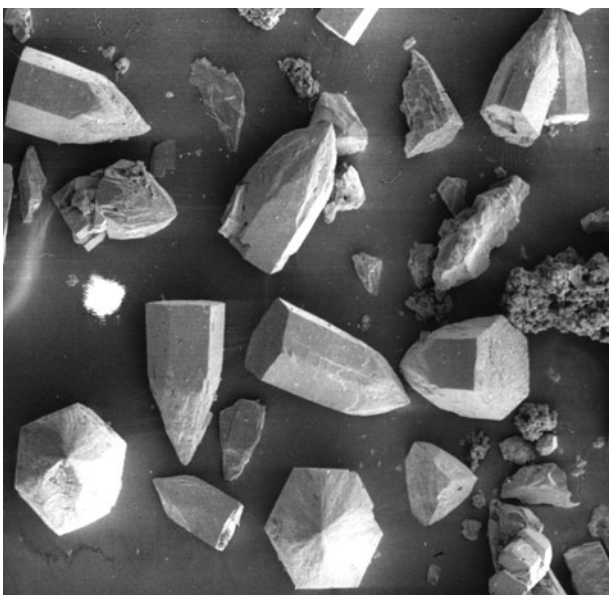

**Manganese (Sedimentary Carbonates and Sulfides), Figure 2** Scanning electron microscope picture of idiomorphic authigenic MnS from the Baltic Sea. Picture width is equivalent to a scale of 950 μm.

## Conclusion

Sedimentary authigenic manganese(II) carbonate minerals, especially investigated in the nowadays brackish-marine Baltic Sea, are indicative of biogeochemical early-diagenetic processes in manganese-rich environments. They have gained a lot of attention in the past 2 decades because of their proxy potential for specific hydrological conditions leading to euxinic water column turnover or glacial-interglacial cycles that are controlled by climate change (e.g., Lepland and Stevens, 1998; Gingele and Kasten, 1994). One of the many open questions within the biogeochemistry and geomicrobiology of manganese in sediments is about the conditions leading to the metastable formation and preservation of manganese(II) sulfides. An interpretation of water profiles in sediments with high manganese load point toward complex interactions between chemical inhibitors, microbial processes, and rates of (temporary) mineral formation processes.

## Bibliography

Banfield, J. F., and Nealson, K. H., 1997. Geomicrobiology: interactions between microbes and minerals. *Reviews in Mineralogy*, **35**, 1.

Baron, G., and Debyser, J., 1957. Sur la prèsence dans des vases organiques de la mer Baltique du sulfure manganeux hexagonal. *Comptes Rendues de l'Académie des Sciences Francais*, **245**, 1148.

Berner, R. A., 1981. Authigenic mineral formation resulting from organic matter decomposition in modern sediments. *Fortschritte Mineralogie*, **59**, 117.

Böttcher, M. E., 1998. Manganese(II) partitioning during experimental precipitation of rhodochrosite-calcite solid-solutions from aqueous solutions. *Marine Chemistry*, **62**, 287.

Böttcher, M. E., and Huckriede, H., 1997. First occurrence and stable isotope composition of authigenic γ-MnS in the central Gotland Deep (Baltic Sea). *Marine Geology*, **137**, 201.

Burke, I. T., and Kemp, A. E. S., 2002. Microfabric analysis of Mn-carbonate laminae deposition and Mn-sulfide formation in the Gotland Deep, Baltic Sea. *Geochimica et Cosmochimica Acta*, **66**, 1589.

Gingele, F. X., and Kasten, S., 1994. Solid-phase manganese in Southeast Atlantic sediments: implications for the paleoenvironment. *Marine Geology*, **121**, 317.

Huckriede, H., and Meischner, D., 1996. Origin and environment of manganese-rich sediments within black-shale basins. *Geochimica et Cosmochimica Acta*, **60**, 1399.

Lepland, A., and Stevens, R. L., 1998. Manganese authigenesis in the Landsort Deep, Baltic Sea. *Marine Geology*, **151**, 1.

Mucci, A., 2004. The behavior of mixed Ca–Mn carbonates in water and seawater: controls of manganese concentrations in marine porewaters. *Aquatic Geochemistry*, **10**, 139.

Peacor, D., Essene, E. J., and Gaines, A. M., 1987. Petrologic and crystal-chemical implications of the cation order-disorder in kutnahorite [CaMn(CO3)2]. *American Mineralogist*, **72**, 319.

## Cross-references

Carbonates
Divalent Earth Alkaline Cations in Seawater
Iron Sulfide Formation
Microbial Degradation
Sulfur Cycle

# MASS EXTINCTIONS, PHANEROZOIC

Joachim Reitner
University of Göttingen, Göttingen, Germany

## Synonyms

Biotic crisis; Extinction event; Extinction-level event

## Definition

A *mass extinction* is a sharp decrease in biodiversity, speciation, and diversification rate among micro- and macroorganisms in the fossil record, often also related with a decrease of biomass. The microbial biodiversity, which probably dominates the entire biodiversity, however, is not to be considered under this aspect, because we have no idea about the real microbial biodiversity through time.

## Mass extinctions

Mass extinctions are generally important events, which have a large impact on evolutionary processes throughout earth's history. Mass extinctions might have also occurred in the Precambrian, however, these are much more difficult to recognize and interpret, because most of them affected microbial communities. Profound extinction events in the Precambrian are related with the Great Oxidation Event 2.5 Gy ago, during which an unknown number of anaerobic microbial communities disappeared from oxygenated shelf areas and were restricted to the still anaerobic deeper parts of the oceans (Canfield Ocean, see Wiese and Reitner, Chapter *Critical Intervals in Earth History*, this volume). It can be suspected that the Neoproterozoic Cryogenian Snowball Earth situations (730–630 My) damaged early earth's ecosystems as decreasing $\delta^{13}C$ values prior to the glaciations suggest a decrease in bioproductivity (e.g., Moczydłowska, 2008; Le Guerroué, et al., 2006a, b; Hoffman, this volume). A first macrofossil extinction of eukaryotic multicellular organisms occurred in the Lower Cambrian, when the Ediacara organisms or Vendobionta, respectively (Raup and Sepkoski, 1982; Brasier et al., 1989; Jensen et al., 1998), became extinct.

Within the Phanerozoic, five major mass extinctions are known (Sepkoski, 1984, 1994; Alroy, 2004; Kiessling and Simpson, 2010), in the literature referred to as "the Big Five" (Figure. 1). All of them have potentially different origins (e.g., impact, volcanisms, glaciations a.o.; see below) or are even multicausal. However, in most cases, the triggering mechanisms and feedback loops are often difficult to understand. Apart from cosmic impacts, mass extinctions are most likely no sudden events but have precursory ecosystem perturbations that prelude the phase of the biotic crisis (further reading see Wiese and Reitner, this volume).

## End-Ordovician mass extinction (ca. 443 My)

The end-Ordovician mass extinction event is the first major extinction event in the Phanerozoic. Brachiopods, bryozoans, trilobites, graptolites, corals, mollusks, conodonts, etc. were strongly decimated. It is estimated that roughly 50% of known taxa died out (further reading Krug and Patzkowsky, 2004; Sheehan, 2001; Sole and Newman, 2002; Webby and Droser, 2004).

### Possible origins

a. One reason might be the paleogeographic constellation of the continents at the Ordovician–Silurian boundary, when Gondwana was positioned at the South Pole. The position of large continental areas at the South Pole triggered a severe cooling, which terminated in the Sahara glaciation in the uppermost Ordovician (Hirnantian). Possibly, it was the heaviest glaciation during the entire Phanerozoic. The associated strong regression and a breakdown of oceanic circulation patterns brought up nutrients from the abyssal waters and affected the diversity of organisms negatively (Sheehan, 2001). A further idea is that the glaciation forced an equatorward migration of warmer water organisms, competition in remaining habitats and extinction of a large number of taxa. In a second step, a severe warming, succeeding the Sahara glaciation, forced a poleward migration of the few remaining cold water assemblages, which then also suffered heavy losses (see also Webby and Droser, 2004).
b. Melott et al. (2004) argued that the end-Ordovician mass extinction could have been caused by a gamma ray burst from a supernova 6,000 light years distant from the Earth. This burst should have destroyed half of the ozone layer, leading to an immediate kill by the heavy UV radiation. However, any hard data that confirm this model do not exist. As the ozone layer buffers the mutagen UV radiation, an increase of UV radiation should in some kind be visible in the fossil record by an increase of pathologically developed invertebrate macrofossils.
c. Young et al. (2009) speculated that $CO_2$ might play a major role in the end-Ordovician mass extinction. Their idea is that through the late Ordovician massive volcanic $CO_2$ outgassing was balanced by strong weathering of the uplifting Appalachian Mountains, which sequestered $CO_2$. Finally, in the end of the Ordovician, the volcanic activity finished and the continued weathering caused a significant decrease of $CO_2$. As a result, the Hirnantian ice age started.

## Late Devonian extinction events (ca. 370 My)

Within the late Devonian, several extinction events severely affected biodiversity. The most important ones were the Upper Devonian Kellwasser events in the Frasnian–Famennian boundary interval and the Hangenberg event at the Devonian–Carboniferous boundary (McGhee, 1996; Walliser, 1995; Sandberg et al., 2002). The

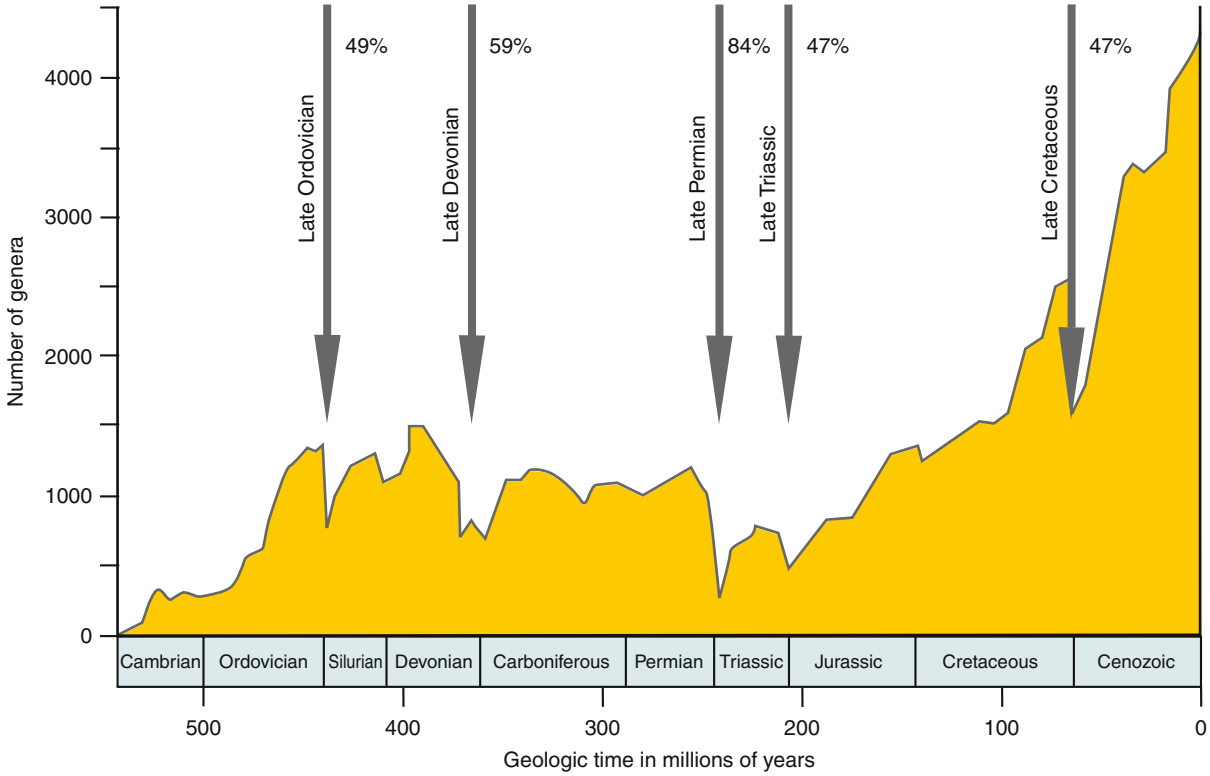


**Mass Extinctions, Phanerozoic, Figure 1** Compilation of the Big Five Phanerozoic extinction events with the assumed percentage of extinction of known genera. These numbers are highly speculative, because the biodiversity of deep water environments during the extinction events are only poorly known (Figure modified after Sepkoski, 1984, 1994; Alroy, 2004).

extinction seems to have only affected marine life. Reef-building organisms were almost completely wiped out, except some microbial reefs with occasionally few sponges. Roughly 60% of the known genera became extinct. The diversity of brachiopods, cephalopods, trilobites, benthic foraminifera, conodonts, rugose and tabulate corals, jawless fish, stromatoporoid sponges, etc. was strongly influenced by these events. However, the decline of biodiversity is probably a reduction in the formation of new species rather than an extinction of already existing taxa.

### Possible origins

Different possibilities have been discussed for the late Devonian mass extinctions such as asteroid impacts, global anoxia, sea-level changes, climatic changes, etc. (Buggisch, 1991; Joachimski, 1997; Joachimski and Buggisch, 1993; Joachimski, 2001). The most intriguing hypothesis is the "Devonian Plant Hypothesis" (Algeo and Sheckler, 1998; Algeo et al., 1995, 2001). Due to the rapid and accelerating evolution of terrestrial plants from the Lower Devonian on, intensified chemical and physical weathering by roots and the increased continental bioturbation resulted in an intensivation of pedogenesis. As a result, several feedback loops established. On the one hand, the increased runoff of nutrients caused eutrophication of the Devonian seas, the genesis of anoxia and black shales, and the extinction of deep water and shelf biota. On the other hand, due to silicate weathering and $CO_2$ withdrawal from the atmosphere, the alkalinity of the sea increased, enhancing precipitation of carbonates and further $CO_2$ withdrawal. As a result, a global cooling occurred, and the associated sea-level fall diminished shelf habitat significantly during the Kellwasser and Hangenberg events (e.g., Sandberg et al., 2002).

## End-Permian mass extinction (ca. 251.4 My)

The Permian–Triassic extinction was the most severe extinction event within the Phanerozoic. Up to 84% of the known Permian taxa (genera) became extinct. Not only marine organisms were affected, but also terrestrial ecosystems. Many of the characteristic Paleozoic organisms like trilobites, representatives of the cephalopoda and corals, marine and terrestrial vertebrates, and also plants disappeared and died out. However, some of the Permian-style organisms like coralline sponges occurred again in the early–middle Triassic and are interpreted as Lazarus-taxa, a widely, only poorly understood phenomenon. The end-Permian extinction cannot be explained by one event only. The combination of various events is

possibly responsible for this tremendous mass extinction (Benton, 2005; Bowring et al., 1998).

### Possible origins

a. Volcanic events are widely discussed to be the major controlling factor of the Permian–Triassic mass extinction. The most important volcanic events were flood basalt eruptions, which produced the Siberian Traps, some of the largest known volcanic provinces in earth's history. These eruptions have an age of $251.2 \pm 0.3$ My, and they fit stratigraphically very well with the estimated age of the mass extinction. The Siberian Traps were estimated to exhibit 20% of pyroclastic material, which heavily reduced insolation by backscatter of sunlight. Furthermore, eruptions caused dust clouds, acidic aerosols, and acidic rain, which – in conjunction with the first – disturbed and disrupted photosynthesis on land and in the sea. The Siberian Trap lava intruded into calcareous sediments and large coal beds, and emitted large amounts of $CO_2$, causing a slight global warming (White, 2002; Saunders and Reichow, 2009; Reichow et al., 2009).
b. There is a worldwide negative excursion of $\delta^{13}C_{carb}$ to values of ca. −10‰. There are various possibilities to explain this excursion. However, the release of huge amounts of methane possibly from collapsing marine and permafrost methane hydrates is the most probable reason (Palfy et al., 2001; Twitchett et al., 2001; Payne et al., 2004).
c. Several pieces of evidence can be brought forward for an impact event in the end of the Permian. There are possible impact craters, which have been proposed as possible causes of the extinction: the Australian Bedout crater and the Wilkes Land crater of East Antarctica. From these sites, shocked quartz and fullerenes, trapping extraterrestrial noble gases, are known. However, this evidence does not really prove the impact event, and the Wilkes Land crater is possibly younger than the Permian–Triassic boundary (Retallack et al., 1998; Becker et al., 2001, 2004). In this respect, the paper by Stanton (2002) is very intriguing, in which he suggests that the Gulf of Mexico is a very huge meteorite crater of end-Permian age – big enough to explain this fatal extinction event.
d. There is evidence of anoxic seawater conditions around the time of end-Permian extinctions. Major players in anoxic seawater are sulfate-reducing bacteria, which could produce high amounts of $H_2S$, which is, however, partly re-mineralized in iron sulfides (e.g., pyrite). Dissolved $H_2S$ is a poison and could be responsible for aquatic mass killing. Perhaps, the release of $H_2S$ in to the atmosphere weakened the ozone layer and increased the UV radiation with fatal effects for plants and land animals. There are indications that anaerobic photosynthesis via green sulfur bacteria occurred in the end of the Permian till the early Triassic (Kump et al., 2005; Grice et al., 2005). The triggering mechanism is believed to be the increase of volcanogenic $CO_2$, which lowered the pH value and increased chemical weathering. As a result, the continental runoff of nutrients increased dramatically, causing eutrophication and finally anoxia with the consequences listed above.
e. Last but not least, sea-level changes are also discussed to explain the mass extinction. Due to the Pangea situation, a very big marine regression is noticed. This reduced the shelfal areas, biodiversity, and the stability of food chains (e.g., Hallam and Wignall, 1999).

## End-Triassic mass extinction (ca. 201.4 My)

The end-Triassic extinction defines the boundary between the Triassic and Jurassic, and it is one of the most important Phanerozoic extinction events. Ca. 47% of the known genera got extinct, such as the conodonts, nearly almost all Triassic taxa of ammonites except the stem groups of the Phylloceratina and the Lytoceratina. Many vertebrates such as a high number of large amphibians, Triassic archosaurs, many therapsids, etc. disappeared. The end-Triassic extinction event also destroyed the widespread shallow water coral reef environments, including many types of corals and especially coralline sponges. The recovery of this coral reef environment took a long time and was more or less completed in the Upper Jurassic (Hallam, 1987, 1997; Palfy et al., 2001; Ward et al., 2001).

### Possible origins

There is only one seriously discussed reason for the end-Triassic extinction. During this time, a tremendous volcanic activity occurred, the Central Atlantic Magmatic Province (CAMP), which produced huge amounts of flood basalts, linked with a high amount of outgassing $CO_2$, sulfur gases, and volcanic ash (Hesselbo et al., 2002). This event heavily influenced the shallow water and terrestrial bioproduction and, probably due to acid rains, also biomineralization. The $\delta^{13}C$ isotopic composition of organic matter from sediments from this time exhibits an unusual negative excursion (Deenen et al., 2010; Ruhl et al., 2009; Whiteside et al., 2010). Most probable trigger for the extinction is the CAMP-induced climatic change, acidification of the ocean surface waters, and a strong sea-level fall.

## End-Cretaceous mass extinction (ca. 65.5 My)

The end-Cretaceous extinction event, also known as the **K**reide–**T**ertiary (K-T) extinction event, was a very short-termed mass extinction event. However, the diversity of some groups of animals like ammonites, belemnites, various Cretaceous bivalves (rudists, inoceramids), dinosaurs, etc. decreased before the K-T event. The most important impact on biodiversity was the extinction of non-feathered dinosaurs, marine large reptiles (mosasaurs, plesiosaurs), pterosaurs, and the decrease of phyto- and zooplankton diversity and biomass in the ocean surface waters. Crocodilian archosaurs, turtles, birds, and small nocturnal mammalian survived the mass extinction event.

Extinction of most taxa of, for example, coccolithophorids and Cretaceous planktonic foraminifera led to a breakdown of primary productivity and calcareous sedimentation rates in the oceans. The K-T boundary layer is worldwide often documented as a black band, which exhibits geochemical anomalies, for example, an enrichment of in iridium and in the Pt-group elements in general. Probably, ca. 47% of the known genera became extinct.

### Possible origins

a. The most discussed reason is that huge impacts of cometary parts or asteroids caused the extinction. This assumption is evidenced by the geochemical anomalies (Ir, Pt-group) and the discovery of a very large impact structure in northern Mexico (Yucatan), the Chicxulub crater, which has an age corresponding to that of the K-T boundary. Some scientists assume that more impacts happened; however, no further impact structures are known. The ecological disaster shortly after the huge meteorite impact (estimated size of impactor more than 10 km) caused the extinction of the above-listed organisms.
b. Beside the bolide impact hypothesis, an increased volcanic activity is also discussed to be responsible for the big extinction event. The Deccan trap basalts have the age of the K-T boundary, and this vast volcanic event might also have influenced the biodiversity and biomass production at that time, which then reflects a comparable scenario like for the Permian–Triassic boundary. It is easily possible that the conjunction of two events – the bolide impact and the Deccan trap volcanism – are responsible for this last large Phanerozoic mega extinction.

## Conclusion

All five major extinction events within Phanerozoic are milestones in the evolution of organisms, community structures, and ecosystems. All of them are critical intervals (see contribution Wiese and Reitner this volume) and of fundamental paleobiological importance. All of the major extinction events are multicausal events and cannot be restricted to only one factor. Most of them are also not short-term events, except the K-T boundary event which is proved to be a large meteorite impact. However, also in this case, the extinction of some important taxa has a prelude in the form of successive decrease in diversity, and the K-T event finally wiped them out.

These catastrophic events are probably very important for the entire biotic evolution on earth and obviously one of major evolutionary driving force.

## Bibliography


Algeo, T. J., and Scheckler, S. E., 1998. Terrestrial-marine teleconnections in the Devonian: links between the evolution of land plants, weathering processes, and marine anoxic events. *Philosophical Transactions of the Royal Society of London* B, **353**, 113–130.

Algeo, T. J., Berner, R. A., Maynard, J. P., and Scheckler, S. E., 1995. Late Devonian oceanic anoxic events and biotic crises: rooted in the evolution of vascular land plants? *Geological Society of America Today*, **45**, 64–66.

Algeo, T. J., Scheckler, S. E., and Maynard, J. B., 2001. Effects of the Middle to Late Devonian spread of vascular land plants on weathering regimes, marine biota, and global climate. In Gensel, P. G., and Edwards, D. (eds.), *Plants Invade the Land: Evolutionary and Environmental Approaches*. New York: Columbia University Press, pp. 213–236.

Alroy, J., 2004. Are Sepkoski's evolutionary faunas dynamically coherent? *Evolutionary Ecology Research*, **6**, 1–32.

Becker, L., Poreda, R. J., Hunt, A. G., Bunch, T. E., Rampino, M., 2001. Impact event at the Permian–Triassic boundary: evidence from extraterrestrial noble gases in fullerenes. *Science*, **291**, 1530–1533.

Becker, L., Poreda, R. J., Basu, A. R., Pope, K. O., Harrison, T. M., Nicholson, C., and Iasky, R., 2004. Bedout: a possible end-Permian impact crater offshore of northwestern Australia. *Science*, **304**, 1469–1476.

Benton, M. J., 2005. When life nearly died: the greatest mass extinction of all time. London: Thames and Hudson.

Bowring, S. A., Erwin, D. H., Jin, Y. G., Martin, M. W., Davidek, K., and Wang, W., 1998. U/Pb Zircon geochronology and tempo of the End-Permian mass extinction. *Science*, **280**, 1039–1045.

Brasier, M. D., 1989. On mass extinctions and faunal turnover near the end of the Precambrian. In Donovan, S. K. (ed.), Mass Extinctions, Processes, and Evidence. New York:Columbia University Press, pp. 73–88.

Buggisch, W., 1991. The global Frasnian-Famennian Kellwasser event. *Geologische Rundschau*, **80**, 49–72.

Deenen, M. H. L., Ruhl, M., Bonis, N. R., Krijgsman, W., Kürschner, W. M., Reitsma, M., and Van Bergen, M. J., 2010. A new chronology for the end-Triassic mass extinction. *Earth and Planetary Science and Letters*, **291**, 113–125.

Grice, K., Cao, C., Love, G. D., Bottcher, M. E., Twitchett, R. J., Grosjean, E., Summons, R. E., Turgeon, S. C., Dunning, W., and Yugan, J., 2005. Photic zone Euxinia during the Permian–Triassic superanoxic event. *Science*, **307**, 706–709.

Hallam, A., 1987. Radiations and extinctions in relation to environmental change in the Marine Lower Jurassic of Northwest Europe. *Paleobiology*, **13**(2), 152–168.

Hallam, A., 1997. Estimates of the amount and rate of sea-level change across the Rhaetian–Hettangian and Pliensbachian–Toarcian boundaries (latest Triassic to early Jurassic). *Journal of the Geological Society*, **154**, 773–779.

Hallam, A., and Wignall, P. B., 1999. Mass extinctions and sea-level changes. *Earth-Science Reviews*, **48**, 217–250.

Hesselbo, S. P., Robinson, S. A., Surlyk, F., and Piasecki, S., 2002. Terrestrial and marine extinction at the Triassic–Jurassic boundary synchronized with major carbon-cycle perturbation: a link to initiation of massive volcanism? *Geology*, **30**, 251–254.

Hillebrandt, V. A., Krystyn, L., and Kürschner, W. M., 2007. A candidate GSSP for the base of the Jurassic in the Northern Calcareous Alps (Kuhjoch section, Karwendel Mountains, Tyrol, Austria). *International Subcommission on Jurassic Stratigraphy Newsletter*, **34**, 2–20.

Jensen, S., Gehling, J. G., and Droser, M. L., 1998. Ediacara-type fossils in Cambrian sediments. *Nature*, **393**, 567–569.

Joachimski, M. M., 1997. Comparision of organic and inorganic carbon isotope patterns across the Frasnian-Famennian boundary. *Palaeogeography, Palaeoclimatology, Palaeoecology*, **132**, 133–145.

Joachimski, M., and Buggisch, W., 1993. Anoxic events in the late Frasnian – causes of the Frasnian-Famennian faunal crisis? *Geology*, **21**, 675–678.

Joachimski, M., Ostertag-Henning, C., Pancost, R., Strauss, H., Freeman, K., Littke, R., Sinninghe Damste, J. S., and Racki, G., 2001. Water column anoxia, enhancedproductivity and concomitant changes in $\delta^{13}C$ and $\delta^{34}S$ across the Frasnian-Famennian boundary (Kowala-Holt' Cross Mountains/Poland). *Chemical Geology*, **175**, 109–131.
Kiessling, W., and Simpson, C., 2010. On the potential for ocean acidification to be a general cause of ancient reef crises. *Global Change Biology*, doi:10.1111/j.1365-2486.2010.02204
Krug, A. Z., and Patzkowsky, M. E., 2004. Rapid recovery from the Late Ordovician mass extinction. *Proceedings of the National Academy of Sciences of the United States of America*, **101**, 17605–17610.
Kump, L. R., Pavlov, A., and Arthur, M. A., 2005. Massive release of hydrogen sulfide to the surface ocean and atmosphere during intervals of oceanic anoxia. *Geology*, **33**, 397–400.
Le Guerroué, E., Allen, P. A., and Cozzi, A., 2006a. Chemostratigraphic and sedimentological framework of the largest negative carbon isotopic excursion in Earth history: the Neoproterozoic Shuram formation (Nafun Group, Oman). *Precambrian Research*, **146**(1–2), 68–92.
Le Guerroué, E., Allen, P. A., Cozzi, A., Etienne, J. L., and Fanning, C. M., 2006b. 50 Myr recovery from the largest negative $\delta^{13}C$ excursion in the Ediacaran ocean. *Terra Nova*, **18**(2), 147–153.
McGhee, G. R. Jr., 1996. *The Late Devonian Mass Extinction: the Frasnian/Famennian Crisis*. New York: Columbia University Press.
Melott, A. L., Lieberman, B. S., Laird, C. M., Martin, L. D., Medvedev, M. V., Thomas, B. C., Cannizzo, J. K., Gehrels, N., and Jackman, C. H., 2004. Did a gamma-ray burst initiate the late Ordovician mass extinction? International Journal of Astrobiology, 3, arXiv:astro-ph/0309415v3.
Moczydłowska, M., 2008. The Ediacaran microbiota and the survival of Snowball Earth Snowball conditions. *Precambrian Research*, **167**, 1–15.
Palfy, J., Demeny, A., Haas, J., Htenyi, M., Orchard, M.J., and Veto, I., 2001. Carbon isotope anomaly at the Triassic– Jurassic boundary from a marine section in Hungary. *Geology*, **29**, 1047–1050.
Payne, J. L., Lehrmann, D. J., Wei, J., Orchard, M. J., Schrag, D. P., and Knoll, A. H., 2004. Large perturbations of the carbon cycle during recovery from the End-Permian Extinction. *Science*, **305**, 506.
Raup, D. M., and Sepkoski, J. J., 19820. Mass extinctions in the marine fossil record. *Science*, **215**(4539), 1501–1503.
Reichow, M. K., Pringle, M. S., Al'Mukhamedov, A. I., Allen, M. B., Andreichev, V. L., Buslov, M. M., Davies, C. E., Fedoseev, G. S., Fitton, J. G., Inger, S., Medvedev, A. Ya., Mitchell, C., Puchkov, V. N., Safonova, I. Yu., Scott, R. A., and Saunders, A. D., 2009. The timing and extent of the eruption of the Siberian Traps large igneous province: implications for the end-Permian environmental crisis. *Earth and Planetary Science Letters*, **277**, 9–20.
Retallack, G. J., Seyedolali, A., Krull, E. S., Holser, W. T., Ambers, C. P., and Kyte, F. T., 1998. Search for evidence of impact at the Permian–Triassic boundary in Antarctica and Australia. *Geology*, **26**, 979–982.
Ruhl, M., Kuerschner, W. M., and Krystyn, L., 2009. Triassic–Jurassic organic carbon isotope stratigraphy of key sections in the western Tethys realm (Austria). *Earth and Planetary Science Letters*, **281**, 169–187.
Sandberg, C. A., Morrow, J. R., and Ziegler, W., 2002. Late Devonian sea-level changes, catastrophic events, and mass extinctions. In Koeberl, C., and MacLeod, K. G. (eds.), *Catastrophic Events and Mass Extinctions: Impacts and Beyond*. Boulder: Geological Society of America. GSA Special Paper 356, pp. 473–487.
Saunders, A., and Reichow, M. K., 2009. The Siberian traps and the End-Permian mass extinction: a critical review. *Chinese Science Bulletin*, **54**, 20–37.
Sepkoski, J. J. Jr., 1984. A kinetic model of Phanerozoic taxonomic diversity. III. post-Paleozoic families and mass extinctions. *Paleobiology*, **10**, 246–267.
Sepkoski, J. J. Jr., 1994. Extinction and the fossil record. *Geotimes*, **39**,15–17.
Sheehan, P., 2001. The late Ordovician mass extinction. *Annual Review of Earth and Planetary Sciences*, **29**, 331–364.
Sole, R. V., and Newman, M., 2002. Extinctions and Biodiversity in the Fossil Record - Volume Two, The earth system: biological and ecological dimensions of global environment change. *Encyclopedia of Global Environmental Change*, New York: Wiley, pp. 297–391.
Stanton, M. S., 2002. http://www.aapg.org/explorer/2002/12dec/gom_impact.pdf
Twitchett, R. J., Looy, C. V., Morante, R., Visscher, H., and Wignall, P. B., 2001. Rapid and synchronous collapse of marine and terrestrial ecosystems during the end-Permian biotic crisis. Geology, **29**, 351–354.
Wallsier, O. H. (ed.), 1995. *Global Events and Event Stratigraphy*. Berlin: Springer.
Ward, P. D., Haggart, J. W., Carter, E. S., Wilbur, D., Tipper H. W., and Evans. T., 2001. Sudden productivity collapse associated with the Triassic–Jurassic boundary mass extinction. *Science*, **292**, 1148–1151.
Webby, B. D., and Droser, M. L. (eds.), 2004. *The Great Ordovician Biodiversification Event*. New York: Columbia University Press.
White, R. V., 2002. Earth's biggest "whodunnit": unravelling the clues in the case of the end-Permian mass extinction. *Philosophical Transactions of the Royal Society of London*, **360**, 2963–2985.
Whiteside, J. H., Olsen, P. E., Eglinton, T., Brookfield, M. E., and Sambrotto, R. N., 2010. Compound-specific carbon isotopes from Earth's largest flood basalt eruptions directly linked to the end-Triassic mass extinction. Proceedings of the National Academy of Sciences, **107**(15), 6721–6725.
Young, S. A., Saltzman, M. R., Foland, K. A., Linder, J. J., and Kump, L. R., 2009. A major drop in seawater 87Sr/86Sr during the Middle Ordovician (Darriwilian): links to volcanism and climate? Geology, 37, 951–954.

## Cross-references

Asteroid and Comet Impacts
Biological Volcanic Rock Weathering
Comets
Critical Intervals in Earth History
Ediacaran Biota
Snowball Earth

# MAT-RELATED SEDIMENTARY STRUCTURES

Hubertus Porada
University of Göttingen, Göttingen, Germany

## Synonyms

Microbially induced sedimentary structures (MISS) (The acronym MISS was introduced by Noffke et al. (2001) for "microbially induced sedimentary structures." Many of the structures addressed, however, are not truly "induced" by microbes, but rather by physical forces

acting on a biostabilized sediment surface or a microbial mat. Since, in this scenario, the biological component significantly influences the shape of evolving structures, it is suggested to write out the acronym MISS as "microbially *influenced* sedimentary structures.").

## Definition

Mat-related sedimentary structures are small- to medium-scale sedimentary structures resulting from growth and extension of microbial populations and communities on a sediment surface, stabilization of surface sediments, trapping and binding of sediment particles, and from the impact of environmental factors, such as inundation, sedimentary deposition, subaerial desiccation, wind- or current-induced traction, on epibenthic microbial mats.

## Introduction

Originally described from and applied to modern microbial mats (Gerdes et al., 2000; Noffke et al., 2001), mat-related sedimentary structures preferentially serve as proxies of the former existence of microbial mats in ancient siliciclastic sediments. Mat-related structures are in a way analogous to trace fossils (Schieber, 2004), whereby the former presence of mats can be inferred, e.g., from observations suggesting "unusual" sediment properties like original cohesiveness, tensile strength, and erosion-resistance of sand (Eriksson et al., 2007); uncharacteristic grain fabrics; and steep geochemical gradients on a mm-scale. Genetic explanation of the structures relies on an actualistic approach; preservation depends on intrinsic biological, and favorable environmental conditions.

In this chapter, the term "mat-related sedimentary structures" is applied to structures that form on, in, or below microbial mats with distinct properties, e.g., coherence, cohesiveness, minor thickness, and adaptation to periodic subaerial exposure. Further conditions include a fine-grained siliciclastic substrate (sand to silt) and lacking dominance of carbonate precipitation. The term also encompasses primary physical structures that have subsequently been microbially influenced.

Today, well-developed (cyanobacterial) microbial mats that meet the above conditions, are observed mainly in the intertidal to lower supratidal zones of low-gradient tidal flats where they grow in a wide range of climate zones from temperate humid to subtropical/tropical semi-arid and arid, at salinities ranging from brackish to hypersaline. Similar mats may also form in other environments, e.g., lacustrine, fluvial, where similar mat-related structures may partly form. Due to lacking vertical bioturbation in the Precambrian, the distribution of microbial mats may previously have been much wider, extending far into the subtidal zone.

Microbial mats are epibenthic, multilayered microbial communities including different functional groups of microorganisms (Stal, 2000) which act together in a kind of "joint venture" widely balancing organic matter production and destruction (van Gemerden, 1993). Thus, microbial mats in coastal environments normally do not exceed a thickness of a few centimeters. The "biological stratification" of microorganisms is superimposed by a biosedimentary lamination resulting from the interplay of microbial growth and seasonal, periodic, or episodic depositional events related, e.g., to tides or storms.

The top layer of the mat system, which periodically is exposed to the atmosphere, usually consists of oxygenic, filamentous cyanobacteria, frequently *Microcoleus* sp., which form a "felty" fabric of interwoven filaments (Gerdes et al., 2000), including also sediment grains incorporated by "trapping and binding" processes (Noffke et al., 2003a, with references). The felty layer may be overlain, or in some cases replaced, by a resistant ("leathery") layer of colloid extracellular polymeric substances (EPS) produced mainly by coccoid cyanobacteria. This top portion of the mat combines high mechanical resistance with low permeability and is the locus at which most of the mat-related sedimentary structures form. Deeper levels of the mat system are much less cohesive. They contain anaerobic bacteria among which sulfate-reducing bacteria produce sulfide leading to precipitation of iron sulfides (FeS) which gradually transform into pyrite. In the ancient record, the stratiform occurrence of pyrite, in some cases siderite or ferroan carbonate, within otherwise well oxidized sediments may serve as a proxy of the former existence of microbial mats.

## Formation and types of structures

Mat-related sedimentary structures may form during all the stages from first microbial colonization of a sediment surface, through establishment and sustainment of a fully developed mat, to its destruction and final erosion.

### Structures related to early microbial colonization

Microbial colonization leads to "biostabilization" (Krumbein et al., 1994) of a sediment surface which then can resist erosion to some degree. This property may lead to "palimpsest ripples" when new sediment is deposited on top a biostabilized rippled surface (Pflüger, 1999); to surfaces with "multi-directional ripple marks" (Noffke, 1998); and to "ripple patches" (Figure 1a) or "erosional pockets" when a biostabilized flat surface or mat is locally eroded (for ancient example, Noffke, 1999; McKenzie, 1972).

### Structures related to microbial growth and mat growth

Depending on availability of water for some time, specific filamentous cyanobacteria (e.g., *Lyngbya aestuarii*) start to produce on the mat surface, a characteristic "reticulate growth pattern" of small, sharp-crested ridges stabilized by EPS (Figure 1b). Ancient structures of this type are named "elephant skin" texture (Gehling, 1999) (Figure 1c). There is considerable variability in respect of polygon size (few mm to few cm) and shape varying from nearly circular to narrow rectangular with almost linear crest orientation. A unifying feature, however, are the

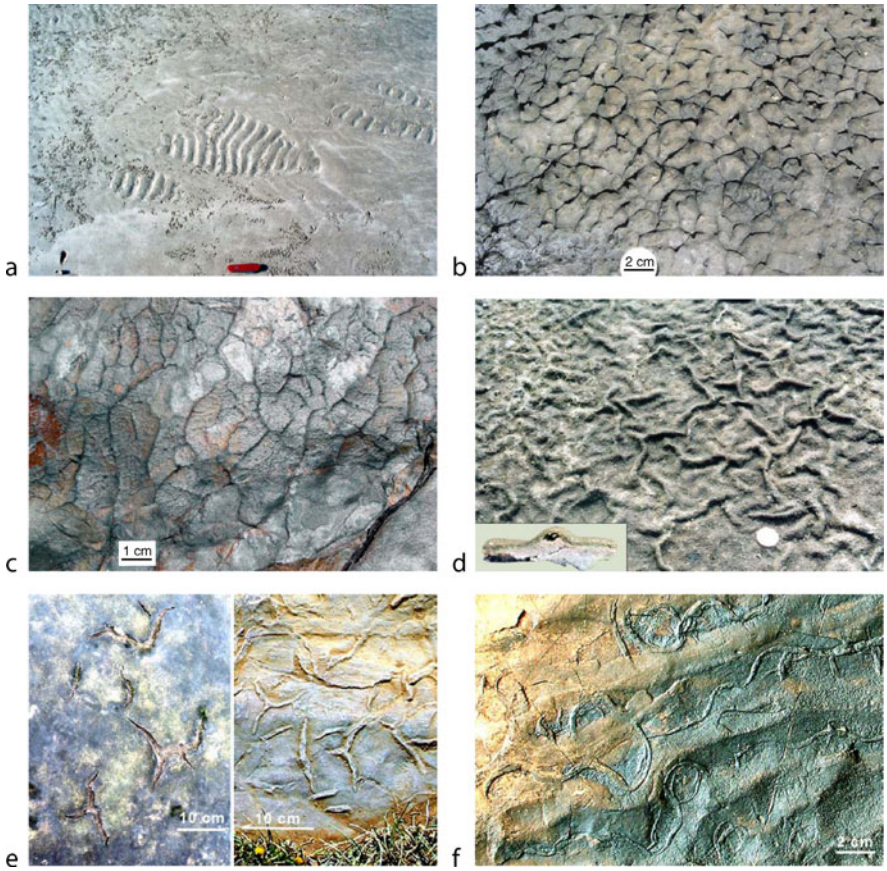


**Mat-Related Sedimentary Structures, Figure 1** Structures related to biostabilization, microbial and mat growth, and desiccation. (**a**) Biostabilized sediment surface with isolated "ripples patches." Scale (knife) is 8 cm. Locality: Trucial Coast, west of Abu Dhabi, U.A.E. (**b**) Reticulate growth pattern produced by *Lyngbya aestuarii*. Locality: Salins du Midi, Réserve Nationale Camargue, southern France. (**c**) Upper surface of sericitic siltstone with "elephant skin" texture representing "reticulate growth pattern" of a previous microbial mat. Locality: Terminal Proterozoic Vingerbreek Member, Nama Group; Farm Haruchas, Namibia. (**d**) "Petees" originating from lateral mat growth and deforming microbial mat into round-crested bulges: *Inset*: Cross-section showing that upper, cohesive part of the mat is deformed and separated from deeper, less cohesive mat layers. Scale (coin) is 24 mm. Locality: Amrum Island, southern North Sea, Germany. (**e**) Modern and ancient shrinkage cracks. *Left photograph*: modern microbial mat with isolated, sigmoidal, and tri-radiate cracks. Locality: Amrum Island, southern North Sea, Germany. *Right photograph*: fillings of ancient, spindle-shaped, and tri-radiate cracks. Locality: Neoproterozoic Tizi n-Taghatine Group; Imi n'Tizi area, Anti-Atlas, Morocco. (**f**) *Manchuriophycus*-type shrinkage cracks meandering in ripple troughs. Locality: Neoproterozoic Tizi n-Taghatine Group; Taghdout area, Anti-Atlas, Morocco.

narrow, sharp-crested ridges preserved on upper bedding surfaces.

A further type of structures related to mat growth are "mat expansion structures," collectively termed "petees" (Gavish et al., 1985; Bouougri et al., 2007), which deform the upper, cohesive part of the mat into bulges and domes, thus enlarging the mat surface (Figure 1d). Occasionally, the bulges may be arranged in a polygonal pattern. Provided, petees are filled by sediment rising up from below, the structures may be preserved. Ancient examples have been named "petee ridges" (Schieber, 2004).

## Structures related to mat desiccation and shrinkage

Subaerial exposure causes dehydration and shrinkage of the EPS and eventually cracking of the mat. Incipient, isolated "shrinkage cracks" are sigmoidal and spindle-shaped, or tri-radiate starting from triple junctions, or occasionally circular in shape (Figure 1e). Crack propagation at progressive shrinkage leads to more or less complete networks of cracks. In general, shrinkage cracks in microbial mats develop a higher degree of curving unlike normal mud cracks. Ancient shrinkage cracks are also termed "sand cracks" referring to their occurrence in sandy sediment without shrinkable mud present. A specific type of shrinkage cracks, characterized by sinusoidal or sub-circular trends and developed mainly in ripple troughs, is referred to as "Manchuriophycus"-type in the ancient record (Porada and Löffler, 2000) (Figure 1f). A characteristic property of many ancient shrinkage cracks is their easy separability from the layers above and below, which is ascribed to soon microbial

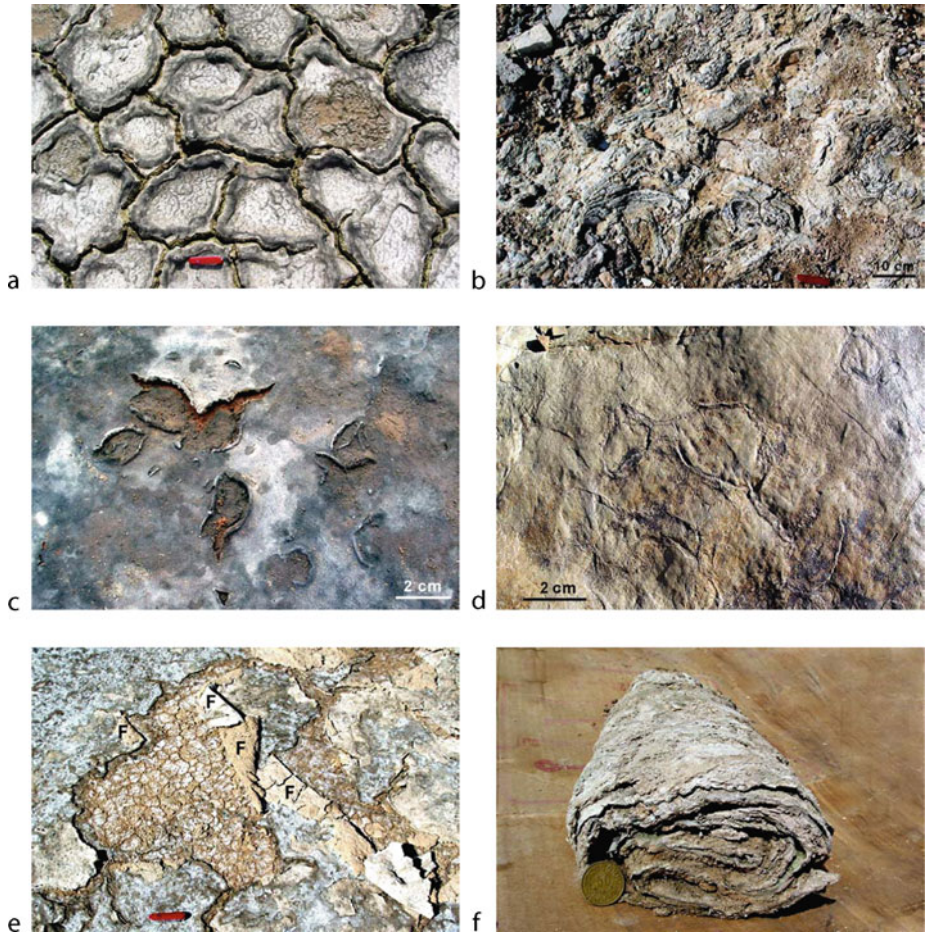


**Mat-Related Sedimentary Structures, Figure 2** Structures related to mat desiccation and deformation. (**a**) Polygonal pattern of shrinkage cracks with upturned margins in thick microbial mat. Scale (knife) is 8 cm. Locality: Trucial Coast, west of Abu Dhabi, U.A.E. (**b**) Surface outcrop of Holocene microbial mat exhibiting relics of polygons with upturned margins. Scale (knife) is 8 cm. Locality: Trucial Coast, west of Abu Dhabi, U.A.E. (**c**) Irregular to subcircular openings with curled margins, formed in a thin microbial mat due to desiccation and shrinkage. Note newly overgrown margin in lower right of photograph. Locality: Sabkha El Gourine, Mediterranean coast of southern Tunisia. (**d**) Upper surface of siltstone layer exhibiting irregular to circular cracks. The structures are interpreted as openings in a previous thin mat that underwent desiccation. Locality: Terminal Proterozoic Vingerbreek Member, Nama Group; Farm Haruchas, Namibia. (**e**) Microbial mat, torn and partly removed by current or wind action. Flip-overs of mat margins are indicated by "F." Note small-scale desiccation cracks in exposed mat substratum. Locality: Sabkhet Mjasser, Mediterranean coast of southern Tunisia. (**f**) "Roll-up" structure ("jelly-roll") consisting of rolled-up microbial mat and adhering sediment. Scale (coin) is 23 mm. Locality: Bhar Alouane, Mediterranean coast of southern Tunisia.

overgrowth of the crack margins and of the sediment trapped in the crack.

Thick mats, frequently dominated by *Microcoleus chthonoplastes*, tend to form polygonal networks of wide cracks with "upturned" or involute, "curled margins" (Figure 2a); individual polygons may range in size from 10 to 60 cm across, depending likely on the thickness of the mat. Ancient examples exhibit a "chaotic" upper surface with irregularly oriented bedding (Figure 2b) and resemble sedimentary structures ascribed to seismic events (Donaldson and Chiarenzelli, 2007).

Thin mats, frequently dominated by coccoid cyanobacteria and vested with a strong EPS top layer, tend to form circular openings with curled margins around (Figure 2c). Ancient examples have been described from thin siltstone layers within heterolithic deposits (Bouougri and Porada, 2007) (Figure 2d).

## Structures related to mat deformation, destruction, and erosion

Cohesive microbial mats may become torn, detached from the substratum and tightly folded, and eventually eroded by strong currents, e.g., during storm and flooding events. Mats are also destructed by complete desiccation after cessation of groundwater supply, and dried mat fragments

may be transported by wind over wide distances and be deposited in environments where mats usually do not grow.

Mat destruction by currents leads to typical structures repeatedly observed in modern environments and in the ancient record: (1) "flip-over" structures (Figure 2e) result when a mat's edge is flipped over; (2) cigar-shaped "roll-up" structures, also named roll-ups or "jelly-rolls" (Figure 2f), may develop when curled margins or flip-overs undergo additional rolling due to current action; and (3) irregular or arcuate belts of "mat deformation folds" form when a torn and detached mat is crumpled by tractional forces (Figure 3a); similar folds may also result from mat slumping on steeps slopes, e.g., along tidal channels. Roll-up structures can withstand transport over some distance and may gather along trash lines, whereas the other structures largely remain in situ. For ancient examples see Schieber et al. (2007).

"Mat chips" (Gerdes et al., 2000) are small fragments of eroded mats or biostabilized sediment. They primarily are irregular in shape with frayed edges, but may become pebble-shaped with transport (Figure 3b). Ancient examples have been named "microbial sand chips" (Pflüger and Gresse, 1996) or "sand clasts" in contrast to intraformational mud clasts (Figure 3c).

## Structures formed beneath microbial mats

From the hydraulic perspective, the sediment beneath cohesive and coherent microbial mats may be addressed and treated as a confined aquifer in which, at sufficient hydraulic head, a potential for liquefaction may develop (Porada et al., 2007). In such case, hydraulic upward

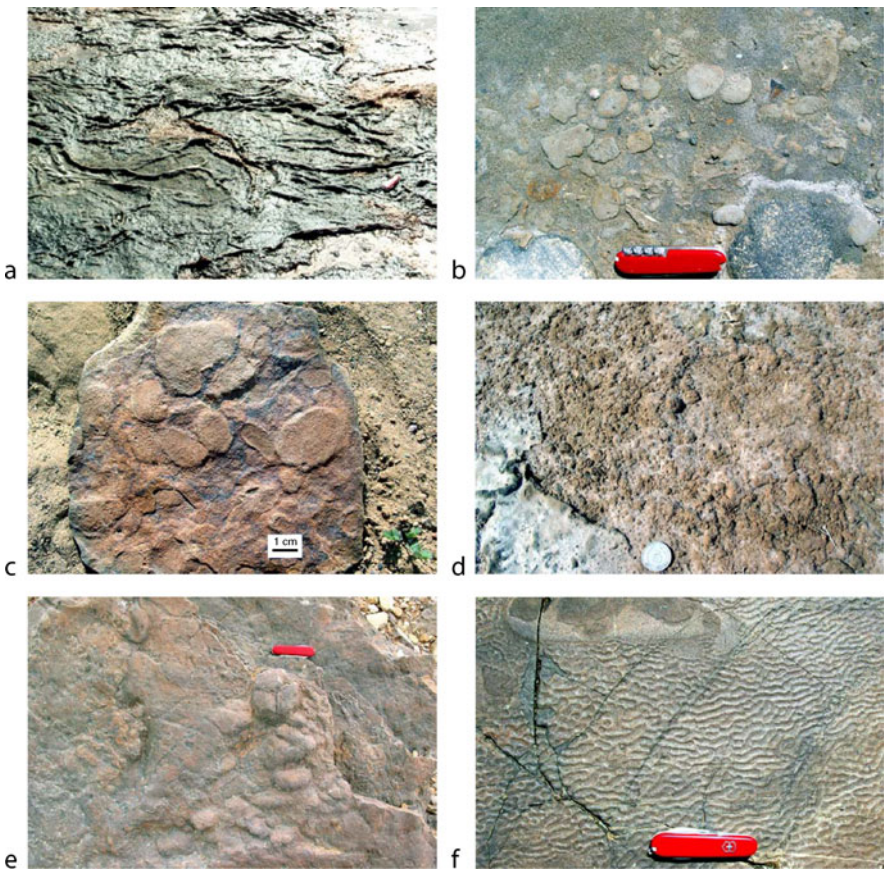


**Mat-Related Sedimentary Structures, Figure 3** Structures related to mat deformation and erosion, and subsurface structures. Scale (knife) in **a**, **b**, **e**, and **f** is 8 cm. (**a**) Detached, thin microbial mat, torn and strongly deformed by current action. Locality: Coastal sabkha between Gabes and Skhirat, Mediterranean coast of southern Tunisia. (**b**) Modern sandy-pebbly sediment surface with subrounded to rounded "mat chips". Locality: Salins du Midi, Réserve Nationale Camargue, southern France. (**c**) Upper surface of sandstone bed carrying subrounded to rounded "sand clasts," interpreted as previous "mat chips.". Locality: Terminal Proterozoic Vingerbreek Member, Nama Group; Farm Haruchas, Namibia. (**d**) Morphological details of a mat subsurface, exposed after removal of the mat. Scale (coin) is 24 mm. Locality: Sabkhet Mjasser, Mediterranean coast of southern Tunisia. (**e**) Upper surface of sandstone layer exhibiting irregular bulges and domes. The structure is considered to represent morphological features of a previous mat subsurface. Note tri-radiate crack in well-developed dome just below scale. Locality: Neoproterozoic Tizin-Taghatine Group; Taghdout area, Anti-Atlas, Morocco. (**f**) Upper surface of sandstone layer with "Kinneyia" structure. Locality: Terminal Proterozoic Vingerbreek Member, Nama Group; Farm Haruchas, Namibia.

pressure will lead to slow, upward movement of sediment grains. As a result, bulges and domes developed in the mat will gradually be filled from below; "petee ridges" have been quoted as an example above.

Thin microbial mats, particularly those dominated by coccoid cyanobacteria, may develop very irregular surfaces with numerous small domes and buckles which also appear as positive features on the subsurface (Figure 3d). Ancient examples of such "subsurface structures" strongly resemble load structures but are clearly distinguished from these by their occurrence as positive features on *upper* bedding surfaces (Figure 3e).

"Kinneyia" (Figure 3f) is a further structure developed in the sediment beneath a microbial mat. The structure is characterized by millimeter-scale, flat-topped, steeply sided, winding ridges separated by equally sized round-bottomed troughs and pits. It resembles small-scale interference ripples including crest-dominated linear and pit-dominated honeycomb-like patterns. The structure has been described from the Archean (Noffke et al., 2003b) to the Jurassic (Bloos, 1976), but not yet from the Recent. Genetic interpretation is thus difficult. Recent models suggest formation by trapping of gas underneath a sealing mat (Pflüger, 1999) or by reversals of groundwater flow in the liquefied mat substratum (Porada et al., 2007).

### Wrinkle structures

The term "wrinkle structure" (Hagadorn and Bottjer, 1997, 1999) is currently used as a collective term for various small-scale irregularities developed on ancient, siliciclastic sediment surfaces. Application of the term implies that a microbial participation in the formation of the structure is suspected, at the least. Within this broad definition, wrinkle structures may originate from very different processes including microbial growth, mat deformation and subsurface processes (Porada and Bouougri, 2007). Included in the term are also structures like elephant skin and Kinneyia which are well defined and for which, if clearly identified, usage of the proper name is recommended.

## Preservation of mat-related structures

As most of the organic matter produced by the cyanobacteria is soon decomposed and mineralized so that organic components or even carbon are rarely preserved in the ancient siliciclastic record, preservation of mat-related structures is largely dependent on the volume of inorganic material bound or produced by the mat or trapped by the structure. Microbially supported processes introducing inorganic material into the mat include "trapping and binding" of silt- to sand-sized grains and possibly clay minerals, formation of authigenic clay minerals during bacterial lysis, formation of iron sulfides and pyrite, and precipitation of carbonates. The mat-related structures themselves, being either positive or negative features on the mat surface, may act as sediments traps. Thus, shrinkage cracks may become filled with sediment by currents or eolian action, and involute (curled) margins may trap grains in their windings.

Another mechanism by which some mat-related structures, e.g., domes and bulges developed in the mat, may become preserved is "filling from below." This process requires comparatively high hydraulic upward pressure enabling liquefaction of the sediment below the sealing mat so that grains are lifted and moved upwards. As a result, a previously flat surface of a sedimentary layer may be transformed into an irregular surface mimicking morphological features of the mat.

## Conclusions

Simplisticly subsumed under the main groups of "wrinkles," "unusual cracks," and mat chips in the fossil record, mat-related sedimentary structures exhibit a wide range of shapes and patterns resulting from various processes and interactions between conflicting biological and physical factors. Due to local microtopographic features and the intrinsic inhomogeneity of microbial mats on a small scale, even well-defined structures, like elephant skin or Kinneyia, may show a high degree of variability. Thus, one structure almost never is like the other and the paradigm of reproducibility is not strictly applicable to them. Nevertheless, the structures are distinctive as exemplified on Figures 1–3.

Mat-related sedimentary structures may serve as tools for detailed facies analysis in siliciclastic peritidal settings. Based on modern analogs, most of the structures form in the intertidal to supratidal zones, but mat extent may have been wider in the Precambrian. Structures requiring (at least temporarily) subaerial exposure for their formation, e.g., types of shrinkage cracks with or without upturned or curled margins, clearly indicate intertidal to supratidal positions, whereas others remain less unequivocal. Subsurface structures including Kinneyia may form down to the shallow subtidal zone, as long as coherent, cohesive mats are present.

In the fossil record, the significance of mat-related sedimentary structures increases greatly if several types are observed in association. Some mat-related structures, e.g., reticulate growth patterns, preferentially occur in heterolithic successions of thinly laminated siltstone and mudstone which, in some cases, may be addressed as "siliciclastic biolaminites" resulting from the interaction of microbial mat growth and sediment supply (Bouougri and Porada, 2007), whereas sand cracks are usually developed on sandstone layers intercalated in the succession. In contrast, Kinneyia structures exclusively occur on upper surfaces of sandstone beds which frequently represent event deposits after storms or floods.

## Bibliography

Bloos, G., 1976. Untersuchungen über Bau und Entstehung der feinkörnigen Sandsteine des Schwarzen Jura α (Hettangium u. tiefstes Sinemurium) im schwäbischen Sedimentations-bereich. *Arb Inst Geol Paläont Univ Stuttgart*, **71**, 1–270.

Bouougri, E. H., and Porada, H., 2007. Siliciclastic biolaminites indicative of widespread microbial mats in the Neoproterozoic Nama Group of Namibia. *Journal of African Earth Sciences*, **48**, 38–48.
Bouougri, E., Gerdes, G., and Porada, H., 2007. Inherent problems of terminology: definition of terms frequently used in connection with microbial mats. In Schieber, J., Bose, P. K., Eriksson, P. G., Banerjee, S., Sarkar, S., Altermann, W., and Catuneanu O. (eds.), *Atlas of Microbial Mat Features Preserved within the Siliciclastic Rock Record*. Amsterdam: Elsevier, pp.145–151.
Eriksson, P. G., Schieber, J., Bouougri, E., Gerdes, G., Porada, H., Banerjee, S., Bose, P. K., and Sarkar, S., 2007. Classification of structures left by microbial mats in their host sediments. In Schieber, J., Bose, P. K., Eriksson, P. G., Banerjee, S., Sarkar, S., Altermann, W., and Catuneanu O. (eds.), *Atlas of Microbial Mat Features Preserved within the Siliciclastic Rock Record*. Amsterdam: Elsevier, pp. 39–52.
Gehling, J. G., 1999. Microbial mats in terminal Proterozoic siliciclastics: Ediacaran death masks. *Palaios*, **14**, 40–57.
Gerdes, G., Klenke, Th., and Noffke, N., 2000. Microbial signatures in peritidal siliciclastic sediments: a catalogue. *Sedimentology*, **47**, 279–308.
Hagadorn, J. W., and Bottjer, D. J., 1997. Wrinkle structures: microbially mediated sedimentary structures common in subtidal siliciclastic settings at the Proterozoic-Phanerozoic transition. *Geology*, **25**, 1047–1050.
Hagadorn, J. W., and Bottjer, D. J., 1999. Restriction of a late neoproterozoic biotope: suspect-microbial structures and trace fossils at the Vendian-Cambrian transition. *Palaios*, **14**, 73–85.
Krumbein, W. E., Paterson, D. M., and Stal, L. J. (eds.), 1994. *Biostabilization of Sediments*, Oldenburg: BIS Verlag, 526 p.
McKenzie, D. B., 1972. Tidal sand flat deposits in Lower Cretaceous Dakota Group near Denver, Colorado. *The Mountain Geologist*, **9**, 269–277.
Noffke, N., 1998. Multidirected ripple marks rising from biological and sedimentological processes in modern lower supratidal deposits (Mellum Island, southern North Sea). *Geology*, **26**, 879–882.
Noffke, N., 1999. Erosional remnants and pockets evolving from biotic-physical interactions in a recent lower supratidal environment. *Sedimentary Geology*, **123**, 175–181.
Noffke, N., Gerdes, G., Klenke, T., and Krumbein, W. E., 2001. Microbially induced sedimentary structures – a new category within the classification of primary sedimentary structures. *Journal of Sedimentary Research* , **71**, 649–656.
Noffke, N., Gerdes, G., and Klenke, T., 2003a. Benthic cyanobacteria and their influence on the sedimentary dynamics of peritidal depositional systems (siliciclastic, evaporitic salty, and evaporitic carbonatic). *Earth-science Reviews*, **62**, 163–176.
Noffke, N., Hazen, R., and Nhleko, N., 2003b. Earth's earliest microbial mats in a siliciclastic marine environment (2.9 Ga Mozaan Group, South Africa). *Geology*, **31**, 673–676.
Pflüger, F., 1999. Matground structures and redox facies. *Palaios*, **14**, 25–39.
Porada, H., and Bouougri, E. H., 2007. Wrinkle structures – a critical review. *Earth-science Reviews*, **81**, 199–215.
Porada, H., and Löffler, T., 2000. Microbial shrinkage cracks in siliciclastic rocks of the Neoproterozoic Nosib Group (Damara Supergroup) of central Namibia. *Communications of the Geological Survey of Namibia*, **12**, 63–72.
Porada, H., Ghergut, J., and Bouougri, E. H., 2008. Kinneyia-type wrinkle structures –critical review and model of formation. *Palaios*, **23**, 63–77.
Schieber, J., 2004. Microbial mats in the siliciclastic rock record: a summary of diagnostic features. In Eriksson, P. G., Altermann, W., Nelson, D., Mueller, W. U., Catuneanu, O., and Strand, K. (eds.), *The Precambrian Earth: Tempos and Events. Developments in Precambrian Geology*. Amsterdam: Elsevier, pp. 663–672.
Schieber, J., Bose, P. K., Eriksson, P. G., Banerjee, S., Sarkar, S., Altermann, W., and Catuneanu O., 2007. *Atlas of Microbial Mat Features Preserved within the Siliciclastic Rock Record*. Amsterdam: Elsevier, 311 p.
Stal, L. J., 2000. Cyanobacterial mats and stromatolites. In Whitton, B. A., and Potts, M. (eds.), The *Ecology of Cyanobacteria*. Amsterdam: Kluwer, pp. 61–120.
Van Gemerden, H., 1993. Microbial mats: a joint venture. *Marine Geology*, **113**, 3–25.

## Cross-references

Biofilms
Extracellular Polymeric Substances (EPS)
Iron Sulfide Formation
Microbial Communities, Structure, and Function
Microbial Mats
Sulfate-Reducing Bacteria
Tidal Flats

# METAGENOMICS

Wolfgang Liebl
Technische Universität München,
Freising-Weihenstephan, Germany

## Definition

Metagenomics is a research discipline that uses molecular biology methods to acquire, analyze, and interpret sequence data and/or functional data from the metagenomes (the collectivity of genomes) present in the environmental samples, without the need to cultivate the organisms in the samples. Related methodologies are so-called metatranscriptomics and metaproteomics that focus on the collective transcriptomes and proteomes, respectively, rather than on the genomes.

## Introduction

Microorganisms constitute major life forms on earth with respect to cell numbers and total biomass, and fulfill essential functions in global element cycles. It has been estimated that the earth's biosphere harbors at least two to three orders of magnitude more prokaryotic cells ($4–6 \times 10^{30}$) than the number of plant and animal cells combined. The total carbon fixed in prokaryotic cells amounts to $3.5–5.5 \times 10^{17}$ g of C which is 60–100% of the estimated total carbon in plants (Whitman et al., 1998).

For many decades since the beginnings of microbiology, research in this field has depended on the isolation and cultivation of individual microorganisms (best illustrated for the area of medical microbiology with the work of Robert Koch on the isolation and characterization of pathogenic bacteria in monocultures, leading to the Koch's postulates) or well-defined syntrophic consortia, and the subsequent in-depth analysis of pure cultures. Until today, microbiological research with traditional cultivation and

subsequent chemical, genetic, and physiological characterization has led to the description of roughly $10^4$ bacterial and archaeal species deposited as pure cultures in microbial culture collections. However, in the course of the past 2 decades, it has become more and more evident that the microbial diversity in most aquatic habitats, soil, as well as oceanic and terrestrial subsurfaces is enormous (Amann et al., 1995; Hugenholtz et al., 1998; Quince et al., 2008; Sleator et al., 2008) and that at least at present the majority (>99%) of microorganisms in many complex habitats are not cultivated by using standard techniques (Amann et al., 1995). Thus, it must be acknowledged that the number of described species contrasts by orders of magnitude with estimates about the number of prokaryotic taxa on earth which may amount to $10^6$–$10^8$ distinct genospecies (Simon and Daniel, 2010). Metagenomics, a relatively young research discipline, can aid in the detection and acquisition of data about this vast majority of uncultured microorganisms. For this methodology, which importantly is independent of cultivation, the collectivity of genomes (the metagenome) present in a given environmental sample is extracted and subjected to completely random or gene-targeted sequence analysis (Figure 1).

Although bacteria and archaea normally are unicellular, they usually occur as highly divers but often poorly characterized consortia in their natural habitats. Individual environmental samples can contain a breathtaking prokaryotic diversity. For example, the numbers of different molecular species or operational taxonomic units (OTUs) in soil samples could be over $10^6$ (Curtis et al., 2002). Statistics-based predictions for a specific Canadian soil sample range from $2 \times 10^4$ to $1.4 \times 10^5$ taxa (Quince et al., 2008). Highly interesting, based on taxonomy assessment results from deep-sea hydrothermal vent samples and statistical follow-up considerations, even samples from extreme environments – which often are believed to contain only limited biodiversity due to the extreme conditions – have revealed enormous microbial biodiversity, for example, $3 \times 10^5$ bacterial taxa at one specific sample site (Quince et al., 2008). These numbers illustrate the problems one faces to reach near-complete metagenomic datasets for complex natural habitats with today's analysis techniques. Thus, even with high-throughput methods, it is difficult if not impossible to generate a complete microbial inventory of a habitat including also most of the rare taxa. However, the methods available do allow the reliable

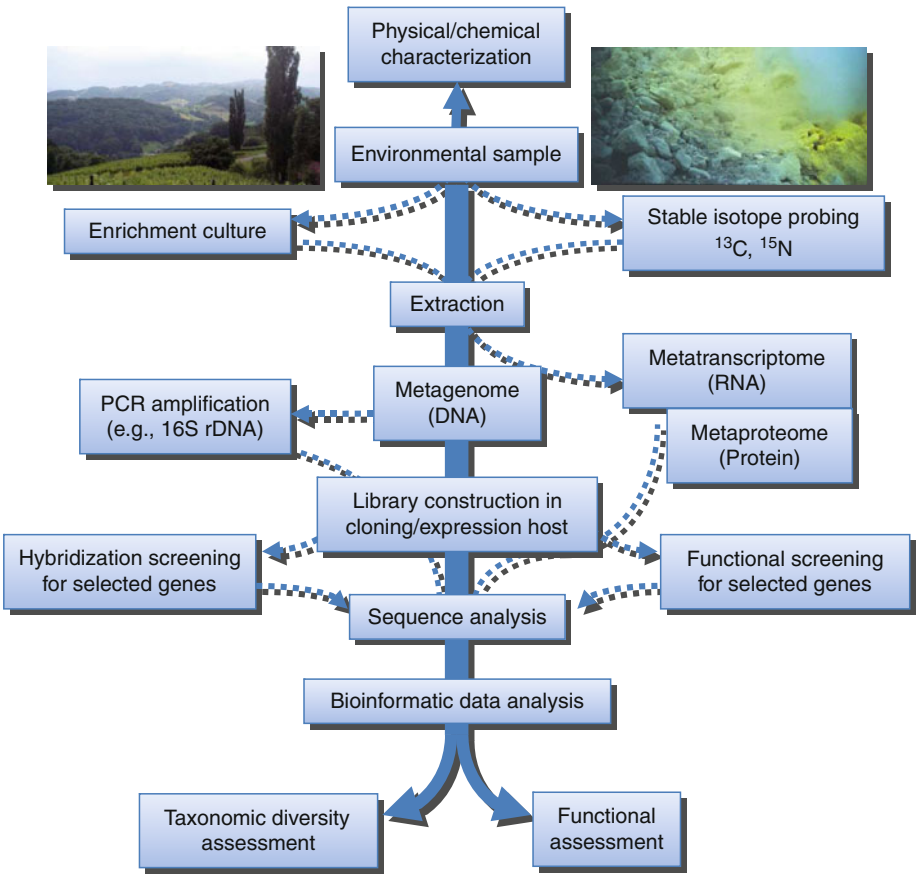


**Metagenomics, Figure 1** Flowchart summarizing steps of environmental meta-analysis.

identification of the abundant taxa that presumably account for the major biogeochemical conversions.

## Uses and applications of metagenome analysis

One major advantage of metagenomic analysis is that one can obtain a wealth of genetic information about organisms that live together in more- or less-complex communities, most of which cannot be cultivated with today's standard techniques. It can be used for extremely diverse purposes, such as the analysis of fundamental aspects of microbial community structure, function, and adaptation in environmental microbiology, but also to explore and exploit the microbial genetic, metabolic, and enzymatic diversity space for the development or improvement of biotechnological processes. Examples for the application of metagenomic techniques in geobiology are the analysis of microbial communities in rock material, sediments, aquifers, as well as in biofilms, on rock surfaces or in subsurface caves and mines, etc. It must be stressed that it is of utmost importance for most metagenomic studies to comprehensively record the sample-associated metadata (the data about the data), like date and position of sampling, physical and chemical characteristics, etc., as has been pointed out by Wooley et al. (2010).

Principally, metagenome analysis can be applied to any kind of habitat, irrespective of the complexity of the microbial communities present. For low-diversity habitats, high-throughput metagenome sequencing can yield a comprehensive overview of genetic information present and can even allow the near-complete or complete assembly of whole prokaryotic genomes, which was nicely shown for the organisms present in acid mine drain fluids (Tyson et al., 2004) or community genome sequencing of an anammox bacterium (Strous et al., 2006). However, the more diverse the community, the higher the sequencing and/or screening effort has to be to arrive at results that cover as comprehensively as possible the target genes of interest present in the sample. In some cases, it is possible to reduce the amount of work and costs by choosing a more specific than a completely random metagenome analysis. For example, if the main interest of a study lies in the analysis of genes involved in a certain metabolic trait (like breakdown and utilization of a specific substrate), one can try to enrich for the corresponding genes by carrying out enrichment cultures wherein the growth of organisms which display this metabolic trait is favored (e.g., by supplying the said specific substrate as the sole carbon source). Enrichment cultivation also has the advantages that (i) more cell material becomes available and that (ii) less organic and inorganic contaminating compounds from the original habitat sample that may interfere with DNA isolation yield and quality are present. An alternative is to enrich for genomic DNA or RNA from microorganisms with a certain substrate utilization capability by feeding a natural microbial community with $^{13}C$- or $^{15}N$-labeled substrate and then to isolate and process only the heavy nucleic acid that stems from organisms that utilized the added $^{13}C$- or $^{15}N$-substrate and incorporated the label into their nucleic acids (stable isotope probing) (Friedrich, 2006; Neufeld et al., 2007). Using enrichment cultures to preselect for microorganisms with certain physiological traits has been successfully done in several cases (e.g., Entcheva et al., 2001) and may be of advantage especially for very complex microbial communities, but it has to be kept in mind that any kind of cultivation step before DNA isolation can result in dramatic changes in community composition and diversity.

## Assessment of phylogenetic and functional diversity

Sequence analysis of conserved marker genes, usually 16S rRNA genes, is widely used for community diversity assessment. To this end, 16S rRNA gene sequences can be amplified with PCR directly from metagenomic DNA samples, followed by cloning into appropriate vectors and sequence analysis. Also, the sequences of conserved marker genes (rRNA genes, but also protein-encoding marker genes) can be retrieved from large sequence datasets compiled by large-scale random sequencing of metagenome DNA and then used for phylogenetic community composition assessment (von Mering et al., 2007).

Recently, massively parallel sequencing specifically of rRNA gene fragments amplified from metagenomic DNA has become possible by the use of the 454 Life Sciences (Roche) high-throughput tag pyrosequencing technology (Huse et al., 2008), but due to the fact that read-length limitations presently only allow the sequencing of incomplete rRNA gene fragments, this technology is suited for the trustworthy phylogenetic assignment at the phylum level but is not as reliable at the genus or species level. Nonetheless, this method allows interesting insights into the affiliation of microorganisms from complex communities to the large phylogenetic lineages, and technological improvements pertaining to the read lengths will surely allow more precise analyses at the genus or species level in the near future.

Bioinformatic tools are available for the comprehensive phylogenetic tree calculation from alignments of conserved marker sequences, for example, the ARB software package (Ludwig et al., 2004). Also, other sequence information than merely phylogenetically conserved genes available from large metagenomic random DNA sequence datasets can be used for diversity assessment. In the past years, various software tools have been developed that are useful for the so-called taxonomic binning of such sequence information (see Simon and Daniel, 2010). While some algorithms work on the basis of oligonucleotide sequence frequencies (composition-based binning, e.g., PhyloPhytia, TETRA; Teeling et al., 2004; McHardy et al., 2007), which are known to vary between different genomes, others use comparative orthologous ORF analysis for this purpose (CARMA, MEGAN, Sort-ITEMS; Huson et al., 2007; Krause et al., 2008; Monzoorul et al., 2009). Importantly, however, since most of these

bioinformatic tools depend on genome sequences and annotations from the available reference genome databases, which presently cover only a minority of the (readily) culturable species (not to speak of the enormous uncultured species diversity present in nature [see above]), our present possibilities for the assignment of short metagenomic DNA sequences to microbial taxa are quite limited.

Current large-scale efforts to sequence the genomes of the prokaryotic species deposited in major microbiological culture collections (GEBA, a Genomic Encyclopedia of Bacteria and Archaea; http://www.jgi.doe.gov/programs/GEBA/; Wu et al., 2009) will surely dramatically improve the reference genome sequence database necessary for a more accurate phylogenetic assignment of metagenomic sequence fragments. Nevertheless, considering that there are still in some cases not a single, in other cases only very few cultured representatives for some deep-rooting phyla, severe limitations in our ability to reliably assign short metagenomic DNA sequences to phylogenetic taxa will remain at least in the near future.

## Screening for genes in metagenomes

Metagenomic studies often include the screening of metagenomic libraries or metagenomic sequence datasets for genes of interest, for example, for genes encoding key enzymes characteristic for habitat-specific physiological traits, or for genes for biotechnologically relevant enzymes. Two fundamentally different approaches are used for this: the sequence-based approach and the function-based approach. Both methods have individual advantages and disadvantages and are explained briefly in the following.

The *sequence-based approach* uses in silico sequence mining, PCR amplification or hybridization methods to detect and isolate genes of interest. Metagenomic sequence datasets can be scored for fragments encoding orthologs of known genes deposited in the available reference databases. Various bioinformatic tools such as BLAST, Pfam, SEED, TIGRFAM, MEX, RAMMCAP, or MG-RAST are available which are helpful for the functional annotation of metagenome sequence data (see Simon and Daniel, 2010; Wooley et al., 2010). Another sequence-driven approach is to design degenerate PCR primers directed against conserved sequence motifs in a gene family of interest and to amplify partial ORFs from metagenomic DNA. The fragments can then be used to isolate the complete ORFs, for example, by using them as hybridization probes to identify clones or metagenomic DNA fragments containing the adjacent, missing ORF sequences, or by metagenome walking (see Simon and Daniel, 2010). Alternatively, DNA microarrays carrying oligonucleotides derived from consensus sequences of known genes have been used for the sequence-directed screening of a metagenomic library for a light, oxygen and voltage (LOV) domain blue light photoreceptor gene (Pathak et al., 2009). The major disadvantage of sequence-based gene detection is that this method depends on prior sequence information from known gene families. Therefore, truly novel genes unrelated to the already known genes encoding for a given function cannot be identified with this approach.

In the *function-based screening approach*, clones from metagenomic libraries are subjected to activity-based assays that indicate the function of interest. The major advantage of this approach is that it allows the recovery of complete genes or gene clusters and of novel types of enzymes without any prior knowledge of the sequence. However, in order to work efficiently, the genes of interest, which often originated from uncultured microorganisms with unknown genetics and physiology, must be compatible with the expression machinery provided by the heterologous screening host with respect to transcription, translation, protein folding, and eventually secretion (Gabor et al., 2004). Therefore, the fraction of the existing enzymatic diversity that can be accessed via functional screening approaches is strongly influenced by the choice of the host organism used. The phylogenetic distance between the gene donor and the cloning/expression host may be crucial for the success of gene expression. Mostly, *Escherichia coli* is used to construct metagenomic libraries for functional screening, but it is clear that the expression of metagenomic genes can be severely biased in this host. Therefore, it is important to establish and improve an alternative host/vector systems in order to enhance the probability of detecting genes from metagenomic samples (Angelov et al., 2009; Steele et al., 2009; Uchiyama and Miyazaki, 2009).

## Some restrictions and problems

Despite the power of metagenomic studies to unravel genetic information from microbes in communities that are not amenable to cultivation and in-depth characterization, a number of restrictions and problems remain, only some of which are listed hereafter.

Huge amounts of data are generated, especially in metagenome random sequencing projects. These data need to be generated, processed, and stored in a complex succession of steps. Special care must be taken with respect to library construction and sequencing quality. Exemplarily, the procedure of a metagenomic sequencing project is described by Kunin et al. (2008). A useful compilation of software tools for composition-based and similarity-based taxonomic binning, functional annotation of metagenomic data, and comparative metagenomics can be found in Wooley et al. (2010).

Interpretation of the sequence data and their connection with biochemical functions of biocatalysts remains a challenging task. The tools for ORF extraction from metagenomic sequence data and bioinformatics-driven function prediction are being improved constantly, but it is of course not feasible to check all gene function predictions experimentally, for example, by heterologous expression and biochemical analysis. Also, if only metagenomic DNA sequence data are available, it is unclear if the genes found are expressed at all. Thus, it has to be kept in mind that in many cases sequence data

obtained from metagenomes only indirectly point to (predicted) enzymes/pathways of the organisms in the sample. In future, performing metatranscriptomics and/or metaproteomics experiments in parallel with metagenomics can help to overcome this problem.

Also, linking phylogenetic and functional metagenomic data with the physiology of living microorganisms in the environmental sample is a crucial but not a trivial step for many studies attempting to correlate environmental data with a microbial community. Due to the species complexity in most microbial communities, it is only rarely possible to obtain assembled genomes. Even if conserved marker sequences point to close relatives of certain well-known microorganisms this does not necessarily prove that the organisms from which the metagenomic sequence information was derived have identical physiologies as the reference organisms. Also, some traits believed to be characteristic for certain phylogenetic groups of microorganisms can get lost by simple mutations. Still, it is possible to extract environment-specific gene fingerprints from unassembled random environmental DNA sequencing data that reflect known characteristics of the sampled environments, thus linking metagenomic sequence information with metabolic functions of the organisms present (Tringe et al., 2005).

Finally, since most conclusions reached from metagenome data analysis rely on comparative sequence analysis and thus are indirect, it will be important to develop and improve new microbiological cultivation and characterization techniques that also allow the cultivation and in vivo analysis of physiologically and quantitatively dominant microbial representatives within the studied communities.

## Summary

Considering the enormous microbial diversity in most environmental samples on one hand and the current shortcoming of the microbiologists' ability to cultivate the vast majority of these organisms on the other hand, it makes sense that metagenomics has become one of the key methods to study the composition and functions of complex microbial communities. The rapid advance of massively parallel sequencing and high-throughput screening technologies will enable even faster and cheaper access to environmental sequence datasets in the future, but connecting the metagenomic data with the physiology of the microorganisms and the environmental data remains challenging, and it will be crucial that the development of experimental setups and bioinformatic tools keep pace in order to be able to derive meaningful conclusions from metagenomic sequence data.

## Bibliography


Amann, R. I., Ludwig, W., and Schleifer, K. H., 1995. Phylogenetic identification and in situ detection of individual microbial cells without cultivation. *Microbiological Reviews*, **59**, 143–169.

Angelov, A., Mientus, M., Liebl, S., and Liebl, W., 2009. A two-host fosmid system for functional screening of (meta)genomic libraries from extreme thermophiles. *Systematic and Applied Microbiology*, **32**, 177–185.

Curtis, T. P., Sloan, W. T., and Scannell J. W., 2002. Estimating prokaryotic diversity and its limits. *Proceedings of the National Academy of Science USA*, **99**, 10494–10499.

Entcheva, P., Liebl, W., Johann, A., Hartsch, T., and Streit, W., 2001. Direct cloning from enrichment cultures, a reliable strategy for isolation of complete operons and genes from microbial consortia. *Applied and Environmental Microbiology*, **67**, 89–99.

Friedrich, M. W., 2006. Stable-isotope probing of DNA: insights into the function of uncultivated microorganisms from isotopically labeled metagenomes. *Current Opinion in Biotechnology*, **17**, 59–66.

Gabor, E. M., Alkema, W. B., and Janssen, D. B., 2004. Quantifying the accessibility of the metagenome by random expression cloning techniques. *Environmental Microbiology*, **6**, 879–886.

Hugenholtz, P., Goebel, B. M., and Pace, N. R., 1998. Impact of culture-independent studies on the emerging phylogenetic view of bacterial diversity. *Journal of Bacteriology*, **180**, 4765–4774.

Huse, S. M., Dethlefsen, L., Huber, J. A., Welch, D. M., Relman, D. A., and Sogin, M. L., 2008. Exploring microbial diversity and taxonomy using SSU rRNA hypervariable tag sequencing. *PLoS Genetics*, **4**, e1000255.

Huson, D. H., Auch, A. F., Qi, J., and Schuster, S. C., 2007. MEGAN analysis of metagenomic data. *Genome Research*, **17**, 377–386.

Krause, L., Diaz, N. N., Goesmann, A., Kelley, S., Nattkemper, T. W., Rohwer, F., Edwards, R. A., and Stoye, J., 2008. Phylogenetic classification of short environmental DNA fragments. *Nucleic Acids Research*, **36**, 2230–2239.

Kunin, V., Copeland, A., Lapidus, A., Mavromatis, K., and Hugenholtz, P., 2008. A bioinformaticians guide to metagenomics. *Microbiology and Molecular Biology Reviews*, **72**, 557–578.

Ludwig, W., Strunk, O., Westram, R., Richter, L., Meier, H., Yadhukumar, Buchner, A., Lai, T., Steppi, S., Jobb, G., Förster, W., Brettske, I., Gerber, S., Ginhart, A. W., Gross, O., Grumann, S., Hermann, S., Jost, R., König, A., Liss, T., Lüßmann, R., May, M., Nonhoff, B., Reichel, B., Strehlow, R., Stamatakis, A., Stuckmann, N., Vilbig, A., Lenke, M., Ludwig, T., Bode, A., and Schleifer, K.-H., 2004. ARB: a software environment for sequence data. *Nucleic Acids Research*, **32**(4), 1363–1371.

McHardy, A. C., Martin, H. G., Tsirigos, A., Hugenholtz, P., and Rigoutsos, I., 2007. Accurate phylogenetic classification of variable-length DNA fragments. *Nature Methods*, **4**, 63–72.

Neufeld, J. D., Vohra, J., Dumont, M. G., Lueders, T., Manefield, M., Friedrich, M. W., and Murrel, J. C., 2007. DNA stable-isotope probing. *Nature Protocols*, **2**, 860–866.

Pathak, G. P., Ehrenreich, A., Losi, A., Streit, W. R., and Gärtner, W., 2009. Novel blue light-sensitive proteins from a metagenomic approach. *Environmental Microbiology*, **11**, 2388–2399.

Simon, C., and Daniel, R., 2010. Achievements and new knowledge unraveled by metagenomic approaches. *Applied Microbiology and Biotechnology*, **85**, 265–276.

Sleator, R. D., Shortall, C., and Hill, C., 2008. Metagenomics. *Letters in Applied Microbiology*, **47**, 361–366.

Steele, H. L., Jaeger, K.-E., Daniel, R., and Streit, W. R., 2009. Advances in recovery of novel biocatalysts from metagenomes. *Journal of Molecular Microbiology and Biotechnology*, **16**, 25–37.

Strous, M., Pelletier, E., Mangenot, S., Rattei, T., Lehner, A., Taylor, M. W., Horn, M., Daims, H., Bartol-Mavel, D., Wincker, P., Barbe, V., Fonknechten, N., Vallenet, D., Segurens, B., Schenowitz-Truong, C., Médigue, C., Collingro, A., Snel, B., Dutilh, B. E., Op den Camp, H. J., van der Drift, C., Cirpus, I., van de Pas-Schoonen, K. T., Harhangi, H. R., van Niftrik, L., Schmid, M., Keltjens, J., van de Vossenberg, J., Kartal, B., Meier, H., Frishman, D., Huynen, M. A., Mewes, H. W., Weissenbach, J., Jetten, M. S., Wagner, M., and Le Paslier, D.,

2006. Deciphering the evolution and metabolism of an anammox bacterium from a community genome. *Nature*, **440**, 790–794.
Teeling, H., Waldmann, J., Lombardot, T., Bauer, M., and Glöckner, F. O., 2004. TETRA: a web-service and a stand-alone program for the analysis and comparison of tetranucleotide usage patterns in DNA sequences. *BMC Bioinformatics*, **5**, 163.
Tringe, S. G., von Mering, C., Kobayashi, A., Salamov, A. A., Chen, K., Chang, H. W., Podar, M., Short, JM, Mathur, E. J., Detter, J. C., Bork, P., Hugenholtz, P., and Rubin, E. M., 2005. Comparative metagenomics of microbial communities. *Science*, **308**, 554–557.
Tyson, G. W., Chapman, J., Hugenholtz, P., Allen, E. E., Ram, R. J., Richardson, P. M., Solovyev, V. V., Rubin, E. M., Rokhsar, D. S., and Banfield, J. F., 2004. Community structure and metabolism through reconstruction of microbial genomes from the environment. *Nature*, **428**, 37–43.
Uchiyama, T., and Miyazaki, K., 2009. Functional metagenomics for enzyme discovery: challenges to efficient screening. *Current Opinion in Biotechnology*, **20**, 616–622.
von Mering, C., Hugenholtz, P., Raes, J., Tringe, S. G., Doerks, T., Jensen, L. J., Ward, N., and Bork, P., 2007. Quantitative phylogenetic assessment of microbial communities in diverse environments. *Science*, **315**, 1126–1130.
Whitman, W. B., Coleman, D. C., and Wiebe, W. J., 1998. Prokaryotes: the unseen majority. *Proceeding of the National Acadamy of Science USA*, **95**, 6578–6583.
Wooley, J. C., Godzik, A., and Friedberg, I., 2010. A primer on metagenomics. *PLoS Computational Biology*, **6**, e1000667.
Wu, D., Hugenholtz, P., Mavromatis, K., Pukall, R., Dalin, E., Ivanova, N. N., Kunin, V., Goodwin, L., Wu, M., Tindall, B. J., Hooper, S. D., Pati, A., Lykidis, A., Spring, S., Anderson, I. J., D'haeseleer, P., Zemla, A., Singer, M., Lapidus, A., Nolan, M., Copeland, A., Han, C., Chen, F., Cheng, J.-F., Lucas, S., Kerfeld, C., Lang, E., Gronow, S., Chain, P., Bruce, D., Rubin, E. D., Kyrpides, N. C., Klenk, H.-P., and Eisen, J. A., 2009. A phylogeny-driven genomic encyclopaedia of Bacteria and Archaea. *Nature*, **462**, 1056–1060.

### Cross-references

Archaea
Bacteria
Biofilms
Endosymbiosis
Exoenzymes
Symbiosis
Terrestrial Deep Biosphere

## METALLOENZYMES

Michael Hoppert
University of Göttingen, Göttingen, Germany

### Synonyms

Metalloprotein (broader term)

### Definition

Enzyme protein containing one or more metal cofactor(s).

### Introduction

Metalloenzymes are enzyme proteins containing metal ions (metal cofactors), which are directly bound to the protein or to enzyme-bound nonprotein components (prosthetic groups). About one-third of all enzymes known so far are metalloenzymes (see Holm et al., 1996 for a general overview). Besides enzymes, other metalloproteins are involved in non-enzyme electron transfer reactions (cytochromes), may act as storage (e.g., ferritin for iron) or transport proteins (e.g., transferrin for iron). In the latter groups of proteins, the metal storage is reversible and the metal is a temporary component. Also ribozymes, i.e., RNA molecules with enzyme function may contain structurally and/or functionally important metal ions (mostly divalent metal ions such as $Mg^{2+}$) and may be therefore termed as metalloenzymes in a broader sense (Sigel and Pyle, 2007).

Though primarily focused on enzyme proteins, i.e., proteins acting as biocatalysts in biochemical reactions, also important non-enzyme proteins (without catalytic activity in the strict sense) and their metal centers are discussed in this article.

In enzyme catalysis, transition metals are of special relevance due to their redox activity, and/or a high charge density, which allows the polarization of enzyme substrates. Vanadium, molybdenum, tungsten, manganese, iron, cobalt, nickel, and copper metal centers have been characterized so far; the metal atoms can occur in mono-, di-, and multinuclear centers with nitrogen, oxygen, and sulfur atoms of the polypeptide chain as possible ligands (Holm et al., 1996; Degtyarenko, 2000; Wilson et al., 2004; Table 1). For analysis of metal centers in proteins, spectroscopic tools for the investigation of small molecules are of relevance, namely electron paramagnetic resonance (EPR) or the related electron-nuclear double resonance (ENDOR) spectroscopy, electron spin resonance (ESR), resonance Raman or Mössbauer spectroscopy. Data obtained from X-ray protein crystallography are inevitable to locate the metal center and its ligands inside a protein molecule. Combination of proteomic approaches with technologies for elemental trace analysis (inductively coupled plasma mass spectrometry or ICP-MS) introduced tools for determination of the entire set of metalloproteins (the metalloproteome) and/or all trace metals (metallome) in an organism (Szpunar, 2005; Barton et al., 2007).

### Metalloenzymes in early evolution

In early evolution, precursors of metal enzymes may have played a key role in catalytic reactions relevant for the synthesis of prebiotic macromolecules. According to the hypotheses originally postulated by Wächtershäuser, surface-bound iron, cobalt, nickel, and other transition metal centers with sulphido, carbonyl, and other ligands were catalysts involved in the synthesis of macromolecular compounds by carbon fixation, thus promoting growth of organic "superstructures" (Wächtershäuser, 1990). The metabolic type of this prebiotic scenario was chemolithoautotrophic, driven by the reducing potential of the outflow from deep-sea hydrothermal vents during

**Metalloenzymes, Table 1** Abundance of some metals in bacterial and algal organisms in g/100 g (dry weight) and some important key functions in enzymes (Barton et al., 2007)

| Element | Algae | Bacteria | Some specific roles in enzymes |
|---|---|---|---|
| K | 1.81 | 1.7 | Protein stabilization |
| Ca | 0.55 | 0.1 | Protein stabilization |
| Mg | 0.35 | 0.25 | Protein stabilization |
| Fe | 0.011 | 0.015 | $O_2$ transport, storage and/or activation; electron transport; superoxide breakdown |
| Mn | 0.006 | 0.005 | $O_2$ evolution; peroxide and superoxide breakdown |
| Zn | 0.001 | 0.005 | Protein stabilization; hydrolytic cleavage |
| Cu | 0.0007 | 0.001 | $O_2$ transport, storage and/or activation; electron transport; superoxide breakdown |
| Mo | 0.0001 | 0.001 | Oxygen transfer; $N_2$ activation |
| Co | 0.0003 | 0.001 | Free radical reactions; nucleophil |

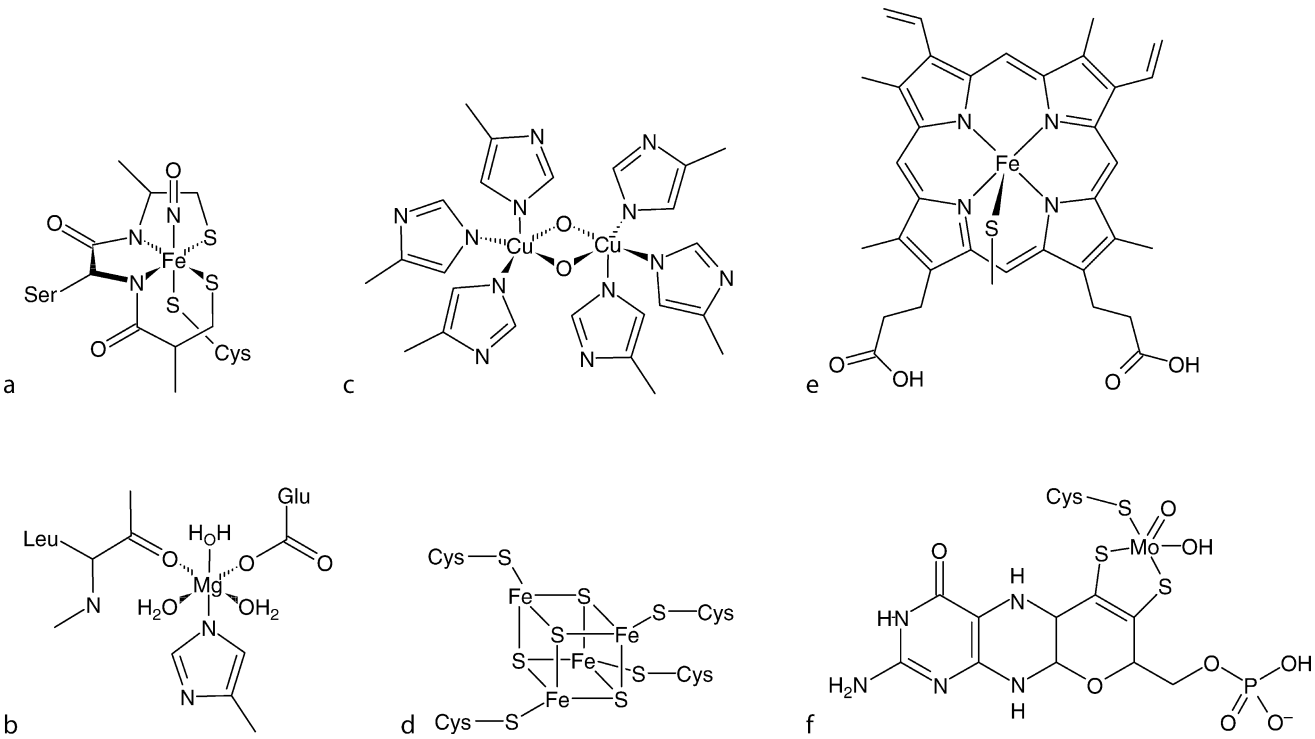


**Metalloenzymes, Figure 1** Various metal centers (from Degtyarenko, 2000) (**a**) mononuclear iron center (nitrile hydratase), (**b**) mononuclear magnesium center (Ni-Fe-hydrogenase from *Desulfovibrio*), (**c**) dinuclear copper center (oxyhemocyanin), (**d**) polynuclear iron–sulfur center, (**e**) heme iron coordination (cytochrome P450), and (**f**) molybdopterin (sulfite oxidase).

the Hadean period. Namely, the acetyl-CoA biosynthetic pathway may be seen as a model for prebiotic energy metabolism, since in this pathway enzymes and other proteins with FeS and (Fe,Ni)S centers are involved (acetyl CoA-synthethase/carbon monoxide dehydrogenase, hydrogenases, ferredoxin); these metal centers are in principle the cubic $Fe_4S_4$ as well as $(SNiS)(Fe_4S_4)(SFeS)$ units of greigite $(Fe(II)Fe(III)_2S_4)$. Later on in evolution, the prebiotic metal centers became parts of peptides and, finally, defined proteins (Wächtershäuser, 1990; Russell and Martin, 2004). Among all metalloproteins, iron metalloproteins and, within this class, iron–sulfur proteins are supposed to be the most important group and ubiquitous in organisms.

Besides FeS-centers, tetrapyrroles as metal-chelating prosthetic groups are interesting from the evolutionary viewpoint. Tetrapyrroles are as cyclic molecules (corrins and porphyrins; e.g., Figure 1e) ideal chelators of cobalt, copper, iron, manganese, and nickel. At the same time, the highly conjugated porphyrin molecules increase the catalytic activities of transition metal ions in electron transfer reactions by several orders of magnitude. Since porphyrins are present in all kingdoms of life, they must have evolved early in evolution, perhaps even in the

prebiotic state. As for FeS centers, the prosthetic groups are found in otherwise completely unrelated metalloproteins, such as methyl-coenzyme M reductase and chlorophylls (see below; Mauzerall, 1998).

Until the Paleozoic era, availability of bioessential transition metals changed by several orders of magnitude. Whereas Cu, Zn, Ni, and Mo concentrations increased in the ocean water, Co, Mn, and particularly iron decreased by several orders of magnitude during the Proterozoic eon (Anbar, 2008). These changes must have had an impact on the biogenic production of greenhouse gases such as nitrous oxide (Cu-dependant) or methane (Ni-dependant) and, hence, respective impact on global climate. The molybdenum cofactor (see below), in particular, plays a key role in the biological nitrogen cycle. It may even be speculated that molybdenum availability in oceans had a tremendous impact on early evolution. Under the reducing atmosphere, molydenum was depleted in the proterozoic ocean, generating a "bottleneck"for the nitrogen cycle. The low availability of nitrogen must have had a retarding effect of total biomass production of all organisms (especially non-nitrogen-fixing eukaryotes), until the oxidizing atmosphere also provided high molybdenum availability and stopped nitrogen limitation (Zerkle et al., 2006; Anbar, 2008). Limited molybdenum availability may also have been overcome in part by (less effective) molybdenum-independent nitrogenases. The evolutionary history of the enzymes is, however, difficult to reconstruct. There is no phylogenetic evidence that these "alternative" nitrogenases preceeded the molybdenum-dependant enzymes (Raymond et al., 2004).

In recent oceans, though, most metal ions relevant for enzyme metal centers are just present in trace amounts in seawater, and/or form hardly soluble salts. Thus, most organisms utilize specialized chelating compounds, uptake and transport systems for metal ion intake.

## Biomimetic metalloenzymes

Metal centers from enzyme proteins may give essential data for the design of biomimetic enzymes in bioorganic synthesis. Biomimetic metal centers from enzymes such as cytochrome oxidases (with Fe-porphyrin), catechol oxidase (based on Mn(IV)-complexes with *o*-aminophenol ligands), or hydrogenase (based, e.g., on six-coordinate Ni-Ru-centers with hydrogen as one of the bridging ligands for NiFe hydrogenase) reveal the biotechnological potential of catalysts derived from biological metal enzymes (Zbaida and Kariv, 1989; Chaudhuri et al., 2005; Song et al., 2005; Ogo et al., 2007).

## Classification of metalloenzymes

Since metalloenzymes are found in all enzymes families, simple classification of metal-containing subgroups based on sequence similarities cannot be applied. Reasonable classification schemes are based upon the bioinorganic motifs (Degtyarenko, 2000; Figure 1), i.e., the metal atom and its ligands (Degtyarenko and Contrino, 2004). Metal centers may be classified by the number of bound metal atoms as mononuclear (for one metal atom, Figure 1a and b) or polynuclear (more than one metal atom, Figure 1c and d) with endogenous ligands (i.e., the polypeptides of the enzyme molecule form a mostly polydentate coordination shell) or exogenous ligands (non-protein component of a conjugated protein such as heme or molybdopterin; Figure 1e and f).

The description given below is, for the sake of simplicity, based on the central atoms. It has to be kept in mind that different metal atoms can be bound to identical or similar bioorganic motifs (e.g., cobalt, copper, iron, magnesium, and nickel by porphyrins or corrins), and different motifs coordinate the same type of metal atom (e.g., either molybdopterin or $Fe_7MoS_9$ homocitrate cofactor for molybdenum; see below).

## Metal centers in metalloenzymes and other metal proteins

*Mononuclear iron proteins* are oxidoreductases (e.g., aromatic amino acid hydroxylases, aromatic ring cleavage dioxygenases, Fe-superoxide dismutase, lipoxygenases, nitrile hydratase, and Rieske oxygenases), or involved in electron transfer (desulforedoxins, rubredoxins, and photosynthetic reaction centers). The amino acid ligands are mostly histidine and/or cysteine such as in nitrile hydratase with three cysteine residues and two amide nitrogens (Figure 1a). *Diiron carboxylate proteins* bind a coupled binuclear iron center using, e.g., four carboxylate and two histidine residues. Oxidoreductases (alkene hydroxylase, methane monooxygenase, and phenol hydroxylase), iron storage (bacterioferritin, ferritin), and oxygen storage/transport proteins are members of this group (hemerythrin, myohemerythrin).

*Hemoproteins* are characterized by an iron porphyrin as prosthetic group (Figure 1e). While four of the iron ligands are occupied by the porphyrin ring, the other two are used for binding of the protein. Hemoproteins are oxidoreductases (catalases, peroxidases), electron transfer proteins (cytochromes), or oxygen transport and storage proteins (globins) (Nordlund and Eklund, 1995; Que and Ho, 1996).

*Iron–sulfur proteins* are characterized by the presence of iron–sulfur clusters containing sulfide-linked di-, tri-, and tetrairon centers in variable oxidation states (Figure 1d). Iron–sulfur clusters are found in ferredoxins, NADH hydrogenases, dehydrogenases, cytochrome c reductases, nitrogenases, and other proteins. Proteins with iron–sulfur clusters have key roles in nearly all respiratory chains, either in bacteria and archaea or in mitochondria of eukaryotic organisms. Other functions include catalysis of stereo-specific isomerization of citrate to isocitrate (aconitase) in the tricarboxylic acid cycle or the redox-dependent gene regulation. The simplest iron–sulfur cluster type consists of two iron ions bridged by two sulfide ions and is coordinated by four cysteinyl ligands or by two cysteins and two histidins. The oxidized proteins

contain two $Fe^{3+}$ ions, whereas the reduced proteins contain one $Fe^{3+}$ and one $Fe^{2+}$ ion. These species exist in two oxidation states, $Fe(III)_2$ and Fe(III)Fe(II). Besides [2Fe-2S], [3Fe-4S], [4Fe-4S], or [8Fe-7S] clusters are known (Bertini et al., 1995).

Also in *copper-containing proteins*, several metal center types occur. Similar to iron proteins, copper proteins are involved in oxygen transport or activation processes and electron transport. *Type I copper centers* have a single copper atom coordinated by two histidine residues and a cysteine residue in a trigonal planar structure and a variable axial amino acid ligand. Type I proteins are, e.g., ascorbate oxidase, ceruloplasmin, laccase, nitrite reductase, auracyanin, and azurin. *Type II copper centers* are square planar coordinated by N or N/O ligands (e.g., in galactose oxidase). *Type III centers* consist of two copper atoms (Figure 1c), each coordinated by three histidine residues (catechol oxidase, hemocyanins, tyrosinase). The *copper A center* in cytochrome c-oxidase consists of two copper atoms, coordinated by two histidine imidazole residues, methionine, carbonyl-oxygen, and two cystein-S bridging the copper atoms. In cytochrome oxidase *copper B centers*, the copper atom is coordinated by three histidine imidazole residues. The *four copper atom center* of nitrous oxide oxidase is coordinated by seven histidine residues. The four centers are bridged by one sulfur atom. Besides cytochrome oxidase, also other copper proteins are frequently oxygenases or dioxygenases (monoamine-oxidase, laccase, caeruloplasmin, superoxide-dismutase, hemocyanine) (Adman, 1991).

*Zinc proteins* represent the third large group of metalloproteins, with one, two, or three zinc ions. Zinc ions in proteins are classified as catalytic, co-catalytic, and structural, where zinc is either directly involved in the opening or closing a chemical bond, or zinc acts in the catalytic reaction in concert with other metal ions, or zinc ions maintain structural integrity of the enzymes. Zinc ions in catalytic sites are generally coordinated to the side chains of three amino acid residues and a water molecule. In structural zinc sites, the ion is coordinated by four amino acid side chains in a tetrahedral symmetry. With a filled *d* orbital, zinc ions do not participate in redox reactions, but rather function as Lewis acids to accept a pair of electrons, which is favorable for reactions like proteolysis or the hydration of carbon dioxide. Important zinc-containing enzymes are the alcohol dehydrogenase (containing both a catalytic and a structural zinc site), metalloproteases, and carbonic anhydrases with catalytic zinc sites. Cocatalytic zinc sites are found in superoxide dismutases, phosphatases aminopeptidases, and β-lactamases. In alcohol dehydrogenases, the zinc catalytic site is responsible for binding of the hydroxyl group oxygen from the alcohol substrate by replacing the zinc-bound water molecule (Lipscomb and Sträter, 1996; McCall et al., 2000).

*Nickel in metalloenzymes* occurs as Ni-4Fe-5S (e.g., nickel-containing CO dehydrogenases), coordinated in a *tetrapyrrole complex* (e.g., in methyl-coenzyme M reductase with glutamine as axial ligand) and as *dinuclear NiNi or NiFe complexes* (e.g., in hydrogenases and urease) or a $[4Fe–4S]^{2+}$ cluster bridged by a cysteine thiolate to a dinuclear NiNi center (acetyl-CoA synthase). Nickel-containing CO-dehydrogenases occur in anaerobic bacteria and archaea (CO-deydrogenases from aerobic bacteria are molybdopterin enzymes), whereby CO is bound by the nickel atom and hydroxyl oxygen (from water) is transferred to the bound carbon atom. After $CO_2$ is released, nickel is reduced ($Ni^{2+} \rightarrow Ni^{+}$) and transfers two electrons to ferredoxin. In the methyl-coenzyme M-reductase reaction, methane and a heterodisulfide are generated from the substrate methyl coenzyme M that reacts with coenzyme B (7-thioheptanoylthreoninephosphate). In nickel-iron hydrogenases, nickel of the Ni-Fe center is coordinated by one apical and three equatorial S-cysteins. The Ni-Fe hydrogenases catalyze both $H_2$ evolution and uptake in vitro, with cytochromes acting as either electron donors or acceptors. Acetyl-CoA synthase catalyzes the reversible formation of acetyl-CoA from carbon monoxide, a methylated corrinoid protein and coenzyme A, and is complexed with a nickel CO dehydrogenase (Ermler et al., 1998).

*Manganese in metalloenzymes* may also act as a simple Lewis acid catalyst. Manganese (normally Mn(II)) can also be oxidized to the (III)- or (IV)-state in biological systems, which allows redox-cycling reactions. *Manganese metal centers* may be mono-, bi-, tri-, or tetranuclear. Mn-superoxide dismutases (SODs) exhibit *mononuclear centers* and are antioxidant metalloenzymes catalyzing the redox disproportionation of the superoxide radical, $O_2^-$. SOD decomposes the highly reactive superoxide anion by a two-step disproportionation reaction which generates oxygen hydrogen peroxide. The active site manganese is five-coordinate, with the metal ligands arranged in distorted trigonal bipyramidal geometry. Two known enzymes with *binuclear centers* are arginase and manganese catalase. Arginase catalyzes the conversion of arginine to urea and ornithine. The manganese ions are five- and six-coordinate, respectively, with square-pyramidal and (distorted) octahedral coordination symmetries. The metal centers are interconnected by a solvent-derived hydroxide and carboxylate residues. This metal-bridging hydroxide acts as nucleophile that attacks the arginine guanidinium carbon. Other binuclear manganese enzymes are aminopeptidase P from *Escherichia coli* and the dinitrogenreductase-activating glycohydrolase from *Rhodospirillum rubrum.*

One of the most important biochemical catalytic reactions in our biosphere, the oxygen-generating photolysis of water, is brought about by the *tetranuclear manganese cluster* in oxygenic photosynthesis of cyanobacteria, eukaryotic algae, and higher plants. In oxygenic photosynthesis, water is oxidized by a cluster of Mn ions. Light is captured by antenna chlorophyll and funneled to the primary reaction center, which contains chlorophyll (P680). The oxidized P680 first oxidizes a redox-active tyrosine. Subsequent oxidation of the Mn cluster occurs via this

generated tyrosine radical. The enzyme can exist in five oxidation levels, corresponding to various oxidation states of the cluster (Wieghardt, 1994; Yocum and Pecoraro, 1999; Carrell et al., 2002).

*Molybdenum* and *tungsten enzymes* catalyze basic metabolic reactions in the nitrogen, sulfur, and carbon cycles. With the exception of the nitrogenase cofactor, molybdenum is associated with the heterocyclic pterin derivative (molybdopterin) that contains a mononucleate center, coordinated to the thiols of the cofactor (Figure 1f). These *molybdenum-cofactor–containing* (*MoCo*) *enzymes* catalyze the transfer of an oxygen atom, derived from or incorporated into water, to or from a substrate in a two-electron redox reaction. Three classes of MoCo enzymes are now distinguished, represented by xanthine oxidase and sulfite oxidase families (with single pterin ligands and either ligand-Mo(VI)OS(OH) or ligand-Mo(VI)$O_2$(S-cys) cores), and DMSO reductase family (with two pterin ligands). The *nitrogenase molybdenum metal center* is not related to the pterin derivatives. In molybdenum nitrogenases, each Mo forms a part of a polynuclear cluster containing 1 Mo, 7 Fe, and 9 S organized into an elongated structure. Within the protein the terminal Fe of the cluster is coordinated by a cysteine residue, while the Mo is coordinated by a histidine residue and a homocitrate ligand.

*Tungsten*, which lies in the chromium group of the periodic system immediately below molybdenum exhibits similar chemical properties and is complexed in a similar way to the pterin cofactors as described for molybdenum. Due to the higher sensitivity of tungsten toward high redox potential, tungsten enzymes are found in (thermophilic) anaerobic bacterial and archaeal microorganisms (Hille, 2002; Williams and Fausto da Silva, 2002).

*Cobalt* is the central metal ion in the tertrapyrrol *corrin ring* in the coenzyme $B_{12}$. Similar to porphyrin rings, four coordination sites are provided by the corrin ring. The $B_{12}$-bearing enzymes catalyzes either the transfer of methyl groups between two molecules or isomerization reactions, i.e., rearrangements of hydrogen atoms with concomitant exchange of a substituent (e.g., an hydroxyl group) between two adjacent carbon atoms in a molecule. In *non-corrin cobalt enzymes*, cobalt is complexed by aminoacids such as in nitrile hydratase (catalyzing the hydration of nitriles to amides; Kobayashi and Shimizu, 1999).

*Vanadium* occurs as V(III), V(IV), or V(V) in biological systems. The respective enzymes catalyze the two-electron oxidation of a halide by hydrogen peroxide. Besides the vanadium-containing enzymes, also heme-containing haloperoxidases and metal-free enzymes are known. In tunicates (ascidians) vanabin binds 20 V(IV) ions. However, the role of vanabins in vanadium accumulation by the ascidian has not yet been determined. In vanadium nitrogenases, vanadium, instead of molydenum is present in a FeVCo-center (Michibata et al., 2003; Crans et al., 2004).

Though frequently not classified as metalloenzymes in the strict sense, numerous (enzyme) *proteins bind* $Na^+$ *and* $K^+$ *ions*. The structures of $Na^+$ and $K^+$-complexes with proteins have a variety of coordination schemes and functions. Usual coordination numbers are five and six. Though the ions are not directly involved in catalytic steps, they activate numerous enzymes. Prominent examples are $Na^+$-activated β-galactosidase or the $K^+$-dependent activity of pyruvate-kinase and glycerol dehydratases (Page and Di Cera, 2006).

Specific *binding of calcium ions* frequently leads to conformational changes and increased protein stability. One large family of calcium-binding proteins is denoted *EF-hand proteins*, comprising a calcium-binding structural domain ("helix-turn-helix" motif). In an EF-hand loop the calcium ion is coordinated in a pentagonal bipyramidal configuration, by atoms of the protein backbone and side chains especially of aspartate and glutamate. Examples for EF-hand proteins are calmodulin and parvalbumin. In *non-EF-hand calcium-binding proteins*, the binding motifs are not conserved, such as α-lactalbumin and thermitase (Yang et al., 2002).

Also *magnesium* has a key function in activation and stabilization of enyzmes. Isocitrate lyase and glutamine synthetase are two examples of $Mg^{2+}$-activated metabolic enzymes. Enzymes catalyzing phosphorylation of proteins typically use magnesium chelates of ATP as cosubstrate. The bound $Mg^{2+}$ serves to facilitate nucleophilic attack at the γ-phosphate of the ATP substrate. Phosphate and phosphoryl transfer reactions require $Mg^{2+}$ as an essential cofactor. In chlorophyll molecules of photosynthetic reaction centers, magnesium ions are coordinated in a terrapyrrole ring system and to an axial *N*-histidin, *O*-aspartate, *O*-formyl-methionin, *O*-leucin, or water as ligands (Figure 1b; Cowan, 2002).

## Conclusion

Since metal centers are present in all enzyme families, and enzymes with metal centers also catalyze a wide variety of different reactions, metal enzymes cannot be assigned to a special group of enzymes or proteins. Thus it is very likely that metal centers developed early in evolution and evolved in several different lineages. Since free transition metal ions are ideal catalysts for numerous reactions in organic chemistry (and biochemistry) at moderate temperatures, they appear to be the natural "precursors" of functional enzyme proteins. Peptides and proteins are, on the other hand, ideal chelators for metal ions. Thus, protein and metal partners may have easily come together frequently during evolution.

## Bibliography

Adman, E. T., 1991. Copper protein structures. *Advances in Protein Chemistry*, **42**, 145–197.

Anbar, A. D., 2008. Oceans. Elements and evolution. *Science*, **322**, 1481–1483.

Barton, L. L., Goulhen, F., Bruschi, M., Woodards, N. A., Plunkett, R. M., and Rietmeijer, F. J. M., 2007. The bacterial metallome: composition and stability with specific reference to the anaerobic bacterium *Desulfovibrio desulfuricans*. *BioMetals*, **20**, 291–302.

Bertini, I., Ciurli, S., and Luchinat, C., 1995. The electronic structure of FeS centers in proteins and models. A contribution to the understanding of their electron transfer properties. *Structure and Bonding*, **83**, 1–53.
Carrell, T. G., Tyryshkin, A. M., and Dismukes, G. C., 2002. An evaluation of structural models for the photosynthetic water-oxidizing complex derived from spectroscopic and X-ray diffraction structures. *Journal of Biological Inorganic Chemistry*, **7**, 2–22.
Chaudhuri, P., Wieghardt, K., Weyhermüller, T., Paine, T. K., Mukherjee, S., and Mukherjee, C., 2005. Biomimetic metal-radical reactivity: aerial oxidation of alcohols, amines, aminophenols and catechols catalyzed by transition metal complexes. *Biological Chemistry*, **386**, 1023–1033.
Cowan, J. A., 2002. Structural and catalytic chemistry of magnesium-dependent enzymes. *BioMetals*, **15**, 225–235.
Crans, D. C., Smee, J. J., Galdamauskas, E., and Yang, L., 2004. Chemistry and biology of vanadium and the biological activities exerted by vanadium compounds. *Chemistry Reviews*, **104**, 849–902.
Degtyarenko, K., 2000. Bioorganic motifs: towards functional classification of metalloproteins. *Bioinformatics Review*, **16**, 851–864.
Degtyarenko, K., and Contrino, S. 2004. COMe: the ontology of bioinorganic proteins. *BMC Structural Biology*, **4**, 3.
Ermler, U., Grabarse, W., Shima, S., Goubeaud, M., and Thauer R. K., 1998. Active sites of transition-metal enzymes with a focus on nickel. *Current Opinon Structural Biology*, **8**, 749–758.
Hille, R., 2002. Molybdenum and tungsten in biology. *Trends in Biochemical Sciences*, **27**, 360–367.
Holm, R., Kennepohl, P., and Solomon, E. I., 1996. Structural and functional aspects of metal sites in biology. *Chemistry Reviews*, **96**, 2239–2314.
Kobayashi, M., and Shimizu, S., 1999. Cobalt proteins. *European Journal of Biochemistry*, **261**, 1–9.
Lipscomb, W. N., and Sträter, N., 1996. Recent advances in zinc enzymology. *Chemistry Reviews*, **96**, 2375–2433.
Mauzerall, D. C., 1998. Evolution of porphyrins. *Clinics Dermatology*, **16**, 195–201.
McCall, K. A., Huang, C.-C., and Fierke, C. A., 2000. Function and mechanism of zinc metalloenzymes. *Journal of Nutrition*, **130**, 1437S–1446S.
Michibata, H., Yamaguchi, N., Uyama, T., and Ueki, T., 2003. Molecular biological approaches to the accumulation and reduction of vanadium by ascidians. *Coordination Chemistry Reviews*, **237**, 41–51.
Nordlund, P., and Eklund, H., 1995. Diiron-carboxylate proteins. *Current Opinion in Structural Biology*, **5**, 758–766.
Ogo, S., Kabe, R., Uehara, K., Kure, B., Nishimura, T., Menon, S. C., Harada, R., Fukuzumi, S., Higuchi, Y., Ohhara, T., Tamada, T., and Kuroki, R., 2007. A dinuclear Ni(μ-H)Ru complex derived from $H_2$. *Science*, **316**, 585–587.
Page, M. J., and Di Cera, E., 2006. Role of $Na^+$ and $K^+$ in enzyme function. *Physiological Reviews*, **86**, 1049–1092.
Que, L. Jr., and Ho, R. Y. N., 1996. Dioxygen activation by enzymes with mononuclear nonheme iron active sites. *Chemistry Reviews*, **96**, 2607–2624.
Raymond, J. R., Siefert, J. L., Staples, C. R., and Blankenship, R. E., 2004. The natural history of nitrogen fixation. *Molecular Biology and Evolution*, **21**, 541–554.
Russell, M. J., and Martin, W., 2004. The rocky roots of the acetyl-CoA pathway. *Trends in Biochemical Sciences*, **29**, 358–363.
Sigel, R. K. O., and Pyle, A. M., 2007. Alternative roles for metal ions in enzyme catalysis and the implications for ribozyme chemistry. *Chemistry Reviews*, **107**, 97–113.
Song, L.-C., Yang, Z.-Y., Bian, H.-Z., Liu, Y., Wang, H.-T., Liu, X.-F., and Hu, Q.-M., 2005. Diiron oxadithiolate type models for the active site of iron-only hydrogenases and biomimetic hydrogen evolution catalyzed by $Fe_2(\mu\text{-}SCH_2OCH_2S\text{-}\mu)(CO)_2$. *Organometallics*, **24**, 6126–6135.
Szpunar, J., 2005. Advances in analytical methodology for bioinorganic speciation analysis: metallomics, metalloproteomics and heteroatom-tagged proteomics and metabolomics. *Analyst*, **130**, 442–465.
Wächtershäuser, G., 1990. Evolution of the first metabolic cycles. *Proceedings of the National Academy of Sciences of the United States of America*, **87**, 200–204.
Wieghardt, K., 1994. A structural model for the water-oxidizing manganese cluster in photosystem II. *Angewandte Chemie International Edition in English*, **33**, 725–728.
Williams, R. J. P, and Frausto da Silva, J. J. P., 2002. The involvement of molybdenum in life. *Biochemical and Biophysical Research Communications*, **292**, 293–299.
Wilson, C. J., Apiyo, D., and Wittung-Stafshede, P., 2004. Role of cofactors in metalloprotein folding. *Quarterly Review of Biophysics*, **37**, 285–314.
Yang, W., Hsiau-Wei, L., Hellings, H., and Yang, J. D., 2002. Structural analysis, identification, and design of calcium-bindung sites in proteins. *Proteins Structure, Function, and Genetics*, **47**, 344–356.
Yocum, C. F., and Pecoraro, V. L., 1999. Recent advances in the understanding of the biological chemistry of manganese. *Current Opinon Structural Biology*, **3**, 182–187.
Zbaida S., and Kariv, R., 1989. Biomimetic models for monooxygenases. *Biopharmaceutics and Drug Disposition*, **10**, 431–442.
Zerkle, A. L., House, C. H., Cox, R. P., and Canfield, D. E., 2006. Metal limitation of cyanobacterial $N_2$ fixation and implications for the Precambrian nitrogen cycle. *Geobiology*, **4**, 285–297.

## Cross-references

Anaerobic Oxidation of Methane with Sulfate
Methane, Orgin
Methane Oxidation (Aerabic)
Nickel, Biology
Siderophores
Zinc

# METALLOGENIUM

Joachim Reitner
University of Göttingen, Göttingen, Germany

## Definition

*Metallogenium* s.str. is a star-shaped enigmatic bacterium oxidizing Mn and iron. It preferentially lives in limnic environments.

*Metallogenium* is a relatively large (2–10 μm) microorganism with bacterial affinities that concentrates manganese and iron oxides in significant amounts. The genus *Metallogenium* has not yet been assigned to any taxonomic group. The cells lack rigid walls and develop flexible, tapering threads from which new cells probably arise. The organism is therefore, star-shaped and is found in various facies, predominantly in limnic environments (Figures 1 and 2). The threads are often heavily encrusted with oxides of iron and/or manganese. The oldest

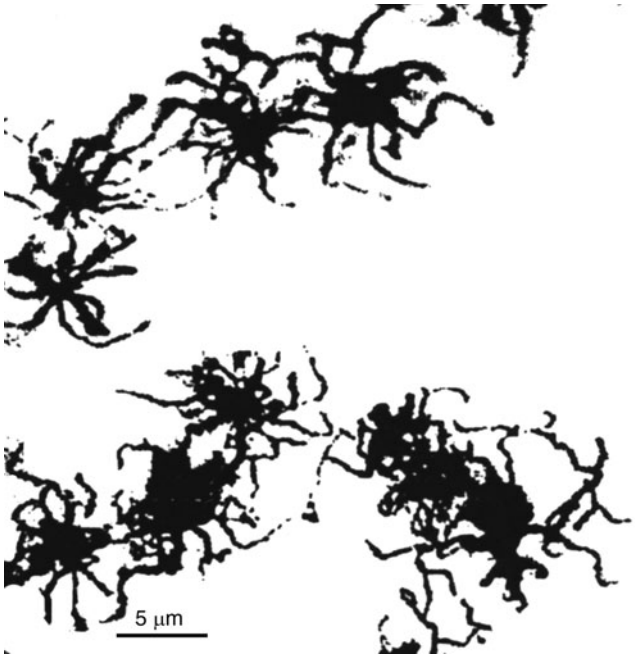


**Metallogenium, Figure 1** *Metallogenium personatum.* (Redrawn from Perfil´ev and Gabe, 1961.)

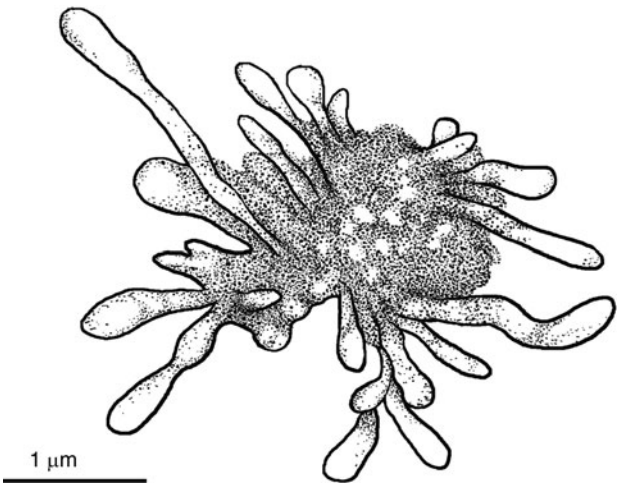


**Metallogenium, Figure 2** *Metallogenium personatum*. (Redrawn from Klaveness, 1999.)

*Metallogenium*-like fabrics are known from the 1.88 Gy old Paleoproterozoic Gunflint Formation (Barghorn and Tyler, 1965).

The first detailed description of *Metallogenium* was carried out by Perfil´ev and Gabe (1961) who called the type species *Metallogenium personatum*. There is an enormous record of publications about this microorganism (Zavarin, 1964a, b; Dubinia, 1970; Schmidt and Overbeck, 1984), and many speculations have been made about its systematic position, for example, within the Mycoplasmatales (Zavarzin and Hirsch, 1974), Chlamydobacteria (Klaveness, 1977), and Hyphomicrobiales (Perfil´ev and Gabe, 1961). Clasen (1969), Schmidt and Overbeck (1984), and Zavarzin (1989), suggested a relationship with the iron bacterium *Leptothrix echinata* (Beger, 1935) which shows a considerable morphological similarity to *Metallogenium*. Unfortunately, valid molecular biological examinations presently do not exist to clarify the phylogenetic position of this organism, although it is common especially in many freshwater lakes (e.g., Klaveness, 1999; Schulte, 1994). Besides *Metallogenium personatum*, which is undoubtedly a prokaryotic organism, "*Metallogenium symbioticum*" was described (Zavarzin, 1964b), which is also an Mn-oxidizing prokaryote preferentially growing on fungal microorganisms (Schweisfurth, 1971).

## Bibliography


Barghorn, E. S., and Tyler, S. A., 1965. Microorganisms from the Gunflint Chert. *Science*, **147**, 563–577.

Beger, H., 1935. *Leptothrix echinata*, ein neues, vorwiegend Mangan fällendes Eisenbakterium. *Zentralbl. Bakteriol. Abt*, **II 92**, 401–406.

Clasen, J., 1969: *Leptothrix echinata* und die Mangankonzentration in der Wahnbachtalsperre. *Städtehygiene*, **20**, 171–174.

Dubinia, G. A., 1970. Untersuchungen über die Morphologie von Metallogenium und die Beziehungen zu Mycoplasma. *Zeitschrift für Allgemeine Mikrobiologie*, **10**, 309–320.

Klaveness, D., 1977. Morphology, distribution and significance of the manganese-accumulating microorganism metallogenium in lakes. *Hydrobiologica*, **56**, 25–33.

Klaveness, D., 1999. Metallogenium – a microbial enigma. In Seckbach, J. (ed.), *Enigmatic Microorganisms and Life in Extreme Environments*. Dordrecht: Kluwer, pp. 539–548.

Perfil´ev, B. V., and Gabe, D. R., 1961. Studies of microlandscape. In *Capillary Methods of Investigating Micro-organisms* (Engl transl. Shewan, J. M., 1969). Toronto: University of Toronto Press, pp. 55–58.

Schmidt, W. D., and Overbeck, J., 1984. Studies of "iron-bacteria" from Lake Pluss.I. Morphology, finestructure and distribution of Metallogenium sp. and Siderocapsa geminata. *Zeitschrift für Allgemeine Mikrobiologie*, **24**, 329–339.

Schulte, N., 1994. Untersuchungen zur Ökologie, Morphologie und Entwicklung von *Metallogenium personatum* in einer Talsperre, Diss., Techn. Univ. Carolo-Wilhelmina Braunschweig.

Schweisfurth, R., 1971. Manganoxidierende Pilze. *Zeitschrift für Allgemeine Mikrobiologie*, **11**, 415–430.

Zavarin, G. A., 1964a. Structure of Metallogenium, Mikrobiologiya (Engl. Transl.). **32**, 864–867.

Zavarzin, G. A., 1964b. Metallogenium symbioticum. *Zeitschrift für Allgemeine Mikrobiologie*, **4**, 390–395.

Zavarzin, G. A., 1989. Genus "Metallogenium" Perfil´ev and Gabe, 1961. In Staley, J. T., Bryant, M. P., Pfennig, N., and Holt, J. G. (eds.), *Bergey´s Manual of Systematic Bacteriology*. Baltimore, MD: Williams & Wilkins, Vol. 3.

Zavarzin, G. A., and Hirsch, P., 1974. Genus Metallogenium Perfilev and Gabe 1961. In *Bergey´s Manual of Determinative Bacteriology,* 8th edn. Baltimore, MD: Williams & Wilkins, pp. 163–165.

## Cross-references

Bacteria
Biofilms
Leptothrix
Microbial Biomineralization
Microbial-Metal Binding
Ores, Microbial Precipitation and Oxidation
Subsurface Filamentous Fabrics
Terrestrial Deep Biosphere

# METALS, ACQUISITION BY MARINE BACTERIA

Alison Butler, Vanessa V. Homann
University of California, Santa Barbara, CA, USA

## Definition

Oceanic bacteria produce siderophores to acquire iron. Given that the iron concentration in surface ocean water is very low, siderophores produced by marine bacteria are tailored to the physical and chemical constraints of the marine environment.

## Introduction

### Microbial iron uptake

Virtually, all bacteria require iron for growth. Bacteria growing under aerobic conditions utilize a variety of pathways to acquire iron, but under conditions of iron starvation, bacteria often produce siderophores (Crosa et al., 2004). Siderophores are low molecular weight, chelating compounds produced by bacteria to facilitate iron(III) uptake (Crosa et al., 2004; Kraemer et al., 2005; Butler, 2007). The Fe(III)-siderophore complex is recognized by a specific outer membrane protein receptor, which catalyzes the transport of the Fe(III)-siderophore complex across the outer membrane (Figure 1).

The study of marine microbial siderophores is relatively new (Butler and Martin, 2005), yet certain characteristic structural features have already begun to emerge: suites of amphiphilic siderophores and photoreactive Fe(III)-siderophores.

## Marine Siderophores

### Amphiphilic marine siderophores

One characteristic of marine siderophores is the predominance of suites of amphiphilic siderophores, comprised of a hydrophilic head group, which coordinates with Fe(III), and one of a series of hydrophobic fatty acid appendages, which confers amphiphilicity (Figure 2). Two types of suites of amphiphilic siderophores are produced by marine bacteria. The aquachelins, marinobactins, and amphibactins are amphiphilic peptidic siderophores produced by distinct genera of marine bacteria (Figure 2) (Martinez et al., 2000, 2003). The relative amphiphilicity of each of these siderophores is

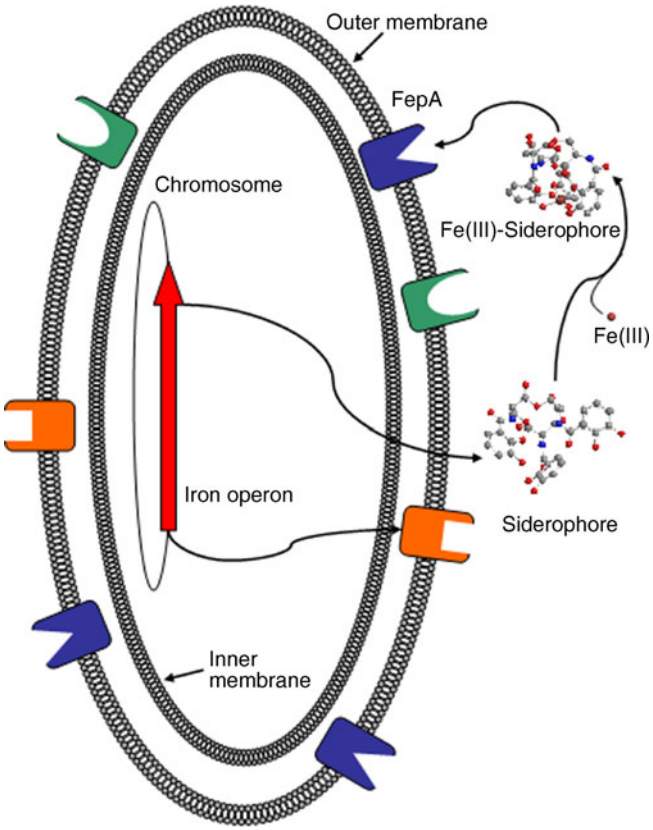


**Metals, Acquisition by Marine Bacteria, Figure 1** Siderophore-mediated iron uptake by a bacterium.

defined by both the number of amino acids in the peptide fraction, compared to the fatty acid chain length (e.g., C12–C18). The amphibactins with only four amino acids and relatively long C18 fatty acids are the most hydrophobic of the amphiphilic peptide siderophores. As a result, they remain cell associated and are extracted from the bacterial pellet during the isolation process (Martinez et al., 2003). In contrast, the marinobactins and aquachelins, with five and six amino acids in the head group and a predominance of the shorter fatty acids, are more hydrophilic and are thus isolated from the supernatant following centrifugation of the bacterial culture to pellet the cells (Martinez et al., 2000).

The synechobactins and ochrobactins (Figure 2) are different suites of amphiphilic siderophores, in which the head group is based on citric acid, as opposed to a peptide. The head group is thus smaller than in the peptidic amphiphilic siderophores. The fatty acids are also shorter than observed for the peptidic amphiphilic siderophores. Nevertheless, the ochrobactins are quite hydrophobic as a result of two fatty acid appendages; these siderophores remain associated with the bacterial pellet (Martin et al., 2006). The synechobactins, with

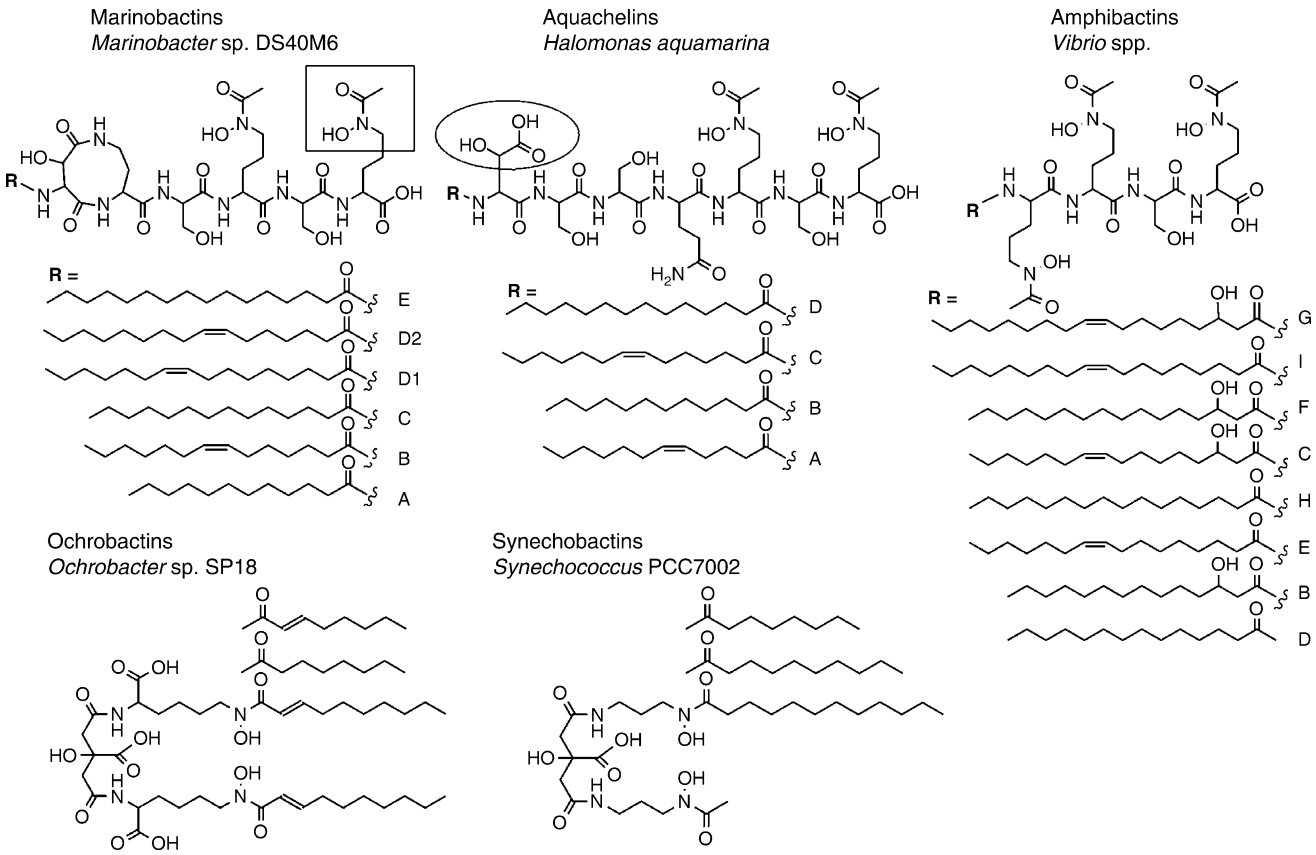


**Metals, Acquisition by Marine Bacteria, Figure 2** Amphiphilic marine siderophores. Marinobactins (Martinez et al., 2000); aquachelins (Martinez et al., 2000); amphibactins (Martinez et al., 2003); ochrobactins (Martin et al., 2006); synechobactins (Ito and Butler, 2005). The boxed portion shows the hydroxamic acid group. The circled portion shows the α-hydroxyacid in β-hydroxyaspartic acid.

only one fatty acid appendage, partition between the culture supernatant and the bacterial pellet (Ito and Butler, 2005).

## Photoreactive Fe(III)-siderophores

The other characteristic of marine siderophores is the predominance of α-hydroxycarboxylic acid moieties in the form of β-hydroxyaspartic acid or citric acid (Figures 2 and 3).

The Fe(III)-complex of an α-hydroxycarboxylic acid moiety is photoreactive in UV light, including natural sunlight, which is a condition experienced by the mixed layer of the upper 30–40 m of the ocean. Upon UV photolysis of the Fe(III)-siderophores containing citric acid, such as the ochrobactins (Martin et al., 2006), the synechobactins (Ito and Butler, 2005), the petrobactins (Bergeron et al., 2003; Hickford et al., 2004), and aerobactin (marine *Vibrio* sp. DS40M5) (Küpper et al., 2006; Haygood et al., 1993), citrate is oxidized to 3-ketoglutarate and Fe(III) is reduced to Fe(II). The resulting ligand photoproduct retains the ability to coordinate Fe(III) with remarkably high stability constant as a result of the 3-ketoglutate moiety and the remaining hydroxamic acid groups (Figure 4, for aerobactin (Küpper et al., 2006).

Other marine siderophores such as the aquachelins, the marinobactins, the alterobactins, and the pseudoalterobactins contain β-hydroxyaspartic acid as the α-hydroxycarboxylic acid group. UV photolysis of the Fe(III)-aquachelins results in ligand oxidation, specifically loss of β-hydroxyaspartic acid, as well as reduction of Fe(III) to Fe(II) (Barbeau et al., 2001). This peptide photoproduct retains the two hydroxamate groups and thus the ability to coordinate with Fe(III), although the conditional stability constant is somewhat reduced (Barbeau et al., 2001). Only catalytic amount of Fe(III) is required to effect the complete oxidation of the aquachelins in aerobic conditions, because the Fe(II) that is produced is oxidized back to Fe(III) and thus can coordinate with another apo aquachelin. The ferric complexes of the alterobactins A and B and the marinobactins are also photoreactive (Barbeau et al., 2003), although the

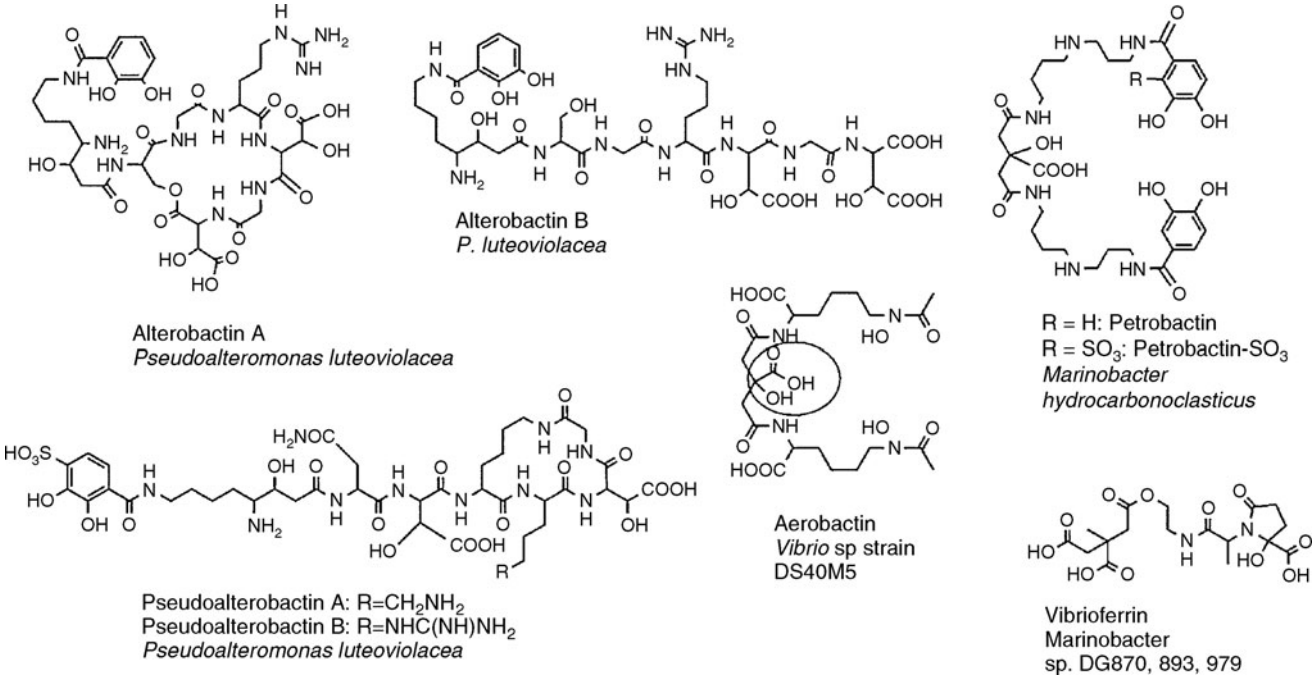


**Metals, Acquisition by Marine Bacteria, Figure 3** Marine siderophores with α-hydroxycarboxylic acid groups. The aquachelins, marinobactins, ochrobactins, and synechobactins shown in Figure 2 also contain α-hydroxycarboxylic acid moiety. Alterobactins (Reid et al., 1993); pseudoalterobactins (Kanoh et al., 2003); aerobactin (Haygood et al., 1993); petrobactin (Bergeron et al., 2003); petrobactin-$SO_3$ (Hickford et al., 2004); vibrioferrin (Amin et al., 2007). The circled portion shows the α-hydroxyacid in citric acid.

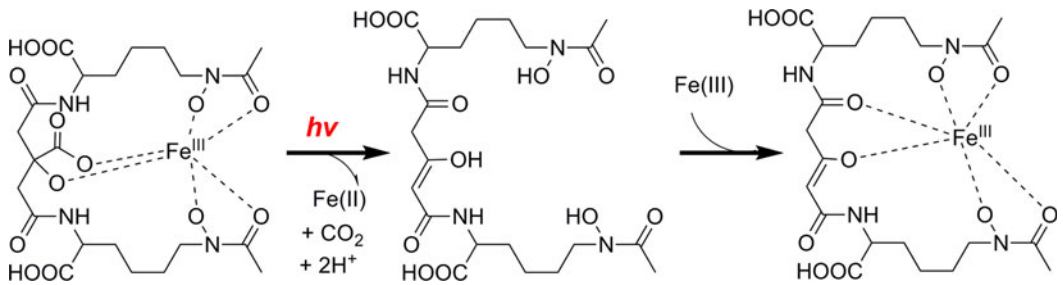


**Metals, Acquisition by Marine Bacteria, Figure 4** Reaction products in the photolysis of Fe(III)-aerobactin. (Adapted from Küpper et al., 2006).

structures of the oxidized ligands have not been completed yet. The ferric complexes of pseudoalterobactins A and B, which are chemically related to the alterobactins (Kanoh et al., 2003), would also be expected to be photoreactive.

## Summary

The preponderance of suites of amphiphilic siderophores and of α-hydroxycarboxylic-acid-containing siderophores produced by marine bacteria suggests that these properties have evolved as common iron acquisition strategies for marine bacteria, although details of the biological advantages conferred by these molecular properties are yet to be elucidated.

## Bibliography

Amin, S. A., Küpper, F. C., Green, D. H., Harris, W. R., and Carrano, C. J., 2007. Boron binding by a siderophore isolated from marine bacteria associated with the toxic dinoflagellate *Gymnodinium catenatum*. *Journal of the American Chemical Society*, **129**, 478–479.

Barbeau, K., Rue, E. L., Bruland, K. W., and Butler, A., 2001. Photochemical cycling of iron in the surface ocean

mediated by microbial iron(III)-binding ligands. *Nature*, **413**, 409–413.
Barbeau, K., Rue, E. L., Trick, C. G., Bruland, K. W., and Butler, A., 2003. The photochemical reactivity of siderophores produced by marine heterotrophic bacteria and cyanobacteria, based on characteristic iron(III)-binding groups. *Limnology and Oceanography*, **48**, 1069–1078.
Bergeron, R. J., Huang, G., Smith, R. E., Bharti, N., McManis, J. S., and Butler, A., 2003. Total synthesis of petrobactin. *Tetrahedron*, **59**, 2007–2014.
Butler, A., 2007. Siderophores. In Bertini, I., Gray, H. B., and Valentine, J. S. (eds.), *Biological Inorganic Chemistry: Structure and Reactivity (Metal Transport and Storage Proteins section)*. Sausalito: University Science Books, (Chap. VIII.3), pp.151–156.
Butler, A., and Martin, J. D., 2005. The marine biogeochemistry of iron. In Sigel, A., Sigel, H., and Sigel, R. K. O. (eds.), *"Biogeochemical Cycles," Metal Ions in Biological Systems*. New York: M. Dekker, Vol. 43, pp. 21–46.
Crosa, J. H., Mey, A. R., and Payne, S. M., 2004. *Iron Transport in Bacteria*. Washington, DC: ASM, p. 499.
Haygood, M. J., Holt, P., and Butler, A., 1993. Aerobactin production by a planktonic marine Vibrio sp. *Limnology and Oceanography*, **38**, 1091–1097.
Hickford, S. J. H., Küpper, F. C., Zhang, G., Carrano, C. J., Blunt, J. W., and Butler, A., 2004. Petrobactin sulfonate, a new siderophore produced by the marine bacterium *Marinobacter hydrocarbonoclasticus*. *Journal of National Products*, **67**, 1897–1899.
Ito, Y., and Butler, A., 2005. Structure of synechobactins, new siderophores of the marine cyanobacterium Synechococcus sp. PCC 7002. *Limnology and Oceanography*, **50**, 1918–1923.
Kanoh, K., Kamino, K., Leleo, G., Adachi, K., and Shizuri, Y., 2003. Pseudoalterobactin A and B, new siderophores excreted by marine bacterium Pseudoalteromonas sp KP20–4. *The Journal of Antibiotics*, **56**, 871–875.
Kraemer, S. M., Butler, A., Borer, P., and Cervini-Silva, J., 2005. Biogenic ligands and the dissolution of iron bearing minerals in marine systems. *Reviews in Mineralogy and Geochemistry: Molecular Geomicrobiology*, **59**, 53–76.
Küpper, F. C., Carrano, C. J., Kuhn, J. U., and Butler, A., 2006. Photoreactivity of iron(III)-aerobactin: Photoproduct structure and iron(III) coordination. *Inorganic Chemistry*, **45**, 6026–6033.
Martin, J. D., Ito, Y., Homann, V. V., Haygood, M. G., and Butler, A., 2006. Structure and membrane affinity of new amphiphilic siderophores produced by Ochrobactrum sp. SP18. *Journal of Biological Inorganic Chemistry*, **11**(5), 633–641.
Martinez, J. S., Zhang, G. P., Holt, P. D., Jung, H. T., Carrano, C. J., Haygood, M. G., and Butler, A., 2000. Self-assembling amphiphilic siderophores from marine bacteria. *Science*, **287**, 1245–1247.
Martinez, J. S., Carter-Franklin, J. N., Mann, E. L., Martin, J. D., Haygood, M. G., and Butler, A., 2003. Structure and membrane affinity of a new suite of amphiphilic siderophores produced by a marine bacterium. *Proceedings of the National Academy of Sciences of the United States of America*, **100**(7), 3754–3759.
Reid, R. T., Live, D. H., Faulkner, D. J., and Butler, A., 1993. A siderophore from a marine bacterium with an exceptional ferric ion stability constant. *Nature*, **366**, 455–457.

## Cross-references

Bacteria
Cyanobacteria
Fe(II)-Oxidizing Prokaryotes
Metalloenzymes
Siderophores

# METEORITICS

Mark A. Sephton
Imperial College London, London, UK

## Definition

Meteorites are fragments of extraterrestrial material that fall on the Earth's surface. Most meteorites are parts of asteroids propelled into Earth-crossing orbits by relatively recent collisions in the asteroid belt, initiated by the gravitational effects of Jupiter's orbit. Relatively small numbers of meteorites originate from larger objects such as the Moon and Mars. The Earth acquires $10^2$ to $10^3$ t of such material each day, but only 1% or less arrives in pieces large enough for identification and recovery (Dodd, 1981). The surface of the meteorite usually melts and emits a glowing tail and a trail of smoke, but the interior of the meteorite is unaffected by passage through the Earth's atmosphere and remains at the temperature of interplanetary space.

## Collection of meteorites

"Falls" are meteorites that have been observed to fall and were subsequently collected; "finds" are meteorites that were not seen to fall. Before the 1970s, the total number of known meteorites amounted to less than 1,000 falls and 1,706 authenticated finds. Since then, it has been recognized that certain parts of the Earth's surface preserve and concentrate meteorites. To date, tens of thousands of meteorites have been collected from the Antarctic ice. Similar numbers of meteorite fragments have also been collected from hot deserts. Most recently, telescope and camera network surveys have produced meteorites with photographed fireballs allowing the calculation of their orbits and assignment to a particular source within the solar system (Bland et al., 2009).

## Chondrites

About 85% of the meteorites observed to fall on the Earth are chondrites, conglomerate rocks with an overall elemental composition similar to the Sun, if the loss of the most volatile elements is ignored. When their near solar makeup is considered alongside radiometric ages of $4.56 \times 10^9$ years, it becomes clear that chondrites are rocks formed during, or shortly after, the birth of the Sun.

## The record in chondrites

Their status as some of the earliest formed solids in the solar system combined with a lack of subsequent processing ensures that chondrites represent a valuable record of extraterrestrial environments. Contributing regions include interstellar space, the solar nebula and the asteroidal meteorite parent bodies.

## Carbonaceous chondrites

Of all the chondrites, the carbonaceous chondrites are considered the most primitive and these objects represent an enthralling window back in time providing views of the earliest solar system (Figure 1). The name "carbonaceous chondrite" is highly descriptive as these meteorites contain a carbon-rich matrix composed primarily of clay minerals, oxides, and organic matter, and most contain spherules of silicate glass termed chondrules.

## Classification of carbonaceous chondrites

The carbonaceous chondrites are classified according to their primary and secondary characteristics (Figure 2). The primary classification (CI, CM, CR, CO, CV, CK) reflects the original properties of the meteorites such as bulk chemistry and mineralogy. The label is derived from the carbonaceous chondrite accepted as the type specimen, for example, CI = Ivuna. The secondary numerical classification reflects petrographic type, which indicates the extent and type of alteration that the meteorite has undergone on its parent body.


**Meteoritics, Figure 1** The Murchison carbonaceous chondrite.

## Carbon in meteorites

The carbon in carbonaceous chondrites is present in several forms and each has its specific source region(s) (Table 1; Sephton et al., 2003). Materials like silicon carbide and graphite condensed from the atmospheres of stars that existed long before our Sun. Nanometer-sized diamonds also originate as condensation products of stellar outflows as well as from catastrophic supernova explosions. Carbonate minerals were formed in the early solar system as aqueous alteration took place on asteroids. Yet all these components are quantitatively subordinate to the main carbonaceous material in carbonaceous chondrites – organic matter.

## Types of organic matter in meteorites

Much of our current understanding of meteoritic organic matter has come from investigations of the Murchison carbonaceous chondrite, approximately 100 kg of which fell in Australia in 1969 (Figure 1). Not all of the organic molecules in meteorites are present in the same form. A minor portion of the organic matter in meteorites is present as small "free" molecules, including various hydrocarbons and the biologically useful amino acids and carboxylic acids (Figure 3), but the majority of organic matter in the carbon-rich meteorites is present as a highly cross-linked organic network or "macromolecular material".

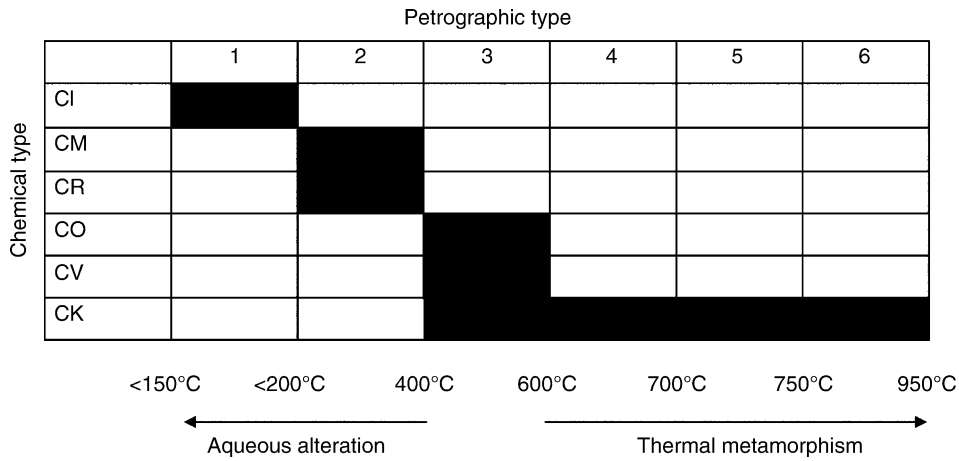


**Meteoritics, Figure 2** The classification system for carbonaceous chondrites.

## Free compounds

### Amino acids

The amino acids found in meteorites have attracted a great deal of attention owing to their role as building blocks for proteins. The search for amino acids in meteorites accelerated in the 1960s (Degens and Bajor, 1962; Kaplan et al., 1963) following reports of microfossils in certain samples (Claus and Nagy, 1961). Amino acids were discovered, but these initially promising results were later found to be the result of terrestrial contamination. It was only when the organic-rich Murchison meteorite fell and was rapidly analyzed that both protein and, importantly, nonprotein amino acids were found in this fresh sample (Kvenvolden et al., 1970). Today it is known that the amino acids in Murchison are present at around 60 ppm. Compounds containing two through eight carbon atoms exist and they exhibit several features, which suggest that they are not terrestrial contaminants but are extraterrestrial and nonbiological or "abiotic" in origin. The meteoritic amino acids display broad structural diversity, a decline in abundance with increasing molecule size, and the presence of unusual and even unique molecular configurations.

A particular characteristic of amino acids is chirality or handedness. One chiral form rotates the polarized light to the left and is termed levorotatory or "L," while the other form rotates the light to the right, and is called dextrorotatory or "D." Chirality is important for theories that link extraterrestrial organic matter with the origin of life, because terrestrial biology preferentially generates L-amino acids whereas abiotic reactions generally have no preference and produce racemic mixtures with equal amounts of L and D forms.

The discussion of whether amino acids in meteorites were racemic (with equal amounts of L and D forms) or nonracemic (with a preference for one or the other) began in the 1950s and continued through the 1960s, (e.g., Mueller, 1953; Nagy et al., 1964) but early results implied that the dominance of L forms was caused by terrestrial contamination and analytical artefacts. Yet following the fall of Murchison in 1969, four protein and seven

**Meteoritics, Table 1** The carbon-bearing components in carbonaceous chondrites

| Carbon-bearing component | Abundance (wt. %) | Environment of formation |
|---|---|---|
| Organic matter | 2.0 | Interstellar space, solar nebula, asteroids |
| Carbonate | 0.2 | Asteroids |
| Diamond | 0.04 | Stars, supernovae |
| Graphite | 0.005 | Stars |
| Silicon carbide | 0.009 | Stars |

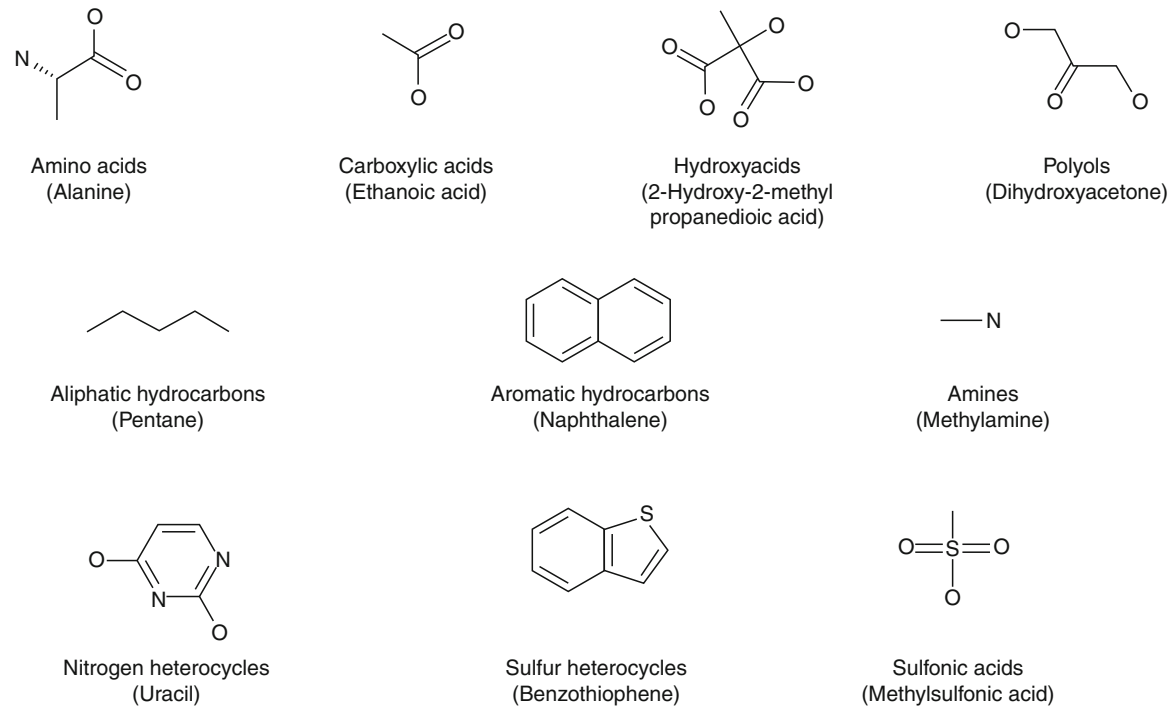


**Meteoritics, Figure 3** Some free compound classes and examples found in carbonaceous chondrites.

nonprotein amino acids were found to be racemic (Kvenvolden et al., 1970, 1971). More modern analyses have reinvigorated the debate over the racemic nature of meteorite amino acids and a slight L-excess in both protein and nonprotein amino acids has been reported (Engel and Nagy, 1982; Pizzarello and Cronin, 2000).

Proposed mechanisms for producing this L-excess in meteoritic amino acids rely on selective destruction of the right-handed form of the amino acids. Currently, popular hypotheses involve ultraviolet circularly polarized light from a neutron star or reflection nebulae (Bailey, 2001; Bonner and Rubenstein, 1987). It is a necessary consequence of this theory that at least some amino acids were already formed in interstellar space so that preferential destruction of D-amino acids could take place. The recent detection of the simplest amino acid, glycine, in interstellar spectra supports this assertion (Kuan et al., 2003).

## Carboxylic acids

Carboxylic acids are another type of biologically useful molecule found in meteorites. In life, they are a convenient and compact store of energy and are common cell membrane molecules. Carboxylic acids in Murchison contain between two and five carbon atoms and display complete structural diversity, a general decrease in abundance with increasing carbon number, and an equal concentration of branched and straight-chain isomers (Lawless and Yuen, 1979; Yuen and Kvenvolden, 1973). The monocarboxylic acids are present in a much higher concentration (332 ppm) than the amino acids and are the most abundant solvent extractable compounds. A structurally diverse suite of dicarboxylic acids containing up to nine carbon atoms are also present in much smaller amounts (26 ppm) (Lawless et al., 1974).

## Hydroxyacids

Hydroxycarboxylic acids (or hydroxyacids) in carbonaceous chondrites contain up to nine carbon atoms and are structurally diverse and present in concentrations of 15 ppm (Peltzer and Bada, 1978). Intriguingly, the hydroxyacids correspond in structure to the more abundant amino acids suggesting that some hydroxy and amino acids may have been produced together on the parent asteroid. The relevant chemical reaction is known as the Strecker-cyanohydrin synthesis. Hydrogen cyanide and aldehydes combine in aqueous solution to produce hydroxyacids but if ammonia is also present then the products become amino acids.

## Sugar-related compounds

Collectively, sugars and their related compounds are called polyhydroxylated compounds or "polyols." They are compounds containing a number of hydroxyl (OH) groups attached to their carbon skeleton. Sugars are important biologically as a source of energy for organisms and, when combined to form larger molecules, they can act as food stores and give structural support. Experiments in the 1960s detected polyols in carbonaceous chondrites, but terrestrial contamination was implied (Degens and Bajor, 1962). More recent experiments on Murchison have discovered a number of sugar-related compounds (sugars, sugar alcohols, and sugar acids) in similar abundances to the amino acids (Cooper et al., 2001). The Murchison polyols display many of the features of extraterrestrial compounds. Progressively larger polyols become less abundant, display almost complete structural diversity, and contain some terrestrially rare compounds implying an abiotic source.

## Aliphatic and aromatic hydrocarbons

Short aliphatic molecules in Murchison are present in amounts of 1.4 ppm and display many nonbiological features, which imply they are indigenous to the meteorite, such as structural diversity and a decrease in amount with increasing molecule size (Yuen et al., 1984). Aromatic hydrocarbons, in free form are present in carbonaceous chondrites at around 30 ppm (Pering and Ponnamperuma, 1971). Compound sizes range from one to seven aromatic rings with the smaller compounds generally being most abundant (Sephton et al., 1998).

## Amines and amides

Amines are derivatives of ammonia ($NH_3$) where hydrogen atoms are replaced by other structures. In Murchison, amine concentration is 8 ppm, amounts of individual amines decrease with increasing carbon number and structural diversity is observed with almost all amine isomers with up to five carbon atoms present (Pizzarello et al., 1994).

Two possible sources of the amines in Murchison have been proposed: they may be directly inherited from the presolar molecular cloud, an assertion supported by the detection of methylamine in interstellar space, or as with the hydroxyl acids, the amines may share a common origin with the amino acids. By simply removing the carboxylic acid group of amino acids, 16 of the 20 amines can be made, a reaction that would take place if the molecules were heated on their parent asteroid.

Amides are structurally analogous to carboxylic acids and, in Murchison, the amide equivalents of monocarboxylic acids, dicarboxylic acids, and hydroxyacids are found in concentrations greater than 70 ppm (Cooper and Cronin, 1995). The amides display complete structural diversity up to and including molecules with eight carbon atoms, a decline in abundance with carbon number, and the presence of many compounds with no terrestrial source. Cyclic amides (lactams) are less abundant (2 ppm) but they are very interesting to

investigators of the origin of life. The chemical structures of cyclic amides permit hydrogen-bonded pair formation and may have acted as parts of a primitive genetic coding apparatus, possible forerunners of the present day nucleic acids.

### Nitrogen heterocycles

Another compound class essential for terrestrial life is that of the nitrogen heterocycles. Some of these compounds are building blocks for nucleic acids that store genetic information. The possible presence of nitrogen heterocycles in water extracts of carbonaceous meteorites was first reported in the early 1960s but the initial optimism was dispelled when they turned out to be laboratory contaminants (Oró, 1963). Later work did confirm the presence of nitrogen heterocycles in meteorites such as Murchison and several classes, including purines, pyrimidines, quinolines/isoquinolines, and pyridines were found. All of the purines and pyrimidines found are biologically common and together account for 1.3 ppm in Murchison (Stoks and Schwartz, 1979, 1981). The quinolines, isoquinolines, and pyridines are structurally diverse, contain a large number of isomeric alkyl derivatives, and are present at concentrations of 7 ppm (Pizzarello et al., 2001; Stoks and Schwartz, 1982). Recent work has confirmed the presence and extraterrestrial origin of xanthine and uracil in the Murchison meteorite (Martins et al., 2008).

### Sulfur heterocycles

Murchison contains small amounts of sulfur-containing compounds such as thiophenes, benzothiophenes, dibenzothiophenes, and benzonaphthothiophenes. The abundance pattern of thiophenes in Murchison is markedly different from those in terrestrial sediments, indicating an abiotic origin for these molecules (Shimoyama and Katsumata, 2001).

### Phosphonic and sulfonic acids

Phosphorus compounds have many biological roles and play a part in cell membranes, energy transactions during metabolism, and the storage and transfer of genetic information. Sulfur compounds are also common in living systems and take part in key biochemical reactions. In Murchison, a series of alkyl phosphonic acids and alkyl sulfonic acids with up to four carbon atoms have been detected (Cooper et al., 1992). As observed for many of the other compound classes in Murchison, the sulfonic and phosphonic acids display an exponential decline in amount with increasing carbon number and exhibit complete structural diversity.

## Macromolecular materials

The solvent soluble substances are only trace components, yet they are often the focus of studies on meteorite organic matter due to their analytical amenability. Essentially, the macromolecular materials can be considered as a cross-linked agglomeration of some of the free compounds but with an overwhelming dominance of aromatic hydrocarbons. The macromolecular materials are generally assumed to be completely indigenous to their meteorite host due to their high molecular weight and immobility.

As the major organic component, the macromolecular material is key to theories of the origin of meteoritic organic matter as a whole. Hence it is interesting to consider that meteoritic organic matter is often compared with that observed in interstellar space. Some scientists believe that the molecular cloud that collapsed to form the solar system bequeathed a significant amount of interstellar organic matter, aliquots of which are preserved in primitive asteroids and the meteorites derived from them. For many years, only one- to four-ring polycyclic aromatic hydrocarbons (PAH) were commonly observed in Murchison macromolecular material breakdown products (Sephton et al., 1998), which contrasted sharply with the greater than 20-ring PAH proposed for the interstellar medium (Pendleton and Allamandola, 2002). Recently, using modern analytical techniques the meteoritic macromolecular material has yielded more information. Up to seven-ring PAH units have been liberated from the macromolecular material in Murchison and it appears that even larger entities are present in the experimental residue (Sephton et al., 2004). These discoveries partly reconcile the apparent disharmony between the meteoritic and interstellar organic inventories and point to a partly presolar origin for this abundant organic component.

## Terrestrial contamination

Although some compound classes in meteorites may contain a record that extends back to interstellar environments before the solar system formed others can be much more recent in the form of terrestrial contamination. Unusual and subtle contamination sources exist and an example is provided by data from the Orgueil carbonaceous chondrite, which has a long curation history since its fall in 1864. Terpene-related compounds have been identified in this meteorite (Watson et al., 2003) and these compounds are structurally specific, and are unlikely to be produced by abiotic reactions. Terpenes are common in essential plant oils, used extensively in cleaning products, and may have percolated their way into the porous Orgueil stones.

A more widespread type of terrestrial contaminant is provided by the long-chain aliphatic hydrocarbons (normal alkanes) in meteorites (Sephton et al., 2001). Unlike the short-chain aliphatic hydrocarbons, the normal alkanes are structurally specific with all carbon atoms arranged in a straight chain. Normal alkanes in meteorites were first detected in Orgueil and were attributed to extraterrestrial biology based on similar distributions

for molecules in the meteorite and those found in butter and marine sediments (Nagy et al., 1961). Subsequent analyses on many different meteorites led to the discovery that these compounds were present in several tens of ppm, were concentrated near to the surfaces of samples, and that they were frequently associated with other, obviously terrestrial, compounds (Oró et al., 1966). A subsequent revival in the belief that these compounds were indigenous occurred when normal alkanes were interpreted as products of an abiotic catalytic reaction called the Fischer–Tropsch synthesis (Studier et al., 1968). Modern measurements of individual normal alkanes reveal terrestrial values that are distinct from the majority of meteoritic organic matter (Sephton et al., 2001) and imply that normal alkanes are simply contributions from our terrestrial environment once the meteorite has fallen on the Earth.

## The location of organic matter in meteorites

In chondrites, organic matter is present within the fine-grained inorganic meteorite matrix, which contains evidence of alteration by liquid water on the parent asteroid. Hence, a general relationship between extraterrestrial organic matter and inorganic aqueous alteration products in carbonaceous chondrites has been recognized for some time. Recently, however, it has been discovered that the association is highly specific to a particular inorganic phase – clay minerals (Pearson et al., 2002). Clay minerals, therefore, may have trapped and concentrated organic matter in the early solar system and organic–inorganic interactions may have played a role in the assembly of increasingly complex organic entities $4.56 \times 10^9$ years ago.

## Relevance to the origin of life on Earth

With the recognition that meteorites contain many biologically useful molecules it is enlightening to consider that the amounts of organic matter extraterrestrial objects can deliver to the Earth's surface are considerable. For example, calculations indicate that comet Halley contains organic matter equivalent to approximately 10% of the current biomass of the Earth (Greenberg, 1993). A connection between life and extraterrestrial material was first proposed in the early 1960s by the biochemist Jan Oró (Oró, 1961). It was suggested that extraterrestrial objects may have seeded the early Earth with an extensive list of ingredients for use in the recipe of life. Modern theories imply that the early Earth had a nonreducing atmosphere composed mainly of carbon dioxide and nitrogen in which the in situ generation of organic matter would be rather sluggish and inefficient. Even if only a small fraction of the molecules delivered by extraterrestrial infall proved biologically relevant, they would have had a significant impact on the prebiotic chemistry of the Earth.

## Outlook

Until space missions begin to return large quantities of extraterrestrial material back to the Earth for analysis in laboratories, meteorites will remain the most accessible and most frequently studied objects to reveal the origin and evolution of the solar system. In particular, the study of carbonaceous meteorites, which contain bona fide prebiotic organic matter is likely to remain our most important means of determining how chemical evolution led to the origin of life.

## Bibliography


Bailey, J., 2001. Astronomical sources of circularly polarized light and the origin of homochirality. *Origins Life Evolution Biosphere*, **31**, 167–183.

Bland, P. A., Spurny, P., Towner, M. C., Bevan, A. W., Singleton, A. T., Bottke, W. F., Greenwood, R. C., Chesley, S. R., Shrbeny, L., Borovicka, J., Ceplecha, Z., McClafferty, T. P., Vaughan, D., Benedix, G. K., Deacon, G., Howard, K. T., Franchi, I. A., and Hough, R. M., 2009. An anomalous basaltic meteorite from the innermost main belt. *Science*, **325**, 1525–1527.

Bonner, W. A., and Rubenstein, E., 1987. Supernovae, neutron-stars and biomolecular chirality. *Biosystems*, **20**, 99–111.

Chang, S., Mack, R., and Lennon, K., 1978. Carbon chemistry of separated phases of Murchison and Allende meteorites. Lunar and Planetary Science, **9**, 157–159.

Claus, G., and Nagy, B., 1961. A microbiological examination of some carbonaceous chondrites. *Nature*, **192**, 594–596.

Cooper, G. W., and Cronin, J. R., 1995. Linear and cyclic aliphatic carboxamides of the Murchison meteorite – hydrolyzable derivatives of amino-acids and other carboxylic-acids. *Geochimica et Cosmochimica Acta*, **59**, 1003–1015.

Cooper, G., Kimmich, N., Belisle, W., Sarinana, J., Brabham, K., and Garrel, L., 2001. Carbonaceous meteorites as a source of sugar-related organic compounds for the early Earth. *Nature* **414**, 879–883.

Cooper, G. W., Onwo, W. M., and Cronin, J. R., 1992. Alkyl phosphonic-acids and sulfonic-acids in the Murchison meteorite. *Geochimica et Cosmochimica Acta*, **56**, 4109–4115.

Cooper, G. W., Thiemens, M. H., Jackson, T. L., and Chang, S., 1997. Sulfur and hydrogen isotope anomalies in meteorite sulfonic acids. *Science*, **277**, 1072–1074.

Cronin, J. R., Pizzarello, S., and Cruikshank, D. P., 1988. Organic matter in carbonaceous chondrites, planetary satellites, asteroids and comets. In Kerridge, J. F., and Matthews, M. S. (eds.), *Meteorites and the Early Solar System*. Tucson, AZ: University of Arizona Press, pp. 819–857.

Degens, E. T., and Bajor, M., 1962. Amino acids and sugars in the Bruderheim and Murray meteorite. *Naturwissenschaften*, **49**, 605–606.

Dodd, R. T., 1981. *Meteorites: A Chemical and Petralogical Synthesis*. London: Cambridge University Press, p. 386.

Engel, M. H., and Nagy, B., 1982. Distribution and enantiomeric composition of amino-acids in the Murchison meteorite. *Nature*, **296**, 837–840.

Greenberg, J. M., 1993. Physical and chemical composition of comets – from interstellar space to the Earth. In Greenburg, J. M., and Pirronello, V. (eds.), *Chemistry of Life's Origins*. Dordrecht: Kluwer, pp. 195–207.

Hayatsu, R., Anders, E., Studier, M. H., and Moore, L. P., 1975. Purines and triazines in the Murchison meteorite. *Geochimica et Cosmochimica Acta*, **39**, 471–488.

Jungclaus, G., Cronin, J. R., Moore, C. B., and Yuen, G. U., 1976a. Aliphatic amines in the Murchison meteorite. *Nature*, **261**, 126–128.
Jungclaus, G. A., Yuen, G. U., Moore, C. B., and Lawless, J. G., 1976b. Evidence for the presence of low molecular weight alcohols and carbonyl compounds in the Murchison meteorite. *Meteoritics*, **11**, 231–237.
Kaplan, I. R., Degens, E. T., and Reuter, J. H., 1963. Organic compounds in stony meteorites. *Geochimica et Cosmochimica Acta*, **27**, 805–834.
Kuan, Y.-J., Charnley, S. B., Huang, H.-C., Tseng, W.-L., and Kisiel, Z., 2003. Interstellar glycine. *The Astrophysical Journal*, **593**, 848–867.
Kvenvolden, K., Lawless, J., Pering, K., Peterson, E., Flores, J., Ponnamperuma, C., Kaplan, I. R., and Moore, C., 1970. Evidence for extra-terrestrial amino acids and hydrocarbons in the Murchison meteorite. *Nature*, **228**, 928–926.
Kvenvolden, K. A., Lawless, J. G., and Ponnamperuma, C., 1971. Nonprotein amino acids in the Murchison meteorite. *Proceedings of the National Academy of Sciences of the United States of America*, **68**, 86–490.
Lawless, J. G., and Yuen, G. U., 1979. Quantification of monocarboxylic acids in the Murchison carbonaceous meteorite. *Nature*, **282**, 396–398.
Lawless, J. G., Zeitman, B., Pereira, W. E., Summons, R. E., and Duffield, A. M., 1974. Dicarboxylic acids in the Murchison meteorite. *Nature*, **251**, 40–42.
Martins, Z., Botta, O., Fogel, M. L., Sephton, M. A., Glavin, D. P., Watson, J. S., Dworkin, J. P., Schwartz, A. W., and Ehrenfreund, P., 2008. Extraterrestrial nucleobases in the Murchison meteorite. *Earth and Planetary Science Letters*, **270**, 130–136.
Meierhenrich, U. J., Munoz Caro, G. M., Bredehoft, J. H., Jessberger, E. K., and Thiemann, W. H. P., 2004. Identification of diamino acids in the Murchison meteorite. *Proceedings of the National Academy of Sciences of the United States of America*, **101**, 9182–9186.
Mueller, G., 1953. The properties and genesis of the carbonaceous complex within the Cold Bokkeveld meteorite. *Geochimica et Cosmochimica Acta*, **4**, 1–10.
Nagy, B., Meinschein, W. G., and Hennessy, D. J., 1961. Mass spectroscopic analysis of the Orgueil meteorite; evidence for biogenic hydrocarbons. *Annals of the New York Academy of Sciences*, **93**, 25–35.
Nagy, G., Murphy, T. J., Modzeleski, V. E., Rouser, G. E., Claus, G., Hennesy, D. J., Colombo, U., and Gazzarini, F., 1964. Optical activity in saponified organic matter isolated from the interior of the Orgueil meteorite. *Nature*, **202**, 228–223.
Oró, J., 1961. Comets and the formation of biochemical compounds on the primitive Earth. *Nature*, **190**, 389–390.
Oró, J., 1963. Ultraviolet absorbing compounds reported present in the Murray meteorite. *Nature*, **197**, 756–758.
Oró, J., Nooner, D. W., Zlatkis, A., and Wisktrom, S. A., 1966. Paraffinic hydrocarbons in the Orgueil, Murray, Mokoia and other meteorites. *Life Sciences and Space Research*, **4**, 63–100.
Pearson, V. K., Sephton, M. A., Kearsley, A. T., Bland, P. A., Franchi, I. A., and Gilmour, I., 2002. Clay mineral-organic matter relationships in the early Solar System. *Meteoritics and Planetary Science*, **37**, 1829–1833.
Peltzer, E. T., and Bada, J., 1978. α-Hydroxycarboxylic acids in the Murchison meteorite. *Nature*, **272**, 443–444.
Peltzer, E. T., Bada, J. L., Schlesinger, G., and Miller, S. L., 1984. The chemical conditions on the parent body of the Murchison Meteorite; some conclusions based on amino, hydroxy and dicarboxylic acids. *Advances in Space Research*, **4**, 69–74.
Pendleton, Y. J., and Allamandola, L. J., 2002. The organic refractory material in the diffuse interstellar medium: mid-infrared spectroscopic constraints. *Astrophysical Journal Supplement Series*, **138**, 75–98.
Pering, K. L., and Ponnamperuma, C., 1971. Aromatic hydrocarbons in the Murchison meteorite. *Science*, **173**, 237–239.
Pizzarello, S., and Cronin, J. R., 2000. Non-racemic amino acids in the Murray and Murchison meteorites. *Geochimica et Cosmochimica Acta*, **64**, 329–338.
Pizzarello, S., Feng, X., Epstein, S., and Cronin, J. R., 1994. Isotopic analyses of nitrogenous compounds from the Murchison meteorite – ammonia, amines, amino-acids, and polar hydrocarbons. *Geochimica et Cosmochimica Acta*, **58**, 5579–5587.
Pizzarello, S., Huang, Y. S., Becker, L., Poreda, R. J., Nieman, R. A., Cooper, G., and Williams, M., 2001. The organic content of the Tagish Lake meteorite. *Science*, **293**, 2236–2239.
Sephton, M. A., Love, G. D., Watson, J. S., Verchovsky, A. B., Wright, I. P., Snape, C. E., and Gilmour, I., 2004. Hydropyrolysis of insoluble carbonaceous matter in the Murchison meteorite: new insights into its macromolecular structure. *Geochimica et Cosmochimica Acta*, **68**, 1385–1393.
Sephton, M. A., Pillinger, C. T., and Gilmour, I., 1998. d13C of free and macromolecular aromatic structures in the Murchison meteorite. *Geochimica et Cosmochimica Acta*, **62**, 1821–1828.
Sephton, M. A., Pillinger, C. T., and Gilmour, I., 2001. Normal alkanes in meteorites: molecular delta C-13 values indicate an origin by terrestrial contamination. *Precambrian Research*, **106**, 47–58.
Sephton, M. A., Verchovsky, A. B., Bland, P. A., Gilmour, I., Grady, M. M., and Wright, I. P., 2003. Investigating the variations in carbon and nitrogen isotopes in carbonaceous chondrites. *Geochimica et Cosmochimica Acta*, **67**, 2093–2108.
Shimoyama, A., and Katsumata, H., 2001. Polynuclear aromatic thiophenes in the Murchison carbonaceous chondrite. *Chemistry Letters*, **3**, 202–203.
Stoks, P. G., and Schwartz, A. W., 1979. Uracil in carbonaceous meteorites. *Nature*, **282**, 709–710.
Stoks, P. G., and Schwartz, A. W., 1981. Nitrogen-heterocyclic compounds in meteorites – significance and mechanisms of formation. *Geochimica et Cosmochimica Acta*, **45**, 563–569.
Stoks, P. G., and Schwartz, A. W., 1982. Basic nitrogen-heterocyclic compounds in the Murchison meteorite. *Geochimica et Cosmochimica Acta*, **46**, 309–315.
Studier, M. H., Hayatsu, R., and Anders, E., 1968. Origin of organic matter in early solar system; I, Hydrocarbons. *Geochimica et Cosmochimica Acta*, **32**, 151–173.
Watson, J. S., Pearson, V. K., Gilmour, I., and Sephton, M. A., 2003. Sesquiterpenoid derivatives in the Orgueil carbonaceous chondrite. *Organic Geochemistry*, **34**, 37–47.
Yuen, G., Blair, N., DesMarias, D. J., and Chang, S., 1984. Carbon isotope composition of low molecular weight hydrocarbons and monocarboxylic acids fron the Murchison meteorite. *Nature*, **307**, 252–254.
Yuen, G. U., and Kvenvolden, K. A., 1973. Monocarboxylic acids in Murray and Murchison carbonaceous meteorites. *Nature*, **251**, 40–42.

## Cross-references

Asteroid and Comet Impacts
Astrobiology
Cosmic Molecular Clouds
Origin of Life

## METHANE OXIDATION (AEROBIC)

Helmut Bürgmann
Eawag, Swiss Federal Institute of Aquatic Science and Technology, Kastanienbaum, Switzerland

### Synonyms

Methanotrophy

### Definition

Methane oxidation is a microbial metabolic process for energy generation and carbon assimilation from methane that is carried out by specific groups of bacteria, the methanotrophs. Methane ($CH_4$) is oxidized with molecular oxygen ($O_2$) to carbon dioxide ($CO_2$).

### Biochemical basis

Methanotrophy is the microbially mediated process of the oxidation of $CH_4$ with $O_2$ to methanol, formaldehyde, formate, and finally $CO_2$ (Figure 1) (Hanson and Hanson, 1996; Madigan et al., 2003; Bowman, 2006). The process is performed by a specialized group of *bacteria* (qv), the methanotrophs ($CH_4$ oxidizing bacteria). They are a subgroup of the methylotrophs, bacteria capable of utilizing single-carbon compounds (Bowman, 2006). Methane is both the energy source (electron donor) and the sole or partial carbon source for methanotrophs. Aerobic oxidation of methane requires specific enzymes, most importantly methane monooxygenase (MMO), which catalyzes the first step in the reaction: the oxidation of methane with molecular oxygen to methanol and water. Two forms of this enzyme are known: particulate methane monooxygenase (pMMO), which is ubiquitous in methanotrophs and contains copper, and the iron-containing soluble methane monooxygenase (sMMO) (Hanson and Hanson, 1996). The reaction mediated by MMO requires additional electrons, which are supplied by cellular redox carriers such as cytochrome C (for pMMO) or NADH (sMMO). Energy is conserved in the subsequent stepwise oxidations of methanol, formaldehyde, and formate. In these reactions, electrons are donated back to a membrane-bound electron transport chain (see Chapter *Aerobic Metabolism*) via a pyrroloquinoline quinone cofactor to cytochrome C (methanol dehydrogenase) or NAD (in formaldehyde oxidation systems and formate dehydrogenase). Electron flow through the membrane ultimately produces a proton motive force that is converted to the cellular energy carrier ATP by the ATPase enzyme complex. $O_2$ is the terminal electron acceptor (see Chapter *Aerobic Metabolism*) (Figure 1) (Madigan et al., 2003). Thus, aerobic methane oxidation can be considered a special case of aerobic

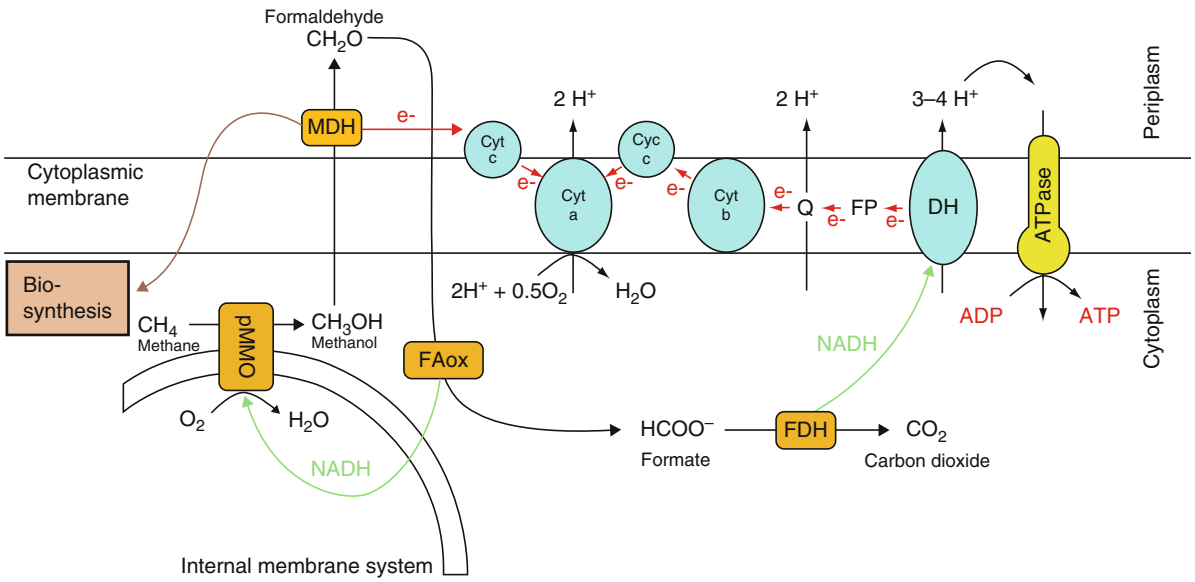


**Methane Oxidation (Aerobic), Figure 1** Pathway of aerobic methane oxidation for energy conservation and carbon assimilation in Type I and II methanotrophs. pMMO, particulate methane mononoxygenase; MDH, methanol dehydrogenase; FAox, formaldehyde oxidation system (tetrahydrofolate- or methanopterin-dependent) FDH, formate dehydrogenase. Methane is oxidized with oxygen by pMMO, a step which requires reducing equivalents (e.g., from NADH) supplied by later oxidations in the pathway. Energy is generated by shuttling electrons generated in the subsequent oxidations of methanol ($CH_3OH$), formaldehyde ($CH_2O$), and formate ($HCOO^-$) through a membrane-bound electron transport chain that creates a proton gradient across the cell membrane (proton motive force) that can be converted into ATP by ATPase (oxidative phosphorylation). Formaldehyde ($CH_2O$) is the starting point for carbon assimilation via the ribulose monophosphate or serine pathways.

respiration. Differences between methanotrophs are thought to exist regarding the enzymes used, especially with regard to formaldehyde oxidation, where different systems are known (Lidstrom, 2006).

## Methanotrophs

Most known methanotrophs fall into two well-defined phylogenetic groups belonging to the gamma- (Type I methanotrophs) and alpha-proteobacteria (Type II) that are also distinguished by morphological traits and differences in carbon assimilation (Hanson and Hanson, 1996; Madigan et al., 2003; Bowman, 2006). Both types share the characteristic extensive intracytoplasmic membrane system (ICM), which is the site of methane oxidation. However, in Type I methanotrophs, the ICM occurs as disk-shaped membrane stacks within the cell, while in Type II methanotrophs, the ICM is located around the periphery of the cell. Both groups are strict aerobes and obligate methylotrophs. The presence of soluble methane monooxygenase (sMMO) seems to be mostly limited to Type II methanotrophs (Hanson and Hanson, 1996; Bowman, 2006). Type I and II methanotrophs employ different carbon assimilation strategies, although both incorporate methane carbon at the level of formaldehyde (Figure 1). Type I methanotrophs use the ribulose monophosphate pathway and obtain all their carbon from methane. Type II methanotrophs use the serine pathway, which in addition to formaldehyde incorporation further involves fixation of one molecule of $CO_2$ per molecule of formaldehyde assimilated. The former pathway is energetically more favorable, requiring only 1/3 ATP per molecule formaldehyde fixed, instead of 1 ATP and reducing power for the serine pathway. This is in accordance with the observed higher growth rates in Type I methanotrophs (Madigan et al., 2003). Most methanotrophs can also grow using other single-carbon compounds, e.g., methanol, which is the first intermediate of methane oxidation.

Within the Type I methanotrophs, the genera *Methylosphaera*, *Methylobacter*, *Methylomicrobium*, *Methylomonas*, *Methylococcus*, and *Methylocaldum* have been described. The latter two genera are often distinguished as "type X methanotrophs," as they are phylogenetically and morphologically distinct from the other Type I genera. The cultivated type II methanotrophs belong to the genera *Methylosinus* and *Methylocystis* (Bowman, 2006). Environmental clone libraries suggest the existence of additional, yet uncultured, genera. Recently, acidophilic methanotrophs belonging to the *Verrucomicrobia* phylum have been isolated, showing for the first time that not all methanotrophs belong to the proteobacteria and that methanotrophs are phylogenetically more diverse than previously thought (Dunfield et al., 2007; Pol et al., 2007). The genome sequence of one isolate revealed the presence of pMMO genes (pmoA), but lacked homologs to known methanol monooxygenases and formaldehyde oxidation genes, indicating a methane oxidation system that deviates from those known from Type I and II methanotrophs (Dunfield et al., 2007).

## Habitats

Although current isolates require high methane partial pressures for growth, some methanotrophs can apparently utilize methane with high affinity at low partial pressures, down to atmospheric levels (Hanson and Hanson, 1996). Therefore, they are ubiquitous in soil and water. Increased populations and activity occur wherever increased methane concentrations, whether from biogenic or other sources, meet oxic conditions. Typical habitats are thus closely tied to sites with methanogenesis (see Chapters *Methane, Origin*; *Methanogens*), e.g., rice paddies, swamps, aquatic and terrestrial sediments, landfill coverings, and the oxycline of stratified water bodies (Hanson and Hanson, 1996). In stratified systems, (e.g., in stratified water bodies or sediments) aerobic methane oxidation will often be located within a relatively narrow band within the oxycline, where methanotrophs can become highly enriched. Methanotrophs also occur as endosymbionts, e.g., of marine mussels found at *cold seeps* (qv) that use methane released to supply their hosts with carbon and energy (Hanson and Hanson, 1996; Bowman, 2006).

## Methods to study aerobic methane oxidation and methanotrophs

Methane oxidation rates in environmental samples are frequently determined by incubation experiments. Samples are placed in a gas-tight container and the consumption of methane over time is determined in the headspace. Alternatively, $^{14}C$ labeled methane can be used to quantify the conversion to $CO_2$ and incorporation into the bacterial biomass. Field methods include the use of push–pull tests (Urmann et al., 2005), or modeling of rates based on methane gradients.

Methanotrophs can be cultured from almost any environment using a nitrate mineral salts medium and a $CH_4$/air atmosphere (Madigan et al., 2003; Bowman, 2006). Since they are relatively easily cultured, viable count methods can be used but will severely underestimate the actual population, due to the prevalence of viable but nonculturable cells. Since they are phylogenetically well defined, methanotrophs can be detected and quantified using ribosomal RNA as a genetic marker, e.g., using specific oligonucleotide probes (e.g., for fluorescent in-situ hybridization) or primers for polymerase chain reaction based detection (PCR) (McDonald et al., 2008). In addition, the gene sequences of functional genes, most frequently the gene encoding pMMO (pmoA), but also genes for sMMO (mmoX) and methanol dehydrogenase (mxaF), are frequently used as molecular markers for

PCR-based detection (Hanson and Hanson, 1996; Bowman, 2006, McDonald et al., 2008). A hybridization microarray was developed for rapid phylogenetic typing of PCR amplified pmoA (Bodrossy et al., 2003). Type I and II methanotrophs also contain biomarkers (see Chapter *Biomarkers (Organic, Compound-Specific Isotopes)*), e.g., specific lipids and phospholipid fatty acids that are useful in tracing community changes (Hanson and Hanson, 1996; Bowman, 2006; Schubert et al., 2006; Blumenberg et al., 2007).

## Geochemical impact

Locally, methanotrophs can be an important basis of the food web, if sufficiently large fluxes of methane are converted to biomass and passed on down the food chain. Since biogenic methane (see Chapters *Methane, Origin*; *Methanogens*) has a strongly $^{13}C$ depleted carbon isotope signature, carbon flow originating from oxidized methane can be studied using isotope measurements (see Chapter *Isotopes (Methods)*).

The primary importance of aerobic methane oxidation for the global *carbon cycle* (qv) is that it represents (together with *anaerobic methane oxidation* (qv) and photochemical methane oxidation in the atmosphere) a major sink for this radiatively active and therefore, important greenhouse gas. Globally, photochemical methane oxidation is by far the dominant process (94%), but microbial oxidation is an important factor to take into account when projecting global warming effects. Obtaining global estimates of microbial aerobic methane oxidation is not trivial due to high spatial and temporal variability and the difficulty in performing rate measurements in environments where methanogenesis and methanotrophy occur simultaneously. The total sink function of soils has been estimated at 29 Tg $year^{-1}$, with an uncertainty range of 7–100 Tg $year^{-1}$ (Smith et al., 2000). In rice paddies, methane oxidation can occur in the rhizosphere and at the soil surface, and is estimated to remove 80% of the methane produced in these systems, but there is uncertainty that $CH_4$ bypass would possibly occur through vascular plants' parenchyma. Methane oxidation rates in soil depend on various factors, e.g., soil bulk density, water content, temperature, and pH (Hanson and Hanson, 1996). The process is also often limited by the rate of methane diffusion into the oxic zone. Further, ammonium is a competing substrate for MMO that is not coupled to energy generation and therefore acts as a poison to methanotrophs at higher concentrations (Madigan et al., 2003). Thus, the methanotroph activity in soil is subject to considerable variability and sensitive to land use changes, and is one factor to be considered for mitigation strategies to reduce atmospheric methane concentrations (Hanson and Hanson, 1996).

Lakes were long considered a minor source of methane, a view that has somewhat changed based on observation of significant methane fluxes from reservoirs (St. Louis et al., 2000). In permanently or temporally stratified water bodies such as lakes, reservoirs, or the Black Sea, a large proportion of the methane is oxidized by aerobic methanotrophs in the chemocline (Schubert et al., 2006; Blumenberg et al., 2007).

While the open ocean is not considered a major source of methane, and methane oxidation activity is generally low, *cold seeps* (qv) release large amounts of methane from sediments and hydrocarbon deposits (including *gas hydrates* (qv)), creating high local fluxes of methane (see Chapter *Methane, Origin*). This creates a situation where symbiotic as well as free-living methane oxidizers are the basis of large oceanic food webs. However, in anoxic marine sediments *anaerobic methane oxidation* (qv) coupled to sulfate reduction is the most important process.

## Summary

Aerobic oxidation of methane is performed by specific bacteria, the methanotrophs, which use a specific metabolic pathway for carbon assimilation and energy generation from methane. Most known methanotrophs belong to the Proteobacteria, but recent discoveries of novel methanotroph *Verrucomicrobia* indicated that the diversity of methanotrophs is not yet fully known. Aerobic methane oxidation is one of the major sinks for the greenhouse gas methane, along with *anaerobic methane oxidation* (qv) and photochemical oxidation in the atmosphere. It is, thus, an important process for the global *carbon cycle* (qv) and an important element in the regulation of the atmospheric concentration of methane.

## Bibliography


Blumenberg, M., Seifert, R., and Michaelis, W., 2007. Aerobic methanotrophy in the oxic-anoxic transition zone of the Black Sea water column. *Organic Geochemistry*, **38**(1), 84–91.

Bodrossy, L., Stralis-Pavese, N., Murrell, J. C., Radajewski, S., Weilharter, A., and Sessitsch, A., 2003. Development and validation of a diagnostic microbial microarray for methanotrophs. *Environmental Microbiology*, **5**(7), 566–582.

Bowman, J., 2006. The methanotrophs - the families methylococcaceae and methylocystaceae. In Dworkin, M. (ed.), The Prokaryotes. New York: Springer, Vol. 5, pp. 266–289.

Dunfield, P. F., Yuryev, A., Senin, P., Smirnova, A. V., Stott, M. B., Hou, S., Ly, B., Saw, J. H., Zhou, Z., Ren, Y., Wang, J., Mountain, B. W., Crowe, M. A., Weatherby, T. M., Bodelier, P. L. E., Liesack, W., Feng, L., Wang, L., and Alam, M., 2007. Methane oxidation by an extremely acidophilic bacterium of the phylum Verrucomicrobia. *Nature*, **450**(7171), 879–882.

Hanson, R. S., and Hanson, T. E., 1996. Methanotrophic bacteria. *Microbiological Reviews*, **60**(2), 439–471.

Lidstrom, M. E., 2006. Aerobic methylotrophic prokaryotes. In Dworkin, M. (ed.), *The Prokaryotes*. New York: Springer, Vol. 2, pp. 618–634.

Madigan, M. T., Martinko, J. M., and Parker, J., 2003. *Brock Biology of Microorganisms*. Upper Saddle River, NJ: Pearson Education.

McDonald, I. R., Bodrossy, L., Chen, Y., and Murrell, C. J., 2008. Molecular ecology techniques for the study of aerobic methanotrophs. *Applied and Environmental Microbiology*, **75**(5), 1305–1315.
Pol, A., Heijmans, K., Harhangi, H. R., Tedesco, D., Jetten, M. S. M., and Op den Camp, H. J. M., 2007. Methanotrophy below pH1 by a new Verrucomicrobia species. *Nature*, **450**(7171), 874–878.
Schubert, C. J., Coolen, M. J. L., Neretin, L. N., Schippers, A., Abbas, B., Durisch-Kaiser, E., Wehrli, B., Hopmans, E. C., Damste, J. S. S., Wakeham, S., and Kuypers, M. M. M., 2006. Aerobic and anaerobic methanotrophs in the Black Sea water column. *Environmental Microbiology*, **8**(10), 1844–1856.
Smith, K. A., Dobbie, K. E., Ball, B. C., Bakken, L. R., Sitaula, B. K., Hansen, S., Brumme, R., Borken, W., Christensen, S., Prieme, A., Fowler, D., Macdonald, J. A., Skiba, U., Klemedtsson, L., Kasimir-Klemedtsson, A., Degorska, A., and Orlanski, P., 2000. Oxidation of atmospheric methane in Northern European soils, comparison with other ecosystems, and uncertainties in the global terrestrial sink. *Global Change Biology*, **6**(7), 791–803.
St. Louis, V. L., Kelly, C. A., Duchemin, E., Rudd, J. W. M., and Rosenberg, D. M., 2000. Reservoir surfaces as sources of greenhouse gases to the atmosphere: a global estimate. *BioScience*, **50**(9), 766–775.
Urmann, K., Gonzalez-Gil, G., Schroth, M. H., Hofer, M., and Zeyer, J., 2005. New field method: gas push-pull test for the in-situ quantification of microbial activities in the vadose zone. *Environmental Science & Technology*, **39**(1), 304–310.

## Cross-references

Aerobic Metabolism
Anaerobic Oxidation of Methane with Sulfate
Bacteria
Biogeochemical Cycles
Carbon Cycle
Cold Seeps
Isotopes (Methods)
Methane, Origin
Methanogens

# METHANE, ORIGIN

Carsten J. Schubert
Eawag, Swiss Federal Institute of Aquatic Science and Technology, Kastanienbaum, Switzerland

## Definition

Methane is a colorless and odorless gas, with the chemical formula $CH_4$. Due to its radiative force, it is a strong greenhouse gas and contributes to the warming of the earth. It is formed in the environment by methanogenesis. The main natural sources are wetlands and termites (30% of total emissions), while anthropogenic sources include rice fields, cattle farming, and energy production (70% of total emissions).

## General aspects

Methane is a colorless and odorless gas and the major component (97% vol.) of natural gas. Methane has a boiling point of −161°C at a pressure of one atmosphere. As a gas, it is flammable only over a narrow range of concentrations (5–15%) in air. It is mainly produced by microorganisms (methanogens) under anoxic conditions in a process called methanogenesis. These conditions exist under water-covered soils, such as rice paddies, tundra, swamps, and marshes, but also in freshwater and marine sediments. Other anoxic environments include ruminant stomachs and termite guts (see Table 1).

Methanogenesis is the final step in the anaerobic degradation of organic carbon, with methane being formed as a waste product. Methanogenesis is performed by strict anaerobes called methanogens, organisms belonging to the Archaea (a domain of life alongside Bacteria and Eukaryota). Methanogens are rather cosmopolitan in respect to environmental conditions (i.e., temperature, pH, salinity; as long as the environment is anoxic) and represent the largest and most diverse group in the Archaea domain (Megonigal et al., 2004; c.f. Boone et al., 1993). Methanogens are able to grow at temperatures between 4°C and 100°C, at pH values from 3 to 9, and at salinities ranging from brines to freshwater. Despite this huge taxonomic diversity, the substrates that can be used by methanogens are rather limited – hydrogen, acetate, formate, some alcohols, and methylated compounds (Zinder, 1993). The most important of these are hydrogen and acetate, which give rise to two different kinds of methanogenesis: (1) the fermentation of acetate to $CO_2$ and $CH_4$ and (2) the reduction of $CO_2$ with $H_2$.

Garcia et al. (2000) showed that over 70% of methanogens use the latter pathway, which is known as hydrogenotrophic methanogenesis or carbon dioxide/hydrogen reduction. Hydrogen in this reaction is used both as an energy source and electron donor, whereas $CO_2$ is the electron acceptor and the carbon source. This reaction yields the most energy of all methanogenic processes – much more than acetate fermentation, which yields the least (see Table 2). Since hydrogen occurs only in very low concentrations in natural environments, it is the limiting substrate in $CO_2/H_2$ reduction.

Only 10% of the methanogenic genera, i.e., *Methanosarcina* and *Methanosaeta*, are able to use the other pathway, called acetate fermentation or acetoclastic

**Methane, Origin, Table 1** Methane properties

| Methane properties | |
|---|---|
| Chemical formula | $CH_4$ |
| Mass | 16.0425 g/mol |
| Melting point | −182.5°C |
| Boiling point | −161.6°C |
| Solubility in water | 3.5 mg/100 ml |

methanogenesis (Garcia et al., 2000). Despite its limited taxonomic distribution, most likely related to the small amount of energy gained from this process (see Table 2), acetate fermentation seems to be the dominant pathway for methane production in the environment.

## Isotopic composition

One of the diagnostic features of methane often used in microbiological, geological, and biogeochemical investigations is its carbon and, to a lesser extent, hydrogen isotopic composition. Due to its biogenic or thermogenic formation, the $^{13}C$ composition is strongly depleted (i.e., more negative values, see Equation 1).

$$\delta^{13}C = (({}^{13}C/{}^{12}C \text{ sample})/({}^{13}C/{}^{12}C \text{standard}) - 1) \times 1,000 \text{ vs. VPDB} \quad (1)$$

(Vienna Pee Dee Belemnite)

**Methane, Origin, Table 2** Reaction and standard changes in Gibbs free energies for methanogenesis (Adapted from Garcia et al., 2000)

| Reaction | $\Delta G^{\circ`}$ (kJ/mol $CH_4$) |
|---|---|
| $4H_2 + CO_2 \rightarrow CH_4 + 2H_2O$ | −135.6 |
| $4\text{Formate} \rightarrow CH_4 + 3CO_2 + 2H_2O$ | −130.1 |
| $2\text{Ethanol} + CO_2 \rightarrow CH_4 + 2\text{Acetate}$ | −116.3 |
| $\text{Methanol} + H_2 \rightarrow CH_4 + 2H_2O$ | −112.5 |
| $4\text{Methylamine} + 2H_2O \rightarrow 3CH_4 + CO_2 + 4NH_4^+$ | −75.0 |
| $4\ 2\text{-Propanol} + CO_2 \rightarrow CH_4 + 4\text{Acetone} + 2H_2O$ | −36.5 |
| $\text{Acetate} \rightarrow CH_4 + CO_2$ | −31.0 |

This is related to a kinetic isotope effect where $^{12}C$ carbon is preferentially used by microorganisms when methane is formed (Whiticar, 1999). This isotopic effect is not as pronounced in the case of methane formed by heating, or with higher pressures during gas formation from a source rock. In Figure 1, mean values of carbon isotopic compositions are shown for various organic and inorganic materials. Whereas carbonates formed in seawater have values around 0‰ VPDB, and atmospheric carbon dioxide shows a global value of around −8‰ VPDB, methane shows highly depleted values between −25‰ and −110‰ VPDB. This significant feature (sometimes in combination with hydrogen isotopes) has been used in numerous studies to reveal, for instance, the origin of methane (Whiticar et al., 1986) or methane oxidation processes in old carbonate rocks, sediments, or water columns of lakes and oceans (Boetius et al., 2000; Peckmann and Thiel, 2004; Schubert et al., 2006). Not only can the formation process (i.e., biological or thermodynamically controlled) be derived, but also changes that occur during its usage and transformation, and therefore the origin/source of methane be determined. Whenever microorganisms use methane as an energy or food source, they preferentially take up the light $^{12}C$ carbon. This leads to very light carbon isotopic compositions of, for instance, the cellular lipid structure, as can be seen in the process of anaerobic methane oxidation (see Chapter *Anaerobic Oxidation of Methane with Sulfate*). In contrast, the remaining methane will be enriched in $^{13}C$, leading to the heavy isotopic values of, for instance, methane in water columns or sediments. Fractionation factors – the relation between the isotopic composition of the original methane and the methane after transformation – provide a tool for quantifying the amount of methane that has reacted.

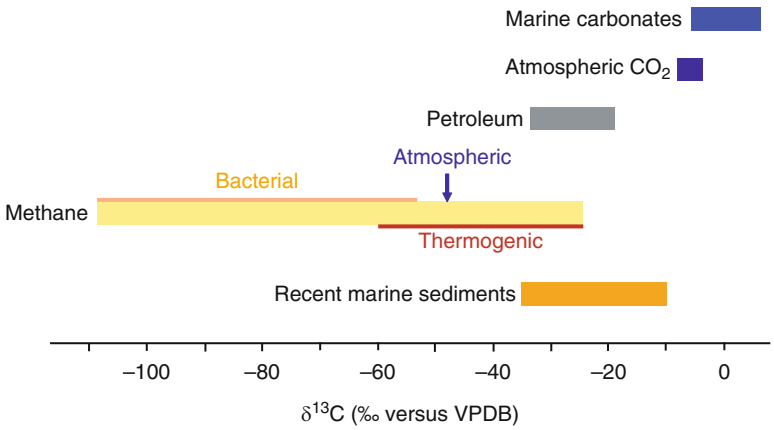


**Methane, Origin, Figure 1** Carbon isotopic composition of various organic and inorganic materials, and recent marine sediments. Note that methane has the widest range of all compounds. Atmospheric methane has a global carbon isotopic value of about −47‰ versus VPDB.

Fractionation factors are also important during methane formation. Whiticar et al. (1986) showed that different microbial formation processes, such as carbon dioxide reduction or fermentation, lead to different isotopic compositions of the methane formed. This is related to the bonds that need to be broken during the methane formation process.

Whereas during acetate fermentation (Equation 2) the methyl group stays intact and therefore only a small overall isotopic fractionation occurs, during hydrogenotrophic methanogenesis (Equation 3) the bond between the oxygen and carbon of the carbon dioxide has to be broken, leading to a much bigger isotope effect.

$$CH_3COOH \rightarrow CH_4 + CO_2 \quad (2)$$

$$CO_2 + 4H_2 \rightarrow CH_4 + 2H_2O \quad (3)$$

The $\delta^{13}CH_4$ from different sources/environments covers a fairly wide range due to variations in methanogenic substrates and mechanisms (Tyler, 1991). Additionally, fractionation associated with oxidation leads to a rather wide $\delta^{13}C$ range. In general, $CH_4$ from geological or thermogenic sources is isotopically heavier (−30‰ to −50‰ VPDB) than that from biological sources (−40‰ to −80‰ VPDB). Also, the $CH_4$ produced by decomposition of either C3 or C4 plant material leads to a distinctive isotopic composition, since the original material is formed via different photosynthesis systems known to fractionate carbon in a different way.

Atmospheric methane has a relatively stable carbon isotopic value globally – around −47‰ VPDB (see compilation in Stevens and Wahlen, 2000).

## Relevance as a greenhouse gas

Methane is the shortest hydrocarbon and the most abundant organic compound in the atmosphere. Due to its ability to absorb on the infrared band, it is a potent greenhouse gas. Taking into account its residence time in the atmosphere (about 10 years), its concentration, and its specific absorbance wavelength, it is about 23 times more potent as a greenhouse gas than $CO_2$ (IPCC, 2001).

Methane mixing ratios in the atmosphere have doubled over the last 200 years, increasing by about 1% per year from 1978 and reaching a value of 1.7 ppm in 1990 (Figure 2a). Since then, the yearly increase has slowed down and values of 1.8 ppm are measured today (Figure 2b).

During the past 15 years, the annual growth rate of tropospheric methane has shown striking changes over 2- to 3-year periods, varying from +1% $year^{-1}$ to slightly negative values (−0.2% $year^{-1}$). These fluctuations are superimposed on an overall slowdown of the $CH_4$ growth rate since the 1980s. The general reduction in atmospheric methane growth seems to be related not to a change in source strength, but to source stabilization and the methane budget approaching a steady state (Dlugokencky et al., 2003).

## Methane sinks

The strongest sink for methane is oxidation by OH radicals in the troposphere (Badr et al., 1992). Approximately, 94% of methane is lost due to oxidation here and in the stratosphere. Due to photochemical reactions, the above-mentioned reaction produces $H_2O$, CO, and $CO_2$, and hence influences concentrations of ozone, hydroxyl radicals, and CO in the troposphere. Another sink term that needs to be taken into account is soils, in which approximately 6% of methane is oxidized by methanotrophic bacteria.

Recently, the focus has been on oxidation processes that take place in aquatic systems. So far, these have not been included in the source/sink budgets, presumably since none of the methane reaches the atmosphere. However, it is mentioned here as it is an important sink that prevents methane from reaching the atmosphere, and therefore from acting as a greenhouse gas. In aquatic systems, two main processes lead to a loss of methane. One is oxidation by methanotrophic bacteria under oxic conditions in the uppermost sediments and overlying water column (see Chapter *Anaerobic Oxidation of Methane with Sulfate*). The other possibility, and probably the major pathway, is oxidation by methanotrophic archaea under anoxic conditions in deeper sediments and water columns lacking oxygen (see Chapter *Anaerobic Oxidation of Methane with Sulfate*). These two main degradation processes largely restrict the emission or ebullition (transport by bubbles) of methane to the atmosphere from aquatic systems. Normally, 95–99% of the methane found in deeper sediments is oxidized either directly in the sediments or later in the water column and does not, therefore, reach the atmosphere.

## Methane sources

In general, methane sources can be divided into abiotic (20%) and biogenic sources (80%). Abiotic sources include fossil carbon sources, such as coal mining, industrial waste treatment, and combustion processes (e.g., aircraft and automobile exhausts), as well as sea floor and volcanic emissions. Biomass burning during deforestation and for heating purposes also falls into this category. However, most methane is produced by biological processes: the major sources are freshwater wetlands and rice paddies, but ruminants and the guts of termites are also important contributors.

The total methane budget may also be divided into emissions from natural or anthropogenic sources (Figure 3). The major sources are discussed in detail below. In considering the various contributors, it should always be borne in mind that estimates for individual sources still vary widely, although ongoing research is seeking to constrain the budget (c.f. Table 7.6 in Denman et al., 2007).

### Wetlands

Wetlands, covering about $5.3 \times 10^{12}$ $m^2$ globally (Matthews and Fung, 1987), are one of the most important

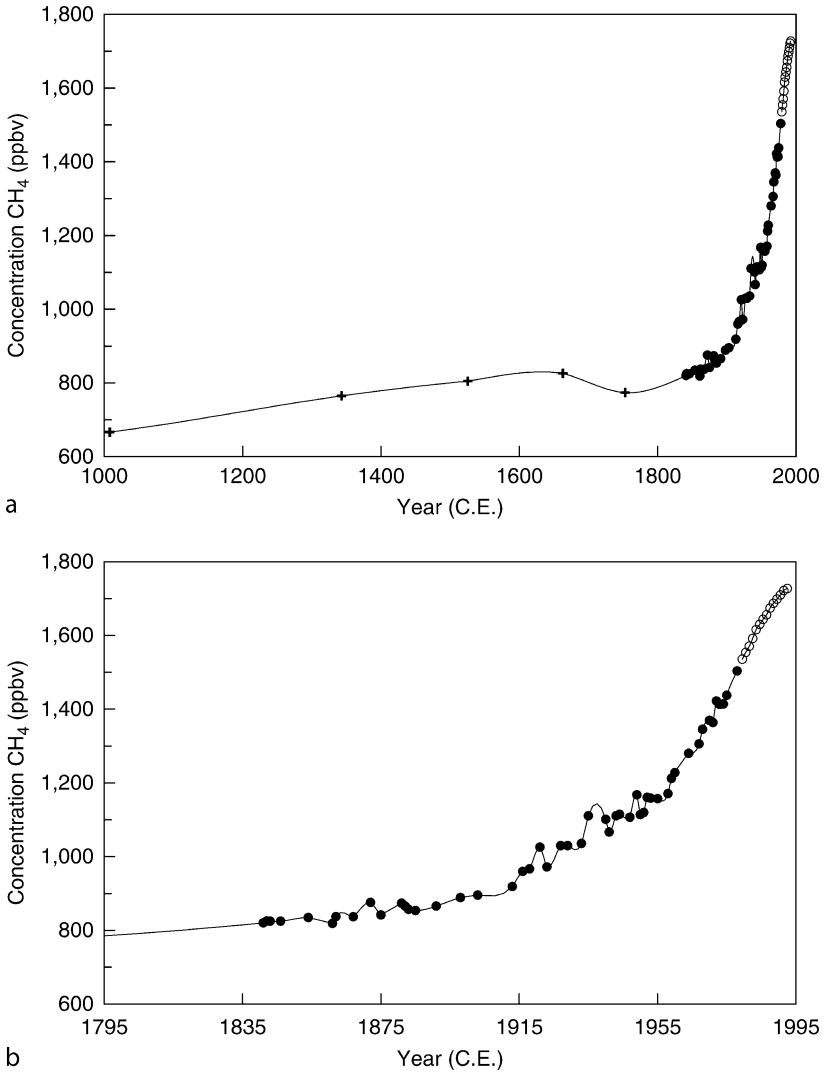


**Methane, Origin, Figure 2** Methane mixing ratios over the last 1,000 years (**a**) and over only the last century (**b**) (adapted from Khalil, 2000). Data from Rasmussen and Khalil (1984) and Etheridge (1992). It is evident from the data obtained from ice cores that the drastic increase only started 200 years ago. During the last 20 years, a slowdown in methane concentrations in the atmosphere is visible.

natural sources of atmospheric methane, with an estimated contribution of 115 Tg $year^{-1}$ (Cicerone and Oremland, 1988). Peat-rich bogs in the northern hemisphere (50−70°N) were mentioned in particular, accounting for 60% of total wetland methane emissions, with tropical and subtropical swamps releasing only 25% of the total (Matthews and Fung, 1987; Fung et al., 1991). The rest was attributed to fens, marshes, and floodplains. However, the high level of emissions from northern wetlands (based on only a few methane emission measurements) was later scaled down, using a process-based methane emission model (Cao et al., 1996). In northern wetlands, according to this publication, $CH_4$ flux rates per square meter are low (40 mg $CH_4$ $m^{-2}day^{-1}$), but the area of wetland is large. Therefore, northern wetlands and moist/dry tundra together contribute 25% to global emissions. The second term includes temperate wetlands with a higher mean flux rate (150 mg $CH_4$ $m^{-2}day^{-1}$) but a much smaller area, leading to a contribution of 19%. Since tropical wetlands – mainly swamps – have an even higher mean daily flux (199 mg $CH_4$ $m^{-2}$), they account for 56% of total wetland emissions despite covering a much smaller area than northern wetlands.

The carbon isotopic composition of methane emitted from wetlands varies from −86‰ to −31‰ VBDP (compilation by Bréas et al., 2001). This rather wide range is, of course, a function of the formation process (methanogenesis by acetate fermentation or $CO_2/H_2$

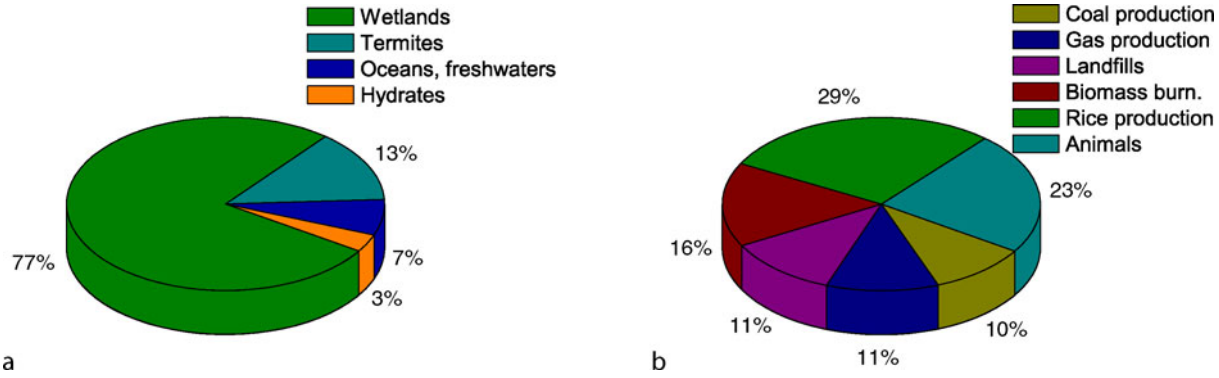


**Methane, Origin, Figure 3** Net emissions of methane stemming from natural (**a**) and anthropogenic sources (**b**). Numbers have been taken from Scenario 7 of Fung et al. (1991). The drastic variations from one study to another are attributable to the wide ranges of emission estimates (for instance, wetland emission estimates vary from 100 to 230 Tg $CH_4$ $year^{-1}$), and freshwater emissions (see below) have yet to be accounted for.

reduction), the original degradation material forming the substrate for methanogenesis (C3 or C4 plants), and more or less strong methane oxidation, leaving behind isotopically heavy methane.

## Termites

Termites feed on all kinds of food, including wood, grass, leaf litter, and agricultural crops. It is very difficult to estimate the amount of methane produced anaerobically in the guts of termites, since it is highly variable between species and colonies. The total amount, mainly produced in tropical savannahs and forests, is estimated at 20 Tg $CH_4$ $year^{-1}$.

The carbon isotopic composition of methane emitted from termites varies from −73‰ to −44‰ VBDP (Tyler et al., 1988). Interestingly, the $\delta^{13}CH_4$ of termite-emitted methane is independent of diet.

## Rice fields

Rice is cultivated either on dry land, from which no methane is emitted, or – in the case of about 80% of global cultivation – on irrigated fields, leading to high methane emissions. Rice is cultivated between 50°N and 50°S on an area of $1.3 \times 10^6$ $km^2$, mostly situated in Asia (90%) (Bréas et al., 2001).

Globally, methane emissions from rice fields are second to those from wetlands and represent the highest anthropogenic budget term (100 Tg $CH_4$ $year^{-1}$). On rice fields, a methane release rate between 0.4 and 0.8 g $m^{-2}$ $day^{-1}$ has been observed (Holzapfel-Pschorn and Seiler, 1986). Methane in rice fields is produced by methanogens which find an ideal environment in flooded soils, i.e., high organic carbon loads and anoxic conditions. The amount of methane produced has been shown to be influenced by several factors, such as soil properties, amount and type of fertilizer, irrigation, etc. The carbon isotopic composition of methane emitted from rice fields also varies widely due to the same variables as found in wetlands and lies between −50‰ and −68‰ VBDP (compilation in Bréas et al., 2001).

## Enteric fermentation in animals

Methane is formed in the rumen of animals as a by-product of carbohydrate chain (e.g., cellulose) degradation. During digestion, ingested macromolecules are broken down into smaller molecules by enzymes. Subsequently, the fermentation of, for example, glucose leads to even smaller molecules, such as acetate, butyrate, $H_2$ and $CO_2$, etc. The $H_2$ produced, together with $CO_2$, is then immediately used by methanogens to form methane.

Global methane emissions mainly from cattle, buffalo, and sheep range between 65 and 100 Tg $CH_4$ $year^{-1}$ (Cicerone and Oremland, 1988) and are therefore comparable to rice cultivation and wetland emissions.

## Biomass burning

Whereas the burning of biomass mainly produces $CO_2$, the subsequent smoldering phase – involving compounds with low combustion efficiency – mainly produces methane. About 85% of methane emissions related to biomass burning stem from tropical areas due to deforestation and fuel wood use. It is estimated that biomass burning accounts for 8–10% (i.e., 40–55 Tg $CH_4$ $year^{-1}$) of total methane emissions (Cicerone and Oremland, 1988; Hein et al., 1997).

## Mining, gas drilling, natural geological sources

During coal mining and gas drilling, methane is produced not by biological processes but from catagenesis of coal or maturation of petroleum and subsequently released into the atmosphere. Cicerone and Oremland (1988) and

Fung et al. (1991) estimated these emissions to be in the order of 75 Tg $CH_4$ $year^{-1}$.

Recently, Kvenvolden and Rogers (2005) estimated the amount of methane emitted from natural geological sources, i.e., not related to petroleum production or mining, to be in the order of 45 Tg $CH_4$ $year^{-1}$. Those geological sources include natural macro- and micro-seeps, mud volcanoes, and other miscellaneous sources such as gas hydrates, magmatic volcanoes, geothermal regions, and mid-ocean ridges.

## Landfills

Globally, methane emitted from landfills following the breakdown of organic material via methanogenesis is estimated to contribute about 43 Tg $CH_4$ $year^{-1}$ (Hein et al., 1997).

## Oceanic emissions

Methane production in the ocean is found basically in two different environments: (1) in anoxic microenvironments of surface waters, e.g., in fish intestines, plankton samples, marine snow, and fecal pellets and (2) in anoxic sediments due to the breakdown of organic material. The first of these is also known as the "Ocean Methane Paradox," since methane production would not be possible normally in oxic ocean water and is therefore restricted to these microenvironments. Although only relatively small amounts of methane are formed by this mechanism, leading to supersaturation of surface waters, the huge area of the oceans is responsible for making this term globally significant. Methane produced in sediments might be released into the water column by diffusion or by methane seeps and vents, or it might be locked up in gas hydrates (see below).

Methane emissions from the various kinds of seeps that occur in the oceans – in shelf regions, slopes, or deep ocean locations – are estimated to be between 1 and 65 Tg $CH_4$ $year^{-1}$ (see compilation in Judd et al., 2002). The best investigated regions in this respect are the Santa Barbara Basin, where at Coal Oil Point an emission of 28 g $CH_4$ $m^{-2}$ $year^{-1}$ was estimated (Hornafius et al., 1999), and the Black Sea, where more than 2,000 seeps were detected in the area west of the Crimean Peninsula alone. The yearly atmospheric methane contribution from seeps in the Black Sea is estimated to range between 0.03 and 0.15 Tg (Dimitrov, 2002).

Since most of the methane from seeps or sediments is oxidized by either aerobic or anaerobic processes in the sediments or in the water column, total oceanic emissions today are estimated to be in the order of 10 Tg $year^{-1}$ (Cicerone and Oremland, 1988; Fung et al., 1991). It has to be taken into account that for methane released into the water column in the form of bubbles, the contribution to the atmosphere may be much higher, depending on the water depth. However, when bubbles travel through the water column, they exchange methane with the ambient water; consequently, most of the gas in the bubbles at the water surface is composed of nitrogen rather than methane (McGinnis et al., 2005).

## Gas hydrates

Gas hydrates are nonstoichiometric solid structures composed of ice-like minerals that form at low temperatures and high pressures in the deep sea or at low temperatures in permafrost regions. They can be thought of as a hydrogen-bonded water framework called a host lattice that traps guest molecules (typically gases). In general, three types of gas hydrates can be distinguished based on the structure in which they crystallize. These are structure I, structure II, and structure H (which occurs more rarely). Hydrates contain gases such as hydrocarbons (including methane, hydrogen sulfide, and carbon dioxide) that glue themselves inside symmetrical cages of water molecules to form hydrate crystals (mainly found in type I structures). Smaller molecules, such as argon, krypton, and nitrogen, are found in smaller cages related to structure II.

Gas hydrates or clathrates are known to occur mainly on continental margins all over the world at depths of around 600 – 3,000 m, depending on the prevailing temperature gradient (see Figure 4). Since pipelines of offshore drilling platforms are also located in these depths, clogging of pipes due to the formation of gas hydrates is a well-recognized problem.

Gas hydrates are confined to the top few hundred meters of marine sediments. They are stable when the temperature is at or below the value $T_3(P)$ for a three-phase equilibrium between clathrate, liquid water, and methane gas (Buffett and Archer, 2004). Experimental determinations of $T_3(P)$ are shown in Figure 4 as a function of depth, assuming a hydrostatic increase in pressure. Superimposed on this figure is a schematic illustration of the temperature profile through the ocean and sediments. The zone of stability is limited by the intersection of the local temperature profile with $T_3(P)$, although clathrate is confined to the sediments because the concentration of methane in the ocean is too low to form clathrate and, even if it did form, the buoyancy of clathrate in seawater would carry it out of the stability zone. Clathrate is unlikely to form below water depths of less than 600 m (except in the cold Arctic Ocean) because the bottom water is too warm for stability. As the depth of the water increases, and the temperature of the seafloor decreases, the zone of stability becomes thicker and capable of accommodating larger volumes of clathrate.

It must be understood that gas hydrates are by no means stable: these structures dynamically trap methane from, or release methane into, the ocean. This feature led Hovland and Judd (1988) to conclude that slides and craters on ocean shelves might be related to rapid hydrate decomposition.

Going back in time, gas hydrates have even been claimed to be responsible for larger environmental

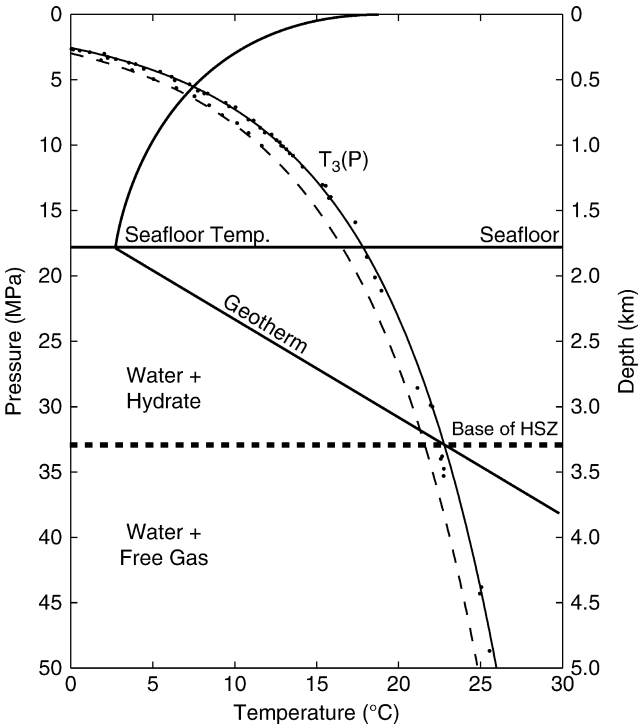


**Methane, Origin, Figure 4** Schematic illustration of temperature through the ocean and uppermost marine sediments (Buffett and Archer, 2004). The temperature for clathrate stability, T3(P), increases with pressure (or depth). Experimental data for T3(P) in pure water (dashed line) and seawater (solid line) are extrapolated using a thermodynamic model (Sloan, 1998). The base of the stability zone is defined by the intersection of the geotherm with T3(P).

catastrophes. Based on light carbon isotopic excursions in the late Paleocene (50 million years ago), Dickens et al. (1995) suggested that methane from gas hydrates might have been released into the atmosphere, leading to significant warming (4°C) during that time.

One of the main features used to find gas hydrates on ocean margins today is the bottom-simulating reflector, which shows up using seismological methods. This is formed by the base of solid gas hydrate and free gas accumulating below in the sediments.

It has been estimated that the amount of carbon (and therefore, energy) stored in gas hydrates (10,000 Gt C) is at least twice as great as in all known oil, gas, and coal fields combined (Kvenvolden and Lorensen, 2001). This would be equal to 2,000 times the atmospheric methane inventory. However, recent estimates have brought the abundance of gas hydrates down from $1 \times 10^{17}$–$10^{18}$ $m^3$ to $(1–5) \times 10^{15}$ $m^3$, also reducing the energy stored in gas hydrates globally to 500–2,500 Gt C (Milkov et al., 2004). Buffett and Archer (2004) estimated that about 3,000 Gt C occurs in clathrate and 1,800 Gt C in methane bubbles. Estimates of the amount of gas hydrate-related methane actually emitted into the atmosphere reach 5 Tg $CH_4$ $year^{-1}$ (Wuebbles and Hayhoe, 2002).

## Freshwater emissions

Recently, freshwater environments, including lakes and reservoirs for hydropower production, have become the focus of attention not only for $CO_2$, but also for methane emissions. Lakes kept in a natural state or with only minor influence by humans undergo normal aerobic degradation of organic material and mainly emit $CO_2$. However, when organic material production is high, natural lakes also turn anoxic either in the water column or in the sediments and release methane due to anaerobic degradation, i.e., methanogenesis. This occurs even more rapidly in systems that are highly eutrophicated, e.g., due to intensive agriculture or effluents from sewage treatment plants.

In contrast, reservoirs are normally man-made. By damming rivers, huge areas are flooded and the water is stored for energy production. If the flooded area is a forest, peatland, or grassland, then – instead of being a sink for $CO_2$ due to photosynthesis – this area will become a source of greenhouse gases due to anaerobic decomposition of the submerged organic material. For example, in the boreal region of Canada, flooded peatlands represent a worst-case scenario, since they possess a large store of organic carbon held in peat, which can decompose and return to the atmosphere as greenhouse gases over a long period (Kelly et al., 1997). It makes a difference to the emission rate whether an area has only been flooded recently or was flooded decades ago. A newly formed reservoir will emit methane at a much higher rate, since fresh organic material is rapidly degraded. In contrast, reservoirs which are already tens of years old show lower methane emissions, since the older and more refractory organic material is harder to degrade.

Due to recent plans to trade or tax carbon dioxide emissions, "green" hydropower is under debate and it is therefore necessary to define the related $CO_2$ and methane emissions.

In a compilation (Table 1 in St. Louis et al., 2000), methane fluxes from temperate reservoirs varied from 1 to 260 mg $m^{-2}$ $day^{-1}$. Tropical reservoirs showed even higher fluxes, evolving from higher productivities, of 2–3,800 mg $m^{-2}$ $day^{-1}$ (St. Louis et al., 2000). Average fluxes were 20 mg $m^{-2}$ $day^{-1}$ $CH_4$ for temperate and 300 mg $m^{-2}$ $day^{-1}$ $CH_4$ for tropical reservoirs. Taking an area of $0.9 \times 10^6$ $km^2$ for temperate and $0.6 \times 10^6$ $km^2$ for tropical reservoirs, a global flux of 70 Tg can be estimated (St. Louis et al., 2000).

Emissions from natural lake systems have been recently evaluated by Bastviken et al. (2004). In these systems, three different pathways for methane emission are described: (1) ebullition, i.e., emission through bubbles, (2) diffusive flux, which mainly depends on surface methane concentrations and wind speed over surface waters, and (3) storage, i.e., methane released during lake

turnover. On average, these various pathways contribute 62%, 31%, and 7% to total emissions, respectively.

Using different regression equations for surface $CH_4$ concentrations, ebullition, diffusive flux, and storage, together with data on lake area and lake numbers (Kalff, 2002), Bastviken et al. (2004) estimated methane emissions from lakes on a global basis. When compared to global nonanthropogenic emission values from Wuebbles and Hayhoe (2002), the estimated lake emissions of 8–48 Tg $CH_4$ $year^{-1}$ represent 6–16% or 2–10% of total emissions.

Taking the two systems (natural lakes and reservoirs) together results in global methane emissions between 78 and 118 Tg $year^{-1}$. These figures are similar to emissions from wetlands, the largest natural contributor, and much higher than estimated oceanic emissions. Although these estimates might be on the high side, they clearly show that emissions from freshwaters have to be included in global methane budgets.

## Summary

Methane is the end product of organic matter degradation under anoxic conditions. In freshwater environments methanogenesis is the main pathway due to the low sulfate concentrations, whereas in the marine environment methogenesis becomes important only after sulfate, as an electron acceptor, has been used up completely. Methane is formed by microorganisms belonging to the Archaea known as methanogens. Methanogens are able to grow at temperatures between 4°C and 100°C, at pH values from 3 to 9, and at salinities ranging from brines to freshwater. Despite this huge taxonomic diversity, the substrates that can be used by methanogens are rather limited – hydrogen, acetate, formate, some alcohols, and methylated compounds. The two main pathways described in nature are hydrogenotrophic methanogenesis (also known as carbon dioxide/hydrogen reduction) which is mainly found in marine environments and acetate fermentation (acetoclastic methanogenesis) which is more dominant in freshwater environments. These two processes can be distinguished from each other by measurements of the carbon or hydrogen isotopic composition of the formed methane, since the fractionation factors between substrate ($CO_2$ or acetate) and methane vary.

Methane is a potent greenhouse gas, ranking second after carbon dioxide as a contributor to global warming. Its concentration has doubled over the past 200 years, although the increase has slowed down over the past 20 years which is thought to be related to source stabilization and the methane budget approaching a steady state.

The main sources of natural emissions are wetlands, termites, and aquatic systems, making up 30% of total global emissions, while the main anthropogenic sources, such as rice paddies, ruminants, energy production, and landfills, account for 70%. Gas hydrates occurring on continental slopes and permafrost regions also store high amounts of methane; however, most of this methane is oxidized to carbon dioxide before it reaches the atmosphere. Recently, lakes and especially reservoirs have been identified to be major contributors to the global methane budget questioning of hydropower as a "green energy" source.

The main sinks for methane are oxidation with OH in the troposphere (accounting for more than 90%), loss in the stratosphere, and oxidation by methanotrophs in soils.

## Bibliography


Badr, O., Probert, S. D., and Ocallaghan, P. W., 1992. Sinks for atmospheric methane. *Applied Energy*, **41**(2), 137–147.

Bastviken, D., Cole, J., Pace, M., and Tranvik, L., 2004. Methane emissions from lakes: dependence of lake characteristics, two regional assessments, and a global estimate. *Global Biogeochemical Cycles*, **18**(4), 1–12.

Boetius, A., Ravenschlag, K., Schubert, C. J., Rickert, D., Widdel, F., Gieseke, A., Amann, R., Jørgensen, B. B., Witte, U., and Pfannkuche, O., 2000. A marine microbial consortium apparently mediating anaerobic oxidation of methane. *Nature*, **407**, 623–626.

Boone, D. R., Whitmann, W. B., and Rouvičre, P., 1993. Diversity and taxonomy of methanogens. In Jerry, J. G. (ed.), *Methanogenesis: Ecology, Physiology, Biochemistry and Genetics*. New York: Chapman Hall, pp. 35–80.

Bréas, O., Guillou, C., Reniero, F., and Wada, E., 2001. Review, the global methane cycle: isotopes and mixing ratios, sources and sinks. *Isotopes in Environmental and Health Studies*, **37**, 257–379.

Buffett, B., and Archer, D., 2004. Global inventory of methane clathrate: sensitivity to changes in the deep ocean. *Earth and Planetary Science Letters*, **227**(3–4), 185–199.

Cao, M. K., Marshall, S., and Gregson, K., 1996. Global carbon exchange and methane emissions from natural wetlands: application of a process-based model. *Journal of Geophysical Research-Atmospheres*, **101**(D9), 14399–14414.

Cicerone, R. J., and Oremland, R. S., 1988. Biogeochemical aspects of atmospheric methane. *Global Biogeochemical Cycles*, **2**(4), 299–327.

Denman, K. L. et al., 2007. Couplings between changes in the climate system and biogeochemistry. In Solomon, S. et al. (eds.), *Climate Change 2007: The Physical Science Basis. Contribution of Working Group I to the Fourth Assessment Report of the Intergovernmental Panel on Climate Change*. Cambridge, UK: Cambridge University Press.

Dickens, G. R., Oneil, J. R., Rea, D. K., and Owen, R. M., 1995. Dissociation of oceanic methane hydrate as a cause of the carbon-isotope excursion at the end of the paleocene. *Paleoceanography*, **10**(6), 965–971.

Dimitrov, L., 2002. Contribution to atmospheric methane by natural seepages on the Bulgarian continental shelf. *Continental Shelf Research*, **22**(16), 2429–2442.

Dlugokencky, E. J. et al., 2003. Atmospheric methane levels off: temporary pause or a new steady-state? *Geophysical Research Letters*, **30**(19).

Etheridge, D. M., Pearman, G. I., and Fraser, P. J., 1992. Changes in tropospheric methane between 1841 and 1978 from a high accumulation-rate Antarctic ice core. *Tellus Series B*, **44**, 282–294.

Fung, I. et al., 1991. 3-dimensional model synthesis of the global methane cycle. *Journal of Geophysical Research-Atmospheres*, **96**(D7), 13033–13065.

Garcia, J. L., Patel, B. K. C., and Ollivier, B., 2000. Taxonomic phylogenetic and ecological diversity of methanogenic Archaea. *Anaerobe*, **6**(4), 205–226.

Hein, R., Crutzen, P. J., and Heimann, M., 1997. An inverse modeling approach to investigate the global atmospheric methane cycle. *Global Biogeochemical Cycles*, **11**(1), 43–76.
Holzapfel-Pschorn, A., and Seiler, W., 1986. Methane emission during a cultivation period from an Italian rice paddy. *Journal of Geophysical Research-Atmospheres*, **91**(D11), 1803–1814.
Hornafius, J. S., Quigley, D., and Luyendyk, B. P., 1999. The world's most spectacular marine hydrocarbon seeps (Coal Oil Point, Santa Barbara Channel, California): quantification of emissions. *Journal of Geophysical Research-Oceans*, **104**(C9), 20703–20711.
Hovland, M., and Judd, A. G., 1988. *Seabed Pockmarks and Seepages: Impact on Geology, Biology and the Marine Environment*. London: Graham and Trotman.
IPCC, 2001. Climate change 2001: the scientific basis. In Houghton, J. T., Ding, Y., Griggs, D. J., Noguer, M., van der Linden, P. J., Dai, X., Maskell, K., and Johnson, C.A. (eds.), *Contribution of Working Group I to the Third Assessment Report of the Intergovernmental Panel on Climate Change*. Cambridge, UK: Cambridge University Press, 881 p.
Judd, A. G., Hovland, M., Dimitrov, L. I., Garcia Gil, S., and Jukes, V., 2002. The geological methane budget at continental margins and its influence on climate change. *Geofluids*, **2**(2), 109–126.
Kalff, J. 2001. Limnology: Inland water ecosystems. Prentice Hall, 592 p.
Kelly, C. A. et al., 1997. Increases in fluxes of greenhouse gases and methyl mercury following flooding of an experimental reservoir. *Environmental Science & Technology*, **31**(5), 1334–1344.
Khalil, M. A. K., 2000. Atmospheric methane: an introduction. In Khalil, M.A.K. (ed.), *Atmospheric Methane*. Berlin, Heidelberg: Springer, pp. 1–8.
Kvenvolden, K. A., and Lorensen, T. D., 2001. The global occurrence of natural gas hydrate. In Paull, C. K., and Dillon, W. D. (eds), *Natural Gas Hydrates: Occurrence, Distribution and Detection*. Geophysical Monograph. Washington, DC: American Geophysical Union.
Kvenvolden, K. A., and Rogers, B. W., 2005. Gaia's breath - global methane exhalations. *Marine and Petroleum Geology*, **22**(4), 579–590.
McGinnis, D. F., Wüest, A., Schubert, C. J., Klauser, L., Lorke, A., and Kipfer, R., 2005. Upward flux of methane in the Black Sea: does it reach the atmosphere? In Lee, J. H. W., and Lam, K. M. (eds.), *Environmental Hydraulics and Sustainable Water Management*. London: Taylor & Francis Group, pp. 423–429.
Matthews, E., and Fung, I., 1987. Methane emission from natural wetlands: global distribution, area, and environmental characteristics of sources. *Global Biogeochemical Cycles*, **1**(1), 61–86.
Megonigal, J. P., Hines, M. E., and Visscher, P. T., 2004. Anaerobic metabolism: linkages to trace gases and aerobic processes. In Schlesinger, W. H. (ed.), *Biogeochemistry.* Oxford: Elsevier-Pergamon, pp. 317–424.
Milkov, A. V., 2004. Global estimates of hydrate-bound gas in marine sediments: how much is really out there? *Earth-Science Reviews*, **66**(3–4), 183–97.
Peckmann, J., and Thiel, V., 2004. Carbon cycling at ancient methane-seeps. *Chemical Geology*, **205**(3–4), 443–467.
Rasmussen, R. A., and Khalil, M. A. K., 1984. Atmospheric methane in the recent and ancient atmospheres: concentrations, trends, and interhemispheric gradient. *Journal of Geophysical Research*, **89**, 11599–11605.
Schubert, C. J. et al., 2006. Aerobic and anaerobic methanotrophs in the Black Sea water column. *Environmental Microbiology*, **8**(10), 1844–1856.
St. Louis, V. L., Kelly, C. A., Duchemin, E., Rudd, J. W. M., and Rosenberg, D. M., 2000. Reservoir surfaces as sources of greenhouse gases to the atmosphere: a global estimate. *Bioscience*, **50**(9), 766–775.
Sloan, E. D., 1998. *Clathrate Hydrates of Natural Gas*, New York: Marcel Dekker.
Stevens, C. M., and Wahlen, M., 2000. The isotopic composition of atmospheric methane and its sources. In Khalil, M. A. K. (ed.), *Atmospheric Methane*. Berlin, Heidelberg: Springer, pp. 25–41.
Tyler, S. C. et al, 1988. Measurements and interpretation of $\delta^{13}C$ of methane from termites, rice paddies, and wetlands in Kenya. *Global Biogeochemical Cycles*, **2**(4), 341–355.
Tyler, S. C., 1991. The global methane budget. In Rogers, J. E., and Whitman, W. B. (eds.), *Microbial Production and Consumption of Greenhouse Gases: Methane, Nitrogen Oxides, and Halomethanes*. Washington, DC: American Society for Microbiology, pp. 7–38.
Whiticar, M. J., 1999. Carbon and hydrogen isotope systematics of bacterial formation and oxidation of methane. *Chemical Geology*, **161**, 219–314.
Whiticar, M. J., Faber, E., and Schoell, M., 1986. Biogenic methane formation in marine and freshwater environments: CO2 reduction vs. acetate fermentation - Isotope evidence. *Geochimica et Cosmochimica Acta*, **50**, 693–709.
Wuebbles, D. J., and Hayhoe, K., 2002. Atmospheric methane and global change. *Earth-Science Reviews*, **57**(3–4), 177–210.
Zinder, S. H., 1993. Physiological ecology of methanogens. In Jerry, J. G., (ed.), *Methanogenesis: Ecology, Physiology, Biochemistry and Genetics*, New York: Chapman Hall, pp. 128–206.

## Cross-references

Anaerobic Oxidation of Methane with Sulfate
Archaea
Bacteria
Cap Carbonates
Carbonates
Cold Seeps
Methane Oxidation (Aerobic)

# METHANOGENS

Please refer to "*Methane, Origin*" and "*Archaea*."

# MICROBIAL BIOMINERALIZATION

Christine Heim
University of Göttingen, Göttingen, Germany

## Synonyms

Microbial biomineral formation

## Definition

Microbial biomineralization describes the formation and deposition of minerals directly mediated or indirectly influenced by microorganisms (Mann, 2001; Weiner and Dove, 2003; Ehrlich, 1999). A huge variety of minerals results from individual biomineralization pathways linked to the phylogeny and metabolic activity of the microorganisms involved (Weiner and Dove, 2003;

Minsky et al., 2002). Moreover, microbial biominerals may differ distinctly from their inorganically formed equivalents in shape, size, crystallinity, isotopic, and trace element composition (Bazylinski et al., 2007; Haferburg and Kothe, 2007; Takahashi et al., 2007; Weiner and Dove, 2003). A compilation of microbial biominerals and their source organisms is given in Table 1.

Two principal modes of microbial biomineralization processes occur, namely biologically induced mineralization (BIM) and biologically controlled mineralization (BCM, Lowenstam, 1981; Lowenstam and Weiner, 1989). These modes are introduced in the following.

## Biologically induced mineralization (BIM)

In BIM, the nucleation and growth of biominerals are extracellular processes triggered by the metabolic activity of the microorganism. Biomineralization takes place because of the changes in the chemical equilibrium of the surrounding environment and may also be linked to

**Microbial Biomineralization, Table 1** Overview of minerals formed by microbial biomineralization and the organism(s) involved

| Chemical formula | Mineral name | Involved microorganism | References |
|---|---|---|---|
| $Fe(OH)_3$ (approx.) | Ferric/iron oxyhydroxide | Fe-oxidizing bacteria | Chan et al. (2009) and Yoshida et al. (2008) |
| $2Fe(OH)_3 \bullet Fe(OH)_2$ (approx.) | Green rust | *Shewanella putrefaciens* | Kukkadapu et al. (2004) and O'Loughlin (2008) |
| α-FeO(OH) | Goethite | *Gallionella ferruginea* | Hallberg and Ferris (2004) |
| γ-FeO(OH) | Lepidocrocite | Marine bacteriophage, *Bacillus subtilis* | Daughney et al. (2004) and Châtellier et al. (2001) |
| $5Fe_2O_3 \bullet 9H_2O$ | Ferrihydrite | *Gallionella ferruginea*, *Leptothrix ochracea*, *Bacillus subtilis* | Hallberg and Ferris (2004) and Kennedy et al. (2004) |
| $Fe_2O_3$ | Hematite | *Gallionella ferruginea* | Hallberg and Ferris (2004) |
| $Fe_3O_4$ | Magnetite | *Shewanella putrefaciens*, (Fe(III)-reducing bacteria), magnetotactic bacteria (e.g., *Magnetospirillum magnetotacticum*), SRB (e.g., *Desulfovibrio magneticus*), thermophilic iron-reducing bacteria | Frankel et al. (1983), Lovley et al. (1987), Lovley (1991), Bazylinski et al. (1993), Zhang et al. (1997), Zhang et al. (1998), Kukkadapu et al. (2004), Bazylinski et al. (2007) and Faivre and Schüler (2008) |
| γ-$Fe_2O_3$ | Maghemite | *Actinobacter* sp., thermophilic iron-reducing bacteria | Zhang et al. (1997) and Bharde et al. (2008) |
| $FeCO_3$ | Siderite | *Shewanella alga*, thermophilic iron-reducing bacteria | Zhang et al. (1997) and Parmar et al. (2000) |
| $FePO_4 \bullet nH_2O$ | Hydrous ferric phosphate | *Acidovorax* sp. | Miot et al. (2009) |
| $Fe_3(PO_4)_2 \bullet 2H_2O$ | Vivianite | *Shewanella putrefaciens*, *Desulfovibrio alaskensis* (SRB), *Alkaliphilus metalliredigens* | Kukkadapu et al. (2004), Zegeye et al. (2007), and Roh et al. (2007) |
| FeS | Cubic FeS (Sphalerite-type) | Magnetotactic bacteria | Pósfai et al. (1998a, b) |
| FeS | Mackinawite (tetragonal FeS) | Magnetotactic bacteria, *Desulfovibrio desulfuricans* | Pósfai et al. (1998a, b) and Ivarson and Hallberg (1976) |
| $Fe_3S_4$ | Greigite | Magnetotactic bacteria, *Actinobacter* sp., SRB | Bharde et al. (2008), Farina et al. (1990), Mann et al. (1990), Heywood et al. (1990), Reitner et al. (2005), and Faivre and Schüler (2008) |
| $Fe_{1-x}S$ | Pyrrhotite | Magnetotactic bacteria | Farina et al. (1990) |
| $FeS_2$ | Pyrite | Magnetotactic bacteria, SRB | Mann et al. (1990), Bazylinski (1996), Folk (2005), Wilkin and Barnes (1997), and Donald and Southam (1999) |
| $KFe_3(SO_4)_2(OH)_6$ | Jarosite | *Sulfobacillus thermosulfidooxidans*, *Acidithiobacillus ferrooxidans*, *Thiobacillus ferrooxidans* | Ding et al. (2007), Daoud and Karamanev (2006), and Ivarson and Hallberg (1976) |
| $Fe_8O_8SO_4(OH)_6$ | Schwertmanite | *Acidithiobacillus ferrooxidans* | Egal et al. (2009) |
| $MnCO_3$ | Rhodochrosite | *Leptothrix discophora* | Zhang et al. (2002) |
| $MnO_2$ | Manganese oxides | *Pseudomonas putida*, *Leptothrix discophora*, *Bacillus* sp. | Tebo et al. (2004), Villalobos et al. (2003), and Brouwers et al. (2000) |
| $Na_4Mn_{14}O_{27} \bullet 9H_2O$ | Birnessite | *Pseudomonas putida* | Villalobos et al. (2003) |
| $S^0$ | Elemental sulfur | *Chromatiaceae*, *Beggiatoa* spp., *Thiothrix*, *Thiovulum*, *Thioploca* | Brune (1989), Brune (1995), Smith and Strohl (1991), Strohl et al. (1981) and Pasteris et al. (2001) |

**Microbial Biomineralization, Table 1** (Continued)

| Chemical formula | Mineral name | Involved microorganism | References |
|---|---|---|---|
| $Au^0$ | Elemental gold | *Bacillus* sp., *Rhodopseudomonas capsulate*, *Shewanella algae*, SRB | Reith et al. (2009), He et al. (2007), Konishi et al. (2007), Konishi et al. (2006), and Lengke and Southam (2006) |
| $CaCO_3$ | Calcite | Communities of SRB and archaea, cyanobacteria, soil bacteria (*Bacillus megaterium*), Algae (e.g., *Halimeda*, *Emiliana huxleyi*) | Boetius et al. (2000), Reitner et al. (2005), Thompson and Ferris (1990), Lian et al. (2006), and de Vrind-de Jong and de Vrind (1997) |
| | Aragonite | Cyanobacteria (*Synechococcus leopoliensis*), *Nesterenkonia halobia*, *Halomonas eurihalina* | Obst et al. (2009) and Rivadeneyra et al. (1998, 2000) |
| | Vaterite | *Kocuria*, *Myxococcus Xanthus*, *Bacillus sphaericus* | Zamarreño et al. (2009), and Rodriguez-Navarro et al. (2007) |
| $CaMg(CO_3)_2$ | Dolomite | *Nesterenkonia halobia* | Rivadeneyra et al. (2000) |
| $SiO_2 \bullet nH_2O$ | Amorphous silica | *Calothrix*, *Fischerella* sp., *Shewanella oneidensis* | Benning et al. (2004), Konhauser et al. (2001), and Furukawa and O'Reilly (2007) |
| $SiO_2$ | Silica | Diatoms, radiolarians, *Thiobacillus*, *Bacillus subtilis* | de Vrind-de Jong and de Vrind (1997), Fortin and Beveridge (1997), and Urrutia and Beveridge (1993) |
| $Ca_5(PO_4)_3(OH)$ | Hydroxyapatite/ calcium phosphate | *Ramlibacter tataouinensis*, *Corynebacterium matruchotii*, *Streptococcus mutans*, *Streptococcus sanguis* | Benzerara et al. (2004), Van Dijk et al. (1998), and Streckfuss et al. (1974) |
| $MgNH_4PO_4 \bullet 6H_2O$ | Struvite | *Myxococcus xanthus*, *Pseudomonas*, *Flavobacterium*, *Acinetobacter*, *Yersinia*, *Corynebacterium*, *Azotobacter* | Da Silva et al. (2000) and Rivadeneyra et al. (1983) |

For comprehensive reading, the following books are recommended: Sigel et al. (2008), Baeuerlein (2000), Banfield and Nealson (1997), Dove et al. (2003), Driessens and Verbeeck (1990), Lovely (2000), Lowenstam and Weiner (1989).

particular metabolic products. The resulting biominerals typically show a poor crystallinity, are chemically heterogeneous, and often closely associated with the cell wall (Frankel and Bazylinski, 2003). An active and a passive mineralization process can be distinguished (Fortin and Beveridge, 2000; Southam, 2000). Active mineralization refers to mineralization by (a) the direct redox conversion of specific metal ions bound to the bacterial surface or (b) the excretion of metabolically produced ions and thereby forming minerals. The term passive mineralization is used when *nonspecific* binding of cations and the involvement of surrounding anions causes nucleation and growth of minerals. Passive mineralization can even be mediated by dead cells, due to the exposure of negatively charged surfaces acting as nucleation sites for metal cations (Urrutia and Beveridge, 1993). Particularly in BIM, extracellular polymeric substances (EPS) are involved in the mineralization process (Chan et al., 2009; Ercole et al., 2007). As an example of BIM, the precipitation of iron oxyhydroxides by the iron oxidizing bacterium *Gallionella ferruginea* is displayed in Figure 1.

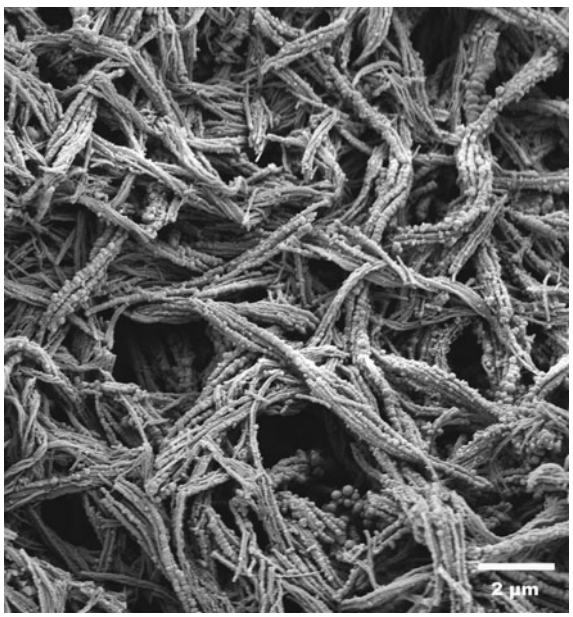


**Microbial Biomineralization, Figure 1** Stalk-shaped extracellular polymeric substances (EPS) produced by the iron oxidizing bacterium *Gallionella ferruginea* are heavily encrusted with iron oxyhydroxide minerals formed by biologically induced mineralization (BIM).

## Biologically controlled mineralization (BCM)

BCM implies that the organism actively controls the nucleation site, growth, morphology, and final location of the mineral (Banfield and Nealson 1997; Bazylinski

and Frankel, 2003). Although the modes of exerting crystallochemical control over the mineralization process may greatly vary across species, the common characteristic of BCM is that mineral formation takes place in a closed, isolated environment. While Weiner and Dove (2003) categorized BCM in *extra-*, *inter-* or *intracellular* mineralization, Mann (2001) differentiated between two key modes of BCM, namely *matrix-mediated* mineralization and *boundary-organized* mineralization. Generally speaking, extracellular mineralization corresponds to matrix-mediated mineralization, whereas inter- and intracellular mineral formation are equivalent to boundary-organized mineralization.

*Extracellular* BCM implies the production of a macromolecular matrix outside the cell. This matrix is typically composed of proteins, polysaccharides, or glycoproteins, forming a three dimensional framework, and the cell actively supplies cations to the matrix for an "on-site" nucleation and growth of the biomineral (Weiner and Dove, 2003).

*Intercellular* BCM occurs mostly in single-celled organisms, existing in a community. This type of mineral formation is not common in bacteria, but is commonly found in calcareous algae, for example, *Halimeda* (de Vrind-de Jong and de Vrind, 1997; Borowitzka, 1982).

*Intracellular* BCM takes place inside specific compartments within the cell, for instance vesicles or vacuoles. Thus, the organism is able to exactly regulate the chemical composition, morphological structure, and particle size of the mineral. The only bacteria known to perform intracellular BCM are magnetotactic bacteria, which use a vacuole-based system for the crystallization of magnetic biominerals (Table 1). Similar systems of intracellular BCM are only known from higher eukaryotic organisms, controlling for example, the bone and teeth formation in mammals (Kirschvink and Hagadorn, 2000). An example of microbial biominerals formed by intracellular BCM is shown in Figure 2.

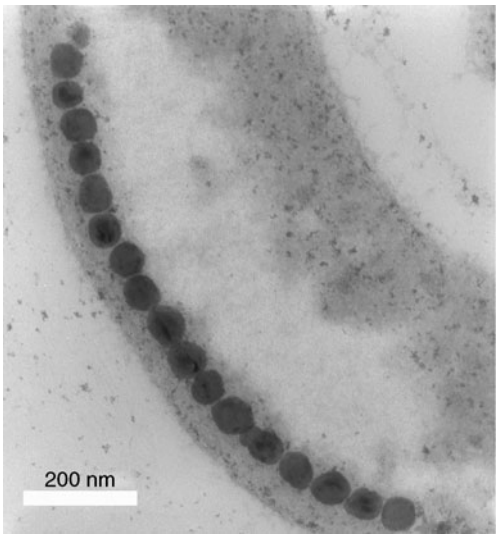


**Microbial Biomineralization, Figure 2** Intracellular iron sulfide (greigite, $Fe_3S_4$) crystals formed by biologically controlled mineralization (BCM) within a magnetotactic bacterium. (Image courtesy of Joachim Reitner.)

## Bibliography


Baeuerlein, E., 2000. *Biomineralization: From Biology to Biotechnology and Medical Application*. Weinheim: Wiley-VCH Verlag GmbH, 316 p.

Banfield, J. F., and Nealson, K. H., (eds.), 1997. *Geomicrobiology: Interactions Between Microbes and Minerals*. *Reviews in Mineralogy*, Ribbe, P. H. (series ed.). Washington, DC: Mineralogical Society of America. Vol. 35, 448 p.

Bazylinski, D. A., 1996. Controlled biomineralization of magnetic minerals by Magnetotactic bacteria. *Chemical Geology*, **132**, 191–198.

Bazylinski, D. A., and Frankel, R. B., 2003. Biologically controlled mineralization in prokaryotes. In Dove, P. M., De Yoreo, J. J., and Weiner, S. (eds.), Rosso, J. J. (series ed.), *Biomineralization. Reviews in Mineralogy and Geochemistry*. Washington DC, USA: Mineralogical Society of America and Geochemical Society, Vol. 54, pp. 217–247.

Bazylinski, D. A., Frankel, R. B., and Konhauser, K. O., 2007. Modes of biomineralization of magnetite by microbes. *Geomicrobiology Journal*, **24**, 465–475.

Bazylinski, D. A., Heywood, B. R., Mann, S., and Frankel, R. B., 1993. $Fe_3O_4$ and $Fe_3S_4$ in a bacterium. *Nature*, **366**, 218.

Benning, L. G., Phoenix, V. R., Yee, N., and Tobin, M. J., 2004. Molecular characterization of cyanobacterial silification using synchrotron infrared micro-spectroscopy. *Geochimica et Cosmochimica Acta*, **68**(4), 729–741.

Benzerara, K., Menguy, N., Guyot, F., Skouri, F., de Luca, G., Barakat, M., and Heulin, T., 2004. Biologically controlled precipitation of calcium phosphate by *Ramlibacter tataouinensis*. *Earth and Planetary Science Letters*, **228**, 439–449.

Bharde, A. A., Paraikh, R. Y., Baidakova, M., Jouen, S., Hannoyer, B., Enoki, T., Prasad, B. L. V., Shouche, Y. S., Ogale, S., and Sastry, M., 2008. Bacteria-mediated precursor-dependent biosynthesis of superparamagnetic iron oxide and iron sulfide nanoparticles. *Langmuir*, **24**, 5787–5794.

Boetius, A., Ravenschlag, K., Schubert, C. J., Rickert, D., Widdel, F., Gieseke, A., Amann, R., Jørgensen, B. B., Witte, U., and Pfannkuche, O., 2000. A marine microbial consortium apparently mediating anaerobic oxidation of methane. *Nature*, **407**, 623–626.

Borowitzka, M. A., 1982. Morphological and cytological aspects of algal calcification. *International Review of Cytology*, **74**, 127–162.

Brouwers, G. J., Vijgenboom, E., Corstjens, P. L. A. M., De Vrind, J. P. M., and De Vrind-De Jong, E. W., 2000. Bacterial $Mn^{2+}$ oxidizing systems and multicopper oxidases: an overview of mechanisms and functions. *Geomicrobiology Journal*, **17**, 1–24.

Brune, D. C., 1989. Sulfur oxidation by phototrophic bacteria. *Biochimica et Biophysica Acta*, **975**, 189–221.

Brune, D. C., 1995. Isolation and characterization of sulfur globule proteins from *Chromatium vinosum* and *Thiocapsa roseopersicina*. *Archives of Microbiology*, **163**, 391–399.

Chan, C. S., Fakra, S. C., Edwards, D. C., Emerson, D., and Banfiled, J. F., 2009. Iron oxyhydroxide mineralization of microbial extracellular polysaccharides. *Geochimica et Cosmochimica Acta*, **73**(13), 3807–3818.

Châtellier, X., Fortin, D., West, M. M., Leppard, G. G., and Ferris, F. G., 2001. Effect of the presence of bacterial surfaces during the synthesis of Fe oxides by oxidation of ferrous ions. *European Journal of Mineralogy*, **13**(4), 705–714.

Da Silva, S., Bernet, N., Delgenès, J. P., and Moletta, R., 2000. Effect of culture conditions on the formation of struvite by *Myxococcus Xanthus*. *Chemosphere*, **40**, 1289–1296.

Daoud, J., and Karamanev, D., 2006. Formation of jarosite during $Fe^{2+}$ oxidation by *Acidithiobacillus ferrooxidans*. *Minerals Engineering*, **19**(9), 960–967.

Daughney, C. D., Châtellier, X., Chan, A., Kenward, P., Fortin, D., Suttle, C. A., and Fowl, D., 2004. Adsorption and precipitation of iron from seawater by a marine bacteriophage (PWH3a-P1). *Marine Chemistry*, **91**, 101–115.

de Vrind-de Jong, E. W., and de Vrind, J. P. M., 1997. Algal deposition of carbonates and silicates. In Banfield, J. F., and Nealson, K. H. (eds.), *Geomicrobiology: Interactions between Microbes and Minerals. Reviews in Mineralogy.* Washington, DC: Mineralogical Society of America, Vol. 35, pp. 267–307.

Ding, J.-N., Gao, J., Wu, X.-l., Zhang, C.-G., and Qiu, G.-Z., 2007. Jarosite-type precipitates mediated by YN22, *Sulfobacillus thermosulfidooxidans*, an their influences on strain. *Transactions of Nonferrous Metals*. *Society of China*, **17**(5), 1038–1044.

Donald, R., and Southam, G., 1999. Low temperature anaerobic bacterial diagensis of ferrous monosulfide to pyrite. *Geochimica et Cosmochimica Acta*, **63**(13/14), 2019–2023.

Dove, P. M., De Yoreo, J. J., and Weiner, S., (eds.), 2003. *Biomineralization. Reviews in Mineralogy and Geochemistry*, Rosso, J. J. (series ed.). Washington DC, USA: Mineralogical Society of America and Geochemical Society, Vol. 54, 381 p.

Driessens, F. C. M., and Verbeeck, R. K., 1990. *Biominerals*. Boca Raton, Florida: CRC Press, 440 p.

Egal, M., Casiot, C., Morin, G., Parmentier, M., Bruneel, O., Lebrun, S., and Elbaz-Poulichet, F., 2009. Kinetic control on the formation of tooeleite, schwertmannite and jarosite by *Acidithiobacillus ferrooxidans* stains in an As(III)-rich acid mine water. *Chemical Geology*, **265**(3–4), 432–441.

Ehrlich, H. L., 1999. Microbes as geologic agents: their role in mineral formation. *Geomicrobiology Journal*, **16**, 135–153.

Ercole, C., Cacchio, P., Botta, A. L., Centi, V., and Lepidi, A., 2007. Bacterially induced mineralization of calcium carboante: the role of exopolysaccharides and capsular polysaccharides. *Microscopy and Microanalysis*, **13**, 42–50.

Faivre, D., and Schüler, D., 2008. Magnetotactic bacteria and magnetosoms. *Chemical Reviews*, **108**, 4875–4898.

Farina, M., Esquivel, D. M. S., and Lins de Barros, H. G. P., 1990. Magnetic iron-sulphur crystals from magnetotactic microorganism. *Nature*, **343**, 256–258.

Folk, R. L., 2005. Nannobacteria and the formation of framboidal pyrite: textural evidence. *Journal of Earth System Science*, **114**(3), 369–374.

Fortin, D., and Beveridge, T. J., 1997. Role of the bacterium *Thiobacillus* in the formation of silicates in acidic mine tailings. *Chemical Geology*, **141**, 235–250.

Fortin, D., and Beveridge, T. J., 2000. Mechanistic routes to biomineral surface development. In Bäuerlein, E. (ed.), *Biomineralization: From Biology to Biotechnology and Medical Application*. Weinheim: Wiley-VCH GmbH, pp. 7–24.

Frankel, R. B., and Bazylinski, D. A., 2003. Biologically induced mineralization by bacteria. In Dove, P. M., De Yoreo, J. J., and Weiner, S. (eds.), Rosso, J. J. (series ed.), *Biomineralization. Reviews in Mineralogy and Geochemistry.* Washington, DC: Mineralogical Society of America and Geochemical Society, Vol. 54, pp. 95–114.

Frankel, R. B., Papaefthymiou, G. C., Blakemore, R. P., and O' Brien, W., 1983. $Fe_3O_4$ precipitation in Magnetotactic bacteria. *Biochimica et Biophysica Acta*, **763**, 147–159.

Furukawa, Y., and O'Reilly, S. E., 2007. Rapid precipitation of amorphous silica in experimental systems with nontronite (Nau-1) and *Shewanella oneidensis* MR-1. *Geochimica et Cosmochimica Acta*, **71**(2), 363–377.

Haferburg, G., and Kothe, E., 2007. Microbes and metals: interactions in the environment. *Journal of Basic Microbiology*, **47**, 453–467.

Hallberg, R., and Ferris, F. G., 2004. Biomineralization by Gallionella. *Geomicrobiology Journal*, **21**, 325–330.

He, S., Gui, Z., Zhang, Y., Zhang, S., Wang, J., and Gu, N., 2007. Biosynthesis of gold nanoparticles using the bacteria *Rhodopseudomonas capsulata*. *Material Letters*, **61**(18), 3984–3987.

Heywood, B. R., Bazylinski, D. A., Garratt-Reed, A., Mann, S., and Frankel, R. B., 1990. Controlled biosynthesis of greigite ($Fe_3S_4$) in magnetotactic bacteria. *Naturwissenschaften*, **77**, 536–538.

Ivarson, K. C., and Hallberg, R. O., 1976. Formation of mackinawite by the microbial reduction of jarosite and its application to tidal sediments. *Geoderma*, **16**, 1–7.

Kennedy, C. B., Scott, S. D., and Ferris, F. G., 2004. Hydrothermal phase stabilization of 2-line ferrihydrite by bacteria. *Chemical Geology*, **212**, 269–277.

Kirschvink, J. L., and Hagadorn, J. W., 2000. 10 a Grand unified theory of Biomineralization. In Bäuerlein, E. (ed.), *The Biomineralisation of Nano- and Microstructures*. Weinheim: Wiley-VCH GmbH, pp. 139–150.

Konhauser, K. O., Phoenix, V. R., Bottrell, S. H., Adams, D. G., and Head, I. M., 2001. Microbial-silica interactions in Iclandic hot spring sinter: possible analogues for some Precambrian siliceous stromatolites. *Sedimentology*, **48**, 415–433.

Konishi, Y., Tsukiyama, T., Ohno, K., Saitoh, N., Nomura, T., and Nagamine, S., 2006. Intracellular recovery of gold by microbial reduction of $AuCl_4^-$ ions using the anaerobic bacterium *Shewanella algae*. *Hydrometallurgy*, **81**(1), 24–29.

Konishi, Y., Tsukiyama, T., Tachimi, T., Saitoh, N., Nomura, T., and Nagamine, S., 2007. Microbial deposition of gold nanoparticles by the metal-reducing bacterium Shewanella algae. *Electrochimica Acta*, **53**(1), 186–192.

Kukkadapu, R. K., Zachara, J. M., Fredrickson, J. K., and Kennedy, D. W., 2004. Biotransformation of two-line silica-ferrihydrite by dissimilatory Fe(III)-reducing bacterium: formation of carbonate green rust in the presence of phosphate. *Geochimica et Cosmochimica Acta*, **68**(13), 2799–2814.

Lengke, M., and Southam, G., 2006. Bioaccumulation of gold by sulfate-reducing bacteria cultured in the presence of gold(I)-thiosulfate complex. *Geochimica et Cosmochimica Acta*, **70**, 3646–3661.

Lian, B., Hu, Q., Chen, J., Ji, J., and Teng, H. H., 2006. Carbonate biomineralization induced by soil bacterium *Bacillus megaterium*. *Geochimica et Cosmochimica Acta*, **704**, 5522–5535.

Lovely, D. (ed.), 2000. *Environmental Microbe-Metal Interactions*. Washington, DC: ASM Press, 395 p.

Lovley, D. R., 1991. Dissimilatory Fe(III) and Mn(IV) reduction. *Microbiology Reviews*, **55**, 259–287.

Lovley, D. R., Stolz, J. F., Nord, Jr. G. L., and Phillips, E. J. P., 1987. Anaerobic production of magnetite by a dissimilatory iron-reducing microorganism. *Nature*, **330**, 252–254.

Lowenstam, H. A., 1981. Minerals formed by organisms. *Science*, **211**, 1126–1131.

Lowenstam, H. A., and Weiner, S., 1989. *On Biomineralization*. New York: Oxford University Press, 324 p.

Mann, S., 2001. *Biomineralization: Principles and Concepts in Bioinorganic Materials Chemistry*. In Compton, R. G., Davies, S. G., and Evans, J. (eds.), *Oxford Chemistry Masters Vol. 5*. New York: Oxford University Press, 216 p.

Mann, S., Sparks, N. H. C., Frankel, R. B., Bazylinski, D. A., and Jannasch, H. W., 1990. Biomineralization of ferrimagnetic greigite ($Fe_3S_4$) and iron pyrite ($FeS_2$) in a Magnetotactic bacterium. *Nature*, **343**, 258–261.

Minsky, A., Shimoni, E., and Frenkel-Krispin, D., 2002. Stress, order and survival. *Nature Reviews Molecular Cell Biology*, **3**, 50–60.

Miot, J., Benzerara, K., Morin, G., Kappler, A., Bernard, S., Obst, M., Férard, C., Skouri-Panet, F., Guigner, J.-M., Posth, N., Galvez, M., Brown, Jr. G. E., and Guyot, F., 2009. Iron biomineralization by anaerobic neutrophilic iron-oxidizing bacteria. *Geochimica et Cosmochimica Acta*, **73**(3), 696–711.

Obst, M., Dynes, J. J., Lawrence, J. R., Swerhone, G. D. W., Benterara, K., Kaznatcheev, K., Tyliszczak, T., and Hitchcock, A. P., 2009. Precipitation of amorphous $CaCO_3$ (aragonite-like) by cyanobacteria: a STXM study of the influence of EPS on the nucleation process. *Geochimica et Cosmochimica Acta*, **73**(14), 4180–4198.

O'Loughlin, E. J., 2008. Effects of electron transfer mediators on the bioreduction of Lepidocrocite (γ-FeOOH) by *Shewanella putrefaciens* CN32. *Environmental Science and Technology*, **42**(18), 6876–6882.

Parmar, N., Warren, L. A., Roden, E. E., and Ferris, F. G., 2000. Soild phase capture of strontium by the iron reducing bacteria *Shewanella alga* strain BRY. *Chemical Geology*, **169**, 281–288.

Pasteris, J. D., Freeman, J. J., Goffredi, S. K., and Buck, K. R., 2001. *Chemical Geology*, **180**, 3–18.

Pósfai, M., Buseck, P. R., Bazylinski, D. A., and Frankel, R. B., 1998a. Reaction sequence of iron sulfide minerals in bacteria and their use as biomarkers. *Science*, **280**, 880–883.

Pósfai, M., Buseck, P. R., Bazylinski, D. A., and Frankel, R. B., 1998b. Iron sulfides from magnetotactic bacteria: structure, compositions, and phase transitions. *American Mineralogist*, **83**, 1469–1481.

Reith, F., Wakelin, S. A., Gregg, A. L., and Schmidt-Mumm, A., 2009. A microbial pathway for the formation of gold-anoumalous calcrete. *Chemical Geology*, **258**(3–4), 315–326.

Reitner, J., Peckmann, J., Blumenberg, M., Michaelis, W., Reimer, A., and Thiel, V., 2005. Concretionary methane-seep carbonates and associated microbial communities in Black Sea sediments. *Palaeogegraphy, Palaeoclimatology, Palaeoecology*, **227**, 18–30.

Rivadeneyra, M. A., Delgado, G., Ramos-Cormenzana, A., and Delgado, R., 1998. Biomineralization of carbonates by *Halomonas eurihalina* in solid and liquid media with different salinities: crystal formation sequence. *Research in Microbiology*, **149**, 277–287.

Rivadeneyra, M. A., Delgado, G., Soriano, M., Ramos-Cormenzana, A., and Delgado, R., 2000. Precipitation of carbonates by *Nesterenkonia halobia* in liquid media. *Chemosphere*, **41**, 617–624.

Rivadeneyra, M. A., Ramos-Cormenzana, A., and García-Cervigon, A., 1983. Bacterial formation of struvite. *Geomicrobiology Journal*, **3**, 151–163.

Rodriguez-Navarro, C., Jiminez-Lopez, C., Rodriguez-Navarro, A., Gonzalez-Muñoz, M. T., and Rodriguez-Gallego, M., 2007. Bacterially mediated mineralization of vaterite. *Geochimica et Cosmochimica Acta*, **71**(5), 1197–1213.

Roh, Y., Chon, C.-M., and Moon, J.-W., 2007. Metal reduction and biomineralization by alkaliphilic metal reducing bacterium, *Alkaliphilus metalliredigens* (QYMF). *Geosciences Journal*, **11**(4), 415–423.

Sigel, A., Sigel, H., and Sigel, R. O. (eds.), 2008. *Biomineralization: from Nature to Application. Metal Ions in Life Sciences*. West Sussex: Wiley and Sons, 4 Vols, 700 p.

Smith, D. W., and Strohl, W. R., 1991. Sulfur oxidizing bacteria. In Shively, J. M., and Barton, L. L., (eds.), *Variations in Autotrophic Life*. London: Academic Press, pp. 121–146.

Southam, G., 2000. Bacterial surface-mediated mineral formation. In Lovley, D. R. (ed.), *Environmental Microbe-Metal Interactions*. Washington DC: ASM Press, pp. 257–276.

Streckfuss, J. L., Smith, W. N., Brown, L. R., and Campbel, M. M., 1974. Calcification of selected strains of *Streptococcus mutans* and *Streptococcus sanguis*. *Journal of Bacteriology*, **120**, 502–506.

Strohl, W. R., Geffers, I., and Larkin, J. M., 1981. Structure of the sulfur inclusions envelopes from four beggiatoas. *Current Microbiology*, **6**, 75–79.

Takahashi, Y., Hirata, T., Shimizu, H., Ozaki, T., and Fortin, D., 2007. A rare earth element signature of bacteria in natural waters. *Chemical Geology*, **244**, 569–583.

Tebo, B. M., Bargar, J. R., Clement, B. G., Dick, G. J., Murray, K. J., Parker, D., Verity, R., and Webb, S. M., 2004. Biogenic manganes oxides: properties and mechanisms of formation. *Annual Review of Earth and Planetary Sciences*, **32**, 287–328.

Thompson, J. B., and Ferris, F. G., 1990. Cyanobacterial precipitation of gypsum, calcite, and magnesite from natural alkaline lake water. *Geology*, **18**, 995–998.

Urrutia, M. M., and Beveridge, T. J., 1993. Mechanism of silicate binding to the bacteria cell wall in *Bacillus subtilis*. *Journal of Bacteriology*, **175**, 1936–1945.

Van Dijk, S., Dean, D. D., Zhao, Y., Cirgwin, J. M., Schwartz, Z., and Boyan, B. D., 1998. Purification, amino acid sequence, and cDNA sequence of novel calcium-precipitating proteolipids involved in calcification of *Corynebacterium matruchotii*, *Calcified Tissue International*, **62**, 350–358.

Villalobos, M., Toner, B., Bargar, J., and Sposito, G., 2003. Characterization of manganese oxide prduced by *Pseduomonas putida*. *Geochimica et Cosmochimica Acta*, **67**(14), 2649–2662.

Weiner, S., and Dove, P. M., 2003. An overview of biomineralization processes and the problem of the vital effect. In Dove, P. M., De Yoreo, J. J., and Weiner, S. (eds.), *Biomineralization. Reviews in Mineralogy and Geochemistry.* Washington DC, USA: Mineralogical Society of America and Geochemical Society, Vol. 54, pp. 1–29.

Wilkin, R. T., and Barnes, H. K., 1997. Formation processes of framboidal pyrite. *Geochimica et Cosmochimica Acta*, **61**(2), 323–339.

Yoshida, H., Yamamoto, K., Murakami, Y., Katsuta, N., Hayashi, T., and Naganuma, T., 2008. The development of Fe-nodules surrounding biological material mediated by microorganisms. *Environmental Geology*, **55**, 1363–1374.

Zamarreño, D. V., Inkpen, R., and May, E., 2009. Studies on carbonate crystals precipitated by freshwater bacteria and their use as a limestone consolidant. *Applied and Environmental Microbiology*, **75**, 5981–5990.

Zegeye, A., Huhuet, L., Abdelmoula, M., Carteret, C., Mullet, M., and Jorand, F., 2007. Biogenic hydroxysulfate green rust, a potential electron acceptor of SRB activity. *Geochimica et Cosmochimica Acta*, **71**, 5450–5462.

Zhang, C., Liu, S., Phelps, T. J., Cole, D. R., Horita, J., Fortier, S. M., Elless, M., and Valley, J., 1997. Physiochemical, mineralogical, and isotopic characterization of magnetite-rich iron oxides formed by thermophilic iron-reducing bacteria. *Geochimica et Cosmochimica Acta*, **61**(21), 4621–4632.

Zhang, C., Vali, H., Romanek, C. S., Phelps, T. J., and Liu, S. V., 1998. Formation of single-domain magnetite by a thermophilic bacterium. *American Mineralogist*, **83**, 1409–1418.

Zhang, J., Lion, L. W., Nelson, Y. M., Shuler, M. L., and Ghiorse, W. C., 2002. Kinetics of Mn (II) oxidation by Leptothrix discophora SS1. *Geochimica et Cosmochimica Acta*, **65**(5), 773–781.

## Cross-references

Banded Iron Formations
Biofilms and Fossilization

Biomining (Mineral Bioleaching, Mineral Biooxidation)
Biosignatures in Rocks
Calcified Cyanobacteria
Calcite Precipitation, Microbially Induced
Extracellular Polymeric Substances (EPS)
Fe(II)-Oxidizing Prokaryotes
Fe(III)-Reducing Prokaryotes
Gallionella
Gold
Iron Sulfide Formation
Leptothrix
Magnetotactic Bacteria
Manganese (Sedimentary Carbonates and Sulfides)
Metallogenium
Metals, Acquisition by Marine Bacteria
Microbial-Metal Binding
Microbialites, Modern
Microbialites, Stromatolites, and Thrombolites
Nanocrystals, Microbially Induced
Ores, Microbial Precipitation and Oxidation
Organomineralization
Shewanella
Stromatolites
Sulfate-Reducing Bacteria
Sulfide Mineral Oxidation
Tufa, Freshwater

# MICROBIAL COMMUNITIES, STRUCTURE, AND FUNCTION

Michael W. Friedrich
University of Bremen, Bremen, Germany

## Definition

*Microbial species.* Microorganisms exhibiting a high degree of phenotypic and genetic similarity; a pragmatic approach to demarcating "microbial species" using molecular biology tools has been 97% 16S rRNA sequence identity or 70% genome identity based on DNA-DNA hybridization (Stackebrandt and Goebel, 1994); thus, microbial species are often defined by operational characteristics (operational taxonomic unit). The microbial species concept is still a matter of controversy.
*Microbial population*. Individual microorganisms (of the same "species") form a population.
*Guild*. Metabolically related populations, e.g., sulfate-reducing microorganisms.
*Microbial community.* All microbial populations in a habitat.
*Microbial community structure*. The composition of a microbial community and the abundance of its members.
*Microbial diversity.* The number of different species in a habitat; sometimes (falsely) used as a synonym for community structure.
*Habitat*. The physical location or dwelling place of a particular organism, where an individual microbial ecotype can be found or isolated from.
*Ecosystem*. A community of microorganisms and their natural environment.
*Ecological niche*. Different from the habitat (spatial), the niche defines the function of an organism.

## Introduction

Microorganisms are an indispensable part of the biogeochemical cycles on Earth, have the longest history in evolution, and represent the largest genetic reservoir. Mostly invisible to the naked eye, microbes represent the largest source of biomass on Earth, with an estimated number of $4–6 \times 10^{30}$ cells, and 350–550 Pg of C (1 Pg = $10^{15}$ g), and have colonized almost any niche available on Earth (Whitman et al., 1998). In their habitats, microorganisms usually do not exist as single, genetically identical population, but live together with other microbial populations as microbial communities carrying out important functions of an ecosystem such as primary production and remineralization of biomass.

A hallmark of microbial life is its diversity. For a long time, only little was known about the magnitude of microbial diversity, as this was based on cultivation. Only about ~7,000 noneukaryotic species have been formally described (Euzeby, 1997) (http://www.bacterio.cict.fr/number.html), and insects were regarded as much more diverse than microorganisms. In microbiology, the term "diversity" is often used to refer to the number of different species in a given habitat, or, when based on molecular data, refers to the number of different sequences present. Diversity reflects the types of microbes present in a habitat, but "community structure" encompasses quantitative information on the different taxa and guilds (Liesack et al., 1997). Eventually, the analysis of community structure will allow for assessing the role and importance of microbes in their habitats and ecosystems. Presently, it is still methodologically difficult to obtain a complete view of microbial diversity and community structure.

## Methods of community structure analysis

*Cultivation*: Traditionally, the diversity of microbial communities has been studied by cultivation, i.e., by viable plate counts or most-probable-number (MPN) dilution techniques. However, the morphology of microorganisms is too simple for reliable identification and classification. Identification of microorganisms by cultivation requires pure cultures for testing physiological, biochemical, and cell biological characterization and suitable media for their growth, which is a major bottle neck. There are no cultivation media available that allow for capturing growth requirements of all microorganisms in a sample, and we often do not even know of their existence and presence. Direct microscopic counts can be of orders of magnitude higher than the counts of bacteria obtained on growth media ("plate counts"). Typically, only a small

fraction of microorganisms grows on standard media, and in some environments this has been estimated to be as low as 0.001–0.1%, e.g., in seawater (Amann et al., 1995).

*Molecular approaches*: The limitations of cultivation-based analysis to describe the diversity of microorganisms adequately were overcome by applying methods of molecular biology. Today, microorganisms are routinely classified by using the RNA of the small ribosomal subunit (small subunit ribosomal RNA – SSU rRNA), or its coding gene (SSU rRNA gene) as a molecular marker. In the 1970s, Carl Woese and coworkers used the sequences of the SSU rRNA to establish a phylogenetic framework for all life, from which the concept of the three domains of life – prokaryotes, archaea, and eukaryotes – emerged (Woese and Fox, 1977; Woese, 1987). Molecular classification of microorganisms was further developed by Norman Pace and his group to cultivation independent analysis of microbial communities in environmental samples by cloning the 16S rRNA gene directly from biomass (Pace et al., 1986). The basic idea is simple: rRNA sequences can be used as identifiers of microorganisms even if they were previously unknown; the sequence allows to establish an evolutionary relationship to other sequences of microorganisms in the databases. Directly extracting DNA from biomass, followed by cloning and sequencing of the (SSU rRNA) sequences of interest, facilitates to examine any environmental habitat. In August 2010, 418, 497 16S rRNA sequences were held in the dedicated database Ribosomal database project II (RDP; http://rdp.cme.msu.edu/), indicating how successful this approach has been. As the number of different microbial species can be very high in certain habitats, computational approaches have been developed to estimate diversity coverage of clone libraries (e.g., DOTUR) (Schloss and Handelsman, 2005). Cloning and sequencing approaches give an overview of microbial species diversity, but this approach is PCR based and therefore, may not adequately reflect the abundance of community members (von Wintzingerode et al., 1997). Analysis of community structure requires quantification of individual groups of microorganisms. Quantitative dot blot hybridization and fluorescent in situ hybridization (see Chapter *Fluorescence In Situ Hybridization (FISH)*), techniques are being used to determine abundance of uncultured prokaryotes using oligonucleotide probes directed against the SSU rRNA (Amann et al., 1995). Specific probes have been designed using SSU rRNA sequences obtained from the habitat studied and public databases; probeBase is an extensive repository of published rRNA-targeting oligonucleotide probe sequences available to the public (http://www.microbial-ecology.de/probebase/).

## How diverse is diversity?

*Microbial diversity in natural environments*: By applying molecular techniques such as DNA reassociation kinetics, it was estimated that 30 g of soil might contain approximately 4,000 different microbial genomes, possibly representing as many as 13,000 different microbial species (Torsvik et al., 1990). Ever since, soils have been regarded as one of the habitats with the most diverse microbial communities; however, a recent comparative study suggests a higher phylogenetic diversity in sediments possibly linked to salinity as major determinant (Lozupone and Knight, 2007). Estimates from PCR-based 16S rRNA gene sequencing suggested up to 100,000 species per gram of soil (Schloss and Handelsman, 2006). However, these estimates were based on relatively low numbers of sequences (up to 1,000). A new DNA sequencing technology, massively parallel pyrosequencing (Margulies et al., 2005), has allowed to sample as many as 53,000 16S rRNA sequences from one soil sample (Roesch et al., 2007); estimates of diversity based on these sequences suggested that the number of unique sequences never exceeded 52,000.

## Function of microbial communities

Ecosystems are individually functioning units including primary producers, consumers, and mineralizing organisms. Microbial communities are the most numerous organisms in any ecosystem, and they control the annual primary production including the recycling of carbon, sulfur, nitrogen, and iron. In a lake ecosystem for instance, photic zone, water column, and sediment harbor functionally different microbial communities. Light energy drives the primary production in the photic zone by a community of phototrophic microorganisms. Photosynthetically fixed carbon and carbon from other sources move through the ecosystem and fuel the community of pelagic chemoorganotrophic aerobes (or anaerobes) in the water column. Eventually, part of the carbon sinks down to the sediment, where a specifically adapted community consisting of several guilds of microorganisms degrades the organic matter in a concerted interdependent manner, resulting in the flow of carbon through the anaerobic microbial food chain (see Chapter *Carbon (Organic, Degradation)*). Several different guilds are involved in the degradation of polymers including polymer hydrolyzing, fermenting bacteria, fatty acid fermenting syntrophs, homoacteogens, and methanogens (Schink and Stams, 2006). As oxygen diffusion into the sediment is severely limited, often microoxic to anoxic conditions occur within a few millimeters depth of the sediment surface because of microbial respiration activity in the very top layer. Concomitantly, anaerobically respiring microorganisms oxidize carbon compounds and transfer electrons to inorganic electron acceptors such as nitrogen oxides, manganese oxides, ferric iron, and sulfate in a sequence that reflects the thermodynamic theory in many environments (Conrad, 1996). Once these electron acceptors are depleted, methanogenesis becomes the terminal electron accepting process, which is typically found in freshwater sediments rich in organic matter, in swamps, or in flooded soils such as rice paddies (Schink and Stams, 2006). The function of the major guilds involved in these processes is known in

principle, mainly because representative microorganisms have been identified by enrichment and isolation techniques. The numerical importance as well as the actual physiological function of such guild representatives in the vast diversity of habitats are still elusive. Although 16S rRNA-based surveys with varying degrees of diversity sampling depths exist for a large number of habitats, mostly, sequences and derived phylogenetic identity alone do not reveal the physiological role these microorganisms have. The SSU rRNA is a very valuable phylogenetic marker, however, most guilds are not monophyletic, i.e., not all microorganisms falling into a coherent phylogenetic cluster have the same physiology. For example, within the Proteobacteria phototrophy is widespread, and thus, a close relative of a phototroph can be a nonphototrophic microorganism. Assignment of physiological characteristics based on close SSU rRNA relationship requires careful evaluation and often is not possible at all. The use of marker genes coding for key enzymes has allowed to target phylogenetically diverse but physiologically coherent guilds of microorganisms (Teske et al., 2003). For example, anaerobic respiratory processes carried out by methanogenic archaea (Friedrich, 2005) or sulphate-reducing (Wagner et al., 2005) prokaryotes can be traced in the environment by targeting the respective key genes.

### Linking identity and function to microbial populations

Our understanding of microbial community functioning, mostly, is of principal nature for many ecosystems. Even for numerically abundant microbial species identified by molecular techniques, their ecophysiology and role in ecosystem functioning remain elusive. A major goal in current microbial ecology research is therefore to understand what uncultured microorganisms do in their habitats. What are their metabolic properties, and which microbial species are responsible for defined processes in their habitat?

An elegant concept for the elucidation of the ecophysiology of uncultivated microorganisms relies on the incorporation of isotopically labeled substrates into biomass and the subsequent identification of the microorganisms actively incorporating the label. This approach enables to link metabolic activity to active microorganisms by measuring label incorporation into biomarkers or even whole cells.

Microautoradiography in combination with FISH (MAR-FISH) can visualize cells actively incorporating radioactively labeled substrates in their natural habitats permitted that samples are suitable for FISH (Lee et al., 1999). Alternatively, oligonucleotide probe array technology detects radiolabel incorporation into rRNA extracted from environmental samples (Adamczyk et al., 2003).

The use of stable isotopes ($^{13}C$, $^{15}N$, $^{18}O$) for labeling active microbial populations has led to a whole suite of approaches that rely on tracing the incorporation of labeled substrates into cell components such as lipids (Boschker et al., 1998), DNA (Radajewski et al., 2000), RNA (Manefield et al., 2002), or even whole cells (Lechene et al., 2006). Tracing $^{13}C$ incorporation into lipids is highly sensitive; however, phospholipids lack phylogenetic resolution and require pure cultures for assigning individual lipids to species. Stable isotope probing (SIP) of nucleic acids represents a direct way to identify microbial populations active in a defined metabolic process. SIP is based on the incorporation of labeled substrate into the cellular biomarker nucleic acids, separation of labeled nucleic acids from unlabeled nucleic acids by density gradient centrifugation, and molecular identification of active populations carrying labeled DNA or RNA. By now, SIP has been used to identify the active players involved in carbon and nitrogen cycling, as well in bioremediation in a large variety of different habitats and has been extended even to metagenomic analysis of labeled DNA (for a recent overview see (Neufeld et al., 2007).

Whereas the original SIP is based on physical separation of labeled nucleic acid from unlabeled nucleic acid, newer approaches target single cells. Raman confocal microscopy detects shifts in vibrational energy of chemical bonds induced by $^{13}C$ labeling of cellular of single microbial cells. In combination with FISH, Raman microscopy enables identification of $^{13}C$ label incorporating active cells (Huang et al., 2007). A conceptually similar approach uses secondary ion mass spectrometry (SIMS) operating at lateral resolution of now down to 33 nm. NanoSIMS has high sensitivity allowing to detect shifts in isotopic signals at per mill rather than the atomic percent range (standard SIP and Raman SIP) and high isotope measurement precision (Lechene et al., 2006). Recently, it has been demonstrated that NanoSIMS analyses can be combined with 16S rRNA targeting oligonucleotide probes by employing halogen atoms as element label allowing in parallel phylogenetic identification and detection of metabolic activity of individual cells (Li et al., 2008).

## Conclusions

Molecular biology based approaches have advanced our understanding of microbial diversity enormously over the last 20 years. However, we are just at the beginning of a new era in surveying microbial diversity: we will be witnessing the rapid accumulation of staggering amounts of sequence data not only for the single phylogenetic marker 16S rRNA, but also for whole metagenomes fueled by parallel DNA sequencing technology. New developments in linking phylogenetic identity to function, including renewed efforts in cultivation, will boost our understanding of the ecophysiology of the uncultivated vast majority of microorganisms. Eventually, this ongoing revolution of microbial ecology will allow to test general ecological theory using microbial systems (Prosser et al., 2007).

## Bibliography


Adamczyk, J., Hesselsoe, M., Iversen, N., Horn, M., Lehner, A., Nielsen, P. H., Schloter, M., Roslev, P., and Wagner, M., 2003. The isotope array, a new tool that employs substrate-mediated labeling of rRNA for determination of microbial community structure and function. *Applied Environmental Microbiology*, **69**, 6875–6887.

Amann, R. I., Ludwig, W., and Schleifer, K. H., 1995. Phylogenetic identification and in situ detection of individual microbial cells without cultivation. *Microbiology Reviews*, **59**, 143–169.

Boschker, H. T. S., Nold, S. C., Wellsbury, P., Bos, D., de Graaf, W., Pel, R., Parkes, R. J., and Cappenberg, T. E., 1998. Direct linking of microbial populations to specific biogeochemical processes by $^{13}$C-labelling of biomarkers. *Nature*, **392**, 801–805.

Conrad, R., 1996. Soil microorganisms as controllers of atmospheric trace gases ($H_2$, CO, $CH_4$, OCS, $N_2O$, and NO). *Microbiology Reviews*, **60**, 609–640.

Euzeby, J. P., 1997. List of bacterial names with standing in nomenclature: a folder available on the Internet. *International Journal of Systematic Bacteriology*, **47**, 590–592.

Friedrich, M. W., 2005. Methyl-coenzyme M reductase genes – unique functional markers for methanogenic and anaerobic methane-oxidizing *Archaea*. *Methods Enzymology*, **397**, 428–442.

Huang, W. E., Stoecker, K., Griffiths, R., Newbold, L., Daims, H., Whiteley, A. S., and Wagner, M., 2007. Raman-FISH: combining stable-isotope Raman spectroscopy and fluorescence in situ hybridization for the single cell analysis of identity and function. *Environmental Microbiology*, **9**, 1878–1889.

Lechene, C., Hillion, F., McMahon, G., et al., 2006. High-resolution quantitative imaging of mammalian and bacterial cells using stable isotope mass spectrometry. *Journal of Biology*, **5**, 20.

Lee, N., Nielsen, P. H., Andreasen, K. H., Juretschko, S., Nielsen, J. L., Schleifer, K. H., and Wagner, M., 1999. Combination of fluorescent in situ hybridization and micro autoradiography – a new tool for structure-function analyses in microbial ecology. *Applied Environmental Microbiology*, **65**, 1289–1297.

Li, T., Wu, T. D., Mazeas, L., Toffin, L., Guerquin-Kern, J. L., Leblon, G., and Bouchez, T., 2008. Simultaneous analysis of microbial identity and function using NanoSIMS. *Environmental Microbiology*, **10**, 580–588.

Liesack, W., Janssen, P. H., Rainey, F. A., Ward-Rainey, N. L., and Stackebrandt, E., 1997. Microbial diversity in soil: the need for a combined approach using molecular and cultivation techniques. In van Elsas, J. D., Trevors, J. T., and Wellington, E. M. H. (eds.), *Modern Soil Microbiology*. New York: Marcel Dekker, pp. 375–439.

Lozupone, C. A., and Knight, R., 2007. Global patterns in bacterial diversity. *Proceedings of National Academy of Sciences United States of America*, **104**, 11436–11440.

Manefield, M., Whiteley, A. S., Griffiths, R. I., and Bailey, M. J., 2002. RNA stable isotope probing, a novel means of linking microbial community function to phylogeny. *Applied Environmental Microbiology*, **68**, 5367–5373.

Margulies, M., Egholm, M., Altman, W. E., et al., 2005. Genome sequencing in microfabricated high-density picolitre reactors. *Nature*, **437**, 376–380.

Neufeld, J. D., Wagner, M., and Murrell, J. C., 2007. Who eats what, where and when? Isotope-labelling experiments are coming of age. *ISME J*, **1**, 103–110.

Pace, N. R., Stahl, D. A., Lane, D. J., and Olsen, G. J., 1986. The analysis of natural microbial populations by ribosomal RNA sequences. *Advances in Microbial Ecology*, **9**, 1–55.

Prosser, J. I., Bohannan, B. J. M., Curtis, T. P., et al., 2007. The role of ecological theory in microbial ecology. *Nature Reviews Microbiology*, **5**, 384–392.

Radajewski, S., Ineson, P., Parekh, N. R., and Murrell, J. C., 2000. Stable-isotope probing as a tool in microbial ecology. *Nature*, **403**, 646–649.

Roesch, L. F., Fulthorpe, R. R., Riva, A., et al., 2007. Pyrosequencing enumerates and contrasts soil microbial diversity. *Isme Journal*, **1**, 283–290.

Schink, B., and Stams, A. J. M., 2006. Syntrophism among prokaryotes. In Dworkin, M. (ed.), *The Prokaryotes*, 3rd edn. New York: Springer, Vol. 2, pp. 309–335.

Schloss, P. D., and Handelsman, J., 2005. Introducing DOTUR, a computer program for defining operational taxonomic units and estimating species richness. *Applied Environmental Microbiology*, **71**, 1501–1506.

Schloss, P. D., and Handelsman, J., 2006. Toward a census of bacteria in soil. *Plos Computational Biology*, **2**, 786–793.

Stackebrandt, E., and Goebel, B. M., 1994. Taxonomic note: a place for DNA-DNA reassociation and 16S rRNA sequence analysis in the present species definition in bacteriology. *International Journal of Systematic Bacteriology*, **44**, 846–849.

Teske, A., Dhillon, A., and Sogin, M. L., 2003. Genomic markers of ancient anaerobic microbial pathways: sulfate reduction, methanogenesis, and methane oxidation. *Biological Bulletin*, **204**, 186.

Torsvik, V., Goksoyr, J., and Daae, F. L., 1990. High diversity in DNA of soil bacteria. *Applied Environmental Microbiology*, **56**, 782–787.

von Wintzingerode, F., Goebel, U. B., and Stackebrandt, E., 1997. Determination of microbial diversity in environmental samples – pitfalls of PCR-based rRNA analysis. *FEMS Microbiology Review*, **21**, 213–229.

Wagner, M., Loy, A., Klein, M., Lee, N., Ramsing, N. B., Stahl, D. A., and Friedrich, M. W., 2005. Functional marker genes for identification of sulphate-reducing prokaryotes. *Methods Enzymology*, **397**, 469–489.

Whitman, W. B., Coleman, D. C., and Wiebe, W. J., 1998. Prokaryotes: the unseen majority. *Proceedings of National Academy of Sciences United States of America*, **95**, 6578–6583.

Woese, C. R., 1987. Bacterial evolution. *Microbiology Reviews*, **51**, 221–271.

Woese, C. R., and Fox, G. E., 1977. Phylogenetic structure of the prokaryotic domain: the primary kingdoms. *Proceedings of National Academy of Sciences United States of America*, **74**, 5088–5090.


## Cross-references


Acetogens
Anaerobic Transformation Processes, Microbiology
Archaea
Bacteria
Carbon (Organic, Cycling)
Carbon (Organic, Degradation)
Chemolithotrophy
Fe(III)-Reducing Prokaryotes
Fluorescence In Situ Hybridization (FISH)
Metagenomics
Methanogens
Photosynthesis
Sulfate-Reducing Bacteria
Sulfur Cycle

# MICROBIAL DEGRADATION

Erika Kothe
Friedrich Schiller University Jena, Jena, Germany

## Synonyms

Mineralization; Nutrient cycling

## Definition

*Microbial*. Processes driven by microorganisms.
*Degradation*. Use of chemical substances as carbon and energy source for metabolism, thereby breaking down larger molecules to smaller ones.

## Introduction

Microorganisms are the basis for the process of mineralization by utilizing organic molecules for their catabolism, thereby returning the elements to the geobiological cycles. In catabolism, or energy conservation, energy-rich adenosine triphosphate (ATP) is formed (for general reading on microbial physiology: Madigan and Martinko, 2006). This is the basis for metabolic degradation performed by microorganisms in a great diversity. The degradation of organic material in terrestrial, limnological, and marine environments is thus based on the growth of microorganisms on organic compounds, which is termed chemoheterotrophic growth style, depending on the availability of organic nutrients for growth. The processes can be dependent on aerobic respiration, but many degradative processes, e.g., in sediments, are performed in the absence of oxygen under anaerobic conditions (Schink, 2002).

## Aerobic and anaerobic respiration

The respiration with oxygen as the terminal electron acceptor is the process yielding the most ATP per mol substance oxidized and thus, aerobic respiration is the preferred route for degradation whenever enough oxygen is available. Under aerobic conditions, the degradation of organic matter is performed following general and ubiquitous pathways such as glycolysis; the pyruvate produced in the glycolytic chain enters the citrate cycle; and the reduction equivalents produced are then reoxidized by the respiratory chain coupled to the reduction of oxygen to water. All building blocks of living cells can be degraded that way, allowing growth of microorganisms. The carbon moieties are released as $CO_2$ into the atmosphere.

Under anaerobic conditions, anaerobic respiratory chains using alternative electron acceptors can ensue. For example, nitrate, nitrite, sulfate, sulfite, sulfur, iron, manganese or fumarate, or carbon dioxide in methanogenesis is then used to accept the electrons, thereby reducing these substances. Halogenated compounds can serve as electron acceptors in dehalorespiration.

All these respiratory chains depend on membrane-bound electron transport, and the reactions of electron transport are coupled to proton export across the cellular membrane to form a proton motif force. The proton motif force is then used to drive ATP formation *via* the enzyme ATP synthase, which can form 1 mol of ATP per 3 mol of protons carried back into the cytoplasm. The electrons for electron transport chains are derived from oxidation of the organic molecules of the nutrient source. If possible, the organic matter is fully oxidized to carbon dioxide. In this way, the organic matter is fully decomposed.

## Fermentation

Another route, independent of respiratory chains, is possible for the fermentative degradation of organic matter. The fermentations performed by microorganisms can use oxidation of substrates to produce ATP and then reduce organic molecules for reoxidation of the reducing equivalents. While ATP yield in these systems is limited when compared to respiration, it still allows growth under conditions when no inorganic electron acceptor is available in sufficient amounts, or when iron as part of the electron carriers in the respiratory chain is not available and therefore, an electron transport chain cannot be synthesized.

In contrast to respiration, both aerobic and anaerobic, during fermentation the organic substrate is not fully oxidized to $CO_2$. Rather, energy conservation is dependent on the oxidation of an organic molecule in which an aldehyde may be formed as intermediate, which subsequently can be oxidized to form an acid. This exergonic reaction is coupled to the activation of an anorganic phosphate moiety which then can be transferred to ADP, thereby forming ATP. This process is called substrate-level phosphorylation in contrast to the electron transport phosphorylation occurring in respiratory chains. The oxidative reaction releases reduction equivalents, which cannot be transferred to an inorganic electron acceptor due to the lack of respiratory chains in fermenting microbes. Thus, the reduction of an organic compound is necessary to release the carrier for a new cycle of oxidation. The reduced organic substance is released into the environment. An alternative is to release the reduction equivalents as $H_2$.

The fermentation of sugars, which are present in large amounts due to photosynthesis products and constituents of plant cell wall material, can be performed using the Embden–Meyerhof pathway of glycolysis, the Entner–Doudoroff pathway, or modifications or parts thereof. Sugars with 5 C moieties, sugar acids, or carbonic acids can be converted by different pathways. Examples for sugar fermentation are homo- or hetero-fermentative lactic acid fermentation, alcoholic fermentation, propionate fermentation, butyrate or butanole fermentation, mixed acid fermentation, solvent fermentation, and many others. The names of the pathways indicate the products released in these different fermentative pathways.

Many bacteria can switch between fermentative and respiratory metabolism, depending on the availability of

electron acceptors for respiratory chains. If they can switch between anaerobic and aerobic metabolism, they are called facultative aerobes, while anaerobes are usually oxygen sensitive and grow exclusively under anaerobic conditions. Within this group, the Gram-positive Clostridia have evolved many fermentation pathways including those to degrade fatty acids, lipids, amino acids and proteins, or nucleic acids under anaerobic conditions. Thus, degradation of all constituents of the cytosol of living organisms under anaerobic conditions can be achieved.

As no oxygen is necessary for the fermentative metabolism, most fermentations will proceed under anoxic conditions. However, aerotolerant microorganisms such as some lactic acid bacteria that are active in decomposition of plant litter can perform this reaction also under oxic conditions, although these anaerobes do not use oxygen as electron acceptor.

## Syntrophic degradation

The reduced compounds released by fermenting microorganisms constitute good nutritional sources for organisms that can use respiratory systems. In turn, the use of the product will allow for the continuous production of this compound, as no restrictions for the fermenting bacteria will inhibit their metabolism. The concomitant occurrence of bacteria in an ecological niche in which both partners are dependent on each other and degradation of the substrate is only possible when both partners are present is termed syntrophy.

The basis is the metabolic activity of one organism which forms a substrate for the other. This constant removal of a metabolic end product is examplified by the release of $H_2$ which is often a link in such syntrophic systems. Use of hydrogen by a second organism allows the first organism to constantly produce this compound. In pure culture, the partial pressure of $H_2$ reaches levels inhibitory to the metabolism of the producing organism which subsequently ceases growth. Since the syntrophic partner constantly removes hydrogen, no cessation of growth is observed due to product inhibition in this coculture. This syntrophy, depending on hydrogen transfer between two microbes present in the same environment, is of special importance, and the term interspecies hydrogen transfer has been coined for this syntrophic relationship. However, many different examples can be given for such syntrophic associations of microorganisms (e.g., Ueda and Beppu, 2007). Degradation of recalcitrant substrates, including, e.g., halogenated compounds, is often seen in syntrophic associations.

## Cometabolic degradation

Recalcitrant substrates are not, or very slowly, degraded because their conversion is not easily or not at all coupled with energy conservation. Thus, the degradation of these compounds is costly for the cell, and the microorganisms do not profit directly from degradation. Instead, the bacteria have to use energy from a different, catabolic reaction to drive the unfavorable degradation process.

An example of immediate importance is lignin degradation, which is performed by white rot fungi. The brown rot fungi degrade lignin mainly in order to get access to the cellulose of plant cell wall which is a good nutrient source but not directly accessible in wood and timber. The recalcitrant nature of lignin is seen under anoxic conditions, where the degradation is not possible and lignin of plant origin is thus the basis for coal formation.

As cometabolic systems are costly, they are mostly linked to respiration. Degradation of plant alcaloids, which are also recalcitrant substrates, often occurs at higher rates in oxic conditions.

## Degradation of plant litter and soil formation

Plant material is composed of the contents of the living cells and the cell wall materials. Within the cell, secondary plant metabolites are stored in the vacuole. Upon leaf fall or death of a plant, especially the secondary metabolites and the wall materials persist, while proteins and lipids are easily degradable in the unsaturated oxygen containing upper soil layers.

Plant cell walls are composed of cellulose, hemicellulose, pectin, polygalacturonans, and lignin. Even in herbaceous plants, a quarter of the secondary cell wall is lignin. This macromolecule can be degraded aerobically, while anoxic conditions lead to the formation of coal, since under these conditions lignin cannot be degraded. Wood rotting fungi, both brown rot and white rot fungi, are able to degrade lignin (Crawford, 1981). The enzymes involved in lignin degradation, peroxidases and laccases, are able to attack the bonds in the macromolecule linking the phenolic monomers to form the high molecular weight lignin. The monomers can then be degraded further and are metabolized to carbon dioxide. These processes have been studied in some detail at the molecular level (Gold and Alic, 1993). Whether bacteria are also able to degrade wood is still under discussion. Streptomycetes are able to perform some partial degradation. However, complete decomposition has yet to be shown with bacterial systems.

An interesting question in wood and lignin degradation is regarding the possible symbiosis of wood degrading fungi and bacterial populations at an oxic/anoxic border. Anaerobic bacteria able to convert lignin decomposition products and partially degrade these compounds have been described. The fermentation products of these organisms may serve as growth substrates for the lignin degrading fungi. Secondary metabolites of plants and microorganisms are often recalcitrant because they contain aromatic rings, heterocycles, and polyketides or are halogenated. Such compounds are not easily degraded, especially under anoxic conditions. If degradation does not lead to complete oxidation of carbon moieties to $CO_2$, the formation of humic acids and fulvic acids and thus the production of humus ensues. This process is the driving force for soil genesis. Under aerobic conditions,

enzymatic reactions known from lignin oxidation are often involved (Bumpus and Aust, 1987; Hammel, 1989).

## Degradation of aromatic and halogenated compounds

Under aerobic conditions, the chemically very stable aromatic ring can be broken by activities of mono- and di-oxygenases. While monooxygenases introduce one of the oxygen atoms of molecular oxygen into the organic molecule forming a hydroxyl group at one site of the ring, dioxygenases incorporate both oxygen atoms which leads to decyclization and ring opening. The linear compound can then be further oxidized after activation and fueled into general metabolic pathways. The aerobic degradation of aromatic compounds can be used to clean oil spills or other anthropogenic contaminations, especially applicable for the residual contamination after a first mechanical cleansing has been performed. Inoculation of a beach after an oil spill could show visible removal of the remaining oil within 1 year.

Under anoxic conditions, the ring opening seems more difficult and it had long been argued that this would not be possible. However, bacterial enrichment cultures could show that an anaerobic degradation of aromatic compounds is possible usually via activation and conversion to benzoyl CoA followed by ring reduction. These energetically unfavorable reactions are feasible with a thermodynamically favorable electron acceptor, e.g., when nitrate is available in an anaerobic respiratory chain. Thus, bacteria related to the nitrogen fixing genus *Azoarcus* link the degradation of aromatic compounds with denitrification. Many gene clusters with different substrate specificities have been identified to perform anaerobic degradation of different organic molecules including aromatic amino acids, benzene and its derivatives, phenols, and heterocyclic compounds. The linearized structures again can be fueled into metabolic pathways via acetyl CoA or propionyl CoA. Anthropogenic aromatic compounds can be degraded by these same processes, thus allowing complete decomposition and natural attenuation. The introduction of bacteria able to anaerobically degrade aromatic compounds into aquifers with (anthropogenic) contaminations opens the road to bioremediation of contaminated groundwater resources. In tertiary oil recovery, introduction of bacteria into the well to partially degrade the high molecular crude oil fraction uses bacterial enzymatic activities to form molecules of lower molecular weight from the tar fraction that then can be recovered.

Many anthropogenic contaminations contain halogen atoms which generally decrease metabolic degradation of the compounds. However, halogenated compounds are also known from natural sources. These include antibiotics with chloride or bromide atoms, plant-derived alkyl halides, or deterrents incorporated into, e.g., marine slugs or tropical frogs. Since nature already has learned to cope with these halogenated compounds, anthropogenic halogenated substances can also be degraded by bacterial consortia, both aerobically and anaerobically (Abraham et al., 2002; Smidt and de Vos, 2004). Not only bacteria are known to be able to perform dehalogenation reactions, but also basidiomycete fungi can also degrade organohalogens (de Jong and Field, 1997). While aerobic dehalogenation is a simple enzymatic reaction, anaerobic dehalorespiration is an interesting field of research. In this case, the dehalogenation is coupled with electron transfer and directly coupled to ATP formation in an anaerobic respiratory process.

## Use of microbes in bioremediation

The properties discussed above make the use of microbia or microbial consortia useful for bioremediation of different contamination scenarios. These include aerobic conditions such as in soil, anoxic condition such as in aquifers or sediments, and all imaginable sources of contamination from oil spill to xenobiotics such as plant protection chemicals or heavy metals. Some recent reviews are included to facilitate further reading on microbial degradation (Holtze et al., 2008; Johnsen and Karlson, 2007; Demnerova et al., 2005; Pieper, 2005; Kim and Rhee, 2003) and bioremediation (Watanabe et al., 2002; Röling and van Versefeld, 2002; Schwitzguebel et al., 2002).

## Summary

The biogeochemical cycles of the macronutrients carbon, nitrogen, sulfur, and phosphorus are dependent on microbial degradation of organic matter. Organic matter originating from carbon dioxide fixation, which is in terrestrial system usually performed by photosynthetically active bacteria and plant, is degraded to form carbon dioxide, either directly in one metabolic reaction or by cocultures in which the intermediate is released and taken up by another microbe. In addition, the formation of methane from $CO_2$ or acetate is possible. Thus, the carbon cycling involves $CO_2$, $CH_4$, and organic molecules. Nitrogen fixation of $N_2$ to $NH_3$ followed by fixation in organic amines constitutes one side of the cycle, while nitrification/denitrification releases the bound nitrogen into the atmosphere. The latter reaction sequences, i.e., oxidation of $NH_3$ to $NO_2^-$ or $NO_3^-$ and nitrate or nitrite respiration leading to $N_2$ formation, are dominant processes in the cycling of nitrogen. For the sulfur cycle, assimilation of sulfates and fixation into organic biomass, the oxidation of sulfur and reduction of sulfate or sulfite to elemental sulfur, or reduction of sulfur to $H_2S$ are the main processes. Sulfur is a constituent of the amino acids cysteine and methionine and of Fe/S clusters in redox enzymes. Phosphate is generally not altered; however, there have recently been reports on the use of phosphite in an unusual energy fixation process.

These elemental cycles in the biogeosphere all involve steps of fixation within living biomass, and the degradation of dead biomass is an essential part in releasing the mineralized elements back into the cycle. Higher

organisms are not capable of using plant litter, e.g., directly and thus entirely dependent on microbial degradation processes to have sufficient minerals available for their nutrition. Properties of microbes for degradation can be useful in bioremediation approaches.

## Bibliography


Abraham, W. R., Nogales, B., Golyshin, P. N., Pieper, D. H., and Timmis, K. N., 2002. Polychlorinated biphenyl-degrading microbial communities in soils and sediments. *Current Opinion in Microbiology*, **5**, 246–253.

Bumpus, J. A., and Aust, D., 1987. Biodegradation of environmental pollutants by the white rot fungus *Phaenorachaete chrysosporium*: involvement of the lignin-degrading system. *Bioessays*, **6**, 166–170.

Crawford, R. L., 1981. *Lignin Biodegradation and Transformation*. New York: Wiley.

de Jong, F., and Field, D. A., 1997. Sulfur tuft and turkey tail: biosynthesis and biodegradation of organohalogens by basidiomycetes. *Annual Review of Microbiology*, **51**, 375–414.

Demnerova, K., Mackova, M., Specakoca, V., Beranova, K., Kochankova, L., Lovecka, P., and Rylslava, E., 2005. Two approaches to biological decontamination of groundwater and soil polluted by aromatics-characterization of microbial populations. *International Microbiology*, **8**, 205–211.

Gold, M. H., and Alic, M., 1993. Molecular biology of the lignin-degrading basidiomycete *Phaenorachaete chrysosporium*. *Microbiology Reviews*, **57**, 605–622.

Hammel, K. E., 1989. Organopollutant degradation by ligninolytic fungi. *Enzyme and Microbial Technology*, **11**, 776–777.

Holtze, M. S., Sorensen, S. R., Sorensen, J., and Aamand, J., 2008. Microbial degradation of the benzonitrile herbicides dichlobenil, bromoxynil and ioxynil in soil and subsurface environments – insights into degradation pathways, persistent metabolites and involved degrader organisms. *Environmental Pollution* **154**, 155–168.

Johnsen, A. R., and Karlson, U., 2007. Diffuse PAH contamination of surface soils: environmental occurrence, bioavailability, and microbial degradation. *Applied Microbiology and Biotechnology*, **76**, 533–543.

Kim, D. Y., and Rhee, Y. H., 2003. Biodegradation of microbial and synthetic polyesters by fungi. *Applied Microbiology and Biotechnology*, **61**, 300–308.

Madigan, M. T., and Martinko, J. M., 2006. *Brock: Biology of Microorganisms*. Upper Saddle River: Prentice-Hall.

Pieper, D. H., 2005. Aerobic degradation of polychlorinated biphenyls. *Applied Microbiology and Biotechnology*, **67**, 170–191.

Röling, W. F., and van Versefeld, H. W., 2002. Natural attenuation: what does the subsurface have in store? *Biodegradation*, **13**, 53–64.

Schink, B., 2002. Anaerobic digestion: concepts, limits and perspectives. *Water Science and Technology*, **45**, 1–8.

Schwitzguebel, J. P., Aubert, S., Grosse, W., and Laturnus, F., 2002. Sulphonated aromatic pollutants. Limits of microbial degradability and potential of phytoremediation. *Environmental Science and Pollution Research International*, **9**, 62–72.

Smidt, H., and de Vos, W. M., 2004. Anaerobic microbial dehalogenation. *Annual Review of Microbiology*, **58**, 43–73.

Ueda, K., and Beppu, T., 2007. Lessons from studies of *Symbiobacterium thermophilum*, a unique syntrophic bacterium. *Bioscience Biotechnology and Biochemistry*, **71**, 1115–1121.

Watanabe, K., Futamata, H., and Harayama, S., 2002. Understanding the diversity in catabolic potential of microorganisms for the development of bioremediation strategies. *Antonie van Leeuwenhoek*, **81**, 655–663.


## Cross-references


Aerobic Metabolism
Anaerobic Transformation Processes, Microbiology
Phosphorus, Phosphorites
Soils


# MICROBIAL ECOLOGY OF SUBMARINE CAVES


Francesco Canganella, Giovanna Bianconi
University of Tuscia, Viterbo, Italy


## Definition

Essential concepts, current investigations, and discussion.

In recent years, the search for the limit of biodiversity in extreme and/or uncommon environments led to the investigation of peculiar ecosystems such as deep-sea, subterranean niches, Antarctic cores, hydrothermal vents, and extraterrestrial sites.

Submarine caves and cavities have also been explored, some were mainly exploited as popular attractions for scuba divers, but some were shown to be of great interest for geologists, biologists, and microbiologists.

Available scientific data on these ecosystems are not abundant, particularly as far as biological disciplines are concerned. Most of the published works have been related to specific submarine cavities known as Blue Holes and Black Holes, as well as to submarine caves showing inner sulfidic emissions. A larger number of data are currently available regarding the microbiology of terrestrial caves, particularly on the microbial ecology of carbonate layers, sediments, bat guano, and flooding waters (Vlasceanu et al., 1997, 2000; Holmes et al., 2001; Engel et al., 2003; Northup et al., 2003; Sugita et al., 2005; Zhou et al., 2007), but these latter ecosystems are not part of the current review.

## Blue holes and black holes

The so-called blue holes are underwater karst systems which can develop horizontally in a very extensive way and appear blue due to a combination of blue sky reflection with the white carbonate sand deposited in the cave (Smart et al., 1988; Mylroie et al., 1995; Schwabe et al., 1997; Marano-Briggs, 2000; Colantoni et al., 2003; Canganella et al., 2004). Most of these sites were found and described in Bahamas and Hawaii.

Other cavern systems are known as "black holes," which are cave systems without known lateral passages and located in the interior regions of the larger Bahamian islands. Most black holes are located in the central to western side of the island of South Andros in the Bahamas (Figure 1), although one has been found on the northern transitional shore of the Grand Bahama Island. They are vertical cave systems which

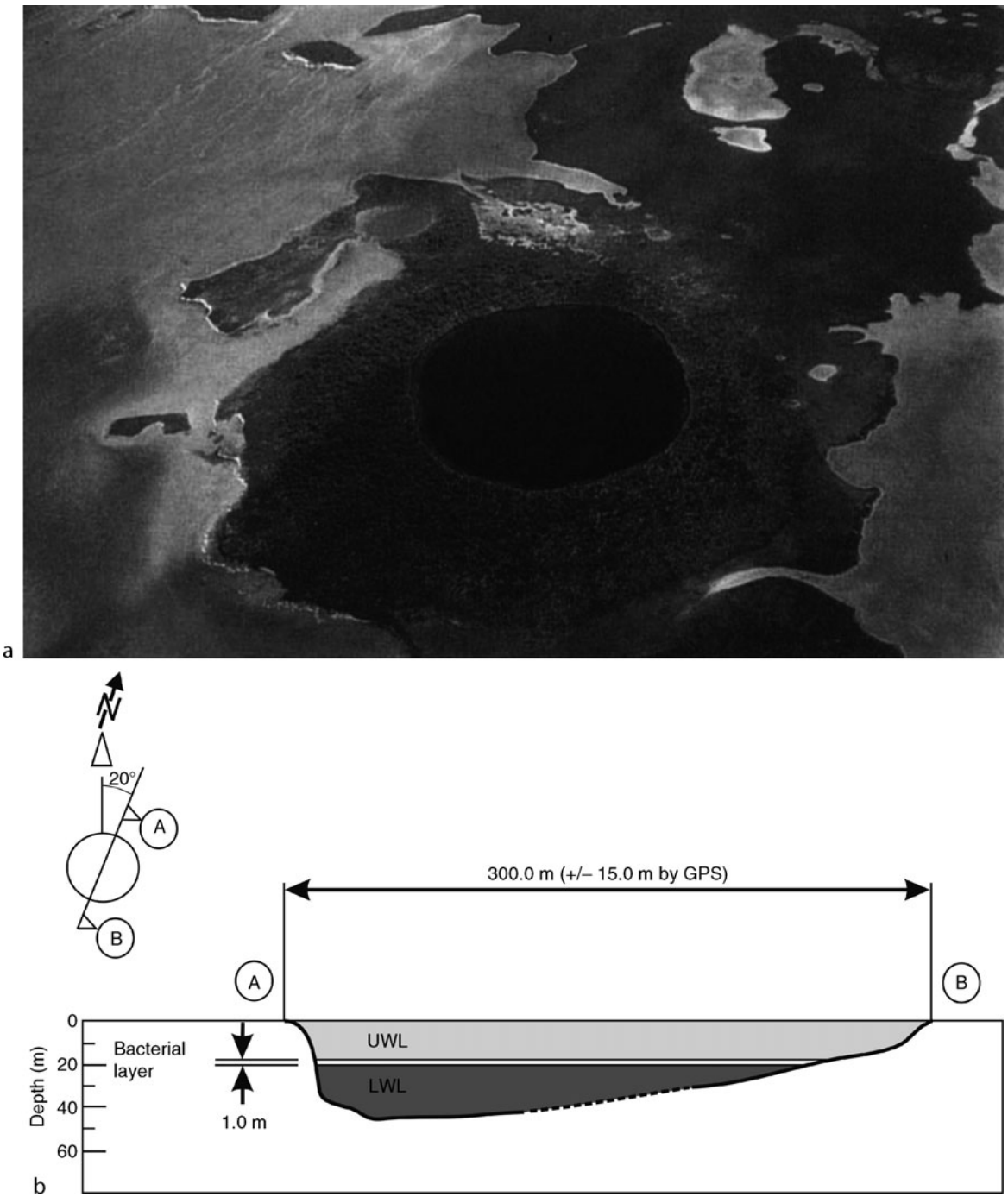


**Microbial Ecology of Submarine Caves, Figure 1** A schematic drawing of the South Andros black hole, (**a**) aerial view and (**b**) bathymetry. UWL, upper water layer; LWL, lower water layer; —, floor area not surveyed. (Reprinted from Schwabe and Herbert, 2004 Black Holes of the Bahamas: what they are and why they are black, Quaternary International 121: 3–11 with permission from Elsevier.)

develop from the surface downward and appear to have no direct link to the sea, except through rock fissures and local porosity (Schwabe, 1998; Schwabe and Herbert, 2004).

In both cave systems, as water exchange is severely restricted, physicochemical gradients are highly stable and even strict anaerobic conditions can develop with remarkable hydrogen sulfide concentrations (from 5 μM to 6 mM).

## Submarine caves with sulfidic water springs

A unique marine ecosystem is represented by the submarine caves of Capo Palinuro (Salerno, Italy), of which 13 have inside sulfidic springs exhibiting temperatures up to 25°C that remarkably affect the surrounding ecosystem.

Preliminary investigations concerning the submarine speleology of the site have been carried out since the mid 1980s, but only after 1990 an extensive biological knowledge was achieved. Several ecological and geological studies were performed (Alvisi et al., 1994a, b; Mattison et al., 1998), particularly on the "Grotta Azzurra" (Figure 2). The cave may be separated into two topographically distinct regions: a weakly illuminated outer region and an inmost dark region (Snow Hall). The latter is characterized by the presence of sulfur springs that arise from fissures in the cave floor. Currently, no other submarine caves with sulfide springs have been reported.

## Microbiological studies

### The blue holes

Abundant microbial development has been observed in these cave systems, usually linked to temperature anomalies in the range of 36–41°C as recorded by investigators. Marano-Briggs (2000) reported temperatures up to 41°C in the Tarpon Blue Hole, supporting the theory that the mass population of anoxygenic phototrophic bacteria present at a specific water layer may dissipate excess light energy by heat. A dense layer of purple sulfur bacteria

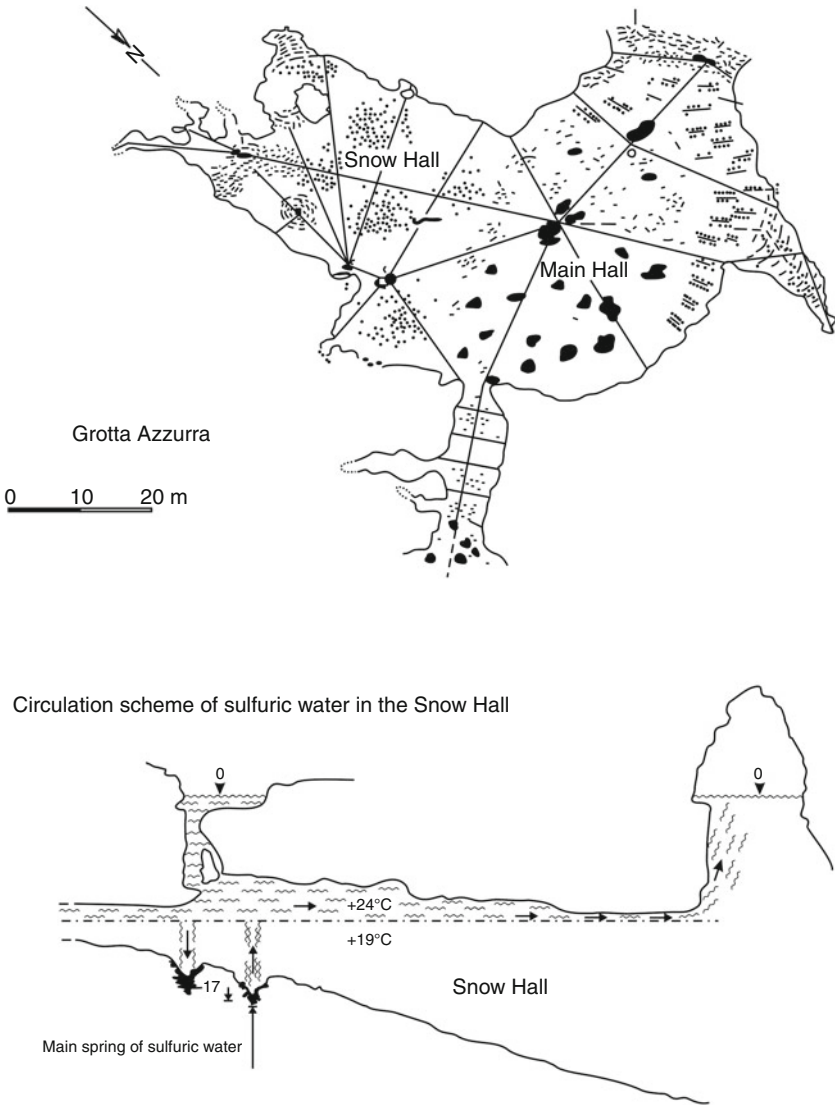


**Microbial Ecology of Submarine Caves, Figure 2** A drawing map of the "Grotta Azzurra" showing both entrances, halls, and freshwater circulation.

was indeed found at 4.5–5.5 m depth in the estuarine Tarpon Blue Hole and the dominant population was represented by *Chromatiaceae* species. These bacteria are capable either of photolithoautotrophic growth with sulfide or elemental sulfur under anoxic conditions in the light or of chemo-organotrophic growth under micro-oxygenic conditions in the dark. Their abundance in the site was consistent with their physiological traits, and among them a phototrophic bacterium in particular was identified as a novel strain of *Marichromatium purpuratum* that contained okenone instead of spirilloxanthin as its major carotenoid.

Recently, microbiological studies on a blue hole discovered in the Indian Ocean (Canganella et al., 2004) were preliminarily performed in order to investigate the distribution of microbial populations along the water column and in the bottom sediment of the cave. In Figure 3, the DGGE analysis carried out shows how bacterial populations are distributed among surface layers, mid- and deep-layers, indicating in particular a similar biodiversity between 30 and 50 m depth. The same was investigated by the Biolog system, particularly for anaerobic populations.

The molecular investigation showed that at surface there was a complex microbial community showing several peculiarities with respect to standard pelagic seawater. Characteristic species were *Thioalkalivibrio* and *Thioploca* within the Gamma-Proteobacteria and *Desulfosarcina* and other Delta-Proteobacteria; sequences within the Delta-Proteobacteria related to sponge symbionts were also found. Subsurface bacteria present in the water column appeared dominated by Alpha-Proteobacteria represented by sequences related to photoorganotrophs (*Rhodovibrio*-related), methanotrophs, and coral surface-related bacteria.

Near the bottom, although the Alpha-Proteobacteria were still well represented, the proportion of Delta-Proteobacteria increased. These Delta-Proteobacteria represent sulfate-reducing bacteria mainly belonging to the Desulfobacteriaceae, or related to *Desulfonanticus*, *Synteophus*, and others related to marine and salt-marsh uncultured bacteria.

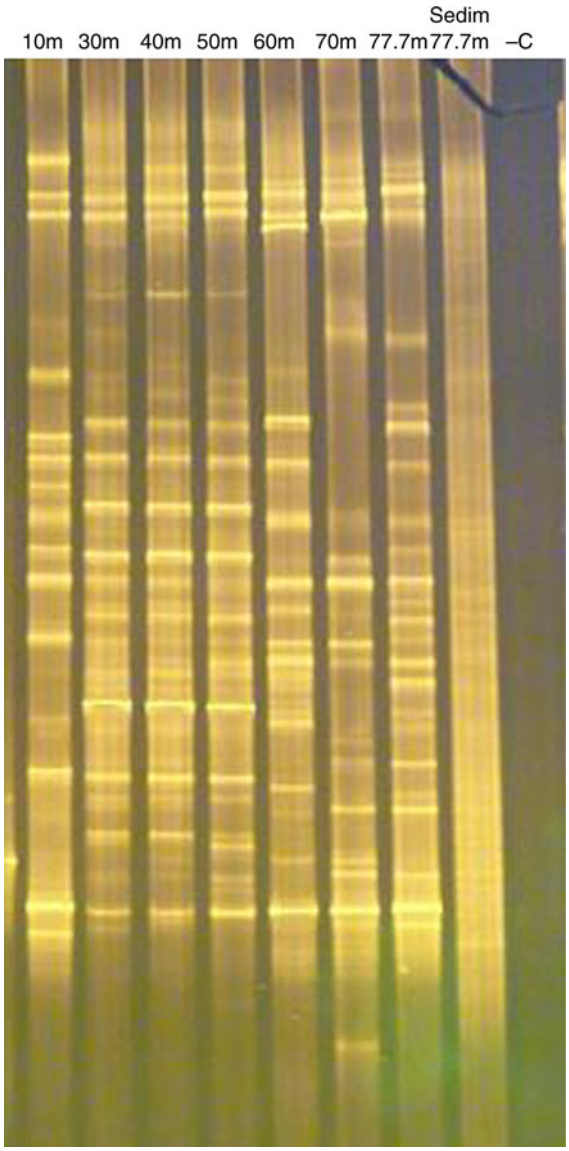


**Microbial Ecology of Submarine Caves, Figure 3** DGGE analysis of the water column and bottom sediment of the blue hole in the Indian Ocean.

## The black holes of the Bahamas

The water in these holes appears black in color due to the presence of a 1 m thick white microbial veil located within the upper third of the water column (18–19 m), at the boundary between the oxygenic low salinity upper water mass and the denser anoxic saline water layer. The boundary between the two water masses is characterized by sharp discontinuities in physicochemical gradients: salinity increased from 12 to 35 psu and temperature from 29°C to 36°C; pH decreased from 8.6 to 6.45 as well as dissolved $O_2$ from 6 mg/l to <1 mg/l. Morphological microscopic observations of collected samples showed mainly nonmotile spherical and motile rod-shaped purple sulfur bacteria. The dominant members of this warm (36°C), saline, and sulfide-rich layer have been identified as anoxygenic phototrophic bacteria belonging to the genera *Allochromatium* and *Thiocapsa* and showed population densities $>10^7$ viable cells/ml. These bacteria grow well in the presence of sulfide and carbon dioxide in the light. During photoautotrophic growth sulfur globules are stored intracellularly as intermediate oxidation products. Moreover, the intracellular photosynthetic membranes are of the vesicular type, and bacteriochlorophyll *a* and carotenoids of the normal spirilloxanthin series are present (Herbert et al., 2005). Calculations made by these authors revealed that the layer of anoxygenic phototrophic bacteria in the South Andros black hole may have a biomass content of approximately 5.06 ton dry weight.

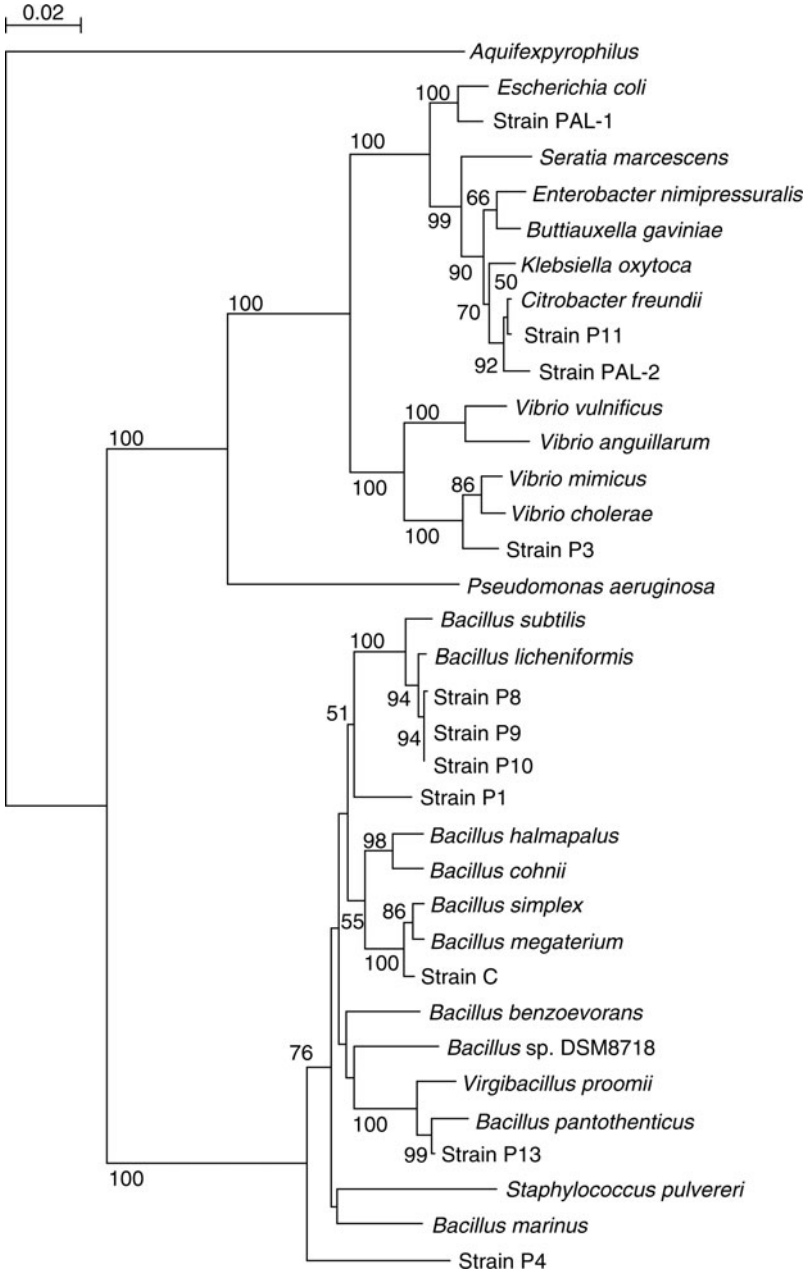


**Microbial Ecology of Submarine Caves, Figure 4** A phylogenetic tree based on 16S rRNA gene sequence comparison, including representative heterotrophic isolates from the "Grotta Azzurra."

## The marine caves of Capo Palinuro

The emergence of sulfidic water in some of the caves (particularly in the "Grotta Azzurra," "Grotta Sulphurea," and "Grotta di Cala Fetente") gives rise to an unusual situation, characterized by abiotic as well as biotic fluctuations, represented by emissions from sulfidic springs and higher concentration of sulfur-utilizing bacteria following each outflowing event, respectively. Warm sulfidic water of reduced salinity enters the Snow Hall (Grotta Azzurra), from fissures in the bottom rocks, and rises above the more dense seawater to form a thermocline and chemocline as a visible boundary at a depth of about 9.5 m. The geochemistry of water samples from the Grotta Azzurra was extensively reported by Mattison et al. (1998): above and below the chemocline temperatures were 24.0 $\pm$ 0.2 and 22.8 $\pm$ 0.3, respectively; NaCl concentrations (%) were 2.6 $\pm$ 0.1 and 3.0 $\pm$ 0.1, respectively; pH values were 7.22 $\pm$ 0.02 and 8.15 $\pm$ 0.25, respectively.

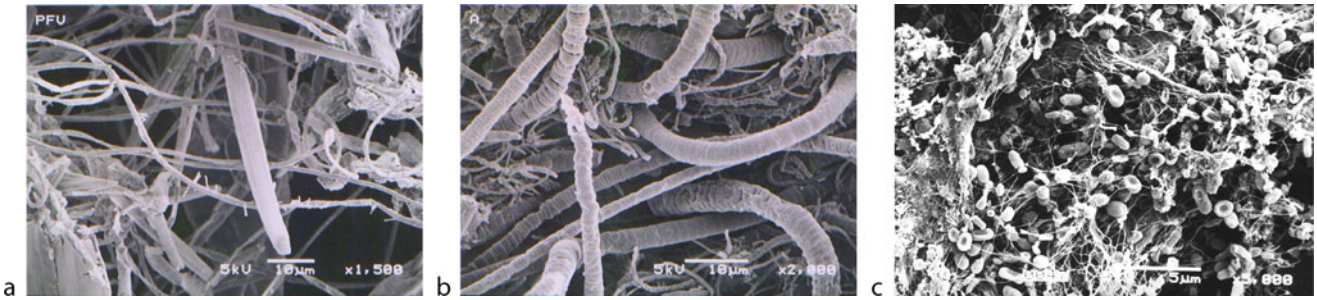


**Microbial Ecology of Submarine Caves, Figure 5 (a)** A SEM picture of a sample collected in the bacterial mat on the vault of the "Grotta Azzurra"; (**b**) a SEM picture of a sample collected in the bacterial mat on the vault of the "Grotta Azzurra"; (**c**) A SEM picture of a sediment sample collected nearby a sulfataric spring along the main entrance of the "Grotta Azzurra."

The present ecosystem is biologically unique particularly because of the following points: (1) the peculiar emissions represent the only available model in shallow waters resembling the deep-sea hydrothermal vents (Canganella, 2001); (2) alike what happens in usual submarine caves, the development of micro- and macrofauna increases with the decrease of irradiation; (3) the freshwater flow is placed above the seawater and, inside the cave, an interface between the warm/anaerobic upper zone ($H_2S$-enriched) and the cold, sulfurless lower zone can be observed; (4) giant forms, particularly among *Cnidaria* and *Porifera*, occur mainly along the aerobic/anaerobic interface (Alvisi et al., 1994a, b).

During the last decade both, "Grotta Azzurra" and "Grotta Sulfurea" have been investigated. Some preliminary data on the lithotrophic microflora were published (Mattison et al., 1998), and other studies were performed in order to (1) investigate the microscopic structure of bacterial mat and (2) to understand both the taxonomy and physiology of heterotrophic bacteria inside the "Grotta Azzurra" (Canganella and Bianconi, 1999, 2003). The 16S rRNA genes analysis (Figure 4) showed that heterotrophic isolates were closely related to the genera *Escherichia*, *Citrobacter*, *Vibrio*, and *Bacillus*.

In addition to the analysis of the heterotrophic microflora, recently a preliminary molecular investigation was performed to evaluate the biodiversity of both eubacterial and archaeal populations (Canganella F. and Bianconi G. 2009).

Some bacterial sequences were closely related to the sulfur-oxidizing bacterial group, involving the genus *Beggiatoa* and *Thiothrix*. Showing that these microorganisms may well represent a major microbial community in the bacterial mat of the cave. Other bacterial sequences were phylogenetically linked to the Delta-proteobacterial group, particularly to sulfate-reducing bacteria. Archaeal sequences were partially related to methanogen archaeal group, but the phylogenetic distance was still remarkable; so the involvement of a novel archaeal group can be considered. Other archaeal sequences were related to MG-1, which is a common uncultivable archaeal group in marine environment.

As regards the microscopic structure of bacterial mat inside the cave and sediments collected nearby a sulfidic spring along the main entrance of the "Grotta Azzurra," the distribution of various morphological forms is shown in Figures 5a–c. Filamentous microbial forms were abundant and morphologically similar to *Beggiatoa*, *Desulfonema*, *Leucothrix*, or *Thiothrix* species; morphology was, however, not enough to identify such organisms. Several cells showing either coccoid or rod morphologies were also observed in samples collected inside as well as outside the mat.

## Conclusions

As regards the blue and black holes, it has been shown that the dominant anoxigenic phototrophic bacteria in the microbial layers are member of the *Chromatiaceae* (Imhoff et al., 1998). The presence of dense phototrophic populations of purple sulfur bacteria particularly explains why the South Andros black hole appears black and not blue. Moreover, the sulfide profile data obtained in this site showed that sulfide concentration was low (30 μM) suggesting that biomass production by the purple sulfur bacteria was sulfide rather than light limited.

Another important point to consider is that the dense microbial phototrophic population probably plays a significant role in enhancing carbonate $CO_2$-mediated dissolution operated by heterotrophic bacteria. The effects of microbiological activity on degradation of limestone deposits have been described by several authors (Ehrlich, 1996; Golubic and Schneider, 1979; Paine et al., 1993) and similar observations were reported for the Bahamas cave systems from Smart et al. (1988).

Recent studies have shown that biotic oxidation of sulfide into sulfuric acid can occur in anoxic marine ecosystems due to chemoautotrophic sulfur-oxidizing bacteria such as *Beggiatoa* (Mattison et al., 1998; Vlasceanu et al., 1997, 2000). This biological process may also be involved in carbonate dissolution for the South Andros black hole but the role of sulfur-oxidizing bacteria needs

to be evaluated by further investigations. The same consideration may be valid for the blue hole in the Indian Ocean. In this site the occurrence of highly toxic sulfide and low oxygen content caused the death of the macrobenthos in deep waters, where a chemolithoautotrophic microbial community settled on the cave walls as mucilaginous and hardened short filaments of bacterial origin whose study is still in progress.

In the "Grotta Azzurra" cave of Capo Palinuro, fluids emitted from active springs with maximum temperatures of 25°C and enriched in dissolved sulfur species ($H_2S$, $S_2O_3^{-2}$) allowed the development of a significant micro- and macro-fauna, resembling in some way what occurs around hydrothermal vent sites (Jeanthon, 2000; Canganella, 2001).

Morphological/physiological observations were previously carried out by Mattison et al. (1998) on microbial mats in the "Grotta Azzurra" of Capo Palinuro. In recent studies both sampling and isolation were carried out regardless of the chemocline. Future investigations on the distribution of microbial populations will eventually lead to discrimination between more thermotolerant and more mesophilic species living above or below the chemocline; the same can be true for noncultivable species.

The characterized heterotrophic isolates partially represent the microbial ecology of the site, showing its biological complexity at a phylogenetic level. Moreover, the wide resistance of isolates to temperature, salinity and pH may be associated with the specific ecological system, an hypothesis that certainly deserves further investigations.

In general terms, similar environmental traits can be described for the blue hole in the Indian Ocean and the submarine caves of Palinuro Cape; first of all, the presence of elevated concentrations of hydrogen sulfide, ranging from 5 μM to 200 mM. A chemocline in the water column may be clearly observed in the blue hole of the Indian Ocean or in the black hole of the Bahamas, whereas in the submarine caves of Palinuro Cape the environmental borderline inside the habitat is represented by the threshold between upper anoxic, sulfide-rich freshwater and lower seawater.

As regards the autoctonous microflora, the blue hole of the Indian Ocean showed the presence of filamentous forms as described in the Palinuro caves but mucilaginous forms on the rocky side walls were not found in the latter; moreover sulfate-reducers and sulfide-oxidizers were also detected in both systems.

Some microbiological features of both systems are also shared with other sulfide-rich environments, such the presence of anaerobic methane oxidizers, filamentous bacteria, anaerobic phototrophs, and archaeal strains. However, the incomplete data set on the inhabitant microflora, the geological diversity of the systems described earlier, and their different geographical locations make a microbiological comparative study difficult. With no doubts the combination of different approaches and techniques may be a powerful tool to investigate further such astonishing ecosystems by a multiphasic approach.

As a matter of fact, further investigations on the microbial diversity in sulfide-rich, either marine or freshwater, caves will be based on traditional techniques of isolation coupled to simultaneous molecular investigations.

## Bibliography


Alvisi, M., Barbieri, F., and Colantoni, P., 1994a. Le grotte marine di Capo Palinuro. In Alvisi, M., Colantoni, P., Forti, P. (eds.), *Grotte Marine d'Italia*. Bologna: Memorie dell'Istituto Italiano di Speleologia, (pp 143–181).

Alvisi, M., Barbieri, F., Bruni, R., Cinelli, F., Colantoni, P., Grandi, F., and Maltoni, P., 1994b. La Grotta Azzurra di Capo Palinuro (Salerno). In Alvisi, M., Colantoni, P., Forti, P. (eds.), *Grotte Marine d'Italia*. Bologna: Memorie dell'Istituto Italiano di Speleologia, (pp 51–56).

Canganella, F., 2001. Hydrothermal vent communities. In *Encyclopedia of Life Sciences*. London: Macmillan.

Canganella, F., and Bianconi, G., 1999. Microbial investigations on submarine caves in the area of Cape Palinuro (Salerno, ITALY) in Brasilian Microbiology Society (Ed). In *Proceedings of the XX Meeting of the Microbiological Brasilian Society*, Oct 21–25, 2001, p. 223, Salvador, BA.

Canganella, F., and Bianconi, G., 2003. Microscopic investigations on the cell structure of autoctonous microflora in a sulphidic submarine cave (transl.). In *Fifth Congress FISV*, Oct 10–13, 2003, p 154, Rimini, Italy.

Canganella, F., Bianconi, G., and Maugeri, T., 2004. A multiphasic approach to investigate the microbial ecology of a Blue Hole in the Indian Ocean. In Extremophiles Meeting, September 19–23, 2004, p 83, Cambridge, MA.

Colantoni, P., Baldelli, G., Bianchi, C. N., Capaccioni, B., Morri, C., Mandrini, M., and Tassi, F., 2003. A cave flooded by marine water with hydrogen sulphide highlights the recent evolution of the Maldives (Indian Ocean): preliminary notes. *Le grotte d'Italia*, **4**, 29–37.

Ehrlich, H. L., 1996. Geomicrobiology, 3rd edn. New York: Marcel Dekker, pp 172–215.

Engel, A. S., Lee, N., Porter, M. L., Stern, L. A., Bennett, P. C., and Wagner, M., 2003. Filamentous "Epsilonproteobacteria" dominate microbial mats from sulfidic cave springs. *Applied and Environmental Microbiology*, **69**, 5503–5511.

Golubic, S. I., and Schneider, J., (1979). Carbonate dissolution. In Trudinger, P. A., Staine, D. J. (eds.), *Biogeochemical Cycling of Mineral-Forming Elements*. Amsterdam: Elsevier, pp. 107–129.

Herbert, R. A., Ranchou-Peyruse, A., Duran, R., Guyoneaud, R., and Scwabe, S., 2005. Characterization of purple sulphur bacteria from the South Andros Black Hole cave system: highlights taxonomic problems for ecological studies among the genera *Allochromatium* and *Thiocapsa*. *Environmental Microbiology*, **7**, 1260–1268.

Holmes, A. J., Tujula, N. A., Holley, M., Contos, A., James, J. M., Rogers, P., and Gillings, M. R., 2001. Phylogenetic structure of unusual aquatic microbial formations in Nullarbor caves, Australia. *Environmental Microbiology*, **3**, 256–264.

Imhoff, J. F., Süling, J., and Petri, R., 1998. Phylogenetic relationships among the *Chromatiaceae*, their taxonomic reclassification and description of the new genera *Allochromatium*, *Halochromatium*, *Isochromatium*, *Marichromatium*, *Thiococcus*, *Thiohalocapsa* and *Thermochromatium*. *International Journal of Systematic Bacteriology*, **48**, 1129–1143.

Jeanthon, C., 2000. Molecular ecology of hydrothermal vent microbial communities. *Antonie van Leeuwen.*, **77**, 117–133.
Marano-Briggs, K., 2000. *Water Chemistry, Bacterial Abundance and Anoxygenic Photosynthetic Bacteria in an Estuarine Blue Hole, Andros Island, The Bahamas*. PhD Thesis, George Mason University, Fairfax, VA.
Mattison, R. G., Abbiati, M., Dando, P. R., Fitzsimons, M. F., Pratt, S. M., Southward, A. J., and Southward, E. C., 1998. Chemoautotrophic microbial mats in submarine caves with hydrothermal sulphidic springs at Cape Palinuro, Italy. *Microbial Ecology*, **35**, 58–71.
Mylroie, J. E., Carew, J. L., and Moore, A. I., 1995. Blue holes: definition and genesis. *Carbonate and Evaporites*, **10**, 225–233.
Northup, D. E., Barns, S. M., Yu, L. E., Spilde, M. N., Schelble, R. T., Dano, K. E., Crossey, L. J., Connolly, C. A., Boston, P. J., Natvig, D. O., and Dahm, C. N., 2003. Diverse microbial communities inhabiting ferromanganese deposits in Lechuguilla and Spider Caves. *Environmental Microbiology*, **5**, 1071–1086.
Paine, S. G., Lingood, F. V., Schimmer, F., and Thrupp, T. C., 1993. *The Relationship of Microorganisms to the Decay of Stone*. London: Philosophical Transactions of the Royal Society, pp. 97–127.
Schwabe, S. J., 1998. The Black Hole. Caves and caving. *British Cave Research Association*, **80**, 1–22.
Schwabe, S. J., and Herbert, R. A., 2004. Black Holes of the Bahamas: what they are and why they are black. *Quaternary International*, **121**, 3–11.
Schwabe, S. J., Parkes, R. J., and Smart, P. L., 1997. Biogeochemical investigation of submerged cave systems (Blue Holes) within Bahamian carbonate platforms. In *97th Applied and Environmental Microbiology General Meeting*, May 4–7, 1997, p. 398. Miami, FL.
Smart, P. L., Dawans, J. M., Whitaker, F., 1988. Carbonate dissolution in a modern mixing zone. *Nature*, **335**, 811–813.
Sugita, T., Kikuchi, K., Makimura, K., Urata, K., Someya, T., Kamei, K., Niimi, M., and Uehara, Y., 2005. Trichosporon species isolated from guano samples obtained from bat-inhabited caves in Japan. *Applied and Environmental Microbiology*, **71**, 7626–7629.
Vlasceanu, L., Popa, R., and Kinkle, B., 1997. Characterization of *Thiobacillus thioparus* LV43 and its distribution in a chemoautotrophically based ecosystem. *Applied and Environmental Microbiology*, **63**, 33123–33127.
Vlasceanu, L., Sarbu, S., Engel, A. S., and Kinkle, B., 2000. Acidic, cave wall biofilms located in the Frasassi George, Italy. *Geomicrobiology*, **17**, 125–139.
Zhou, J., Gu, Y., Zou, C., and Mo, M., 2007. Phylogenetic diversity of bacteria in an earth-cave in Guizhou province, southwest of China. *Journal of Microbiology*, **45**, 105–112.

## Cross-references

Bacteria
Beggiatoa
Biofilms
Hydrothermal Environments, Marine
Karst Ecosystems
Metals, Acquisition by Marine Bacteria
Microbial Communities, Structure, and Function
Microbial Mats
Nanocrystals, Microbially Induced
Siderophores
Sulfate-Reducing Bacteria
Sulfide Mineral Oxidation
Sulfur Cycle

# MICROBIAL MATS

Joachim Reitner
University of Göttingen, Göttingen, Germany

## Synonyms

Algal mats; Bacterial mats; Biomats; Thick biofilms

## Definition

Microbial mats are often centimeter-thick multilayered structures of microorganisms, mainly bacteria, archaea, fungi, and sometimes these mats are enriched with protozoans. Microbial biofilms are in contrast much thinner (10–100 μm) than microbial mats and have a different architecture (Characklis and Wilderer, 1989). Microbial mats grow at interfaces between different types of material, mostly on moist surfaces, but some of them are also found in dry environments like deserts (e.g., Stal and Caumette, 1994; Characklis and Wilderer, 1989). They colonize environments located in high altitude, they are common in the Deep Biosphere, in subterranean environments with temperatures from −40°C to +120°C. There are also common as endosymbiontic structures, for example, in animals. They are very common in extreme environments like hydrothermal vents, cold seeps, and alkaline and hypersaline lakes (Van Dover, 2000; Pedersen, 2006; Arp et al., 2003; Riding and Awramik, 2000).

## Geobiological implications

A microbial mat consists of several layers dominated by specific types of microorganism (Figures 1 and 2). Although the composition of individual mats varies depending on the environment, as a rule the by-products of each group of microorganisms serve as energy source for other groups. Different types of microorganisms dominate different layers based on their comparative advantage (Canfield and Des Marais, 1993; Allison et al., 2000). Ecological relationships between different groups are a combination of competition and cooperation. The metabolic capabilities of bacteria and archaea are generally depend on their phylogeny. In a wet environment where sunlight is available, the upper layers are generally dominated by aerobic consortia like cyanobacteria (Figure 1), while the lowest layers are normally dominated by anaerobic microorganisms such as sulfate-reducing bacteria, methanogenic and/or methanotrophic archaea, or general archaea. Marine mats may grow to a few centimeters in thickness, of which only the top few millimeters are oxygenated. Microbial mats are held together and bound to their substrates by sugar- and protein-rich extracellular polymeric substances (EPS), which they secrete (Decho et al., 2005; Wingender et al., 1999). In many cases, some of these microorganisms form filaments (threads), which tangle and thus increase the microbial


**Microbial Mats, Figure 1** Phototrophic 5-cm-thick microbial mat from a hypersaline lake (Lake 21) on Kiritimati Island (Kiribati, Line Islands). 1 – Orange layer with cyanobacteria; 2 – Green layer with green bacteria, zone with the highest diversity of prokaryotes; 3 – Purple layer, zone with photosynthetic non-sulfur purple bacteria (alpha-, and beta proteobacteria); 4 – Gray layer with sulfate-reducing bacteria and archaea, zone of heavy carbonate and gypsum mineralization within degrading extracellular polymeric substances (EPS). The entire mat is interspersed with authigenic, spherulitic aragonite, and gypsum crystals that are growing within EPS.

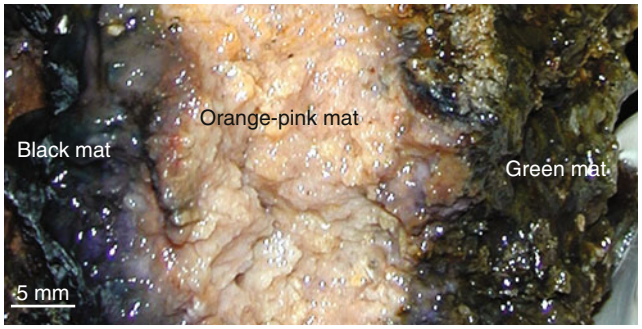


**Microbial Mats, Figure 2** Anaerobic microbial mat from a cold seep environment of the Black Sea. Black mat represents the outer margin of the microbial mat. This mat is dominated by ANME 2 archaea and greigite-bearing sulfate reducing bacteria (GHOSTDABS field, for details see Reitner et al., 2005; Reitner, 2010). Orange-pink mat represents an archaea-(ANME1)-dominated mat portion. The green mat represents the inner most area close to the methane vent. This mat is also dominated by ANME archaea, Crenarcheota, and anaerobic bacteria. The entire mat is stabilized by authigenic methane-related aragonite and calcite crystal aggregates, which are also growing within EPS.

colonies structural strength, especially if the filaments have sheaths.

Microbial mats are the earliest complex form of life on Earth. There is a fossil record from 3,500 million years ago, and they have always been the most important members and maintainers of earth ecosystems (Allwood et al., 2006; van Kranendonk, 2007). Early Precambrian microbial mats are the first evolved highly complexly organized multicellular organisms. Microbial mats occasionally mineralize if the ionic strength in the aquatic environment allows it. The mineralized structures are known as stromatolites and thrombolites and they represent the most important organo-sedimentary fabrics since the early beginning of microbial life on earth (Burne and Moore, 1987; Riding, 2000). Originally, microbial mats first occurred at hydrothermal vents for energy. Since the late Precambrian microbial mats have also played an important role at cold hydrocarbon seeps, so-called Cold Seeps. Most of the Cold Seeps are methane vents coupled with hydrogen sulfur microbial metabolism (Reitner et al., 2005) (Figure 2). However, phototrophic microorganisms such as cyanobacteria, unicellular algae (e.g., diatoms), and related consortia are the most abundant microorganisms in the formation of microbial mats (e.g., Arp et al., 2010). Within subterranean environments iron-oxidizing microbial consortia show a strong ability to form thick microbial mats (Kurz et al., 2010).

Microbial mats are the context within which the first multicellular organisms evolved. Sponges are, for example, highly evolved microbial mats with a mutual relationship with eukaryote choanoflagellates. May be the Vendobionta, large Ediacaran organisms with characteristic quilt bauplan are part of well-developed microbial mats and may themselves be large colonies of various microbial communities (Seilacher, 1999; Schieber et al., 2007; Steiner and Reitner, 2001).

## Conclusion

Microbial mats are normally cm-thick microbial communities often related with microbially induced mineral precipitates (calcite, aragonite, iron-oxides etc.). Characteristic for these mats is a multilayered structure which represents various microbial communities with different metabolic activities. In phototrophic microbial mats (e.g., cyanobacteria) dominate the uppermost layers whereas within the deep layers of the mats anaerobic microbes dominate like sulphate reducing bacteria and archaea. Microbial mats are complex multicellular systems which exhibit some accordance to basic metazoans like sponges. It is speculated that microbial mats are a model for the basic metazoan bauplan.

## Bibliography

Allison, D. G., Gilbert, P., Lappin-Scott, H. M., and Wilson, M., 2000. *Community Structure and Co-operation in Biofilms*. Cambridge: Cambridge University Press, 349 p.

Allwood, A. C., Walter, M. R., Kamber, B. S., Marshal, C. P., and Burch, I. W., 2006. Stromatolite reef from the Early Archaean era of Australia. *Nature*, **441**,714–717.

Arp, G., Reimer, A., and Reitner, J., 2003. Microbialite formation in seawater of increased alkalinity, Satonda Crater Lake, Indonesia. *Journal of Sedimentary Research*, **73**, 105–127.

Arp, G., Bissett, A., Brinkmann, N., Cousin, S., de Beer, D., Friedl, T., Mohr, K. I., Neu, T. R., Reimer, A., Shiraishi, F., Stackebrandt, E., and Zippel, B., 2010. Tufa-forming biofilms of German karstwater streams: microorganisms, exopolymers, hydrochemistry and calcification. In Rogerson, M., and Pedley, M. M. (eds.), *Tufas and Speleothems: Unravelling the Microbial and Physical Controls*. London: Geological Society Special Publication 336, pp. 83–118.
Burne, R. V., and Moore, L., 1987. Microbialites; organosedimentary deposits of benthic microbial communities. *Palaios*, **2**, 241–254.
Canfield, D. E., and Des Marais, D. J., 1993. Biogeochemical cycles of carbon, sulfur, and free oxygen in a microbial mat. *Geochimica et Cosmochima Acta*, **57**, 3971–3984.
Characklis, W. G., and Wilderer, P. A., 1989. Structure and function of Biofilms. *Life Sciences Research Report*, **46**, 1–387 (Wiley).
Decho, A. W., Visscher, P. T., and Reid, P., 2005. Production and cycling of natural microbial exopolymers (EPS) within a marine stromatolite. *Palaeogeography, Palaeoclimatology, Palaeoecology*, **219**, 71–86.
Kurz, J., Simon, K., Heim, C., Reitner, J., Nadia-Valérie Quéric, N.-V., and Volker Thiel, V., 2010. Trace element and biomarker signatures in iron-precipitating microbial mats from the tunnel of Äspö (Sweden). In Reitner, J., Quéric, N.-V., and Arp, G. (eds.), *Advances in Geobiology of Stromatolite Formation, Proceedings of the Kalkowsky Symposium held in Göttingen 2008*. Lecture Notes of Earth Sciences (Springer).
Pedersen, K., 2006. Microbial life in deep granitic rock. *FEMS Microbiology Reviews*, **20**, 399–414.
Reitner, J., 2010. Architecture of archaeal-dominated microbial mats from Cold Seeps in the Black Sea (Dnjepr Canyon, Lower Crimean Shelf). In Seckbach, J., and Oren, A. (eds.), *Microbial Mats, Modern and Ancient Microorganisms in Stratified Systems. - Cellular Origin, Life in Extreme Habitats and Astrobiology*, 14 (Springer).
Reitner, J., Peckmann, J., Reimer, A., Schumann, G., and Thiel, V., 2005. Methane-derived carbonate build-ups and associated microbial communities at cold seeps on the lower Crimean shelf (Black Sea). *Facies*, **51**, 66–79.
Riding, R., and Awramik, S. M. (eds.), 2000. *Microbial Sediments*. Berlin: Springer, 331 pp.
Riding, R., 2000. Microbial carbonates: the geological record of calcified bacterial-algal mats and biofilms. *Sedimentology*, **47**(Supplement 1), 179–214.
Schieber, J., Bose, P. K., Eriksson, P. G., Banerjee, S., Sarkar, S., Altermann, W., and Catuneanu, O., 2007. *An Atlas of Microbial Mat Features Preserved Within the Siliciclastic Rock Record*. Amsterdam, The Netherlands: Elsevier.
Seilacher, A., 1999. Biomat-related lifestyles in the Precambrian. *Palaios*, **14**, 86–93.
Stal, L., and Caumette, P., 1994. Microbial mats. NATO ASI Series, Series G. *Ecological Sciences*—. Berlin: Springer, Vol. 35, pp. 1–463.
Steiner, M., and Reitner, J., 2001. Evidence of organic structures in Ediacara-type fossils and associated microbial mats. *Geology*, **29**, 1119–1122.
Van Dover, C. L., 2000. *The Ecology of Deep-Sea Hydrothermal Vents*. Princeton: Princeton University Press, 424 p.
Van Kranendonk, M. J., 2007. A review of the evidence for putative Paleoarchean life in the Pilbara Craton. In Van Kranendonk, M. J., Smithies, R. H., and Bennet, V. (eds.), *Earth's Oldest Rocks – Developments in Precambrian Geology*. Amsterdam, The Netherlands: Elsevier, pp. 855–896.
Wingender, J., Neu, T. R., and Flemming, H.-C., 1999. Microbial Extracellular Polymeric Substances; Characterization, Structure, and Function. Berlin: Springer, 258 p.

## Cross-references

Anaerobic Oxidation of Methane with Sulfate
Archaea
Bacteria
Biofilms and Fossilization
Calcite Precipitation, Microbially Induced
Chemolithotrophy
Cold Seeps
Cyanobacteria
Diatoms
Ediacaran Biota
Extracellular Polymeric Substances (EPS)
Mat-Related Sedimentary Structures
Microbial Biomineralization
Microbial Communities, Structure, and Function
Microbial Degradation
Microbial-Metal Binding
Microbialites, Modern
Mud Mounds
Ores, Microbial Precipitation and Oxidation
Protozoa (Heterotroph, Eukaryotic)

# MICROBIAL SILICIFICATION – BACTERIA (OR PASSIVE)

Kurt O. Konhauser, Brian Jones
University of Alberta, Edmonton, Alberta, Canada

## Definition

The encrustation, impregnation, and/or replacement of microbial tissue by silica minerals, usually opal-A.

## Overview

Silica precipitation is an important geological process in many modern geothermal systems where venting of supersaturated solutions leads to the formation of finely laminated siliceous sinters around geyser and hot spring vents and on their discharge aprons. The spring waters, which typically originate from deep, hot reservoirs, at equilibrium with quartz, commonly contain dissolved silica concentrations significantly higher than the solubility of amorphous silica at 100°C (Fournier, 1985). Therefore, when these fluids are discharged at the surface, decompressional degassing, rapid cooling to ambient temperatures, evaporation, mixing, and changes in solution pH collectively cause the solution to suddenly become supersaturated with respect to amorphous silica (also known as opal-A). In such supersaturated solutions, the discharged monomeric silica, $Si(OH)_4$, polymerizes, initially to oligomers (e.g., dimmers, trimers, and tetramers), and eventually to polymeric species with spherical diameters of 1–5 nm, as the silanol groups (-Si-OH-) of each oligomer condense and dehydrate to produce the siloxane (-Si-O-Si-) cores of larger polymers. The polymers grow in size through Ostwald ripening such that a bimodal

composition of monomers and particles of colloidal dimensions (>5 nm) are generated. The latter stay in suspension due to the external silanol groups exhibiting a residual negative surface charge, they coagulate via cation bridging and nucleate homogenously, or they precipitate heterogeneously on a solid substratum (Ihler, 1979).

Siliceous sinters commonly contain numerous mineralized microorganisms (e.g., bacteria, algae, fungi) in varying stages of preservation (Jones et al., 1997; Konhauser et al., 2001). Examination under the scanning or transmission electron microscopes (SEM/TEM) shows that their preservation typically involved the precipitation of spheroidal, amorphous silica grains on (i.e., encrustation) or within (i.e., impregnation, replacement) the walls and/or sheaths of the microbes. The manner in which a particular microbe is preserved depends upon the balance between the timing of opal-A precipitation/impregnation and decay of the soft tissues of the microbe (Figure 1). In many cases, a microbe merely acts as a template as opal-A is precipitated around its outer surface. Such encrustation begins with the attachment of preformed silica colloids, on the order of only 10 s of nanometers in diameter, to the cell surfaces (Figure 2a). Those silica particles then grow in size, and may reach micrometer diameters in size. If opal-A precipitation is sustained, those particles invariably coalesce until the individual precipitates are no longer distinguishable, resulting at times in entire colonies being cemented together in a siliceous matrix (Figures 2b and 3a–d).

Replacement, which involves impregnation of the organic tissue by opal-A, can lead to superb preservation of the microbes (Figure 3e). Jones et al. (2001, their Fig. 8), for instance, illustrated silicified specimens of *Calothrix* in which the sheath and outer splayed lamina are still evident. Septa may also be preserved in this way (Figure 3h). If encrustation is the sole process, then many silicified filamentous microbes will be evident only as hollow tubes (Figure 3g and i). Subsequent filling of that tube with opal-A will produce a solid opal-A rod, with the size of the original lumen/filamentous microbe only being apparent if there is a discontinuity preserved (e.g., Figure 3f). Irrespective of the nuances, the silicification of microbes must take place quickly if they are to be preserved, and certainly before the microbes undergo any degree of desiccation and degradation (Jones et al., 2001). This notion is supported by the fact that the three-dimensional form of most microbes is still apparent following silicification (Figure 3j–l). Indeed, some microbes are coated with silica while they are still viable (Phoenix et al., 2000) and it seems that silicification must take place in a matter of days in order for the three-dimensional morphology to be preserved.

Plant material bathed in the polymerizing solutions may be encrusted, impregnated, and/or replaced with opal-A similar to microbes. In many of the hot spring systems of New Zealand, for example, grass stems, pieces of wood, and leaves are heavily encrusted with opal-A but their tissues have usually not been replaced. In fact, the grass is commonly still growing even though encased by opal-A. In contrast, wood and leaves on the discharge apron around Geysir, Iceland that have been superbly preserved through replacement have not been encrusted with opal-A. Similar comparisons apply to some of the microbes. The factors that dictate encrustation as opposed to replacement are currently not understood as there are no obvious correlations between preservation style and the chemical attributes of the associated waters.

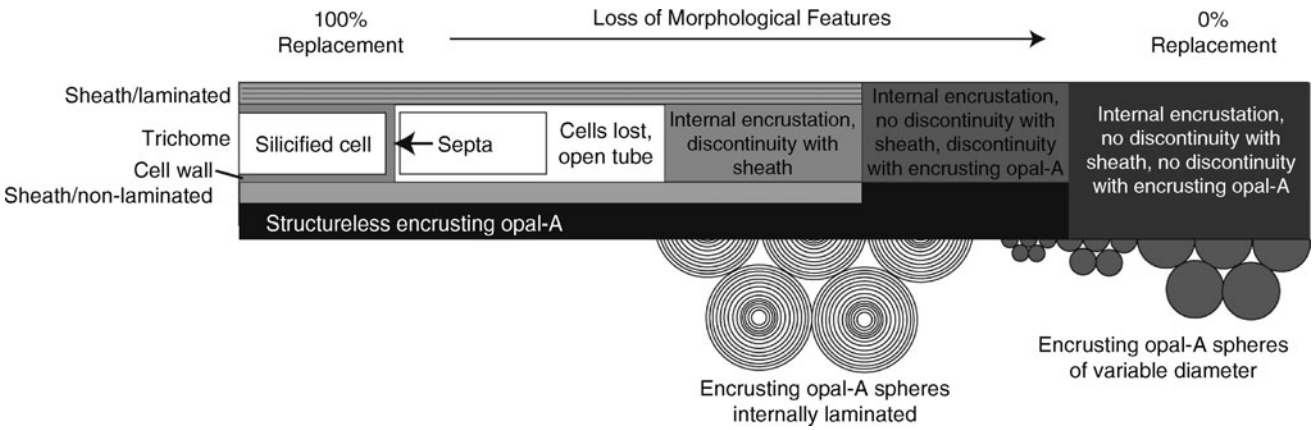


**Microbial Silicification – Bacteria (or Passive), Figure 1** Schematic longitudinal cross-section of a sheathed filamentous microbe showing morphological variations that can develop as a result of silicification. Modified form Jones et al. (2001, their Fig. 10).

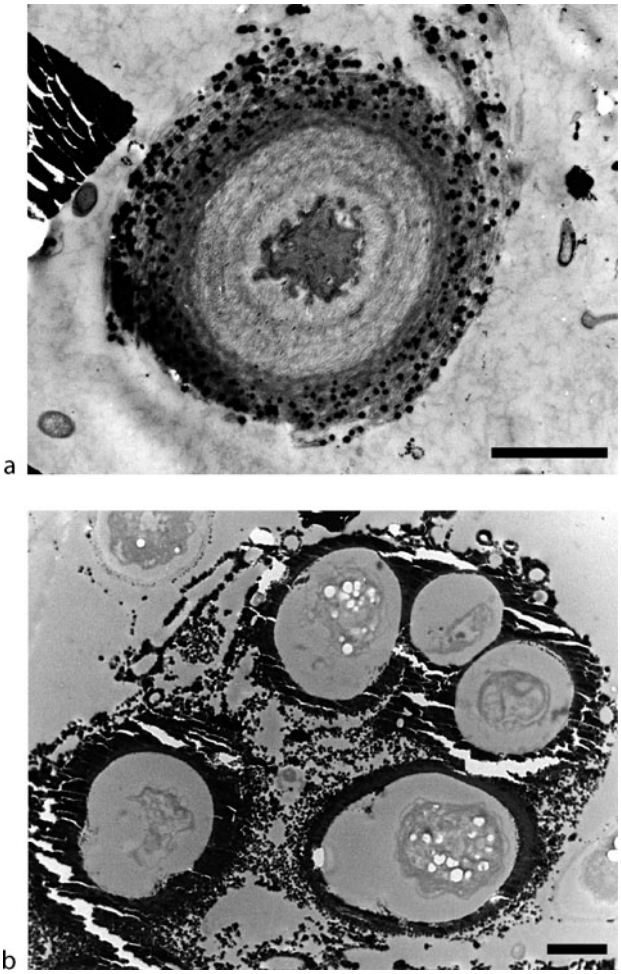


**Microbial Silicification – Bacteria (or Passive), Figure 2** Transmission electron micrographs (TEM) of cyanobacteria from a geyser outflow channel at Strokkur, Iceland. (**a**) Cell showing abundant silica spheres on, and within the surrounding sheath material. (**b**) Colony of unidentified cyanobacteria that are completely encrusted by silica matrix. Remnants of cytoplasm are still evident inside some cells. Scale bars = 3 μm.

Despite the fact that many silicified microbes appear to be superbly preserved, only a limited number of features are usually apparent. Even in the best-preserved specimens, features are generally limited to overall morphology, filament diameter, presence/absence of branching, presence/absence of a sheath, and/or size of cells. Identification in terms of extant taxa is usually difficult because the limited numbers of morphological features apparent in the silicified forms are insufficient unless they are particular distinctive in some way. This issue is compounded by the fact that many extant taxa are defined by their DNA characteristics and/or the conditions under which they were cultured in a laboratory setting. In most cases, therefore, the identification of silicified microbes must be done with caution.

The role that the microbes (and some plant material) play in their own silicification has been a matter of debate. Being soft-bodied organisms they do not "actively" mediate amorphous silica formation in the manner of diatoms, radiolarians, and sponges. In contrast, bacteria, algae, and fungi facilitate silica precipitation by creating a suitable microenvironment and/or template for opal-A precipitation. For example, they may produce organic ligands that promote the mineralization process (Lalonde et al., 2005), or they may change the pH immediately around the cell through their metabolic activity, and in this regard, induce supersaturation with respect to opal-A (Amores and Warren, 2007). At other times, the microbes may simply act as solid surfaces for silica precipitation and exert no direct influence over the process (Walter et al., 1972).

Experimental evidence seems to indicate that the microbial role in the silicification processes is incidental and not limited to any particular taxa. First, microbes have little affinity for monomeric silica, even at high bacterial densities and low pH conditions where most organic functional groups are fully protonated and neutrally charged (Fein et al., 2002). Second, at supersaturated conditions, there appears to be very little difference in the rates or magnitude of silica precipitated between microbial and microbial-free systems (Yee et al., 2003; Benning et al., 2004). Third, silicification occurs on dead cells, and continues autocatalytically and abiogenically for some time after their death due to the high reactivity of the newly formed silica. This notion is supported by microscopic examination of thermal spring deposits where it has been shown that the silica precipitated in the porous spaces between filaments has the same basic motif as the silica precipitated on the original filaments (Jones et al., 1998). From these observations, it can be inferred that at high silica levels there is such a strong chemical driving force for silica polymerization, homogeneous nucleation, and ultimately silica precipitation that there is no obvious need for microbial catalysis.

Despite the observations above, the fact that there are species-specific patterns of silicification infers that some microbes may influence silicification in some way. The initial coating of opal-A spheres around microbes in Iodine Pool in the Waimangu geothermal area, for example, are consistent in size and highly organized in terms of their distribution (Jones et al., 2004, their Fig. 9). In contrast, the outer layer of opal-A beads is larger, variable in diameter, and follows no set distribution pattern. Thus, it seems that some aspect of the microbes may have influenced the initial phase of opal-A precipitation but not later phases. This seems feasible given that the initial layer of opal-A precipitates would have effectively encased the microbes and thereby isolated their surfaces from the water. Furthermore, different microbes exhibit different degrees of silicification. This is not surprising

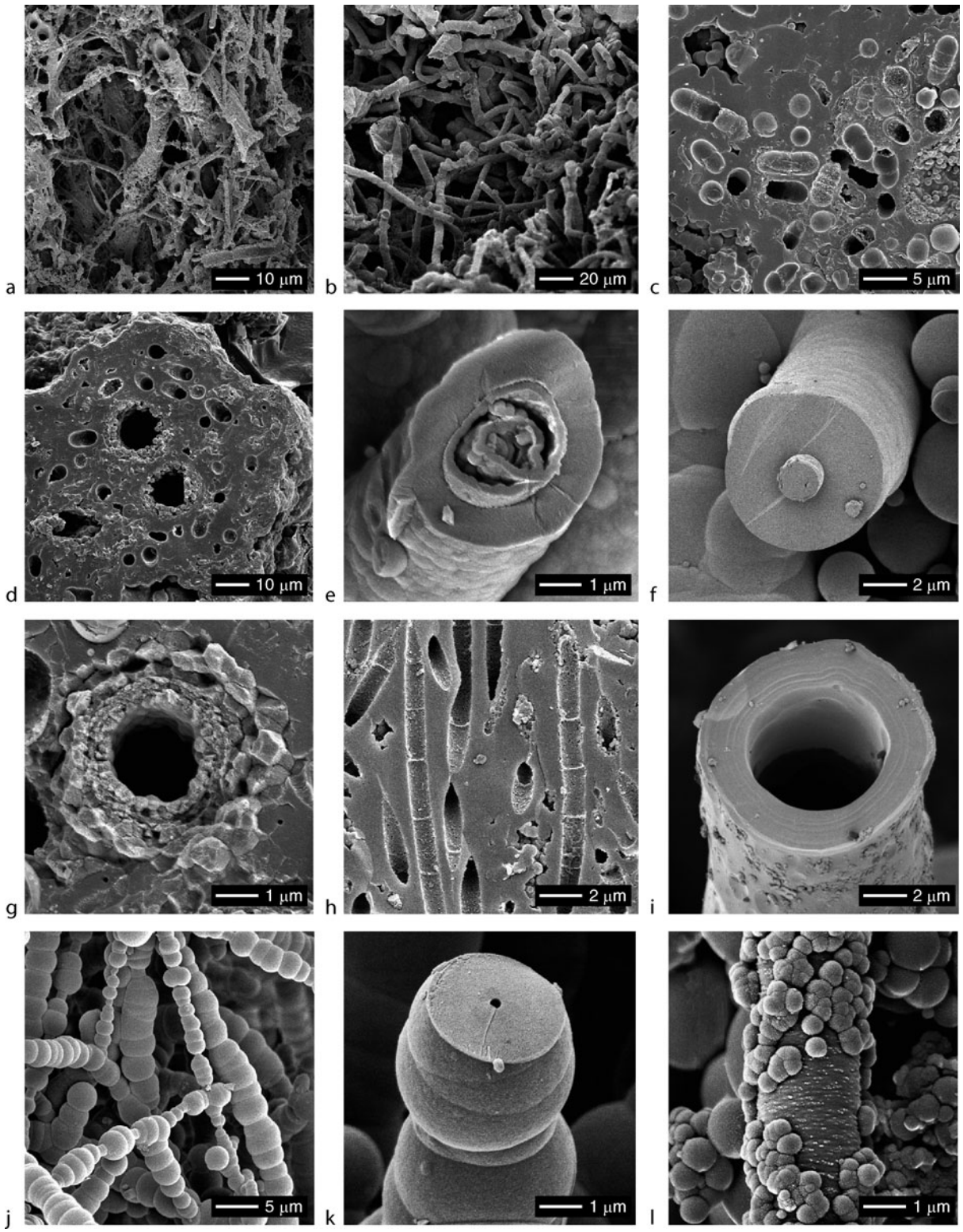


**Microbial Silicification – Bacteria (or Passive), Figure 3** (Continued)

given that the actual mechanisms of silicification rely, in part, on the microbes providing reactive surface ligands that adsorb silica from solution, and accordingly, reduce the activation energy barriers to heterogeneous nucleation (Konhauser et al., 2004). This means that cell surface charge may have a fundamental control on the initial silica sorption process.

At present there appears to be three different mechanisms by which microbes bind dissolved/colloidal silica; (1) hydrogen bonding, (2) cation bridging, and (3) electrostatic interactions (Figure 4). In the first instance, Phoenix et al. (2002) showed that the polysaccharide-rich sheath of *Calothrix* is electrically neutral at pH 7, and opal-A precipitation occurs through hydrogen bonding between the hydroxy groups associated with the sugars and the hydroxyl ions of the dissolved silica. Second, the highly anionic nature of most bacteria, such as *Bacillus subtilis*, limits opal-A from ocurring on the cell wall, likely as a result of electrostatic charge repulsion between the anionic ligands of the organic functional groups and the negatively-charged silica species (Phoenix et al., 2003). Therefore, in order for silica to sorb, some form of cation bridge (e.g., $Fe^{3+}$, $Al^{3+}$) is necessitated (Fein et al., 2002). Third, some species, such as *Aquificales*, produce protein-rich biofilms that contain sufficient cationic amino groups ($NH_4^+$) to electrostatically react with dissolved silica (Lalonde et al., 2005).

Given that a wide assortment of microbes live in environments where opal-A is being precipitated, it is important to determine if those species survive the mineralization process. In this regard, Phoenix et al. (2000) tested cell viability during biomineralization, and observed that experimental encrustation of *Calothrix* by silica was not notably detrimental to the organisms. Even after 12 days of incubation in a 600 mg $l^{-1}$ silica solution, during which many of the filaments developed extensive mineral crusts up to 5 μm thick, the cells still fluoresced, they continued to generate oxygen and the mineralized colonies exhibited comparable rates of photosynthesis to the non-mineralized colonies. Interestingly, silica precipitation only occurred upon the outer surface of sheath material from viable cyanobacterial cells – no viable cells exhibited internal or cell wall mineralization. This contrasts with dead and lysed cells where mineralization of the cell wall and cytoplasm had occurred. In a more recent study with the thermophilic chemolithoautotroph *Sulfurihydrogenibium azorense*, Lalonde et al. (2005) showed that the bacterium, when grown as a $H_2$-oxidizer, reacted to increasing silica concentrations by producing excess protein that appears linked to biofilm production. Since silicification was not observed directly on the cell surface, they proposed that *S. azorense* may prevent cellular silicification to some degree by providing abundant reactive sites in the biofilm matrix and regulating biofilm production appropriately, with potential contributions from metabolic effects. Thus, it appears that some microbes can thrive in silica-rich environments because they form protective layers that isolate the cells from the potentially damaging effects of silicification.

## Summary

Microbial silicification includes the encrustation, impregnation, and replacement of cells by amorphous silica. Most microbes play a passive role in the mineralization process by providing organic surfaces that facilitate the binding of silica polymers and colloids from solution. These sorption reactions can occur by either (1) hydrogen bonding between dissolved silica and cell hydroxy functional groups, (2) cation bridging between anionic cell functional groups and the silica, or (3) direct electrostatic interaction of silica with cell surface ammonium groups.

**Microbial Silicification – Bacteria (or Passive), Figure 3** Examples of silicified microbes from various hot-spring sinters in the Taupo Volcanic Zone of the North Island of New Zealand. (**a**) Silicified microbial mat formed of small-diameter filamentous microbes wrapped around erect, large-diameter filamentous microbes. Tokaanu geothermal area. (**b**) Silicified microbial mat formed of interwoven small-diameter filaments. Waiotapu geothermal area. (**c**) Group of silicified bacteriform microbes embedded in opal-A matrix. Tokaanu geothermal area. (**d**) Two large-large diameter filamentous microbes (*Calothrix*?) with small-diameter filamentous microbes (*Phormidium*?) wrapped around them, all encased by opal-A. Tokaanu geothermal area. (**e**) Transverse cross-section through silicified microbe showing what appears to be opal-A encrusting a sheath; note possible silicified microbial material inside the sheath. Tokaanu geothermal area. (**f**) Transverse cross section through a silicified filamentous microbe showing opal-A encrusted around a solid opal-A core. Iodine Pool, Waimangu. (**g**) Transverse cross-section through a laminated sheath, probably from *Calothrix*, with open lumen. Tokaanu geothermal area. (**h**) Longitudinal cross-section through small-diameter filamentous microbes showing septa, and hence cell-size. Tokaanu geothermal area. (**i**) Transverse cross-section through a silicified filamentous microbe. Note growth lines in encrusting silica that record progressive precipitation of opal-A around the original filament. Waikite Geyser, Whakarewarewa. (**j**) General view of group of filamentous microbes that have been encrusted by opal-A spheres of variable diameter. Waikite Geyser, Whakarewarewa. (**k**) Cross-section through filamentous microbe showing small open lumen and variable diameter of encrusting opal-A. Waikite Geyser, Whakarewarewa. (**l**) Filamentous microbe showing silicified cell wall or sheath encrusted by small opal-A spheres. Iodine Pool, Waimangu.

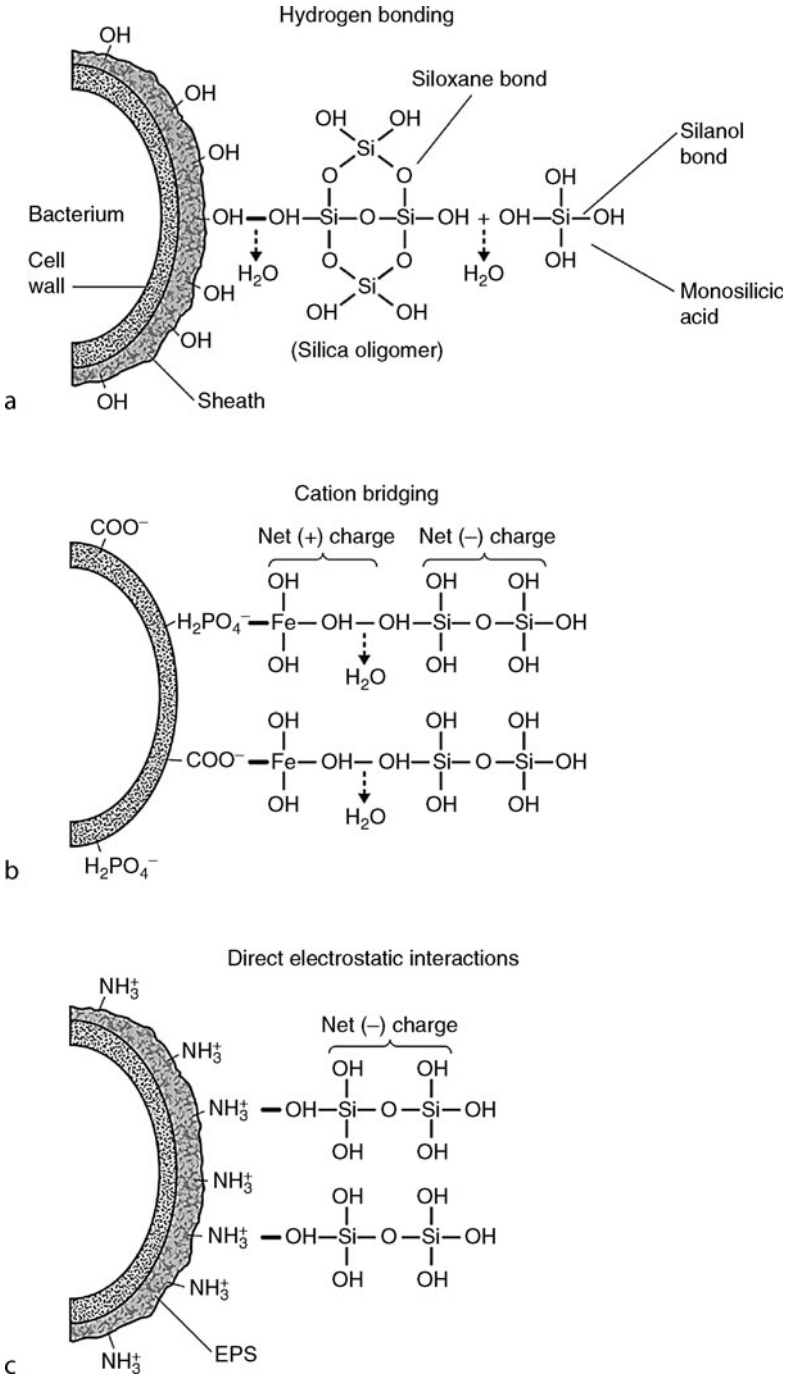


**Microbial Silicification – Bacteria (or Passive), Figure 4** Three mechanisms by which microorganisms silicify: (**a**) hydrogen bonding between silica polymers with hydroxy groups in sheaths of *Calothrix*; (**b**) cation bridging between negatively-charged cell walls in *Bacillus subtilis* and silica; and (**c**) electrostatic interactions between silica and positively-charged amino groups in the biofilm of *Sulfurihydrogenibium azorense*. Reproduced from Konhauser (2007) with permission of Wiley-Blackwell.

## Bibliography

Amores, D. A., and Warren, L. A., 2007. Identifying when microbes biosilicify: the interconnected requirements of acidic pH, colloidal $SiO_2$ and exposed microbial surface. *Chemical Geology*, **240**, 298–312.

Benning, L. G., Phoenix, V. R., Yee, N., and Konhauser, K. O., 2004. The dynamics of cyanobacterial silicification: an infrared micro-spectroscopic investigation. *Geochimica et Cosmochimica Acta*, **68**, 743–757.

Fein, J. B., Scott, S., and Rivera, N., 2002. The effect of Fe and Si adsorption by *Bacillus subtilis* cell walls: insights into non-metabolic bacterial precipitation of silicate minerals. *Chemical Geology*, **182**, 265–273.
Fournier, R. O., 1985. The behaviour of silica in hydrothermal solutions. *Reviews in Economic Geology*, **2**, 45–61.
Ihler, R. K., 1979. *The Chemistry of Silica*. New York: Wiley-Interscience.
Jones, B., Renaut, R. W., and Rosen, M. R., 1997. Biogenicity of silica precipitation around geysers and hot-spring vents, North Island, New Zealand. *Journal of Sedimentary Research*, **67**, 88–104.
Jones, B., Renaut, R. W., and Rosen, M. R., 1998. Microbial biofacies in hot-spring sinters: a model based on Ohaaki Pool, North Island, New Zealand. *Journal of Sedimentary Research*, **68**, 413–434.
Jones, B., Renaut, R. W., and Rosen, M. R., 2001. Taphonomy of silicified filamentous microbes in modern geothermal sinters – implications for identification. *Palaios*, **16**, 580–592.
Jones, B., Konhauser, K. O., Renaut, R., and Wheeler, R., 2004. Microbe silicification in Iodine Pool, Waimangu geothermal area, North Island, New Zealand: implications for recognition and identification of ancient silicified microbes. *Journal of the Geological Society of London*, **161**, 983–993.
Konhauser, K. O., Phoenix, V. R., Bottrell, S. H., Adams, D. G., and Head, I. M., 2001. Microbial-silica interactions in modern hot spring sinter: possible analogues for Precambrian siliceous stromatolites. *Sedimentology*, **48**, 415–435.
Konhauser, K. O., Jones, B., Phoenix, V. R., Ferris, F. G., and Renaut, R. W., 2004. The microbial role in hot spring silicification. *Ambio*, **33**, 552–558.
Lalonde, S. V., Konhauser, K. O., Reysenbach, A.-L., and Ferris, F. G., 2005. Thermophilic silicification: the role of Aquificales in hot spring sinter formation. *Geobiology*, **3**, 41–52.
Phoenix, V. R., Adams, D. G., and Konhauser, K. O., 2000. Cyanobacterial viability during hydrothermal biomineralization. *Chemical Geology*, **169**, 329–338.
Phoenix, V. R., Martinez, R. E., Konhauser, K. O., and Ferris, F. G., 2002. Characterization and implications of the cell surface reactivity of the cyanobacteria *Calothrix* sp. *Applied and Environmental Microbiology*, **68**, 4827–4834.
Phoenix, V. R., Konhauser, K. O., and Ferris, F. G., 2003. Experimental study of iron and silica immobilization by bacteria in mixed Fe-Si systems: implications for microbial silicification in hot-springs. *Canadian Journal of Earth Sciences*, **40**, 1669–1678.
Walter, M. R., Bauld, J., and Brock, T. D., 1972. Siliceous algal and bacterial stromatolites in hot spring and geyser effluents of Yellowstone National Park. *Science*, **178**, 402–405.
Yee, N., Phoenix, V. R., Konhauser, K. O., Benning, L. G., and Ferris, F. G., 2003. The effect of cyanobacteria on silica precipitation at neutral pH: implications for bacterial silicification in geothermal hot springs. *Chemical Geology*, **199**, 83–90.

## Cross-references

Cherts
Cyanobacteria
Diatoms
Hydrothermal Environments, Terrestrial
Microbial Biomineralization
Microbial Surface Reactivity
Radiolaria

# MICROBIAL SURFACE REACTIVITY

David A. Fowle, Kurt O. Konhauser
University of Alberta, Edmonton, Alberta, Canada

## Definition

The chemical charge on a cell surface caused by the deprotonation/protonation of organic functional groups.

## Overview

Similar to an aqueous organic acid, bacterial cell surfaces can either bind or release protons ($H^+$) into solution depending upon the solution pH. In the case of the latter, this deprotonation process, which accurately mimics a number of the functional groups associated with cell surfaces, leads to the formation of an organic anion, or ligand. Unlike an aqueous organic acid, which exhibits proton buffering over a narrow pH range ( $\pm$1–2 units), bacterial cell walls have continuous buffering capacity over a wide range of pH values which span most geologic settings (pH 2–10). Ultimately, most surface reactivity of bacteria with its external environment results from the enhanced electronegativity of the cell wall as these functional groups deprotonate. In its most simplistic form, deprotonation can be expressed by the following equilibrium reaction:

$$B - AH^0 \leftrightarrow B - A^{-1} + H^{+1}, \quad (1)$$

where B denotes a bacterium to which each protonated ligand type, A, is attached. The distribution of protonated and deprotonated sites can be quantified with the corresponding mass action equation:

$$K_a = \frac{[B - A^{-1}][H^{+1}]}{[B - AH^0]}, \quad (2)$$

where $K_a$ is the dissociation constant; $[B{-}A^{-1}]$ and $[B{-}AH^0]$ represent the concentration of exposed deprotonated and protonated ligands on the bacterium, respectively (in mol $l^{-1}$); and $[H^+]$ represents the activity of protons in solution. Each functional group has its own $K_a$, and based on equation (2), the pH at which $[B{-}A^{-1}]$ and $[B{-}AH]$ are equivalent is known as the p$K_a$ value, where $pK_a = -\log_{10}K_a$. At pH $<$ p$K_a$ surfaces are protonated and at pH $>$ p$K_a$ they are deprotonated.

The ionization of functional groups provides an electrical charge ($[L]_T$ represented in mol $mg^{-1}$), which in the laboratory can be calculated as a function of pH from the difference between total base or acid added to a suspension of organic material and the equilibrium $H^+$ and $OH^-$ ion activities (Reaction 3):

$$[L]_T = \frac{C_a - C_b \pm [OH^-] - [H^{+1}]}{S} \quad (3)$$

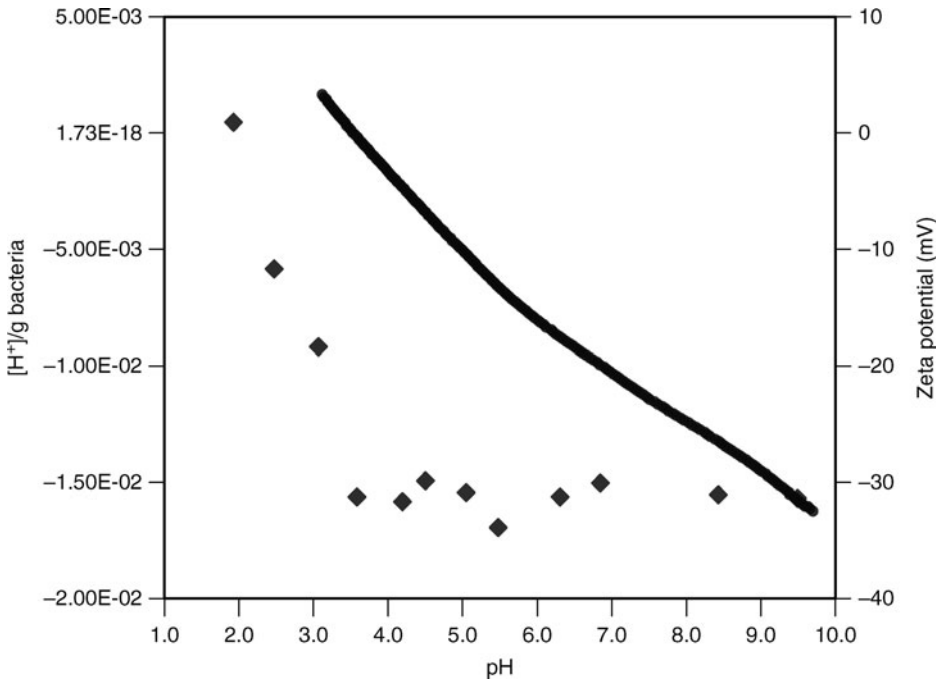


**Microbial Surface Reactivity, Figure 1** Experimental data demonstrating the buffering capacity of *Bacillus subtilis* during acid–base titration (circles; molality of protons added normalized with respect to the wet weight of bacteria present) and zeta potential (diamonds) gathered from titrations of *Bacillus subtilis* in 0.01 M $NaNO_3$ that were cultured in tryptocase soy broth.

The components, $C_a$ and $C_b$, are the concentrations of acid and base added, respectively; $n_{OH}$ and $n_{H+}$ are the number of moles of $OH^-$ and $H^+$ in the solution at the measured pH, respectively; while "S" is the quantity of the solid (usually expressed in dry weight, i.e., mg). When such calculations are done over an entire pH range, an acid–base titration curve is created that shows the pH range over which some functional groups are chemically active and how the net surface charge of the organic surface varies with pH (Figure 1). A large difference in the total base or acid added and the free $H^+$ ion activity indicates significant pH buffering and a high concentration of surface functional groups. On the titration curve this is shown by a steep slope. A small difference in the total base or acid added and the free $H^+$ ion activity indicates weak pH buffering and a low concentration of surface functional groups. This translates into a gentle slope on a titration curve. In terms of microbial biomass, carboxyl groups account for the buffering capacity from pH 2–6 (Reaction 4), phosphate groups from pH 5–8 (Reaction 5), amino groups at pH $>$ 8 (Reaction 6), and hydroxy groups deprotonate at pH values above 10 (Reaction 7) (see Konhauser, 2007).

$$R - COOH^0 + OH^- \rightarrow R - COO^- + H_2O \quad (4)$$

$$R - PO_4H_2^0 + OH^- \rightarrow R - PO_4H^- + H_2O \quad (5)$$

$$R - NH_3^+ + OH^- \rightarrow R - NH_2 + H_2O \quad (6)$$

$$R - OH^0 + OH^- \rightarrow R - O^- + H_2O \quad (7)$$

As a consequence of the deprotonation reactions, the microbial surface develops an electrical charge. Therefore, when subjected to an electric field, microorganisms move in the direction, and at a rate, commensurate with the polarity and density of the overall surface charge. This process is termed electrophoresis, and the electrophoretic mobility of a microbial suspension can be quantified by measuring their velocity in an electric field. This measurement can, in turn, be used to calculate the zeta potential ($\zeta$), using the Smoluchowski equation below (Hunter, 2001):

$$\zeta = \frac{\eta\mu}{\varepsilon_0\varepsilon} \quad (8)$$

The component "$\mu$" is the electrophoretic mobility of a particle; $\varepsilon_0$ and $\varepsilon$ are the relative dielectric constants of the vacuum and solution, respectively; and $\eta$ is the viscosity of the solution. The zeta potential reflects the electrical potential at the interfacial region (viewed as a shear plane) separating an inner layer, where cations are held tightly in place and move with the bacterium, and an outer layer where ions are mobile (Wilson et al., 2001). The greater the absolute value of the $\zeta$ potential, the greater the charge

density on the surface (Blake et al., 1994). The electrophoretic mobility (and zeta potential) is pH dependent because the activity of protons in solution controls the ionization reactions of functional groups at the microbial surface (Ahimou et al., 2001) (Figure 1). This leads us to the concept of isoelectric point, which is defined as the pH value where the net surface charge of a solid is zero. The isoelectric point can be estimated from acid–base titrations, but it can also be directly measured with electrophoretic mobility experiments because at the isoelectric point microbes do not exhibit motion in an electric field. The isoelectric point of bacterial cell walls is typically between pH 2–4 (Harden and Harris, 1953). This means that at low pH, when the surface functional groups are fully protonated, bacteria are either neutral or positively-charged, the latter being the result of a cell possessing abundant amino groups. Meanwhile, at the growth pH of most bacteria, cells inherently display a net negative charge and the magnitude of negativity increases with higher pH values. As a result, under low pH conditions, most bacterial surfaces behave hydrophobically, but with an increasingly hydrophilic nature with increasing pH.

One of the major challenges faced by the researchers today is how to translate acid–base titration data in terms of cell wall biochemistry. Ascribing p$K_a$ values from a titration curve to specific functional groups can be problematic because there is often significant variation in p$K_a$ values for the same functional group. This occurs because the magnitude of the dissociation constant is controlled by the structure of the molecule to which it is attached (see Martell and Smith, 1977 for details). Consequently, a single carboxyl group in two different organic acids will have different p$K_a$ values, as will an organic acid with multiple carboxylic groups. As might then be expected, the p$K_a$ for a carboxyl group on one microbial species versus another could yield widely different values simply because of subtle conformational variations within the wall macromolecules. Furthermore, titration experiments are only able to resolve those groups that contribute significant amounts of protons to solution. Minor groups are simply undetectable with the resolution of current techniques. It is thus important to keep in mind that the model-derived binding sites do not directly represent the functional groups of the cell surface; their identity can only be inferred by comparison of the functional group p$K_a$ values with p$K_a$ values of model compounds. Unequivocal identification of the types of functional groups responsible for acid–base buffering may be obtained by spectroscopic techniques, such as Fournier transform infrared spectroscopy (FTIR), calorimetry or gas/liquid chromatography of cell wall extracts. For instance, Yee et al. (2004) and Jiang et al. (2004) used infrared spectroscopy to examine the pH dependence of deprotonation of bacterial cell-wall functional groups. Although not all pH conditions were studied, it was clear that the vibrational frequencies of carboxyl type groups increased with increasing pH. Calorimetic measurements of protonation reactions on bacterial surfaces indicate these reactions are exothermic with relatively small site-specific entropies (Gorman-Lewis et al., 2006). This provides more evidence that (1) hydrogen bonding between protonated and deprotonated sites likely stabilizes the cell wall, and (2) bacterial cell wall functionalities are similar to multifunctional organic acids rather than simple organic acids.

## Summary

Microbial surface reactivity results from the protonation and deprotonation of the organic moieties of microbial cell surfaces including carboxyl, phosphate, amino, and potentially hydroxyl groups. These groups behave similarly to multifunctional organic acids – they hydrogen bond with each other which leads to negative charge on the cell wall as pH increases. At most environmentally relevant pH values, microbial cell surfaces will possess a net negative charge, and therefore, will interact with positively charged cations or mineral surfaces.

## Bibliography


Ahimou, F., Paquot, M., Jacques, P., Thonart, P., and Rouxhet, P. G., 2001. Influence of electrical properties on the evaluation of the surface hydrophobicity of *Bacillus subtilis*. *Journal of Microbiological Methods*, **45**, 119–126.

Blake, R. C., Shute, E. A., and Howard, G. T., 1994. Solubilization of minerals by bacteria: electrophoretic mobility of *Thiobacillus ferrooxidans* in the presence of iron, pyrite, and sulfur. *Applied and Environmental Microbiology*, **60**, 3349–3357.

Gorman-Lewis, D., Fein, J. B., and Jensen, M. P., 2006. Enthalpies and entropies of proton and cadmium adsorption onto *Bacillus subtilis* bacterial cells from calorimetric measurements. *Geochemica et Cosmochimica Acta*, **70**, 4862–4873.

Harden, V. P., and Harris, J. O., 1953. The isoelectric point of bacterial cells. *Journal of Bacteriology*, **65**, 198–202.

Hunter, R. J., 2001. *Foundations of Colloid Science*. New York: Oxford University Press.

Jiang, W., Saxena, A., Song, B., Ward, B. B., Beveridge, T. J., and Myneni, S. C. B., 2004. Elucidation of functional groups on Gram-positive and Gram-negative bacterial surfaces using infrared spectroscopy. *Langmuir*, **26**, 11433–11442.

Konhauser, K. O., 2007. *Introduction to Geomicrobiology*. Oxford: Blackwell Publishing.

Martell, A. E., and Smith, R. M., 1977. *Critical Stability Constants. III. Other Organic Ligands*. New York: Plenum Press.

Wilson, W. W., Wade, M. M., Holman, S. C., and Champlin, F. R., 2001. Status of methods for assessing bacterial cell surface charge properties based on zeta potential measurements. *Journal of Microbiological Methods*, **43**, 153–164.

Yee, N., Benning, L. G., Phoenix, V. R., and Ferris, F. G., 2004. Characterization of metal-cyanobacteria sorption reactions: a combined macroscopic and infrared spectroscopic investigation, *Environmental Science and Technology*, **38**, 775–782.


## Cross-references


Metalloenzymes
Metals, Acquisition by Marine Bacteria
Microbial Biomineralization
Microbial-Metal Binding
Organomineralization
Siderophores

# MICROBIALITES, MODERN

Christophe Dupraz[1], R. Pamela Reid[2], Pieter T. Visscher[1]
[1]University of Connecticut, Storrs, CT, USA
[2]University of Miami, Miami, FL, USA

## Synonyms

"Cryptalgal sedimentary rock" (Aitken, 1967); Microbolite (Riding, 1991)

## Definition

*Microbialite*: "Organosedimentary deposits that have accreted as a result of a benthic microbial community trapping and binding sediment and/or forming the locus of mineral precipitation" (Burne and Moore, 1987), or "Benthic microbial deposits" (Riding, 1991).

## Introduction

In this encyclopedia, microbialite is discussed under two chapters: (1) modern and (2) fossil. This part discusses modern microbialites, with emphasis on processes of formation. The fossil extension and classification of microbial deposits (fossil forms being more diverse) are treated in the "fossil microbialite" section of the encyclopedia (see Chapter *Microbialites, Stromatolites, and Thrombolites*). Microbialites are composed of trapped, bound, and/or precipitated sediment, and exhibit a range of mineralogies (Figure 1). This chapter focuses on carbonate microbialites, which are the most widespread and the most studied.

Microbialites are "rocks" that are produced, induced, or influenced by benthic microbial communities, primarily bacteria and sometimes also microeukaryotes, such as diatoms. These microbial communities are organized in mats or biofilms (e.g., Stolz, 2000), consisting of microscopic organisms enveloped in an organic matrix of extracellular polymeric substances (EPS; Decho, 1990; Bhaskar and Bhosle, 2005; see Chapter *Extracellular Polymeric Substances (EPS)*). Because the microbial mat is dominantly organic, it is rarely preserved in the fossil record. In some unusual cases, exceptional taphonomic conditions can preserve intact cells and even the EPS structure (e.g., silicification or preserved remnants of EPS matrices, Golubic and Hofmann, 1976; Barbieri et al., 2004; Barbieri and Cavalazzi, 2005; Altermann et al., 2006; Benzerara et al., 2006; Kumar and Pandey, 2008; Lepot et al., 2008). More commonly, the organic matter decomposes to carbon dioxide ($CO_2$) or methane ($CH_4$), although in some cases incomplete degradation can lead to organic matter enrichment of the sediment. Evidence of the original microbial mat or biofilm is generally indirect (e.g., specific sedimentary (bio)structure, micromorphology, organic biomarkers, and stable isotopic fractionation). Microbial mats can help preserve sedimentary structures in the fossil record ("microbially-induced sedimentary structures" – MISS; Noffke et al., 2003). The most spectacular examples are carbonate microbialites. Examples of modern microbialites in the following section are followed by a discussion of processes of formation.

## Types of modern microbialite

Microbialite descriptions incorporate a range of scales, from macrometers to micro/nanometers (e.g., Shapiro, 2000). Megastructure relates to the geographical extension of a microbial deposit and overall deposit morphology (e.g., ridges, biostrome, and bioherm). Macrostructure characterizes the morphology of an individual buildup (e.g., domal, branching, knobby). Mesostructure refers to structures visible with the naked eye, such as lamination. Microstructure is observed with a microscope, such as light, confocal, scanning electron (SEM), or transmission electron microscope (TEM).

Microbialite classification is based on mesostructure with four common types (Figure 2): laminated microbialites classified as stromatolites, thrombolites are clotted, leiolites are structureless, and dendrolites are dendritic (Burne and Moore, 1987; Riding, 1991, 2000; Dupraz and Strasser, 1999, 2002). All of these structures exhibit a wide range of microstructures including micropeloidal, densely micritic, or agglutinated microfabrics (Riding, 1991; Dupraz and Strasser, 1999). Three types of modern microbialites are described in the following section; dendrolites have not yet been found in modern environments. For further description of microbialite classification and microstructure see Chapter *Microbialites, Stromatolites, and Thrombolites*.

### Stromatolite

The term stromatolite is derived from the Greek "stroma," meaning mattress or stratum and "lithos," meaning rock. The term was first introduced by Kalkowsky in 1908 to refer to "laminated benthic microbial deposits" (see also Riding, 1999; Chapter *Microbialites, Stromatolites, and Thrombolites*). The first modern stromatolites were found in the Shark Bay, Western Australia in 1954 in the hypersaline water of Hamelin Pool. Until this date, scientists believed that stromatolites were extinct, found only in the fossil record. Although the biogenicity of 3.5 Ga stromatolites has been questioned (Buick et al., 1981; Lowe, 1994; Grotzinger and Knoll, 1999; Lindsay et al., 2003), all modern microbialites called stromatolites are associated with microbial communities that induce, or serve as organic substrate for, precipitation (Riding, 2000). Modern stromatolites are found in many different locations including marine, hypersaline, freshwater, and even continental environments.

### Open marine stromatolites

The Bahamas hosts the only known examples of open marine stromatolites. These structures are found at a variety of locations on the margins of Exuma Sound including Schooner Cays, Lee Stocking Island, Stocking Island Highborne Cay, and Darby Island (Dravis, 1983;

**Carbonates**
Calcite - $CaCO_3$
Mg-Calcite - $(Mg_xCa_{1-x})CO_3$
Aragonite - $CaCO_3$
Vaterite - $CaCO_3$
Monohydrocalcite - $CaCO_3 \bullet H_2O$
Protodolomite - $MgCa(CO_3)$
Hydrocerussite - $Pb_3(CO_3)_2(OH)_2$
Amorphous forms - $CaCO_3 \bullet H_2O$ or $CaCO_3$

**Phosphates**
Octacalcium phosphate - $Ca_8H_2(PO_4)_6$
Brushite - $CaHPO_4\ 2H_2O$
Francolite - $Ca_{10}(PO_4)6F_2$
Carbonated-hydroxylapatite (dahllite) - $Ca_5(PO_4,CO_3)3(OH)$
Whitlockite - $CaI_8H_2(Mg,Fe)_2{+}2(PO_4)I_4$
Struvite - $Mg(NH_4)(PO_4) \bullet 6H_2O$
Vivianite - $Fe_3{+}2(PO_4)_2 \bullet 8H_20$
Amorphous Calcium Phosphate (at least 6 forms) variable
Amorphous Calcium Pyrophosphate - $Ca_2P_2O_7 \bullet 2H_2O$

**Sulfates**
Gypsum - $CaSO_4 \bullet 2H_2O$
Barite - $BaSO_4$
Celestite - $SrSO_4$
Jarosite - $KFe_3^{+3}(SO_4)_2(OH)_6$

**Sulfides**
Pyrite - $FeS_2$
Hydrotroilite - $FeS \bullet nH_2O$
Sphalerite - ZnS
Galena - PbS
Hydrotroilite $FeS \bullet nH_2O$
Sphalerite ZnS
Wurtzite ZnS
Greigite $Fe_3S_4$
Mackinawite $(Fe,Ni)_9S_8$
Amorphous Pyrrhotite $Fe_{1-x}S$ (x = 0–0.17)
Acanthite $Ag_2S$

**Arsenates**
Orpiment - $As_2S_3$

**Hydrated Silica**
Amorphous Silica - $SiO_2 \bullet nH_2O$

**Chlorides**
Atacamite - $Cu_2Cl(OH)_3$

**Fluorides**
Fluorite - $CaF_2$
Hieratite - $K_2SiF_6$

**Oxides**
Magnetite - $Fe_3O_4$
Amorphous Iron Oxide - $Fe_2O_3$
Amorphous Mn Oxide - $Mn_3O_4$
Amorphous Ilmenite $Fe^{+2}TiO_3$

**Metals**
Sulfur - S

**Hydroxides and Hydrous Oxides**
Goethite - $\alpha$ -FeOOH
Ferrihydrite - $5Fe_2O_3 \bullet 9H_2O$
Lepidocrocite -$\gamma$-FeOOH
Ferrihydrite - $5Fe_2O_3 \bullet 9H_2O$
Todorokite - $(Mn^{+2}CaMg)Mn_3^{+4}O_7 \bullet H_20$
Birnessite - $Na_4Mn_{14}O_{27} \bullet 9H_2O$

**Organic Crystals** following Lowenstam & Weiner (1989)
Whewellite - $CaC_2O_4 \bullet H_2O$
Weddelite - $CaC_2O_4 \bullet (2+x)H_2O$
Mn Oxalate - $Mn_2C_2O_4 \bullet 2H_2O$
Earlandite - $Ca_3(C_6H_5O_2)_2 \bullet 4H_2O$
Glushinskite - $MgC_2O_4 \bullet 4H_2O$
Manganese Oxalate - $Mn_2C_2O_4 \bullet 2H_2O$
Sodium urate - $C_5H_3N_4NaO_3$
Uric Acid - $C_5H_4N_4O_3$
Ca tartrate - $C_4H_4CaO_6$
Ca malate - $C_4H_4CaO_5$
Paraffin Hydrocarbon
Guanine - $C_5H_3(NH_2)N_4O$

**Microbialites, Modern, Figure 1** Nomenclature and chemical compositions of minerals produced by biologically-related mineralization processes. (Modified from Weiner and Dove, 2003; data from Lowenstam and Weiner, 1989; Simkiss and Wilbur, 1989; Mann, 2001; Weiner and Addadi, 2002.)

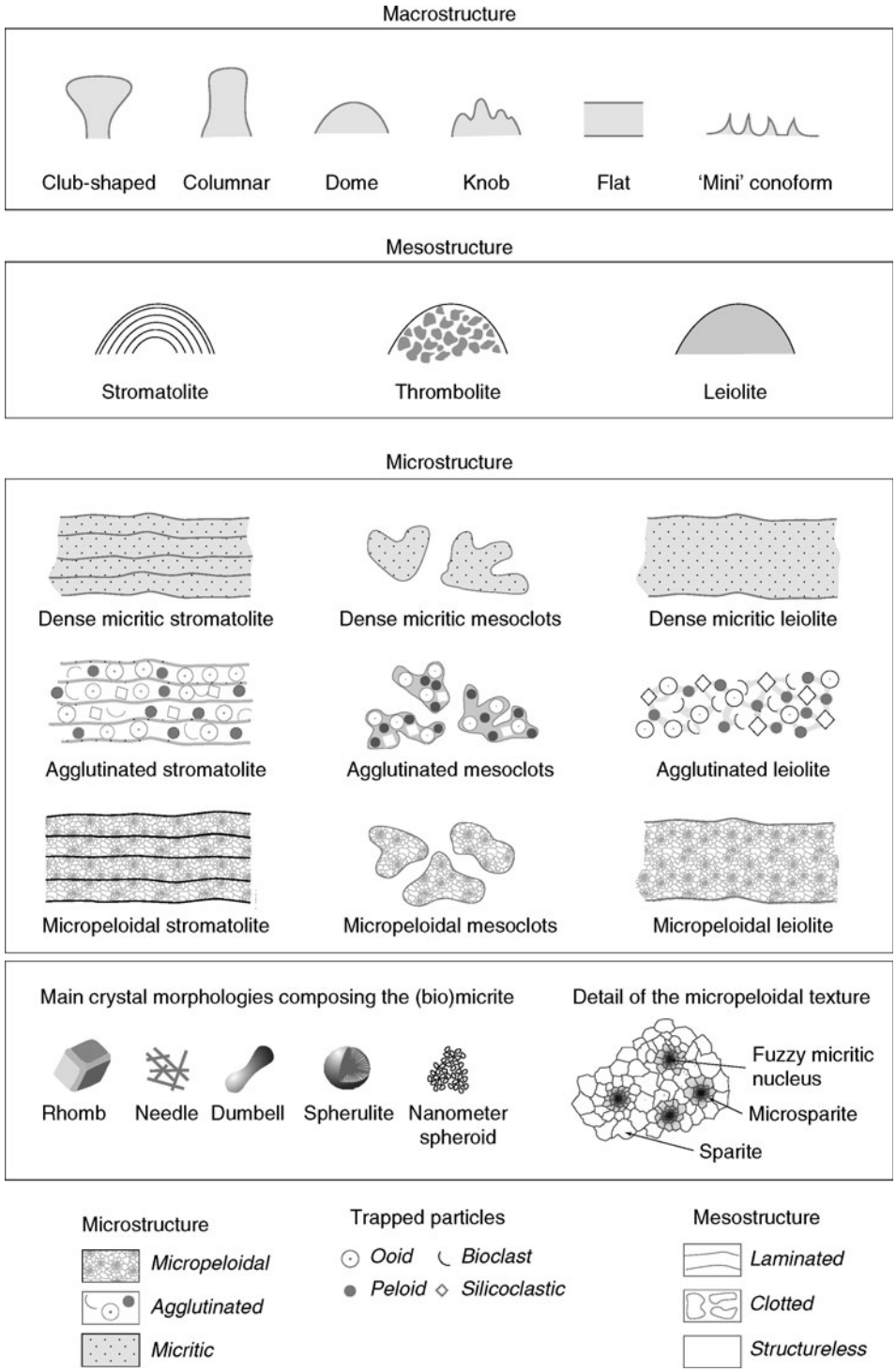


**Microbialites, Modern, Figure 2** Descriptive terminology for microbialite macro-, meso, and microfabrics. (From Kennard and James, 1986; Riding, 1991; Schmid, 1996; Dupraz and Strasser, 1999; Shapiro, 2000.)

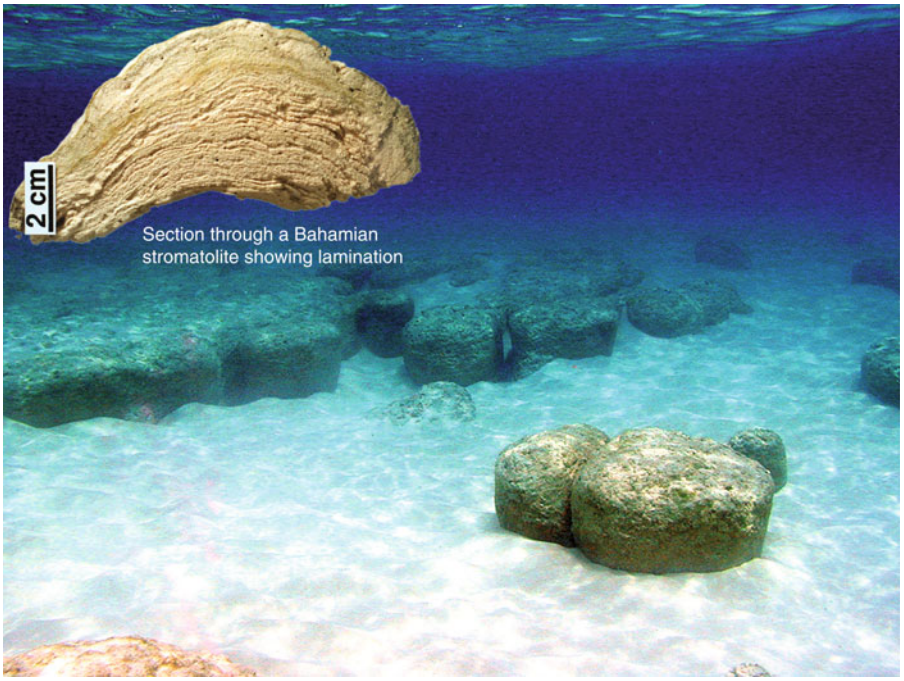


**Microbialites, Modern, Figure 3** Underwater photograph showing shallow subtidal stromatolites (Darby Island, Bahamas) with a vertical section (upper left hand insert) showing well-developed lamination.

Dill et al., 1986; Reid et al., 1995). These stromatolites are coarse grained structures, composed of ooid sand; they form in intertidal and subtidal environments, exposed to high wave energy and strong tidal currents (e.g., Gebelein, 1976; Reid et al., 2000). Many of the stromatolites exhibit well-developed laminae (Figure 3; e.g., Reid et al., 2000). The lamination results from iterative growth of different types of microbial mats on the top of the build-ups (Figure 4). Each microbial mat forms a distinct mineral product, which can be recognized in thin section and SEM (Figure 5; Reid et al., 2000). The first mat type (1) is dominated by the filamentous cyanobacterium *Schizothrix,* which traps and binds ooids. The stickiness of the mat EPS results in the trapping of particles, which are subsequently bound by the upward growth of the cyanobacterial filaments. Other microorganisms (e.g., diatoms that produce copious amounts of EPS) can also participate in trapping grains. The second mat community (2) consists of a thin biofilm with abundant heterotrophic bacteria. Precipitation of aragonite within this biofilm forms a micritic lamina, which caps the underlying ooids. The third mat type (3) is characterized by an abundance of the endolithic coccoid cyanobacterium *Solentia* spp. *Solentia* tunnels through grains, leaving bore holes filled with EPS. Aragonite precipitation within the EPS results in micritization of the grains and, when tunnels cross between grains, welds the grains together. This process forms a well-cemented layer (Macintyre et al., 2000; Reid and Macintyre, 2000; Reid et al., 2000). The in situ precipitation of carbonate, which leads to early lithification of the stromatolite-forming mats, is a result of prokaryotic activity (Visscher et al., 2000; Reid et al., 2003a).

Dominance of prokaryotic communities on the surfaces of modern marine stromatolites, is favored by the selective environmental pressure of periodic burial by sand (Andres and Reid, 2006; Kromkamp et al., 2007). In contrast to eukaryotes, which are typically killed when buried for periods of weeks to months, prokaryotes such as cyanobacteria are able to survive and recover from long burial events (Kromkamp et al., 2007). This attribute may contribute to the success of stromatolites in modern and past environments. Eukaryotic colonization (macroalgae: e.g., *Batophora*), during week- to month-long periods of exposure disrupts the lamination resulting from the cycling of prokaryotic mats, producing intervals of crude to no lamination within the stromatolite head.

It should be noted that trapping and binding alone does not form a stromatolite. The key factor in allowing development of a lithified laminated buildup is a hiatus in sediment accretion and corresponding development and lithification of a microbial biofilm. During long hiatal periods (i.e., several weeks), surfaces infested with the coccoid bacterium *Solentia* forms thicker, well-cemented lamina of fused ooid grains. Precipitation of aragonitic needles associated with the activity of sulfate-reducing bacteria is a key feature in carbonate precipitation within Bahamian stromatolites (Visscher et al., 2000). Precipitation resulting from anaerobic heterotrophic activity is supported by isotopic data (Andres et al., 2005).

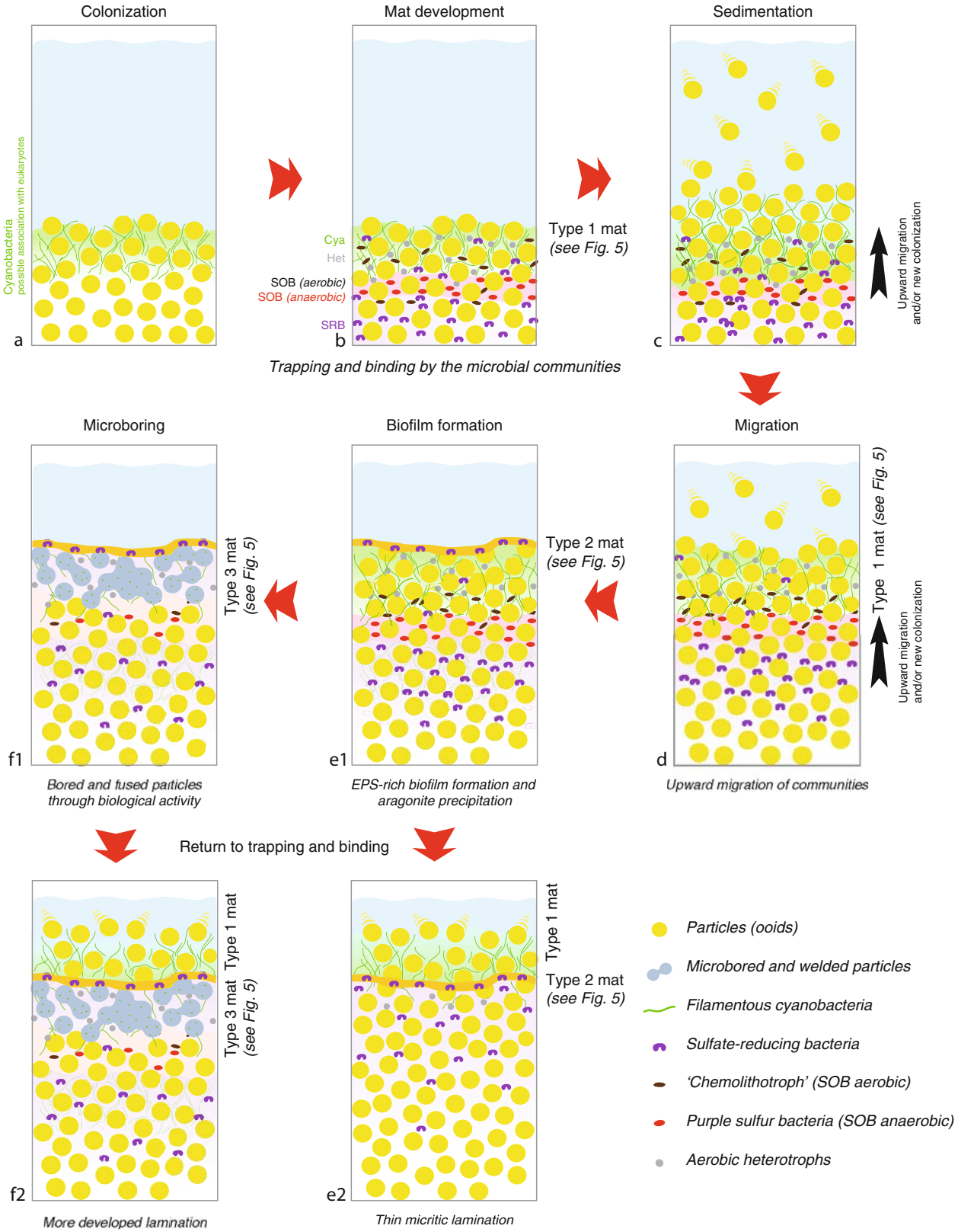


**Microbialites, Modern, Figure 4** (Continued)

Factors leading to the cycling of surface communities responsible for lamination in Bahamian stromatolites are currently under investigation (Andres and Reid, 2006). Both biological and environmental factors may be important (Figure 6; Seong-Joo et al., 2000; Reid et al., 2003a). Biological factors include microbial ecological interactions, and production and consumption of organic and inorganic compounds. Extrinsic factors include temperature, light, nutrients, and hydrodynamics, which could affect the stickiness of EPS and/or sediment supply (Figure 6).

## Hypersaline and saline stromatolites

In contrast to open marine environments, where modern stromatolites are rare, living stromatolites are more common in hypersaline environments. This is because microbial communities are able to cope with high salinity, whereas most eukaryotes, such as macroalgae and burrowing/grazing invertebrates, which compete with or ingest cyanobacteria and disrupt lamination, are largely excluded (Fischer, 1965; Awramik, 1971, 1982, 1992; Walter and Heys, 1985; Riding, 2006).

Stromatolites in Shark Bay, Western Australia are the most famous stromatolites thriving in hypersaline water. They are found in the Hamelin Pool Marine Nature Reserve of the Shark Bay UNESCO World Heritage Site. Ranging from 55–70 ppt throughout the year (Playford, 1990), Hamelin Pool has approximately double normal marine salinity and hosts abundant and diverse stromatolites. Shark Bay stromatolites were discovered in 1954 by Johnstone, Playford, and Chase of the West Australian Petroleum Pty. Ltd (Playford and Cockbain, 1976). They were the first modern stromatolites discovered with sizes and shapes comparable to fossil counterparts (Logan, 1961; Logan et al., 1974; Playford and Cockbain, 1976; Playford, 1979; Bauld et al., 1979; Bauld, 1981; Burns et al., 2004). Like Bahamian stromatolites, Shark Bay structures are formed by both (1) microbial trapping and binding and (2) microbial precipitation. Both processes are important in the intertidal zone, forming coarse grained sandy stromatolites. Microbial precipitation is the primary accretionary mechanism in the subtidal zone of Shark Bay, forming muddy, micritic stromatolites (Reid et al., 2003b).

As a result of the dominant sandy textures of Shark Bay stromatolites and open marine stromatolites in the Bahamas, some authors have proposed that these stromatolites are not appropriate analogs for fossil stromatolites, which are generally display fine-grained, micritic microstructures (Awramik and Riding, 1988). Despite their overall coarse-grained texture, these modern stromatolites have micritic laminae formed as a result of microbially-induced precipitation (Reid et al., 2000; Visscher et al., 2000). Moreover, the ecological model developed for Bahamian stromatolites, in which lamination results from the cycling of prokaryotic communities on the stromatolite surface, is likely applicable to the growth of Shark Bay stromatolites. Indeed, a model of iterative accretion of laminae, which record both microbial and environmental fingerprints and progressively shape the emergent morphology, may serve as a conceptual model for the growth of fossil stromatolites.

In addition to Shark Bay, living stromatolites are also present in many other saline and hypersaline environments. Several saline lakes in Australia habor stromatolites, including Lake Thetis, near Cervantes, lakes on Rottnest Island (Reitner et al., 1996), and Lake Clifton near Mandurah (e.g., Grey et al., 1990). Cyanobacterial stromatolitic domes have been described in the intertidal zone of Bermuda (e.g., Sharp, 1969; Golubic and Focke, 1978) and small crudely laminated knobs have been found in a hypersaline lake on Bonaire Island in the Netherlands Antilles (Golubic and Focke, 1978). Various islands in the Bahamas also have hypersaline lakes with well-developed microbial mats and stromatolites, including Storr's Lake on San Salvador. Storr's lake harbors alternating stromatolitic and thrombolitic buildups (Mann and Hoffman, 1984; McNeese, 1988; Neumann et al., 1988; Mann and Nelson, 1989; Pentecost, 1989; Zabielski, 1991).

## Fresh water and continental stromatolites

Numerous examples of freshwater laminated microbialite have been published. One of the most widespread examples of these microbialites is travertines. Tufa stromatolites (meteogene travertine following Pentecost (2005)) are freshwater fluviatile tufas, which locally exhibit thick laminated crusts formed by calcified cyanobacteria (Pentecost, 1978; Riding, 1991b, 2000). Most of the precipitation of carbonate in these travertines results from physicochemical

**Microbialites, Modern, Figure 4** Model of coarse-grained open-marine stromatolite formation. (**a**) Cyanobacteria colonize and stabilize mobile ooid sand (trapping and binding). (**b**) A complex microbial mat develops in the upper few millimeters of the sediment (*Cya* cyanobacteria; *SRB* sulfate reducing bacteria; *SOB* sulfide oxidizing bacteria (aerobic and anaerobic); *Het* aerobic heterotrophs; see also Figure 8). (**c**–**d**) As a result of sediment accretion, the microbial mat migrates upward, continuing trapping and binding. Cyanobacteria (and heterotrophs) can survive massive burial. No significant in situ precipitation is observed at this stage, which corresponds to the *Type 1 mat in Figure 5*. (**e**) During a hiatus in sediment accretion, an EPS-rich biofilm develops, draping over the ooids (Type 2 mat, Figure 5). This biofilm rapidly lithifies due to the activity of anaerobic heterotrophs (i.e., SRB), forming a thin lamina of micritic aragonite (see Figure 5b4). (**f**) A prolonged hiatus in trapping and binding results in colonization of ooid grains under the biofilm by the endolithic cocoid cyanobacteria *Solentia* sp. (Type 3 mat, Figure 5) Precipitation of aragonite in the bore holes made by these endoliths destroys the internal microstructure of ooids, changing their color from golden brown to gray. Precipitation in bore holes crossing between grains fuses them together (Figure 5$c_{2-4}$). Resumption of trapping and trapping corresponds to formation of a new Type 1 mat ($e_2$, $f_2$). The iterative succession of these three different mat types is responsible for the lamination observed in open-marine stromatolite (Figure 3).

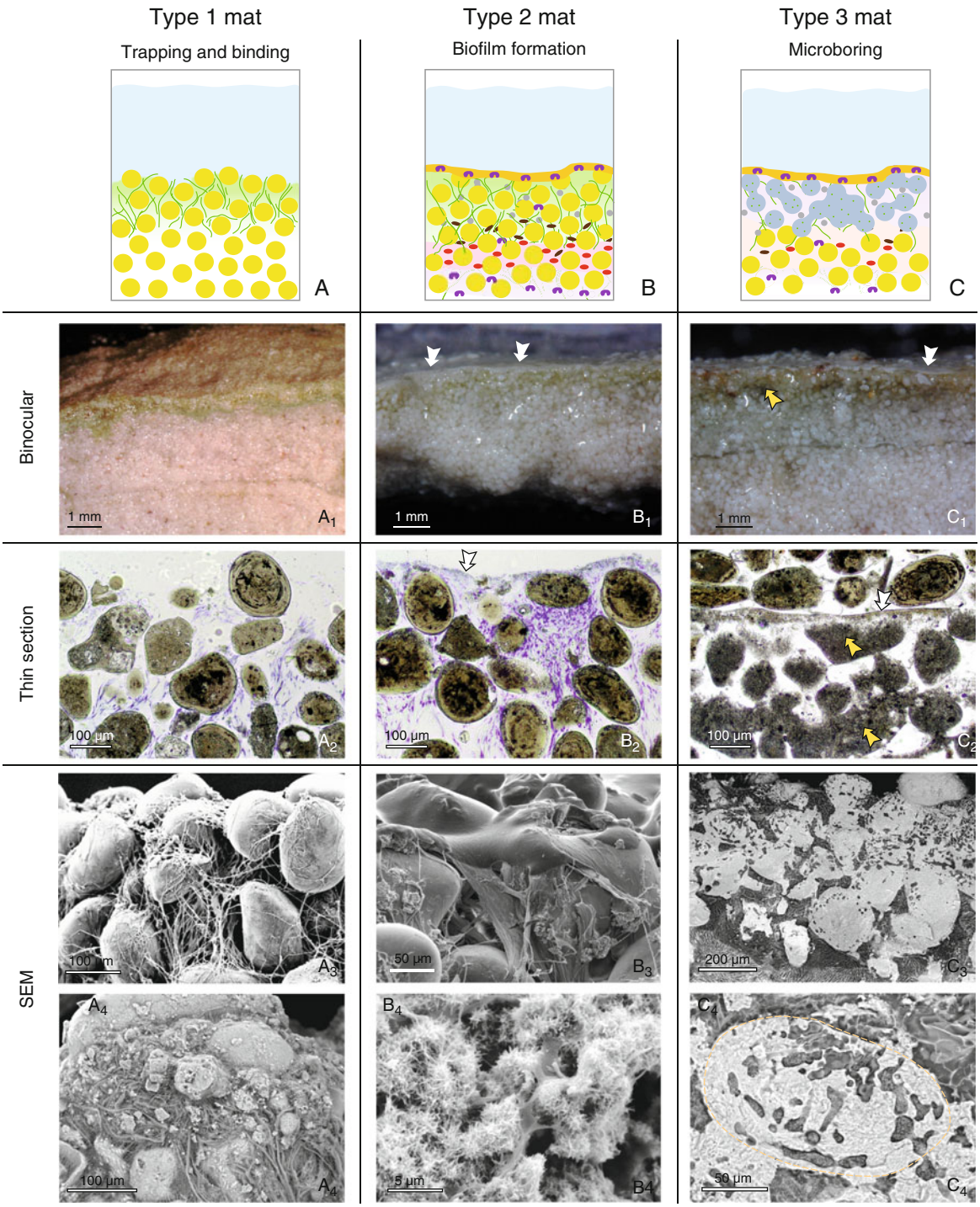


**Microbialites, Modern, Figure 5** Micrographs illustrating the main features of the surface mats responsible for the formation of modern marine stromatolites. Stromatolite lamination results from the iterative growth at the surface of the build up of three mat types: (1) Type 1 mats are dominated by filamentous cyanobacteria, which trap carbonate sand grains through EPS stickiness ($A_{1\text{-}4}$); (2) Type 2 mats consist of a continuous biofilm, drapping the stromatolite surface (white arrows in $B_{1\text{-}3}$); the biofilm is composed of extracellular polymeric substances (EPS, $B_3$) containing numerous heterotrophic bacteria. This biofilm rapidly lithifies as a result of precipitation of aragonite needles within the biofilm ($B_4$); (3) Type 3 mats are characterized by endolith-infested ooid grains (yellow arrows in $C_{1\text{-}2}$), which appear gray and are fused together, below a surface biofilm.($A_1$-$B_1$-$C_1$) binocular micrographs, ($A_2$-$B_2$-$C_2$) petrographic micrographs, ($A_3$-$B_3$-$B_4$) high vacuum scanning electron microscope images (SEM; chemical drying), and ($A_4$-$C_3$-$C_4$) cryo-SEM (frozen samples) images.

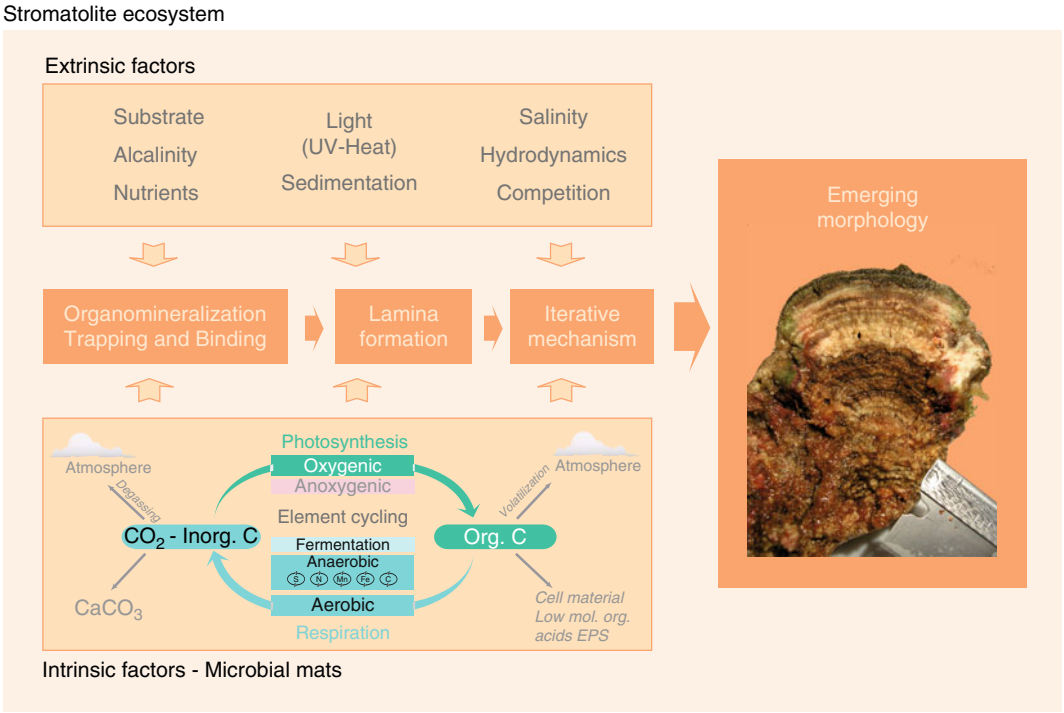


**Microbialites, Modern, Figure 6** Interactive processes within the stromatolite ecosystem. Intrinsic (microbial mat-related) and extrinsic (environment-related) factors work together to determine the emergent stromatolite morphology and fabric, which can be described at microscale (biomineralization, trapping, and binding), mesoscale (laminae formation), and macroscale (iterative mechanism leading to morphology) levels.

degassing of $CO_2$ through resurgence, cascades, or waterfalls. Photosynthetic uptake of $CO_2$ by cyanobacteria can, however, be responsible for the precipitation of calcium carbonate in slow running and low DIC streams (Verrecchia et al., 1995; Merz-Preiss and Riding, 1999; Arp et al., 2001). Relatively low DIC and high $Ca^{2+}$ concentration is required for photosynthesis to influence carbonate alkalinity and enable precipitation (Arp et al., 2001, 2003).

Fresh water stromatolites are also present in Antarctic lakes, which are permanently ice-covered (Parker et al., 1981). These lakes are seasonally fed by glaciers, which modify salinity from fresh-to-saline while oxygen levels vary from anoxic to supersaturated. The stromatolites are formed through sediment trapping and binding as well as carbonate precipitation in cyanobacterial-dominated (e.g., *Phormidium*, *Oscillatoria*) microbial mats. Other non-marine environments with stromatolites include alkaline lakes, such as the Caldera lakes of Niuafo'ou Island (Tonga), with spectacular laminated buildups (Kazmierczak and Kempe, 2006).

Laminated deposits, referred to as terrestrial stromatolites (Verrecchia et al., 1995; Riding, 2000), are observed in "non-water-saturated" environments. These deposits have also been called lichen stromatolites (Klappa, 1979) and subaerial stromatolites (Riding, 1991b). They consist of laminar calcretes formed by microbial activity or in close association with microbial communities. Determining between biogenic and non-biogenic calcretes is often difficult as carbonate precipitation may be caused by physicochemical evaporation (e.g., Read, 1976), and/or cyanobacterial activity (e.g., Verrecchia et al., 1995).

## Thrombolite

The term thrombolite was introduced by Aitken (1967) for microbial "structures related to stromatolites, but lacking lamination and characterized by a macroscopic clotted fabric". Since this initial definition, thrombolites and stromatolites have been recognized as two distinct microbialite structures (Kennard and James, 1986). The key microstructure of thrombolites is mesoclots, which produce the clotted fabric (Shapiro, 2000). The mesoclots consist of polymorphic (simple spheroids to polylobate), millimeter to centimeter-sized, aggregates which display a variety of forms, from simple spheroids to polylobate masses (e.g., Shapiro, 2000). Clotted mesostructures have been described for many fossil thrombolites, which are mostly composed of fine-grained carbonate. Therefore, many authors define mesoclots as mostly composed of micrite or micropeloids (Kennard, and James, 1986; Dupraz and Strasser, 1999; Shapiro, 2000). However, modern thrombolites, as well examples from the Miocene, show agglutinated, clotted fabrics (Riding, 2000). The mesoclots of modern thrombolites thus consist of micrite, micropeloids, or agglutinated particles (Figure 2).

The clotted fabric of thrombolites can have a variety of origins. The fabric can be attributed "to the in situ calcification of coccoid or coccoid-dominated microbial communities" (Kennard and James, 1986). Other mechanisms involve bioturbation and bioerosion, and thrombolitic mesostructures within large Bahamian stromatolites are often due to disruption of the lamination by eukaryotic colonization (e.g., *Batophora* sp. and other algae).

In some cases, environmental conditions may trigger changes between thrombolite and stromatolitic fabrics. In Storr's Lake (San Salvador, Bahamas), well-developed thrombolites alternate with stromatolitic layers (McNeese, 1988; Mann and Nelson, 1989). This alternation might be triggered by lake-level fluctuations and associated turbidity variability. This mechanism results in a succession of phototrophic-dominated (stromatolites) to heterotrophic-dominated communities (thrombolites) as surface communities, as modeled by Dupraz et al. (2006).

Many other modern lakes host thrombolite deposits: Lake Clifton, Lake Tethys, Lake Richmond and different lakes on Rottnest Island (Australia), Kelly and Pavillon lakes (British Columbia, Canada), lakes on Bonaire Island (Netherlands Antilles, southern Caribbean; Kobluk and Crawford, 1990), Lago Sarmiento (Patagonia, Chile), Poza Azul lake (Cuatro Cienegas, Mexico), Yellow Stone National Park (USA), Green Lake (Fayetteville, New York, USA). In addition, travertines showing thrombolitic features have been referred to as "Tufa Thrombolite" (Riding, 2000).

### Leiolite

The term leiolite comes from the Greek word "leios," meaning uniform or smooth and "lithos," (meaning rock) and was originally applied to late Miocene (Messinian) deposits in Spain (Figure 2; Braga et al., 1995). Leiolite is characterized by relatively structureless, aphanitic, mesostructure, lacking lamination or clots, and can be a synonym for "cryptomicrobial" as used by Kennard and James (1986). Most authors tend to classify microbialites as either stromatolites or thrombolites, despite the fact that many of these deposits lack the defining mesostructures and would more appropriatedly be termed leiolite (see Riding, 2000). No examples of modern leiolite have been published. However, examples could include non-laminated, non-thrombolitic portions of Bahamian or Shark Bay stromatolites, carbonate crust formation in hypersaline lakes (Dupraz et al., 2004), and biological stabilization of sand dune by chasmolithic microorganisms (Hillgaertner et al., 2001).

### Other types of microbialites

Microbial processes or the presence of microbes are often intimately related to sedimentary processes in modern carbonate systems, although the resulting deposits may not be considered as true microbialite and classified as stromatolite, thrombolite, or leiolite. These microbial carbonate deposits include meteogene and thermogene travertine (Pentecost, 2005), where microbial influence creates specific microfabrics. Spectacular examples of travertines can be observed in many alkaline lakes, forming carbonate towers (e.g., Pyramid Lake, Nevada (Benson, 1994)), Lake Can, Turkey (Kempe et al., 1991), and Mono Lake, California (e.g., Bischoff et al., 1993; Riding, 2000). Carbonate chimneys are also formed in hydrothermal systems, where microbial activity is important (e.g., "Lost City" Hydrothermal Field; Kelley et al., 2001; Ludwig et al., 2006).

Other deposits that are difficult to classify include microbial calcrete – a terrestrial carbonate the formation of which is strongly influenced by bacteria and fungi (Jones and Wilson, 1986; Wright et al., 1988; Verrecchia and Verrecchia, 1994; Verrecchia et al., 1995). In addition, in continental environments, the formation of needle fiber calcite (NFC) is related to fungi activity (Verrecchia and Verrechia, 1994; Cailleau et al., 2004, 2005). Mondmilch or Moonmilch – a soft paste-like or powdery cave deposit – includes important microbial populations, which influence precipitation (Thrailkill, 1976; Canaveras et al., 2006). Microbial mats are also involved in the formation of oncoids, which are unattached spherical stromatolites (e.g., Bathurst, 1966), and microbial activity may play a role in the formation of "whitings" (Thompson, and Ferris, 1990; Robbins, and Blackwelder, 1992).

## Processes of microbialite formation

Early lithification is a key process in the formation of modern carbonate microbialites and is critical for the preservation of these structures in the fossil record. Lithification processes start at the time of deposition and continue during burial (diagenesis). Lithification consists of in situ precipitation of minerals, which progressively cement trapped grains (if present), and preserve the biosedimentary structures. Two closely coupled components are fundamental in carbonate precipitation within microbial mats: (1) the alkalinity engine and (2) the organic matrix in which this mineral is forming.

### The alkalinity engine

The precipitation of carbonate minerals depends on the availability of carbonate ions, specific cations (e.g., $Ca^{2+}$, $Mg^{2+}$), and suitable nucleation sites. Carbonate minerals may precipitate when a solution is saturated with respect to that mineral. The degree of saturation is calculated via the saturation index of the specific mineral:

$$SI = \log(IAP/K_{ps}) \quad (1)$$

IAP is the "ion activity product" and $K_{sp}$ is the solubility product of the corresponding mineral (solid phase). In the case of $CaCO_3$, both the carbonate alkalinity and the activity of the available cations are taken into account

when calculating the saturation index (Stumm and Morgan, 1996):

$$SI_{CaCO3} = Log(\{Ca^{2+}\} * \{CO_3{}^{2-}\}/K_{sp}). \quad (2)$$

The activity of a given chemical compound corresponds to the concentration of that compound multiplied by the activity coefficient. The solubility products for aragonite and calcite are $10^{-6.19}$ and $10^{-6.37}$, respectively, at 25°C, 1 bar atmospheric pressure and 35 PSU salinity (Zeebe and Wolf-Gladrow, 2001). A solution is supersaturated with respect to a given mineral when SI is greater than 0, meaning that $K_{sp}$ is smaller than IAP. Experimental evidence showed that a supersaturation must be greater than 0.8 in order to have spontaneous precipitation of $CaCO_3$ (Kempe and Kazmierczak, 1994). Arp et al. (2001) used SI greater than 1 (i.e., a 10-fold supersaturation) as a prerequisite for carbonate precipitation in nonmarine environment.

Carbonate ion activity, $\{CO_3{}^{2-}\}$, depends on the carbonate equilibrium. $CO_2$ dissolves in water to form carbonic acid ($H_2CO_3$). The amount of dissolved $CO_2$ is proportional to the partial pressure of $CO_2$ ($pCO_2$) in the gas phase in contact with the liquid (i.e., Henry's Law). This value varies with pressure and temperature. Low temperature and high pressure allow for more $CO_2$ dissolution in water. Carbonic acid is weak acid that will only partially dissociate in an aqueous solution to produce $H^+$ ion and the conjugate base. It will depronotate as follows (with p*K*s value for fresh water):

$$H_2CO_3{}^* \rightleftharpoons HCO_3{}^- + H^+$$
$$K_{a1} = 4.30 \times 10^{-7}; \quad pK_{a1} = 6.36. \quad (3)$$

$$HCO_3{}^- \rightleftharpoons CO_3{}^{2-} + H^+$$
$$K_{a2} = 5.61 \times 10^{-11}; \quad pK_{a2} = 10.25 \text{ at } 25°C. \quad (4)$$

The two p*K*s values vary as a function of the salinity. For seawater conditions, $pK_{a1}$ and $pK_{a2}$ are 5.9 and 8.9, respectively (at 25°C, 1 bar atmospheric pressure and 35 PSU salinity; Zeebe and Wolf-Gladrow, 2001).

Availability of carbonate ions is a prerequisite for precipitation of carbonate minerals. The amount of bicarbonate and carbonate ions in solution denotes carbonate alkalinity, which is a part of total alkalinity, including borate, hydroxide, phosphate, and silicate. In marine and most of freshwater environments, phosphate and silicate are minor components, and the carbonate equilibrium typically drives global alkalinity. Various processes can have an impact of carbonate alkalinity, indirectly promoting precipitation or dissolution of carbonate mineral. The sum of processes that creates alkalinity represents the "alkalinity engine." This engine is intrinsically driven when alkalinity is affected by microbial communities, or extrinsically driven when physicochemical processes of the macro-environment cause alkalinity shifts (Figure 7).

## Intrinsic alkalinity engine (metabolism)

The way microbial communities acquire their energy and their source of carbon (i.e., through metabolism) can have a strong impact on local carbonate alkalinity. In a simplified view of the microbial carbon cycle, the production of organic matter through photosynthesis (oxygenic or anoxygenic) is coupled with the oxidation of organic carbon by aerobic (oxygen as oxidant) or

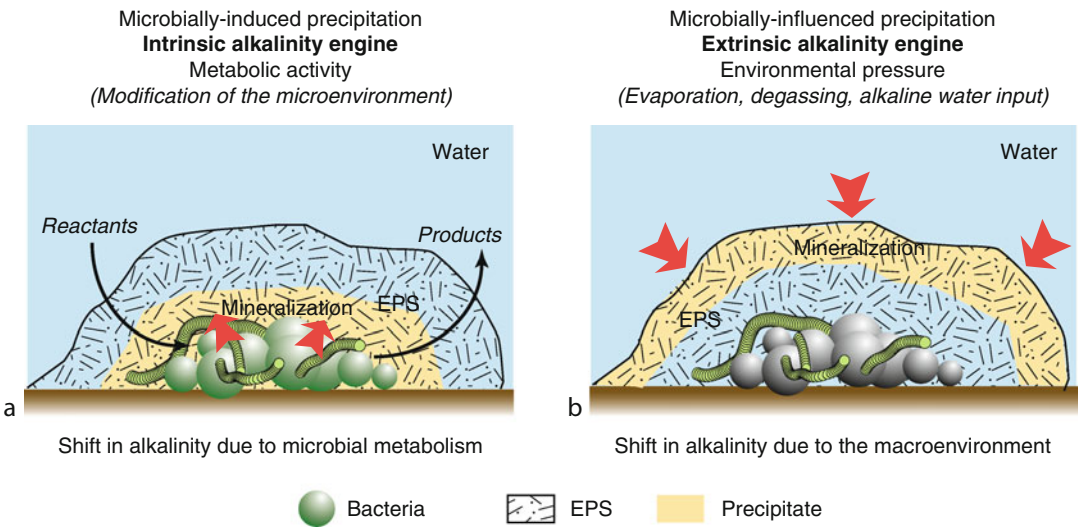


**Microbialites, Modern, Figure 7** Model of carbonate precipitation within biofilms. Increases in alkalinity leading to precipitation can be (**a**) intrinsic, resulting from microbial metabolism or (**b**) extrinsic, resulting from environmental factors (**b**). In both the cases, the EPS matrix, which embeds the microbial communities, has a pivotal role in determining mineral morphology, composition, and mineralogy.

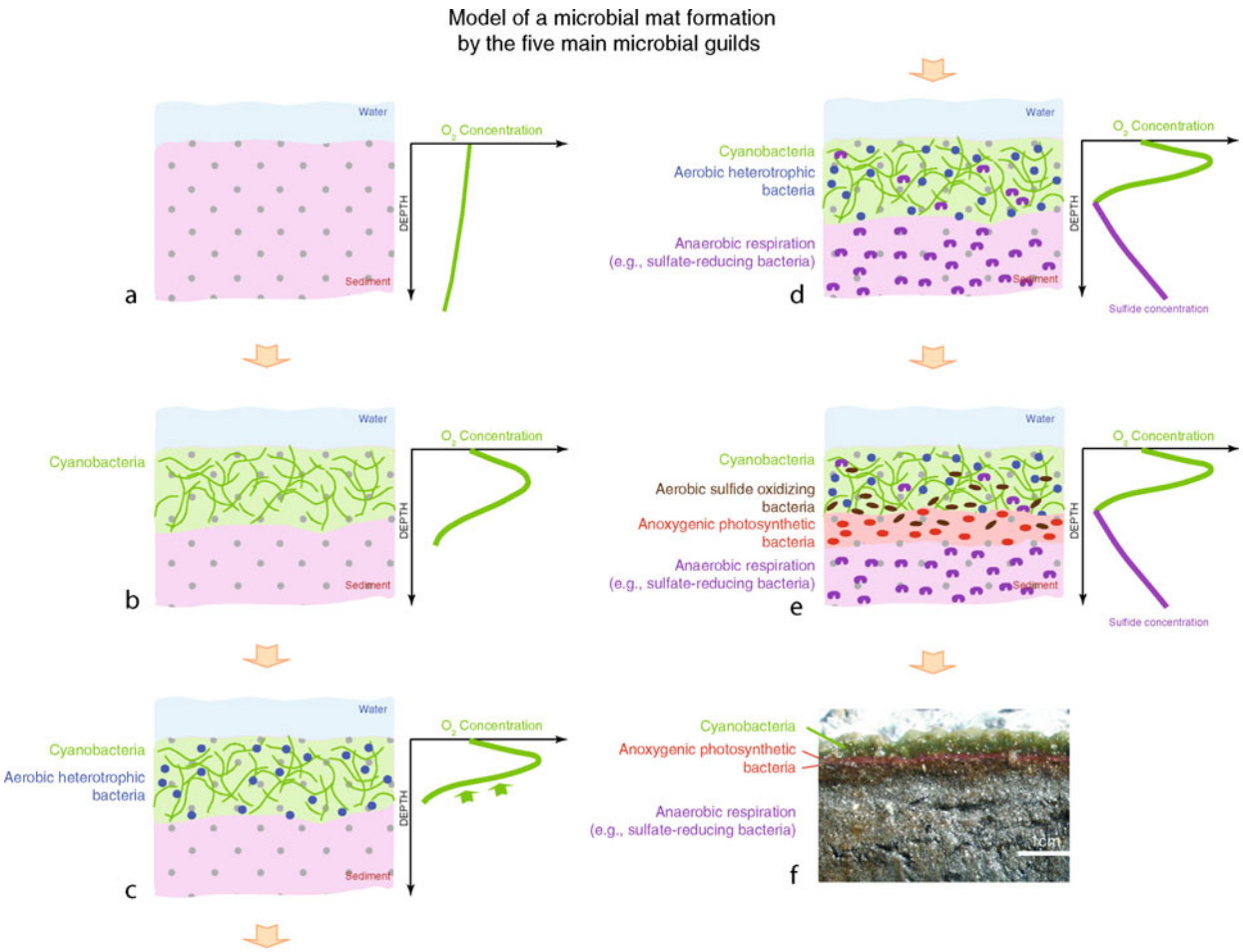


**Microbialites, Modern, Figure 8** Model of microbial mat formation by the five main guilds (van Gemerden, 1993). (**a**) Typical diffusion of $O_2$ through the water-sediment interface in the absence of microbial activity. (**b**) Cyanobacteria colonize the sediment, fixing (reduce) $CO_2$ to form biomass using solar energy (photosynthesis) and using water as electron donor. $O_2$ is a byproduct (visible in the upper millimeter of the depth profile). (**c**) The autotrophically-produced organic carbon is degraded by aerobic heterotrophs (aerobic respiration) using $O_2$ as final electron acceptor. The consumption of oxygen results in, or is reflected by, a sharper $O_2$ gradient in the sediment (arrows) and the formation of an anoxic zone below the active cyanobacterial layer. (**d**). Anaerobic heterotrophs then develop in the anoxic zone (mostly SRB in this example). (**e**) SRB produces sulfide compounds, which can then feed anoxygenic photosynthesis and aerobic sulfide oxidation. (**f**) Examples of a hypersaline mat from the Bahamas showing classical zonation of bacterial guilds.

anaerobic ($SO_4^{2-}$, $NO_3^-$, $Fe^{3+}$, etc. as oxidant) respiration (Figure 8). Most microbial metabolites (products of metabolism) are efficiently recycled within the mats, completely closing the cycles of major elements. Many microbial mats function as light-driven engines, fueled only by sunlight.

The biogeochemical niche of microorganisms can be described through three overarching metabolic characteristics related to energy generation and biomass acquisition: the energy source, the electron donor used for energy generation, and the carbon source for biomass production. Each of these three properties have two possibilities: potential energy sources are light (photo-) or chemical redox reactions (chemo-), electron donors can be organic (organo-) or inorganic (litho-), and biomass can be derived from $CO_2$ fixation (autotrophy) or from carbon that is already fixed (heterotrophy). For example, a cyanobacterium derives energy from light (photo) uses water as electron donor (litho) and fixes $CO_2$ for biomass (auto-); it is hence designated as a photolithoautotroph (trophos means "to feed"). A typical aerobic bacterium that uses organic carbon is a chemoorganoheterotroph, etc.

Different types of metabolism impact carbonate precipitation and dissolution by taking up (autotrophy) or releasing (respiration) $CO_2$ and through production or consumption of organic acids. Changes in organic acid concentrations modify alkalinity and pH of the mats (Ehrlich, 1996; Visscher and Stolz, 2005). Mechanisms

that can promote precipitation of carbonate minerals include the following:

1. *Oxygenic photosynthesis* (producing $O_2$) by cyanobacteria (photolithoautotrophy). Uptake of $CO_2$ during photosynthetic activity leads to precipitation of carbonate in the sheath or in the direct vicinity of the cyanobacteria (Pentecost and Riding, 1986; Freytet and Verrecchia, 1998, 1999; Merz-Preiss and Riding, 1999; Riding, 2000) (Figure 9). The increase in alkalinity is attributed to an exchange of $HCO_3^-$ and $OH^-$ through the cell membrane (Figure 9). Photosynthesis is an important mechanism for microbialite formation in freshwater environment (Arp et al., 2001), where it may help overcome the kinetic barrier for $CaCO_3$ precipitation, even in highly supersaturated freshwater settings (Shiraishi et al., 2008).
2. *Aerobic respiration* (chemoorganoheterotrophy) generally dissolves calcium carbonate through production of $CO_2$. However, precipitation can occur in a well-buffered alkaline environment when $CO_2$ produces carbonate ions. Carbonate minerals can also be formed when aerobic respiration consumes strong organic acids and produce $CO_2$ that will be degassed. This process is proposed for carbonate precipitation in tropical soil associated to the oxalate-carbonate cycle (Braissant et al., 2004). In the absence of $O_2$, some bacteria can generate energy through fermentation, which process uses the same compound (e.g., organic carbon, inorganic sulfur) both as electron donor and acceptor. Most fermentation of organic carbon will lead to dissolution of carbonate (Visscher and Stolz, 2005).
3. *Anaerobic respiration*: certain bacteria can oxidize organic matter using respiratory chains that do not use $O_2$ as final electron acceptor (also chemoorganoheterotrophy). These bacteria can use, e.g., sulfate (sulfate-reduction), nitrate (nitrate-reduction), iron (iron-reduction), manganese (manganese reduction), or even $HCO_3^-$. These types of metabolism can promote precipitation of carbonate through various processes (e.g., Visscher and Stolz, 2005): consumption of organic acid, production of base (e.g., $NH_3$), removing precipitation inhibition (removing of $SO_4^{2-}$), etc. Sulfate reduction is the main process in marine environment due to high concentration of $SO_4^{2-}$ in seawater.
4. *Chemolithoautotrophy*: Some bacteria do not oxidize organic matter to generate energy. They will instead use the chemical energy (chemo) produced by the oxidation of inorganic (litho) electron donors such as $H_2$, CO, $Fe^{2+}$, $NH_4^+$ and $HS^-$ in order to fix $CO_2$ (autotrophy). Sulfide (in sediments) and ammonium (in the water column) oxidation are the most abundant chemolithoautotrophic electron donor in marine environment. Aerobic sulfide oxidation and ammonium oxidation is likely to induce dissolution of carbonate minerals, whereas anaerobic sulfide oxidation (e.g., using nitrate as electron acceptor) may induce precipitation (Visscher and Stolz, 2005). However, most of these types of metabolism are all autotrophic, i.e., fixing $CO_2$. The uptake of $CO_2$ can increase carbonate alkalinity and induce precipitation of carbonates in similar way that physicochemical degassing of $CO_2$ does.

## Extrinsic alkalinity engine

The determination of alkalinity-driving forces that form microbialites is generally a complex task. In many cases, a combination of intrinsic and extrinsic factors is responsible for precipitation. There are however, a few examples where the macroenvironment acts as a major player in microbial mat lithification. The two important physicochemical processes that can lead to carbonate precipitation in microbial mats are water evaporation and $CO_2$ degassing. Even in these cases, however, the microbial communities of the mats can serve as substrates for physicochemical carbonate precipitation and affect mineral mineralogy or morphology.

In the marine environment, solar evaporation of water may lead to the formation of evaporitic minerals (e.g., Warren, 2006). Although a variety of carbonate minerals can be produced through this mechanism (e.g., calcite, ikaite, aragonite, Mg-calcite, dolomite, and magnesite), evaporites largely consist of halite and gypsum. Examples of microbial mats associated with gypsum deposits have been described (e.g., Babel, 2004). Moreover, bacteria trapped in gypsum crystals are able to survive for millions of year (Vreeland et al., 2000, 2007). The specific role of microbes in gypsum nucleation is, however, not clear as the evaporation processes generally obscure microbial signatures. For reviews on evaporites, see Yechieli, and Wood (2002) or Warren (2006).

Precipitation of carbonate can also result from degassing of $CO_2$ and forms travertines. Travertines represent chemically-mediated continental carbonate deposits that form around sinter sources along streams and lakes (Pentecost, 2005). The precipitated minerals, consisting of aragonite or calcite, are mainly related to the release of $CO_2$ from the system, resulting in supersaturation with respect to calcium carbonate. This can be illustrated by the buffering equation of the carbonate:

$$Ca^{2+} + 2HCO_3^- \longleftrightarrow CaCO_3 + CO_2 + H_2O \qquad (5)$$

Removal of $CO_2$ through degassing will drive this equation to the right, promoting precipitation of $CaCO_3$. Similarly, increasing dissolved $CO_2$ drive the equation to the left, resulting in dissolution of calcium carbonate.

Travertines can be classified based on the source of the $CO_2$ that is degassed (Pentecost, 2005). "Meteogene travertines" are formed by degassing of meteoric carbon dioxide, whereas "thermogene travertines" are formed by the degassing of hydrothermal $CO_2$. In meteogene travertines, the $CO_2$ can originate from the atmosphere or from the soil-zone. In thermogene travertines, the bulk of the $CO_2$

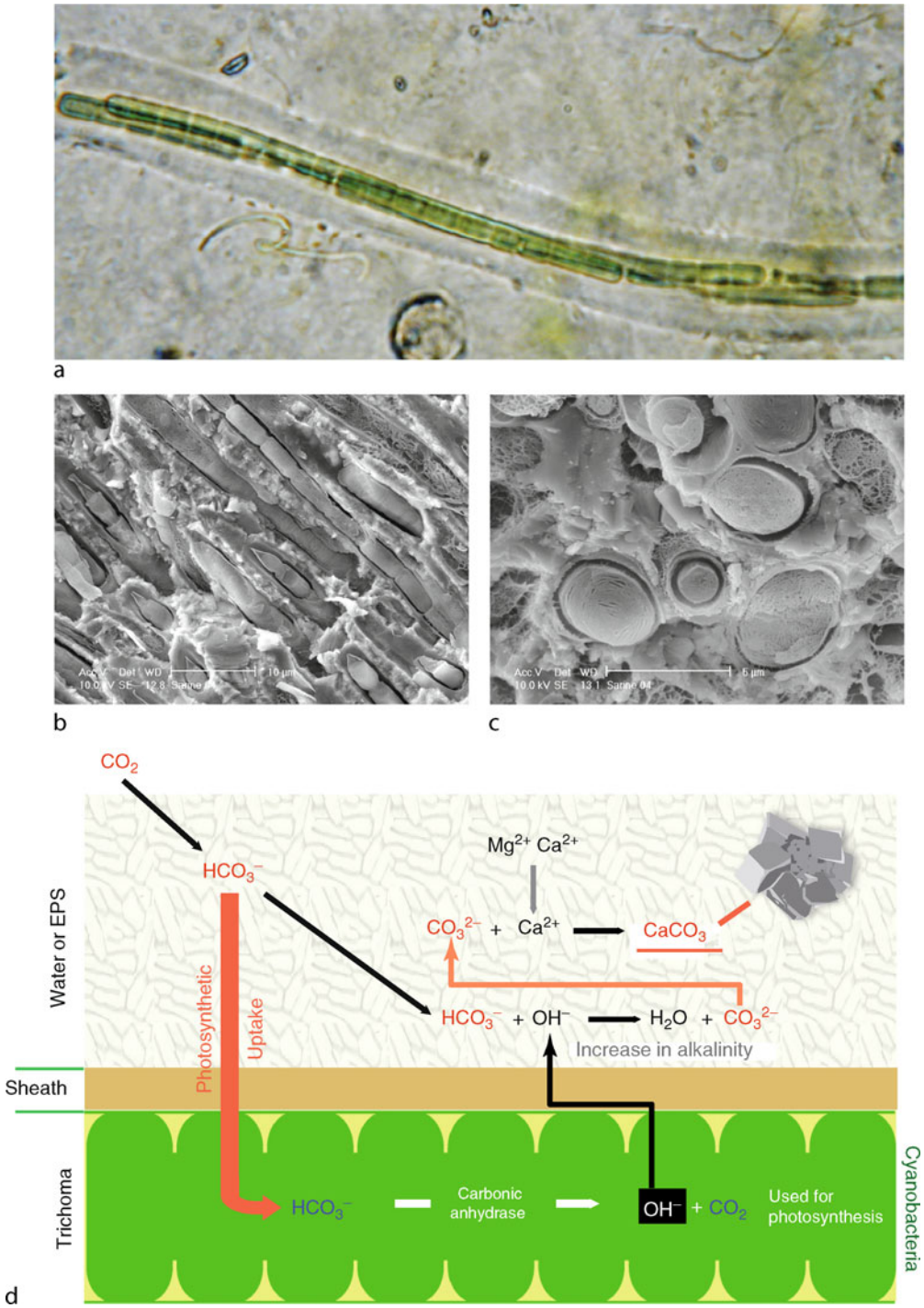


**Microbialites, Modern, Figure 9** Role of photosynthesis in the precipitation of carbonate minerals. (**a**) Photomicrograph of *Microcoleus* spp., a filamentous cyanobacterium showing the trichoma (chains of cells) embedded in a sheath. (**b**) Longitudinal section through a freshwater travertine (Sarine River, Switzerland) showing precipitation of $CaCO_3$ in the sheath of the filamentous cyanobacteria *Oscillatoria* sp. and *Phormidium* sp. (**c**) Perpendicular section through the same travertine. (**d**) Model of photosynthetically-driven carbonate precipitation. $CO_2$ dissolve in water, forming bicarbonate ions (the most common form of DIC between pH 5 and 9). The bicarbonate is taken up by cells of the trichoma; the enzyme carbonic anhydrase inside the cells produces $CO_2$ (used for photosynthesis) and $OH^-$. The release of hydroxyl ions outside the trichoma increases the alkalinity in the surrounding area of the cyanobacteria and induces precipitation of $CaCO_3$ (provided $Ca^{2+}$ ions are available).

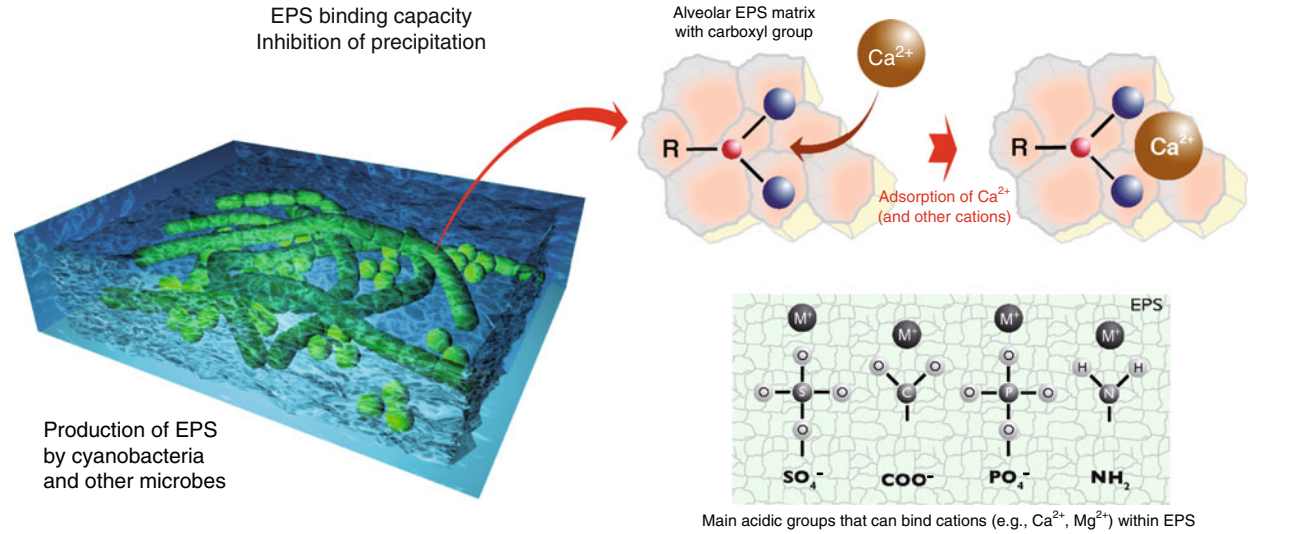


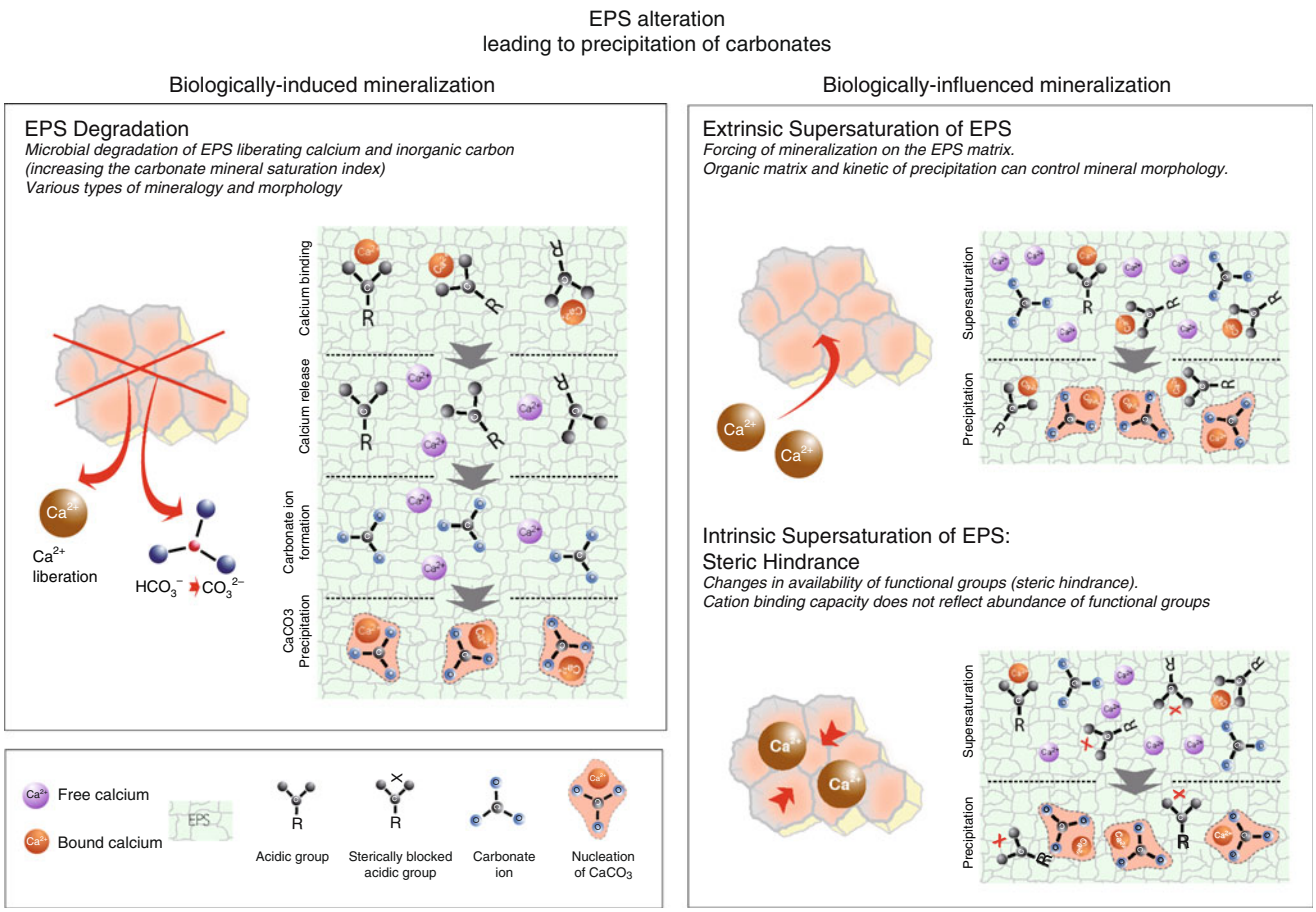


**Microbialites, Modern, Figure 10** Mechanistic role of the organic EPS matrix in microbial mat lithification. The exopolymeric substances are produced by various groups of bacteria (especially cyanobacteria). EPS can bind large amounts of cations (i.e., $Ca^{2+}$), reducing the calcium carbonate saturation index, inhibiting precipitation. Alteration of the EPS matrix can end this inhibition, allowing carbonate precipitation to commence. EPS alteration is achieved via two main pathways: (1) EPS degradation, (2a) extrinsic, and (2b) intrinsic supersaturation of the EPS binding capacity (modified from Dupraz and Visscher, 2005).

originates from thermal processes. These hydrothermal systems are commonly associated with region of recent volcanic or tectonic activities. It is important to note that the term travertine has variable usage in the literature. Many authors use travertine only for hot water deposits, using "tufa" for cold-water deposits (Pedley, 2000). Other authors use tufa for actively-forming deposits and travertine for non-active, fossil forms (see Chapter *Tufa, Freshwater*).

Although carbonate precipitation in travertines and tufas is driven by abiotic processes, precipitation often initiates on organic substrates, e.g., leaves, woods, algae, or microbial mats. In theses cases, mineralogy and morphology are strongly influenced by the organic matrix (e.g., Fouke et al., 2000; Farmer, 2000; Pentecost, 2005; Turner and Jones, 2005). Microbial mats at hot springs, for example, can therefore have a profound impact on thermogene travertine by providing templates for mineralization, even though precipitation is due to vigorous $CO_2$ degassing (Farmer, 2000; Fouke et al., 2000). Travertine formation is thus an example of biologically-influenced mineralization, since the carbonate precipitation is not due to biological activity, but microorganisms indirectly affect the characteristics of the resulting minerals.

## The organic matrix (EPS)

Microbial communities generally produce extracellular polymeric substances (EPS; see Chapter *Extracellular Polymeric Substances (EPS)*). This organic matrix is an important part of the microbial mat, preventing desiccation, retaining essential nutrients, protecting against UV radiation, and providing water channels for transport of metabolites and signaling compounds (Decho, 1990, 2000). Cyanobacteria are often considered to be the major producers of EPS. However, many other bacteria can produce EPS matrix, including aerobic and anaerobic (chemoorgano)heterotrophs, anoxygenic phototrophs, and chemolithoautotrophs (De Philippis et al., 1998, 2001; Stal, 2000, 2003; Richert et al., 2005). Anaerobic bacteria, especially sulfate-reducing bacteria, which play a key role in carbon metabolism in marine microbial mats (Thode-Andersen, and Jorgensen, 1989; Canfield and DesMarais, 1991; Visscher et al., 1991), are known to produce large amounts of EPS (Bosak and Newman, 2005; Braissant et al., 2007).

The EPS matrix is generally the location where the carbonate minerals nucleate and grow (Dupraz et al., 2004). EPS contains negatively-charged acidic groups (e.g., carboxyl, sulfhydril, amine, hydroxyl groups), which can bind a large amount of mono- and divalent cations, notably $Ca^{2+}$ (Braissant et al., 2007). This binding capacity may inhibit the precipitation of carbonate minerals by depleting calcium from the surrounding microenvironment (Figure 10). The saturation index of calcite depends on the carbonate alkalinity and the availability in calcium. Even if carbonate ions are in solution, the lack of free $Ca^{2+}$ may inhibit precipitation (Dupraz and Visscher, 2005). Therefore, the physicochemical properties of the polymer matrix, such as the acidity or composition of the functional groups associated with the EPS, are key factors in the formation of modern microbialites.

In order to precipitate calcium carbonate in microbial mats, the $Ca^{2+}$-binding capacity of the EPS has to be reduced. Various mechanisms have been proposed (e.g., Dupraz and Visscher, 2005), which can be grouped into two main processes (Figure 10): (1) degradation of the EPS matrix and (2) intrinsic or extrinsic supersaturation of cation-binding sites (e.g., Dupraz and Visscher, 2005). As EPS is a sugar polymer, it serves as metabolic substrate for (chemoorgano) heterotrophic bacteria. Depolymerization (hydrolysis) of EPS, possibly by fungi and heterotrophs, including spirochetes (Harwood and Canale-Parola, 1984; Weaver and Hicks, 1995), must occur before sugar monomers are available. Microbial degradation of EPS liberates the calcium and produces inorganic carbon (under alkaline conditions, the dominant species is carbonate ion). Alternatively, if the amount of Ca exceeds the number of binding sites in the EPS, free calcium will be present and available for precipitation. These conditions can be achieved through extrinsic factors (the environment) through continuous input of Ca. It can also result from the steric hindrance of acidic groups within the EPS. Although EPS may indeed possess abundant functional groups capable of binding $Ca^{2+}$ or $Mg^{2+}$ ions, these groups may be "sterically-inhibited" (i.e., blocked) via molecular-scale interactions into a structurally complex EPS (Figure 10).

## Summary

Microbialites are "organosedimentary deposits that accrete as a result of a benthic microbial community, which traps and binds sediment and/or forms the locus of mineral precipitation" (Kennard and James, 1986). Living examples of these structures can be found in many modern environments including marine, hypersaline, freshwater, and even continental settings. Microbialites are classified based on mesostructure as stromatolites (laminated), thrombolites (clotted), and leiolites (structureless). Among the most spectacular examples are modern stromatolites, which were first discovered in a hypersaline lagoon of Shark Bay in 1954. The only known examples of stromatolites presently forming in open marine environments are in the Bahamas. Lamination in these coarse-grained structures results from the iterative growth of three different types of microbial mats on the surfaces of the build-ups. These microbial communities are responsible for successive "trapping and binding" of sediment (type 1) and in situ precipitation of calcium carbonate (types 2 and 3). Both processes are essential for stromatolites formation. Modern thrombolites and leiolites are less well-studied than modern stromatolites.

Early lithification is a key process in the formation of modern microbialites. Lithification consists of in situ precipitation of minerals, which preserves the biosedimentary structures. Two key and closely coupled components

involved in carbonate precipitation within microbial mats are (1) the alkalinity engine and (2) the organic matrix. The alkalinity engine, which effectively changes the saturation index, is *intrinsically driven* when microbial metabolism is the dominant process causing carbonate precipitation. The alkalinity engine is *extrinsically driven* when the macroenvironment is responsible for microbial mat lithification. In both the cases, the organic matrix of extracellular polymeric substances (EPS), which embed the microbial communities, is the physical location where carbonate minerals nucleate and grow. Fresh EPS contains negatively-charged acidic groups, which bind large amount of cations (e.g., $Ca^{2+}$), inhibiting $CaCO_3$ precipitation. In order to precipitate carbonate, this inhibition has to be reduced by degradation of the EPS or by oversaturation of the cation-binding capacity. Microbial activity is ultimately responsible for EPS production and degradation leading mineral precipitation.

## Bibliography


Aitken, J. D., 1967. Classification and environmental significance of cryptalgal limestones and dolomites, with illustrations from the Cambrian and Ordovician of southwestern Alberta. *Journal of Sedimentary Petrology*, **37**, 1163–1178.

Altermann, W., Kazmierczak, J., Oren, A., and Wright, D. T., 2006. Cyanobacterial calcification and its rock-building potential during 3.5 billion years of Earth history. *Geobiology*, **4**, 147–166.

Andres, M. S., and Reid, R. P., 2006. Growth morphologies of modern marine stromatolites: a case study from Highborne Cay, Bahamas. *Sedimentary Geology*, **185**, 319–328.

Andres, M. S., Sumner, D. Y., Reid, R. P., and Swart, P. K., 2005. Isotopic fingerprints of microbial respiration in aragonite from Bahamas stromatolites. *Geology*, **34**, 973–976.

Arp, G., Reimer, A., and Reitner, J., 2001. Photosynthesis-induced biofilm calcification and calcium concentrations in Phanerozoic oceans. *Science*, **292**, 1701–1704.

Arp, G., Reimer, A., and Reitner, J., 2003. Microbialite formation in seawater of increased alkalinity, Satonda Crater Lake, Indonesia. *Journal of Sedimentary Research*, **73**, 105–127.

Awramik, S. M., 1971. Precambrian columnar stromatolite diversity: reflection of metazoan appearance. *Science*, **174**, 825–827.

Awramik, S. M., 1982. Precambrian columnar stromatolite diversity: reflection of metazoan appearance. *Science*, **216**, 171–173.

Awramik, S. M., 1992. The history and significance of stromatolites. In Schidlowski, M., Kimberley, M. M., McKirdy, D. M., and Trudinger, P. A. (eds.), *Early Organic Evolution: Implications for Energy and Mineral Resources*. Berlin: Springer, pp. 435–449.

Awramik, S. M., and Riding, R., 1988. Role of algal eukaryotes in subtidal columnar stromatolite formation. *Proceeding of National Academy of Science, USA*, **85**, 1327–1329.

Babel, M., 2004. Models for evaporite, selenite and gypsum microbialite deposition in ancient saline basins. *Acta Geologica Polonica*, **54**, 219–249.

Barbieri, R., and Cavalazzi, B., 2005. Microbial fabrics from Neogene cold seep carbonates Northern Apennine, Italy. *Palaeogeography, Palaeoclimatology, Palaeoecology*, **227**, 143–155.

Barbieri, R., Ori, G. G., and Cavalazzi, B., 2004. A Silurian cold-seep ecosystem from the Middle Altlas, Morocco. *Palaios*, **19**, 527–542.

Bathurst, R. G. C., 1966. Boring algae, micrite envelopes and lithification of molluscan biosparite. *Geological Journal*, **5**, 15–32.

Bauld, J., 1981. Geobiological role of cyanobacterial mats in sedimentary environments: production and preservation of organic matter. *BMR Journal of Australian Geology and Geophysics*, **6**, 307–317.

Bauld, J., Chambers, L. A., and Skyring, G. W., 1979. Primary productivity, sulfate reduction and sulfur isotope fractionation in algal mats and sediments of Hamelin pool, Shark Bay, W. A. Australian. *Journal of Marine and Freshwater Research*, **30**, 753–764.

Benson, L., 1994. Carbonate deposition, Pyramid Lake Subbasin, Nevada; 1, Sequence of formation and elevational distribution of carbonate deposits (tufas). *Palaeogeography Palaeoclimatology and Palaeoecology*, **109**, 55–87.

Benzerara, K., Menguy, N., Lopez-Garca, P., Yoon, T.-H., Kazmierczak, J., Tyliszczak, T., Guyot, F., and Brown, G. E. Jr., 2006. Nanoscale detection of organic signatures in carbonate microbialites. *PNAS*, **103**, 9440–9445.

Bhaskar, P. V., and Bhosle, N. B., 2005. Microbial extracellular polymeric substances in marine biogeochemical processes. *Current Science*, **88**, 45–53.

Bischoff, J. L., Stine, S., Rosenbauer, R. J., Fitzpatrick, J. A., and Stafford, T. W., 1993. Ikaite precipitation by mixing of shoreline springs and lake water, Mono Lake, California, USA. *Geochimica Cosmochimica Acta*, **57**, 3855–3865.

Bosak, T., and Newman, D. K., 2005. Microbial kinetic controls on calcite morphology in supersaturated solutions. *Journal of Sedimentary Research*, **75**, 190–199.

Braga, J. C., Martin, J. M., and Riding, R., 1995. Controls on microbial dome fabric development along a carbonate-siliciclastic shelf-basin transect, Miocene, SE Spain. *Palaios*, **10**, 347–361.

Braissant, O., Cailleau, G., Aragno, M., and Verrecchia, E. P., 2004. Biologically induced mineralization in the tree Milicia excelsa (Moraceae): its causes and consequences to the environment. *Geobiology*, **2**, 59–66.

Braissant, O., Decho, A. W., Dupraz, C., Glunk, C., Przekop, K. M., and Visscher, P. T., 2007. Exopolymeric substances of sulfate-reducing bacteria: interactions with calcium at alkaline pH and implication for formation of carbonate minerals. *Geobiology*, **5**, 401–411.

Buick, R., Dunlop, J. S. R., and Groves, D. I., 1981. Stromatolite recognition in ancient rocks: an appraisal of irregularly laminated structures in an Early Archaean chert-barite unit from North Pole, Western Australia. *Alcheringa*, **5**, 161–181.

Burne, R. V., and Moore, L. S., 1987. Microbialites: organosedimentary deposits of benthic microbial communities. *Palaios*, **2**, 241–254.

Burns, B. P., Goh, F., Allen, M., and Nellan, B. A., 2004. Microbial diversity of extant stromatolites in the hypersaline marine environment of Shark Bay, Australia. *Environmental Microbiology*, **6**, 1096–1101.

Cailleau, G., Braissant, O., and Verrecchia, E. P., 2004. Biomineralization in plants as a long-term carbon sink. *Naturwissenschaften*, **91**, 191–194.

Cailleau, G., Braissant, O., Dupraz, C., and Verrecchia, E. P., 2005. Biological control on CaCO3 accumulations in ferrallitic soils of Biga, Ivory Coast. *Catena*, **59**, 1–17.

Canaveras, J. C., Cuezva, S., Sanchez-Moral, S., Lario, J., Laiz, L., Gonzales, J. M., and Saiz-Jimenez, C., 2006. *Naturwissenschaften*, **93**, 27–32.

Canfield, D. E., and DesMarais, D. J., 1991. Aerobic sulfate reduction in microbial mats. *Science*, **251**, 1471–1473.

Decho, A. W., 1990. Microbial exopolymer secretions in ocean environments: their role(s) in food webs and marine processes. *Oceanography and Marine Biology Annual Review*, **28**, 73–154.

Decho, A. W., 2000. Exopolymer microdomains as a structuring agent for heterogeneity within microbial biofilms. In Riding,

R. E., and Awramik, S. M. (eds.), *Microbial Sediments*. New York: Springer, pp. 1–9.
De Philippis, R., Margheri, M. C., Materassi, R., and Vincenzini, M., 1998. Potential of unicellular cyanobacteria from saline environments as exopolysaccharide producers. *Applied and Environmental Microbiology*, **64**, 1130–1132.
De Philippis, R., Sili, C., Paperi, R., and Vincenzini, M., 2001. Exopolysaccharide-producing cyanobacteria and their possible exploitation: a review. *Journal of Applied Phycology*, **13**, 293–299.
Dill, R. F., Shinn, E. A., Jones, A. T., Kelly, K., and Steinen, R. P., 1986. Giant subtidal stromatolites forming in normal salinity water. *Nature*, **324**, 55–58.
Dravis, J. J., 1983. Hardened subtidal stromatolites, Bahamas. *Science*, **219**, 385–386.
Dupraz, C., and Strasser, A., 1999. Microbialites and micro-encrusters in shallow coral bioherms (Middle to Late Oxfordian, Swiss Jura Mountains). *Facies*, **40**, 101–130.
Dupraz, C., and Strasser, A., 2002. Nutritional modes in coral-microbialite reefs (Jurassic, Oxfordian, Switzerland). *Palaios*, **17**, 449–471.
Dupraz, C., and Visscher, P. T., 2005. Microbial lithification in marine stromatolites and hypersaline mats. *Trends in Microbiology*, **13**, 429–438.
Dupraz, C., Visscher, P. T., Baumgartner, L. K., and Reid, R. P., 2004. Microbe-mineral interactions: early CaCO3 precipitation in a Recent hypersaline lake (Eleuthera Islands, Bahamas). *Sedimentology*, **51**, 745–765.
Dupraz, C., Patissina, R., and Verrecchia, E. P., 2006. Simulation of stromatolite morphospace using 'DLA-CA' growth model': translation of energy in morphology. *Sedimentary Geology*, **185**, 185–203.
Ehrlich, H. L., 1996. *Geomicrobiology*, 3rd edn. (revised and expanded). New York: Marcel Dekker, Inc.
Farmer, J. D., 2000. Hydrothermal systems: doorways to early biosphere evolution. *GSA Today*, **10**, 1–10.
Fischer, A. G., 1965. Fossils, early life, and atmospheric history. In *Proceeding National Academy of Science. USA*, *Washington*, Vol. 53, pp. 1205–1215.
Fouke, B. W., Farmer, J. D., Des Marais, D. J., Pratt, L., Sturchio, N. C., Burns, P. C., and Discipulo, M. K., 2000. Depositional facies and aqueous-solid geochemistry of travertine-depositing hot springs (Ange Terrace, Mammoth Hot Springs, Yellowstone National Park, USA). *Journal of Sedimentary Research*, **70**, 565–585.
Freytet, P., and Verrecchia, E. P., 1998. Freshwater organisms that build stromatolites: a synopsis of biocrystallization by prokaryotic and eukaryotic algae. *Sedimentology*, **45**, 535–563.
Freytet, P., and Verrecchia, E. P., 1999. Calcitic radial palisadic fabric in freshwater stromatolites: diagenetic and recrystallized feature or physicochemical sinter crust. *Sedimentary Geology*, **126**, 97–102.
Gebelein, C. D., 1976. The effects of the physical, chemical and biological evolution of the earth. In Walter, M. R. (ed.), *Stromatolites*. Developments in Sedimentology. Amsterdam: Elsevier, Vol. 20, pp. 499–515.
Golubic, S., and Focke, J. W., 1978. Phormidium hendersonii Howe: identify and significance of a modern stromatolites building microorganism. *Journal of Sedimentary Petrology*, **48**, 751–764.
Golubic, S., and Hofmann, H. J., 1976. Comparison of Holocene and mid-Precambrian Entophysalidaceae (Cyanophyta) in stromatolitic algal mats; cell division and degradation. *Journal of Paleontology*, **50**, 1074–1082.
Grey, K., Moore, L. S., Burne, R. V., Pierson, B. K., and Bauld, J., 1990. Lake Thetis, Western Australia: an example of saline lake sedimentation dominated by benthic microbial processes. *Austalian Journal of Marine and Freshwater Research*, **41**, 275–300.
Grotzinger, J. P., and Knoll, A. H., 1999. Stromatolites in Precambrian carbonates: evolutionary mileposts or environmental dipsticks? *Annual Review of Earth and Planetary Science*, **27**, 313–358.
Harwood, C. S., and Canale-Parola, E., 1984. Ecology of spirochetes. *Annual Review of Microbiology*, **38**, 161–192.
Hillgaertner, H., Dupraz, C., and Hug, W. A., 2001. Microbially induced stabilization of carbonate sands in marine phreatic environments or are micritic meniscus cements good indicators for vadose diagenesis? *Sedimentology*, **48**, 117–131.
Jones, D., and Wilson, M. J., 1986. Biomineralization in crustose lichens. In Leadbeater, B. S. C., and Riding, R. (eds.), *Biomineralization in Lower Plants and Animals*. The Systematics Association, Special Volume 30. New York: Oxford University Press, pp. 91–105.
Kalkowsky, E., 1908. Oolith und Stromatolith im nord-deutchen Buntsandstein. *Zeitschrift der deutschen geologischen Gesellschaft*, **60**, 68–125.
Kazmierczak, J., and Kempe, S., 2006. Genuine modern analogues of Precambrian stromatolites from caldera lakes of Niuafo'ou Island, Tonga. *Naturwissenschaften*, **93**, 119–126.
Kelley, D. S., Karson, J. A., Blackman, D. K., Frueh-Green, G. L., Butterfield, D. A., Lilley, M. D., Olson, E. J., Shrenk, M. O., Roe, K. K., Lebon, G. T., and Rivizzigno, P., and the AT3–60 Shipboard Party, 2001. An off-axis hydrothermal vent field near the Mid-Atlantic ridge at 30° N. *Nature*, **412**, 145–149.
Kempe, S., and Kazmierczak, J., 1994. The role of alkalinity in the evolution of ocean chemistry, organization of living systems, and biocalcification processes. *Bulletin de l'Institut oceanographique, Monaco*, **13**, 61–117.
Kempe, S., Reimer, A., Lipp, A., Kazmierczak, J., Landmann, G., and Konuk, T., 1991. Largest known microbialites discovered in Lake Van, Turkey. *Nature*, **349**, 605–608.
Kennard, J. M., and James, N. P., 1986. Thrombolites and stromatolites: two distinct types of microbial structures. *Palaios*, **1**, 492–503.
Klappa, C. F., 1979. Lichen stromatolites; criterion for subaerial exposure and a mechanism for the formation of laminar calcretes (caliche). *Journal of Sedimentary Petrology*, **49**, 387–400.
Kobluk, D. R., and Crawford, D. R., 1990. A modern hypersaline organic mud- and gypsum dominated basin and associated microbialites. *Palaios*, **5**, 134–148.
Kromkamp, J. C., Perkins, R., Dijkman, N., Consalvey, M., Andres, M., and Reid, R. P., 2007. Resistance to burial of cyanobacteria in stromatolites. *Aquatic Microbial Ecology*, **48**, 123–130.
Kumar, S., and Pandey, S. K., 2008. Discovery of organic-walled microbiota from the black-bedded chert, Balman Limestone, the Bhander Group, Lakheri area, Rajasthan. *Current Science*, **94**, 797–800.
Lepot, K., Benzerara, K., Brown, G. E. Jr., and Philippot, P., 2008. Microbially influenced formation of 2.724-million-year-old stromatolites. *Nature Geoscience*, **1**, 118–121.
Lindsay, J. F., Brasier, M. D., McLoughlin, N., Green, O. R., Fogel, M., McNamara, K., Steele, A., and Mertzman, S. A., 2003. Abiotic Earth – establishing a baseline for earliest life, data from the Archaean of Western Australia. *Lunar and Planetary Institute, Annual Meeting. Lunar, Planetary Institute Contribution*, **1156**, 1137.
Logan, B. W., 1961. Cryptozoon and associate stromatolites from the Recent, Shark Bay, Western Australia. *The Journal of Geology*, **69**, 517–533.
Logan, B. W., Hoffman, P., and Gebelein, C. D., 1974. Algal mats, cryptalgal fabrics and structures, Hamelin Pool, Western Australia. *AAPG Memoir*, **22**, 140–194.

Lowe, D. R., 1994. Abiological origin of described stromatolites older than 3.2 Ga. *Geology*, **22**, 387–390.
Lowenstam, H. A., and Weiner, S., 1989. *On Biomineralization*. New York: Oxford University Press.
Ludwig, K. A., Kelley, D. S., Butterfield, D. A., Nelson, B., and Früh-Green, G., 2006. Formation and evolution of carbonate chimneys at the Lost City Hydrothermal Field. *Geochemica Cosmochimica Acta*, **70**, 3625–3645.
Macintyre, I. G., Prufert-Bebout, L., and Reid, R. P., 2000. The role of endolithic cyanobacteria in the formation of lithified laminae in Bahamian stromatolites. *Sedimentology*, **47**, 915–921.
Mann, S., 2001. *Biomineralization: Principles and Concepts in Bioinorganic Materials Chemistry*. New York: Oxford University Press.
Mann, C. J., and Hoffman, L. R., 1984. Algal mounds in Storr's Lake, San Salvador, Bahamas. In *Proceeding of the 2nd Symposium on Geology of the Bahamas*, CCFL Bahamian Field Station, pp. 41–51.
Mann, C. J., and Nelson, W. M., 1989. Microbialitic structures in Storr's Lake, San Salvador Island, Bahamas Islands. *Palaios*, **4**, 287–293.
McNeese, L. R., 1988. *The stromatolites of Storr's Lake, San Salvador, Bahamas*. MSc thesis, University of North Carolina at Chapel Hill, Department of Geology.
Merz-Preiss, M., and Riding, R., 1999. Cyanobacterial tufa calcification in two freshwater streams; ambient environment, chemical thresholds biological processes. *Sedimentary Geology*, **126**, 103–124.
Neumann, C. A., Bebout, B. M., McNeese, L. R., Paul, C. K., and Paerl, H. W., 1988. Modern stromatolites and associated mats: San Salvador, Bahamas. In *Proceedings of the 4th Symposium on the geology of the Bahamas*. Bahamas Field Station, San Salvador, pp. 235–251.
Noffke, N., Gerdes, G., and Klenke, T., 2003. Benthic cyanobacteria and their influence on the sedimentary dynamics of peritidal depositional systems (siliciclastic, evaporitic salty, and evaporitic carbonatic). *Earth-Science Reviews*, **62**, 163–176.
Parker, B. C., Simmons, G. M., Love, F. G. Jr., Wharton, R. A., and Seaburg, K. G. Jr., 1981. Modern stromatolites in Antarctic Dry Valley Lakes. *BioScience*, **31**, 656–661.
Pedley, M., 2000. Ambient temperature freshwater microbial tufas. In Riding, R., and Awramik, S. M. (eds.), *Microbial Sediments*. Berlin: Springer, pp. 179–186.
Pentecost, A., 1978. Blue-green algae and freshwater carbonate deposits. *Proceedings of the Royal Society of London*, **200**, 43–61.
Pentecost, A., 1995. The quaternary travertine deposits of Europe and Asia Minor. *Quaternary Science Reviews*, **14**, 1005–1028.
Pentecost, A., 2005. *Travertine*. Berlin: Springer.
Pentecost, A., and Riding, R., 1986. Calcification in cyanobacteria. In Leadbeater, B. S. C., and Riding, R. (eds.), *Biomineralization in Lower Plants and Animals*. The Systematic Association, Special Volume 30, pp. 73–90.
Perry, R. S., Mcloughlin, N., Lynne, B. Y., Sephton, M. A., Oliver, J. D., Perry, C. C., Campbell, K., Engel, M. H., Farmer, J. D., Brasier, M. D., and Staley, J. T., 2007. Defining biominerals and organominerals: Direct and indirect indicators of life. *Sedimentary Geology*, **201**, 157–179.
Playford, P. E., 1979. Stromatolite research in Western Australia. *Journal of the Royal Society of Western Australia*, **62**, 13–20.
Playford, P. E., 1990. Geology of the Shark Bay area, Western Australia. In Berry, P. F., Bradshaw, S. D., and Wilson, B. R. (eds.), *Research In Shark Bay*. West Australian Museum, pp. 13–31.
Playford, P. E., and Cockbain, A. E., 1976. Modem algal stromatolites at Hamelin Pool, a hypersaline barred basin in Shark Bay. Western Australia. In Walter, M. R. (ed.), *Stromatolites*. Developments in Sedimentology. Amsterdam: Elsevier, Vol. 20, pp. 389–411.
Read, J. F., 1976. Calcretes and their distinction from stromatolites. In Walter, M. R. (ed.), *Stromatolites*. Developments in Sedimentology. Amsterdam: Elsevier, Vol. 20, pp. 55–71.
Reid, R. P., and Macintyre, I. G., 2000. Microboring versus recrystallization: further insight into the micritization process. *Journal of Sedimentary Research*, **70**, 24–28.
Reid, R. P., Macintyre, I. G., Browne, K. M., Steneck, R. S., and Miller, T., 1995. Modern marine stromatolites in the Exuma Cays, Bahamas: uncommonly common. *Facies*, **33**, 1–18.
Reid, R. P., Visscher, P. T., Decho, A. W., Stolz, J. K., Bebout, B. M., Dupraz, C., Mactintyre, I. G., Paerl, H. W., Pinckney, J. L., Prufert-Bebout, L., Steppe, T. F., and Des Marais, D. J., 2000. The role of microbes in accretion, lamination and early lithification of modern marine stromatolites. *Nature*, **406**, 989–992.
Reid, R. P., Dupraz, C., Visscher, P. T., Decho, A. W., and Sumner, D. Y., 2003a. Microbial processes forming modern marine stromatolites: microbe-mineral interactions with a three-billion-year rock record. In Krumbein, W. E., Paterson, D. M., and Zavarzin, G. A. (eds.), *Fossil and Recent Biofilms - A Natural History of Life on Earth*. Dordrecht: Kluwer, pp. 103–118.
Reid, R. P., James, N. P., Macintire, I. G., Dupraz, C. P., and Burne, R. V., 2003b. Shark Bay Stromatolites: microfabrics and reinterpretations of origins. *Facies*, **49**, 243–270.
Reitner, J., Paul, J., Arp, G., and Hause-Reitner, D., 1996. Lake Thetis Domal Microbialites – a complex framework of calcified biofilms and organomicrites (Cervantes, Western Australia). In Reitner, J., Neuweiler, F., and Gunkel, F. (eds.), *Global and Regional Controls on Biogenetic Sedimentation. I.* Reef Evolution. Research Reports. Göttingen: Göttinger Arb. Geol. Paläont., Sonderband, Vol. 2, pp. 85–89.
Richert, L., Golubic, S., Le Guedes, R., Ratiskol, J., Payri, C., and Guesennec, J., 2005. Characterization of exopolysaccharides produced by cyanobacteria isolated from Polynesian microbial mats. *Current Microbiology*, **51**, 379–384.
Riding, R., 1991. Classification of microbial carbonates. In Riding, R. (ed.), *Calcareous Algae and Stromatolites*. Berlin: Springer, pp. 21–51.
Riding, R., 1999. The term stromatolite: towards an essential definition. *Lethaia*, **32**, 321–330.
Riding, R., 2000. Microbial carbonates: the geological record of calcified bacterial-algal mats and biofilms. *Sedimentology*, **47**, 179–214.
Riding, R., 2006. Microbial carbonate abundance compared with fluctuations in metazoan diversity over geological time. *Sedimentary Geology*, **185**, 229–238.
Robbins, L. L., and Blackwelder, P. L., 1992. Biochemical and ultrastructural evidence for the origin of whitings; a biologically induced calcium carbonate precipitation mechanism. *Geology*, **20**, 464–468.
Schmid, D. U., 1996. Marine microbolithe und mikroinkrustierer aus dem Oberjura. *Profil*, **9**, 101–251.
Seong-Joo, L., Browne, K. M., and Golubic, S., 2000. On stromatolites lamination. In Riding, R. E., and Awramik, S. M. (eds.), *Microbial Sediments*. New York: Springer, pp. 16–24.
Shapiro, R. S., 2000. A comment on the systematic confusion of thrombolites. *Palaios*, **15**, 166–169.
Sharp, J. H., 1969. Blue-green algae and carbonates – Schizothrix calcicola and algal stromatolites from Bermuda. *Limnology and Oceanography*, **14**, 568–578.
Shiraishi, F., Bissett, A., de Beer, D., Reimer, A., and Arp, G., 2008. Photosynthesis, respiration and exopolymer calcium-binding in biofilm calcification (Westerhoefer and Deinschwanger Creek, Germany). *Geomicrobiology Journal*, **25**, 83–94.

Simkiss, K., and Wilbur, K., 1989. *Biomineralization. Cell Biology and Mineral Deposition*. San Diego: Academic.
Stal, L. J., 2000. Microbial mats and stromatolites. In Whitton, B. A., and Potts, M. (eds.), *The Ecology of Cyanobacteria. Their Diversitty in Time and Space*. Dordrecht: Kluwer.
Stal, L. J., 2003. Microphytobenthos, their extracellular polymeric substances, and the morphogenesis of intertidal sediments. *Geomicrobioly Journal*, **20**, 463–478.
Stolz, J. F., 2000. Structure of microbial mats and biofilms. In Riding, R. E., Awramik, S. M. (eds.), *Microbial Sediments*. New York: Springer, pp. 1–9.
Stumm, W., and Morgan, J. J., 1996. *Aquatic Chemistry*. New York: Wiley, 1022 pp.
Thode-Andersen, S., and Jorgensen, B. B., 1989. Sulfate reduction and the formation of $^{35}$S-labeled FeS, $FeS_2$, and S(0) (elemental sulfur) in coastal marine sediments. *Limnology and Oceanography*, **34**, 793–806.
Thompson, J. B., and Ferris, F. G., 1990. Cyanobacterial precipitation of gypsum, calcite, and magnesite from natural alkaline lake water. *Geology*, **18**, 995–998.
Thrailkill, J., 1976. Speleothems. In Walter, M. R. (ed.), *Stromatolites*. Developments in Sedimentology. Amsterdam: Elsevier, Vol. 20, pp. 73–86.
Turner, E. C., and Jones, B., 2005. Microscopic calcite dendrites in cold-water tufa: implications for nucleation of micrite and cement. *Sedimentology*, **52**, 1043–1066.
Van Gemerden, H., 1993. Microbial mats: a joint venture. *Marine geology*, **113**, 3–25.
Verrecchia, E. P., and Verrecchia, K. E., 1994. Needle-fiber calcite: a critical review and a proposed classification. *Journal of Sedimentary Research*, **64**, 650–664.
Verrecchia, E. P., Freytet, P., Verrecchia, K. E., and Dumont, J. L., 1995. Spherulites in calcrete laminar crusts: biogenic CaCO3, precipitation as a major contributor to crust formation. *Journal of Sedimentary Research*, **A65**, 690–700.
Visscher, P. T., and Stolz, J. F., 2005. Microbial mats as bioreactors: populations, processes and products. *Paelogeography Paleoclimatology, Paleooecology*, **219**, 87–100.
Visscher, P. T., Beukema, J., and van Gemerden, H., 1991. *In situ* characterization of sediments: measurements of oxygen and sulfide profiles. *Limnology and Oceanography*, **36**, 1476–1480.
Visscher, P. T., Reid, R. P., and Bebout, B. M., 2000. Microscale observations of sulfate reduction: correlation of microbial activity with lithified micritic laminae in modern marine stromatolites. *Geology*, **28**, 919–922.
Vreeland, R. H., Rosenzweig, W. D., and Powers, D. W., 2000. Isolation of a 250 million year old halotolerant bacterium from a primary salt crystal. *Nature*, **407**, 897–900.
Vreeland, R. H., Lowenstein, T., Timofeeff, M., Satterfield, C., DiFerdinando, J., Jones, J., Monson, A., Rosenzweig, W. D., Cho, B. C., Park, J. S., Wallace, A., and Grant, W. D., 2007. The isolation of live cretaceous (121–112 million years old) halophilic *Archaea* from primary salt crystals. *Geomicrobiology Journal*, **24**, 275–282.
Walter, M. R., and Heys, G. R., 1985. Links between the rise of Metazoa and the decline of stromatolites. *Precambrian Research*, **29**, 149–174.
Warren, J. K., 2006. *Evaporites: Sediments, Resources and Hydrocarbons*. New York: Springer.
Weaver, D. T., and Hicks, R. E., 1995. Biodegradation of *Azotobacter vinelendii* exopolymer by Lake Superior microbes. *Limnology and Oceanography*, **40**, 1035–1041.
Weiner, S., and Addadi, L., 2002. At the cutting edge. Perspectives. *Science*, **298**, 375–376.
Weiner, S., and Dove, P. M., 2003. An overview of biomineralization and the problem of the vital effect. In Dove, P. M., Weiner, S., and De Yoreo, J. J. (eds.), *Biomineralization*. Review in Mineralogy and Geochemistry. Washington: Mineralogical Society of America, Vol. 54, pp. 1–31.
Wright, V. P., Platt, N. H., and Wimbledon, W. A., 1988. Biogenic laminar calcrete: evidence of calcified root-mat horizons in paleosols. *Sedimentology*, **35**, 603–620.
Yechieli, Y., and Wood, W. W., 2002. Hydrogeologic processes in saline systems: playas, sabkhas, and saline lakes. *Earth-Science Reviews*, **58**, 343–365.
Zabielski, V. P., 1991. The depositional history of Storr's Lake San Salvador, Bahamas. Unpublished PhD thesis, University of North Carolina.
Zeebe, R. E., and Wolf-Gladrow, D. (eds.), 2001. *CO2 in Seawater: Equilibrium, Kinetics and Isotopes*. Amsterdam: Elsevier, 346 pp.

## Cross-references

Biofilms
Extracellular Polymeric Substances (EPS)
Microbial Biomineralization
Microbial Mats
Microbialites, Stromatolites, and Thrombolites
Organomineralization
Sediment Diagenesis – Biologically Controlled
Tidal Flats
Tufa, Freshwater

# MICROBIALITES, STROMATOLITES, AND THROMBOLITES

Robert Riding
University of Tennessee, Knoxville, TN, USA

## Microbialite

### Definition

Microbialites are "organosedimentary deposits that have accreted as a result of a benthic microbial community trapping and binding detrital sediment and/or forming the locus of mineral precipitation" (Burne and Moore, 1987, pp. 241–242).

### Introduction

Microbial carbonates are produced by the interaction of microbial growth and metabolism, cell surface properties, and extracellular polymeric substances (EPS) with mineral precipitation and grain trapping. The early lithification that is essential for the accretion and preservation of benthic microbial carbonates is both biologically mediated and environmentally dependent. Consequently, microbialite history reflects not only microbial mat evolution, but also long-term changes in seawater and atmospheric chemistry that have influenced microbial metabolism and seawater carbonate saturation state.

Microbialites are in place benthic sediments produced by microbial processes. The term "microbialite" has been most widely used to describe carbonate stromatolites, thrombolites, and similar structures that occur as domes and columns in the shallow waters of lakes and seas, but it can also apply to many additional authigenic accumulations in which microbes are locally conspicuous, such as

some tufa, travertine, speleothem and spring, seep, and vent deposits. A series of terms and definitions were proposed between 1967 and 1987 in attempts to distinguish benthic sediments formed by microbial sediment trapping and/or precipitation. The first term, *cryptalgal*, was proposed by Aitken (1967, p. 1163) for rocks or rock structures "believed to originate through the sediment-binding and/or carbonate precipitating activities of non-skeletal algae." The second was redefinition of *stromatolite* by Awramik and Margulis' (1974) as "organosedimentary structures produced by sediment trapping, binding and/or precipitation as a result of growth and metabolic activity of organisms, primarily blue-green algae." Both Aitken (1967, p. 1163) and Awramik and Margulis (1974) used blue-green algae to indicate cyanobacteria, and therefore Kennard and James (1986, p. 496) replaced cryptalgal by *cryptomicrobial*. The third term was *microbialite* (Burne and Moore, 1987), which effectively repeated Awramik and Margulis' (1974) definition of stromatolite, thereby broadening its scope. The primary focus of all these definitions was stromatolites and thrombolites.

Research during the 1900s revealed many details concerning the nature and history of stromatolites, but it also led to nomenclatural uncertainty as it became necessary to accommodate newly recognized deposits, such as thrombolites. Aitken (1967, p. 1164) sought to clarify use of "algal" in carbonate rock descriptions by distinguishing "rocks composed of the remains of skeletal calcareous algae . . . from those formed by noncalcareous blue-green . . . and green . . . algae." He termed the latter *cryptalgal*, defined as rocks or rock structures "believed to originate through the sediment-binding and/or carbonate-precipitating activities of nonskeletal algae" (Aitken, 1967, p. 1163). Aitken (1967, Fig. 1) regarded both thrombolites and stromatolites as cryptalgal deposits, distinguishing by their respective clotted and laminated macrofabrics. However, Awramik and Margulis' (1974) proposed a broader definition of stromatolite as "megascopic organosedimentary structures produced by sediment trapping, binding and/or precipitation as a result of growth and metabolic activity of organisms, primarily blue-green algae." This therefore subsumed thrombolite as a category within stromatolite.

As a result of these and other developments, by the 1980s stromatolites could variously be regarded as (1) microbial and laminated (e.g., Kalkowsky, 1908; Hofmann, 1969; Krumbein, 1983), (2) microbial but not necessarily laminated (Awramik and Margulis, 1974), and (3) laminated but not necessarily organic (Semikhatov et al., 1979) (see Riding, 1999, p. 324). Since the wording of Burne and Moore's (1987, pp. 241–242) definition of microbialite closely followed that of Awramik and Margulis' (1974) definition of stromatolite, it therefore required return to a narrower definition of stromatolite, as layered or laminated structures. This relatively narrow definition was intended by Kalkowsky (1908) and is implied by his term stromatolith; *stromat*, Greek for "to spread out," suggests a layer. Burne and Moore's (1987) new term, *microbialite*, encompassed more diverse benthic microbial deposits. The outcome of these developments was that stromatolite and thrombolite could be considered as equal categories within microbialite, mirroring Aitken's (1967, Fig. 1) classification of stromatolites and thrombolites within cryptalgal carbonates. Subsequently, these and other varieties of microbialite have commonly been distinguished by their dominant internal macrofabric: stromatolite (laminated), thrombolite (clotted), dendrolite (dendritric), and leiolite (aphanitic) (Riding, 2000, pp. 189–195) (Figure 1).

Given the importance of stromatolites in the development of these concepts, this orderly arrangement of terms under the microbialite umbrella relied heavily on stromatolites being microbial structures. However, as soon as Kalkowsky's (1908) article was published, researchers began to point out similarities between stromatolites and abiogenic precipitates (Reis, 1908; Bucher, 1918), and this chorus has continued ever since. Logan et al. (1964, p. 69) suggested recognition of "inorganic stromatolites"; Hofmann (1973, Fig. 5) showed the difficulty of distinguishing stromatolites from other laminites; and Semikhatov et al. (1979, p. 994) proposed a descriptive rather than purely genetic definition of stromatolite. Reports of essentially abiogenic stromatolites have persisted, especially in the Proterozoic (Grotzinger and Read, 1983; Grotzinger, 1989a; Pope et al., 2000). Attempts to separate abiogenic and biogenic stromatolites are obstructed by *hybrid stromatolites* (see below, Stromatolites) consisting of millimetric alternations of abiogenic crust and lithified microbial mat (Riding, 2008). Consequently, although microbial mat models seem to apply well to all or most thrombolites, dendrolites and leiolites, they do not account for all stromatolite-like deposits, particularly in the Precambrian. The implications of this complication for stromatolite interpretation as well terminology have still to be worked out.

## Microbialites in space and time

Microbes occupy a very broad range of environments, including waters of widely differing chemistry and composition, and their involvement in sedimentation is equally varied. Most microbialites are carbonate (e.g., aragonite, calcite, dolomite) in composition, but siliceous, phosphatic, iron, manganese, and sulfate examples also occur. The microbes in microbialites are dominantly bacteria, including cyanobacteria, together with small algae. From the perspective of biocalcification, microbialite carbonates are bioinduced. Bacteria in general exert relatively weak control over the organic site and mineralogy of calcification, and present-day microbial carbonates appear to be most widespread in environments where precipitation is inorganically favored. This environmental dependence means that where rapid cooling and degassing strongly favor mineral precipitation irrespective of organic intervention, as in hot water springs and vents, the overall sedimentary contribution of microbes may be

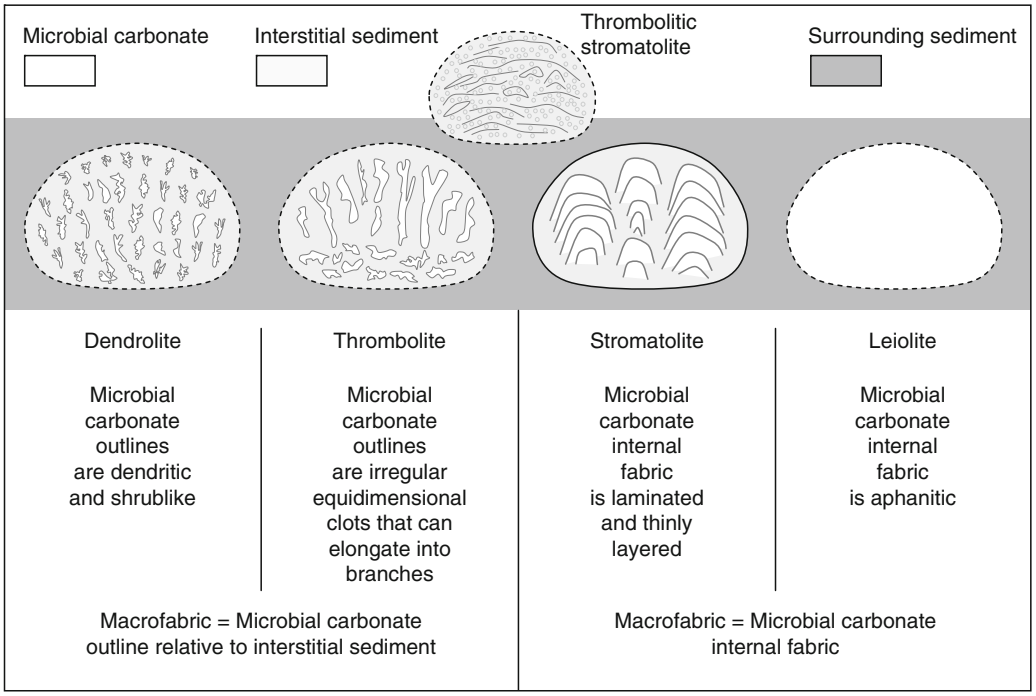


**Microbialites, Stromatolites, and Thrombolites, Figure 1** Microbial carbonates defined by macrofabric: leiolite (aphanitic), stromatolite (laminated), thrombolite (clotted), dendrolite (dendritic). Examples show domes and associated sediment. Not to scale. All categories are integradational. In addition to domes/mounds, overall shape can include columns, layers, and irregular masses. A complication is that leiolite and stromatolite macrofabrics are defined by features within (i.e., internal to) the microbial carbonate, such as lamination. In contrast, thrombolite and dendrolite macrofabrics are defined by the external shape of individual masses of microbial carbonate, such as clots or small shrub-like masses. Thrombolitic stromatolite (Aitken, 1967), typified by some Shark Bay columns, is internally weakly clotted and crudely laminated. It is essentially agglutinated, in contrast to Neoproterozoic and early Palaeozoic thrombolites with calcified microbial microfabrics. In the latter, the clots may be prostrate and irregular, and also vertically extended into amalgamated elongate branches (e.g., *Favosamaceria*).

relatively minor. In such cases, they influence the fabric more than the process of deposition. In contrast, where waters are less saturated for minerals, microbial activity can play a major role in sediment precipitation. These differing roles are reflected in the form and fabrics of the resulting deposits.

Sensitivity to environmental influence is also reflected in the secular distribution of microbialites. Without ruling out the influence of other factors – such as competition with other organisms – marine microbial carbonate abundance through time significantly reflects fluctuation in carbonate saturation state (Fischer, 1965; Grotzinger, 1990; Riding and Liang, 2005). Microbial carbonates can therefore be relatively sensitive proxies for seawater carbonate chemistry, and for atmospheric composition, since cyanobacterial sheath calcification is promoted by increased bicarbonate uptake (Merz, 1992) when $CO_2$ levels decline (Riding, 2006).

### Scope

The term microbialite, with its emphasis on benthic microbial deposits, encompasses a wide range of sediments; what does it not cover? "Benthic" would seem to exclude both allochthonous and interstitial microbial sediments. If so, then biogenic "whiting" deposits produced by photosynthetically induced nucleation of small $CaCO_3$ crystals in the water column are not microbialites, and neither are diagenetic bacterially induced precipitates such as cements and concretions. However, these somewhat artificial distinctions could be blurred, as in some soil crust and beachrock deposits. On the other hand, "microbial" must exclude abiogenic stromatolites, identified in both Precambrian and Phanerozoic sediments (Grotzinger and Read, 1983; Pope et al., 2000). This is a complication, especially since microbialite (Burne and Moore, 1987) is based on a preexisting definition of stromatolite proposed by Awramik and Margulis (1974), and arose from a need for a general term to encompass stromatolite, thrombolite, and related deposits. Such difficulties of definition should be resolved by increased understanding of both present-day and ancient examples of these important and geologically widespread deposits.

## Stromatolites

### Definition

Stromatolites are laminated benthic microbial deposits (Riding, 1991).

## Introduction

Kalkowsky (1908) proposed the term stromatolite (*Stromatolith*) for columns and domes in early Triassic playa lake oolites, but similar structures were already long known from examples such as those in the late Cambrian of New York State that Steele (1825, pp. 17–18, pl. 2) described as "calcareous concretions" and Hall (1883) named *Cryptozoon* (Figure 2). The search for present-day analogs of these ancient stromatolites led from freshwater tufa (Walcott, 1914; Roddy, 1915) and marsh deposits (Black, 1933) to marginal marine domes (Ginsburg et al., 1954) and columns (Logan, 1961). These discoveries strongly supported Kalkowsky's (1908) inference that stromatolites are essentially microbial deposits. But optimism that they could provide appropriate analogs for all ancient marine stromatolites was tempered by studies of Precambrian examples that include significant abiogenic precipitated components (e.g., Serebryakov, 1976, p. 633; Grotzinger and Knoll, 1999, p. 314). Some definitions of stromatolite have therefore encompassed both microbial and abiogenic layered/laminated authigenic crusts that characteristically form domical and columnar morphologies.

Definitions of stromatolite range from that of Kalkowsky (1908) to that of Semikhatov et al. (1979, p. 993): "a stromatolite is . . . an attached, laminated, lithified, sedimentary growth structure, accretionary away from a point or limited surface of initiation. Although characteristically of microbial origin and calcareous composition, it may be of any origin, composition, shape, size, or age." Understanding of Kalkowsky's view has been hindered by a definition incorrectly attributed to him by Krumbein (1983, p. 499): "stromatolites are organogenic, laminated, calcareous rock structures, the origin of which is clearly related to microscopic life, which in itself must not be fossilised." Kalkowsky (1908) did not write this (see Riding, 1999, p. 323), but it has been repeated as if it were a literal translation from his paper (e.g., Ginsburg, 1991, p. 25; Feldmann and McKenzie, 1998, p. 201; Grotzinger and Knoll, 1999, p. 316; McLoughlin et al., 2008, p. 96). Compounding this mistake, the somewhat awkward wording (use of "must not" rather than "need not") has been cited as "paradoxical," and "confusion" to be avoided, and also as an example of the deficiencies of genetic definitions (Grotzinger and Knoll, 1999, p. 316; McLoughlin et al., 2008, p. 96). In his 1908 paper, Ernst Kalkowsky did not provide a specific definition of stromatolite, but he did repeatedly emphasize that it is a laminated organic structure. He thought that the life forms involved were "*niedrig organisierte planzliche Organismen*" (simple plantlike organisms, Kalkowsky, 1908, p. 125). It is therefore reasonable to conclude that Kalkowsky essentially regarded stromatolites as laminated microbial deposits (Riding, 1999).

**Microbialites, Stromatolites, and Thrombolites, Figure 2** Late Cambrian (late Franconian–early Trempealeauan) stromatolite (*Cryptozoon*), Hoyt Limestone, Petrified Gardens, Saratoga Springs, New York, USA. Coin diameter ~3 cm.

However, at the same time that support was growing for Kalkowsky's (1908) biogenic interpretation of stromatolites, the contrary view was also being expressed. Reis (1908) interpreted stromatolites as inorganic precipitates, Bucher (1918) compared them with hot spring sinter. Semikhatov et al. (1979, p. 994) were also concerned by the similarities between microbial stromatolites and "morphologically similar structures of nonmicrobial origin" such as those in caves and hot springs, and therefore suggested their descriptive definition. Subsequent research has shown that some stromatolite-like deposits are essentially abiogenic (e.g., Grotzinger and Read, 1983; Grotzinger and James, 2000, p. 9). Pope et al. (2000, p. 1139) contrasted microbial and abiogenic stromatolites, and considered "isopachous stromatolites to have been dominated by chemogenic precipitation in the absence of microbial mats, and the growth of peloidal stromatolites to have been controlled by sedimentation in the presence of microbial mats."

Fabric criteria can be used to distinguish abiogenic evenly layered sparry crust from fine-grained lithified microbial mats with uneven layering. In well-preserved examples, it should therefore be possible to tell abiogenic and biogenic stromatolites apart. However, as noted under microbialite, the millimetric interlayering of these two fabrics that can occur in hybrid stromatolites (Riding, 2008) makes such straightforward separation impossible. Consequently, stromatolites are regarded here, essentially, as laminated benthic microbial deposits, but they can contain abiogenic precipitates and be intimately inter-layered with them. In the marine realm, there is a strong secular perspective to this. Many Phanerozoic and Neoproterozoic stromatolites are probably essentially lithified microbial mats, whereas many older examples probably contain at least some precipitated abiogenic crust.

## Stromatolite types

Stromatolite micro- and macrofabrics commonly intergrade with those of dendrolites and thrombolites (Figure 3). Their formation can involve up to three main processes: microbial precipitation, inorganic precipitation, and grain trapping (Figure 4).The main types represent

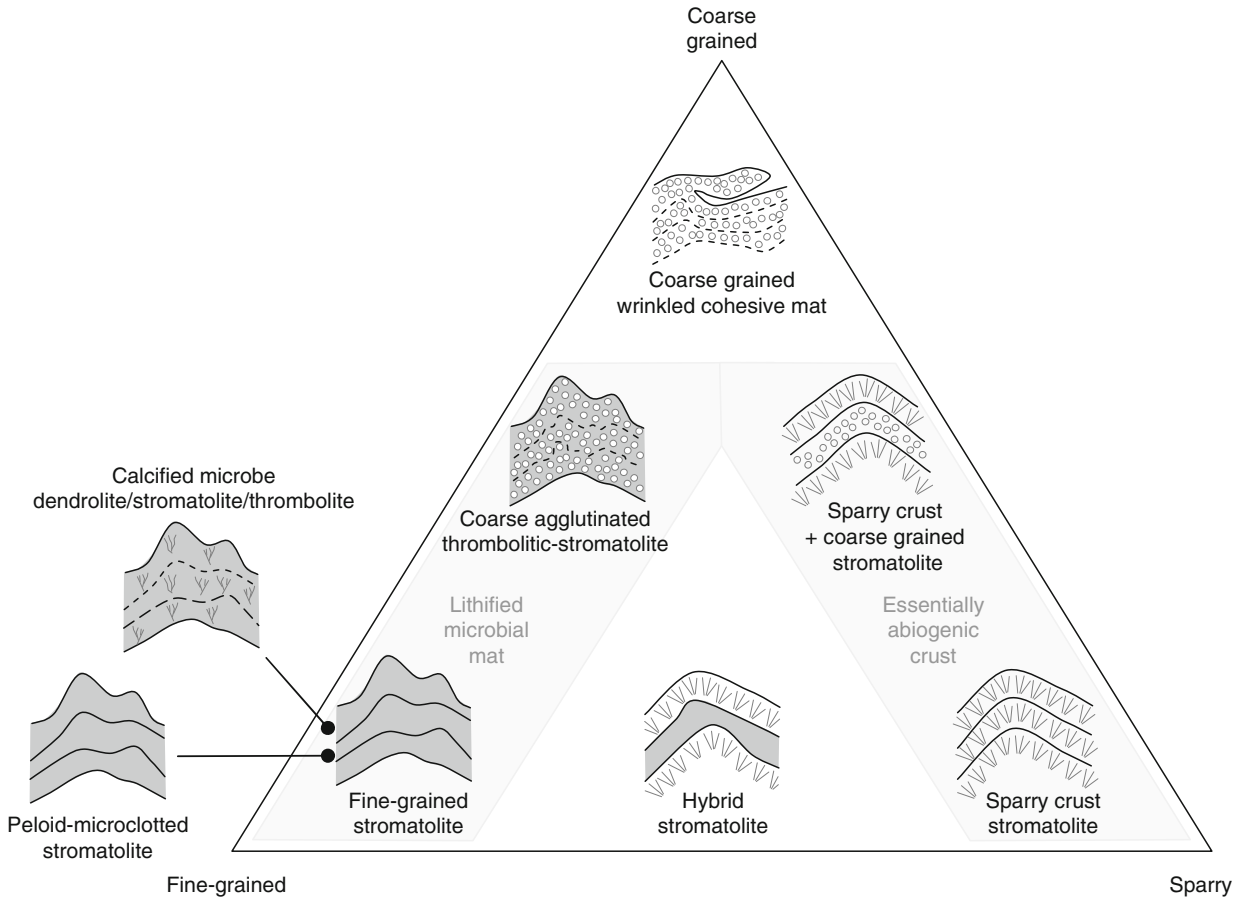


**Microbialites, Stromatolites, and Thrombolites, Figure 3** Stromatolites and thrombolites based on micro/macrofabric. All except wrinked cohesive mats are synsedimentarily lithified by microbial and/or abiogenic processes. Fine-grained varieties include two distinctive types: (i) stromatolites with peloidal-microclotted microfabrics and (ii) dendrolites and thrombolites with abundant filamentous and other calcified microbial microfossils.

lithified microbial mat, sparry crust, and combinations of these ("hybrid stromatolite").

*Lithified microbial mat stromatolites* exhibit a variety of intergradational fabrics. Two main types are fine-grained and coarse agglutinated. They form diverse stratiform, domical and columnar structures and, overall, tend to show relatively uneven to discontinuous layers with relatively poor inheritance and can include abundant fenestrae. Fine-grained stromatolites appear mainly to be products of synsedimentary microbial precipitation and are dominated by fine-grained (micrite, microspar) and filamentous fabrics. Fine-grained microfabrics are typically clotted and peloidal and are probably largely produced by heterotrophic bacterial calcification (e.g., dissimilatory sulfate reduction) of EPS and other cell products. Filamentous microfabrics are dominated by tubiform microfossils such as *Girvanella* that reflect photosynthetic cyanobacterial sheath calcification, but they too have fine-grained matrices. On their own, peloid-microclotted fabrics tend to be stromatolitic, and have been termed spongiostrome (Gürich, 1906; Pia, 1927, p. 36). Filamentous fabrics tend to be more crudely layered and grade to thrombolitic. They have been termed porostromate (Pia, 1927, pp. 36–40), skeletal (Riding, 1977), and calcimicrobial (James and Gravestock, 1990). Coarse agglutinated stromatolites/thrombolites are produced by trapping sandy sediment by uncalcified EPS and erect filaments that can include microalgae. Present-day examples include some Shark Bay and Lee Stocking Island columns. They often have crudely layered macrofabrics (Logan, 1961) and have been termed thrombolitic stromatolites (Aitken, 1967).

*Sparry crust* (Riding, 2008) can form stromatolite-like abiogenic precipitates (Grotzinger and Rothman, 1996) characterized by even, often isopachous, laterally persistent layers with good inheritance (Pope et al., 2000). They have been most widely recognized in the Palaeoproterozoic and Mesoproterozoic (Grotzinger and Knoll, 1999, Fig. 6a, b), with microdigitate forms occupying peritidal environments (Grotzinger and Read, 1983) and isopachous laminite (Jackson, 1989) relatively deeper water facies.

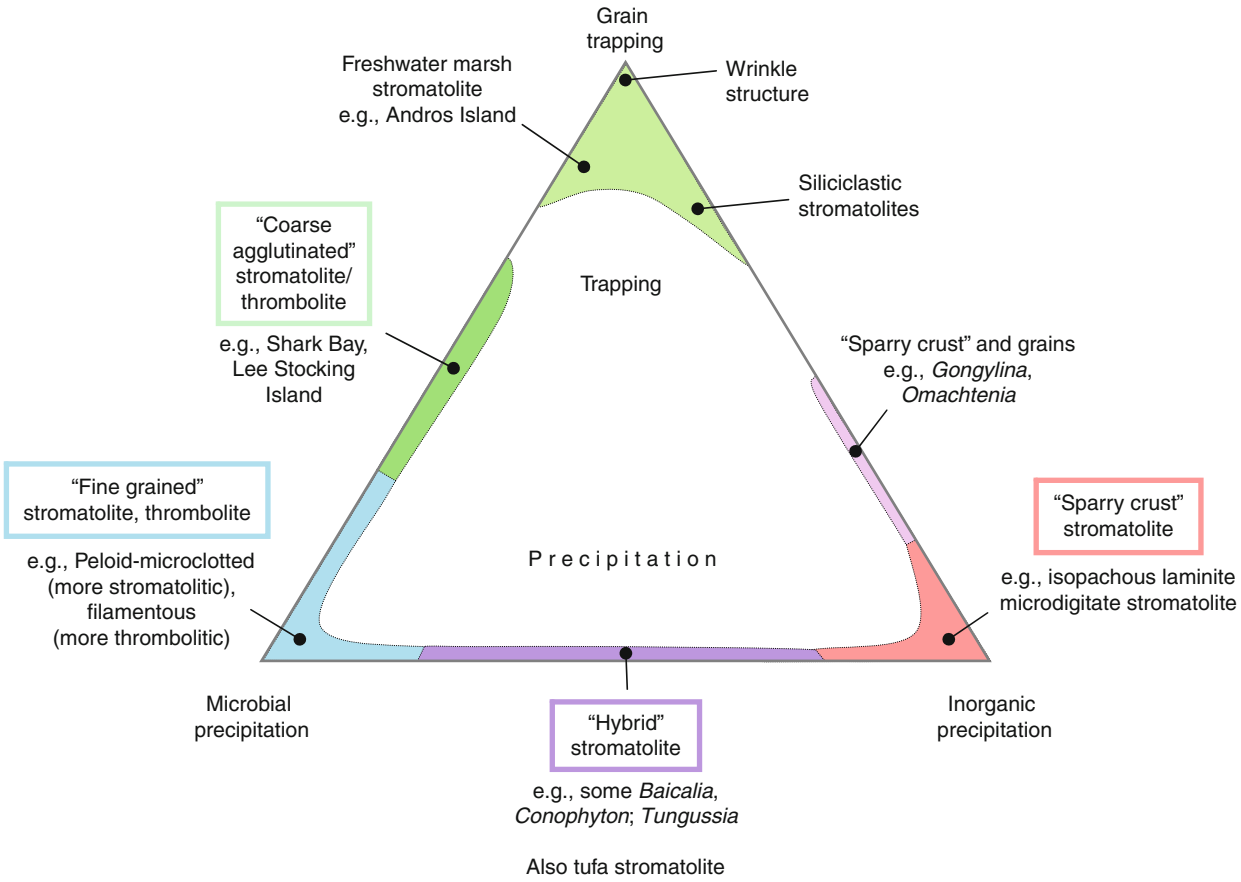


**Microbialites, Stromatolites, and Thrombolites, Figure 4** Stromatolitic and thrombolitic carbonates related to grain trapping, and synsedimentary microbial and inorganic precipitation. Developed from Riding (2008, Fig. 12). Principal categories are coarse agglutinated, fine-grained, hybrid and sparry crust. Those dominated by microbial precipitation and/or grain trapping are microbial mats. Sparry crusts are essentially abiogenic precipitates. Hybrid stromatolites are combinations of lithified microbial mat and sparry crust. Fine-grained varieties include filamentous (also termed porostromate, skeletal, and calcimicrobial) which is more thrombolitic and peloidal-microclotted (also termed spongiostromate) which is more stromatolitic. Microbial mats dominated by trapping, but with relatively minor early lithification include freshwater marsh stromatolites (Black, 1933) and wrinkle marks (Runzelmarken, Häntzschel and Reineck, 1968) mainly in siliciclastic sands and silts. For secular distributions see Fig. 11.

*Hybrid crust stromatolites* (Riding, 2008) typically consist of light-dark, often millimetric, alternations of sparry and fine-grained crust. These build stromatolites with well-developed even, although not usually isopachous, layering that is laterally quite persistent with generally good inheritance, as in some *Conophyton* (e.g., Walter, 1972, p. 86) (Figure 5). This layering is therefore intermediate in regularity between that of stromatolite-like sparry crust and fine-grained crust stromatolites. Hybrid crust appears to be a major component of Palaeoproterozoic (e.g., Sami and James, 1996) and Mesoproterozoic stromatolites (e.g., Petrov and Semikhatov, 2001), which can include very large domical and conical examples. Laminated freshwater cyanobacterial mats in shallow lakes of Andros Island show similarities to hybrid stromatolite, with fine-grained incipiently lithified cyanobacterial mats alternating with laminar fenestrae and elongate open voids (Monty, 1976, Fig. 4). If this structure were early lithified, it could resemble some *Conophyton* and *Baicalia* fabrics, as Bertrand-Sarfati (1976) suggested.

## Intertidal mats and wrinkle structures

At the present day, intertidal and supratidal sediments are commonly colonized by cyanobacteria dominated mats in siliciclastic (e.g., Cameron et al., 1985; Stal et al., 1985), evaporitic (e.g., Gerdes et al., 2000), and carbonate (Black, 1933; Logan et al., 1974) environments (Figure 6). Where these mats are cohesive, but insufficiently early lithified, they do not show significant accretion but nonetheless stabilize layers of sediment. These microbialites that were unlithified during their formation can be preserved in place, and also imprinted and disrupted, e.g., by desiccation and water movement. They and their incorporated sediment may be cracked, curled, and folded, and this synsedimentary deformation can be preserved after burial. Such patterned surfaces in

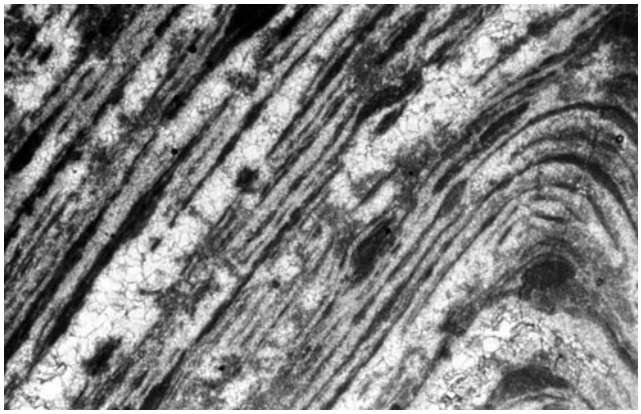

**Microbialites, Stromatolites, and Thrombolites, Figure 5** *Conophyton garganicum*. The fabric is interpreted as Hybrid stromatolite composed of alternating submillimetric layers of fine-grained lithified microbial mat and and light-colored essentially abiogenic sparry layers. Middle Riphean, Russia, stratigraphic unit and locality not known. Specimen donated to Geological Survey of Canada by M.A. Semikhatov; photograph courtesy of Hans Hofmann. Width of view 8 mm.

**Microbialites, Stromatolites, and Thrombolites, Figure 6** Wrinkled microbial mat with carbonate sediment; supratidal flat, Crane Key, Florida Bay, USA. Red pen cap ~5 cm long.

Mesoproterozoic limestones were named *Kinneyia* by Walcott (1914, p. 107, pl. 11, Fig. 3) and subsequently linked to "Runzelmarken" (wrinkle marks, Häntzschel and Reineck, 1968) and other mat-related structures (Hagadorn and Bottjer, 1997). They have also been termed microbially induced sedimentary structures (MISS) (Noffke et al., 1996). The exact origins of these bedding plane structures are probably complex and varied (Porada et al., 2008) but they have been widely linked to deformation of microbial mats and have been used to infer the presence of mats in the Proterozoic (Horodyski, 1982) and Archaean (Noffke et al., 2006).

### Siliciclastic stromatolites

In contrast to wrinkle structures, siliciclastic stromatolites can possess large domical morphologies and considerable synoptic relief. They are much scarcer than carbonate stromatolites, and are only known from mixed siliciclastic-carbonate environments that provide both siliciclastic grains and the early lithification required to maintain their support (Martín et al., 1993). Most examples are Palaeozoic, e.g., Ordovician (Davis, 1968), Devonian (Draganits and Noffke, 2004), Carboniferous (Bertrand-Sarfati, 1994), and Permian (Harwood, 1990), but diverse examples also occur in the late Miocene of South-east Spain (Martín et al., 1993; Braga and Martín, 2000). Based on the proportion of siliciclastic grains they contained, Martín et al. (1993) recognized three compositional types: "carbonate," <10%; "siliciclastic-carbonate," 10–50%; and "sandstone," >50%. They are typically metric, locally decametric, domes with both stromatolitic and thrombolitic macrofabrics, associated with marginal marine beach (Braga and Martín, 2000), fan-delta and conglomeratic debris-flow deposits (Martín et al., 1993), and also with oolitic stromatolites–thrombolites (Braga et al., 1995). Sediment within the more siliciclastic domes includes abundant quartz, mica, and lithic fragment sand, and occasional quartz and metamorphic rock granules and pebbles.

## Thrombolites

### Definition

Thrombolites (Greek: *thrombos*, clot; *lithos*, stone) are "cryptalgal structures related to stromatolites, but lacking lamination and characterized by a macroscopic clotted fabric" (Aitken, 1967, p. 1164).

### Introduction

Aitken's (1967) seemingly straightforward definition of thrombolite contained the seeds of more confusion than might have been anticipated. Since stromatolites are generally regarded as internally laminated; it could be expected that thrombolites are internally clotted. However, stromatolitic laminae are internal features of microbial carbonate, whereas "clot" could be used to describe both the external shape and internal structure of microbial carbonate (Figure 1). Aitken's (1967) descriptions of Cambro-Ordovician examples, and his emphasis that thrombolite clotted fabric is macroscopic, have directed most researchers to regard "clots" as centimetric patches of microbial carbonate within interstitial sediment. In this view, a thrombolite dome consists of numerous such clots within lighter colored interstitial detrital matrix. Consequently, the dome has an overall macroclotted fabric, but the individual clots themselves are not necessarily internally composed of smaller clots, although they can be. This contrasts with stromatolitic domes in which each individual stromatolite is internally laminated and its shape is described separately, e.g., as domical, columnar, digitate, etc.

Aitken's (1967) concept of clots as patches of microbial carbonate within matrix is appropriate where they are irregularly rounded, but in digitate thrombolites the patches elongate into decimetric branches (e.g., Armella, 1994, Fig. 9) and use of "clot" to describe these is awkward. If some of Aitken's (1967) thrombolite domes contain dendritic fabrics, as seems likely, then why did he stress their clotted macrofabric? A likely explanation is that, in domes composed of radial branches, any section other than a vertical one through the dome center (e.g., Armella, 1994, Fig. 9) tends to show clot-like rounded outlines of oblique sections of branches. If this is correct, then to be consistent the branches should also be regarded as clots. This approach was followed by Armella (1994) and Kennard (1994) (although they used *thromboid* as an equivalent term to clot) to describe rounded lobate patches and elongate columns alike. There seems little doubt that this is what Aitken (1967) intended, and Shapiro (2000, p. 166) recognized that he used clot to describe the thrombolite columns themselves. Nonetheless, in describing similar branched Cambro-Ordovician thrombolites (*Favosamaceria*), Shapiro (2000) and Shapiro and Awramik (2006) broadened "clot" to refer to both millimetric clots within the branches and centimetric clots embedded in interstitial sediment. And there is a further complication. Aitken (1967) suggested that poorly laminated columns at Shark Bay are "thrombolitic stromatolites." As a result, in addition to describing Cambro-Ordovician domes with well-defined fine-grained clots, thrombolite has been applied to agglutinated present-day microbial columns in which the clots are much less distinct patchy fabrics.

These complications of usage still require clarification. At present, it is safe to say that "clot" (and the equivalent terms mesoclot and thromboid) has not been used consistently in thrombolite studies. It has been applied to millimetric patches within microbial carbonate, to centimetric lobate patches and also extended columns of microbial carbonate surrounded by detrital carbonate sediment, to transverse sections of these columns (here termed pseudoclots), and to diffuse patches of trapped sand, as well as to secondarily enhanced clots. Given these complications, it is understandable that earlier workers often referred to thrombolites as "unlaminated stromatolites" (e.g., Aitken, 1967, p. 1166; Pratt, 1982a; Schopf and Klein, 1992, p. 1202). Nonetheless, thrombolites can generally be regarded as benthic microbial carbonates with macroclotted fabric.

## Thrombolite types

Two main types of thrombolite are calcified microbe and coarse agglutinated (Riding, 2000, pp. 192–193). Both intergrade with microbial mat stromatolites and primarily reflect the presence of major components that form irregular aggregates rather than thin layers. Nonetheless, the two types have quite distinct origins:

(i) *Calcified microbe thrombolites* include the classic Cambro-Ordovician examples described by Aitken (1967) and also by Pratt and James (1982) and Kennard and James (1986). Aitken (1967) noted that burrows and trilobite fragments are common in these thrombolites, and examples of similar age often show mottled interiors and stromatolitic outer coatings (Figure 7). They consist of clots composed of framework whose most recognizable components are calcified microfossils, such as *Girvanella* filaments and *Renalcis* botryoids. The clots may be irregular centimetric amoeboid forms (Figure 8) or extend vertically into elongate (Armella, 1994, Fig. 9) meandriform and laterally amalgamated (Pratt and

**Microbialites, Stromatolites, and Thrombolites, Figure 7** Late Cambrian (Trempealeauan) thrombolite column with mottled interior (within *dotted line*) and dark stromatolitic coating (between *white arrows*). Smoky Member, Nopah Fm, Dry Mountain, California, north-western Death Valley National Park, USA. Pen ~15 cm long.

**Microbialites, Stromatolites, and Thrombolites, Figure 8** Late Cambrian (Trempealeauan) thrombolite, Smoky Member, Nopah Fm, Dry Mountain, California, north-western Death Valley National Park, USA.

James, 1982, Figs. 9, 12) branches named *Favosamaceria* by Shapiro and Awramik (2006), (Figure 1). The clots are surrounded by detrital sediment infill. Progression from irregular clots to elongate branches has confused descriptive terminology. Shapiro (2000) suggested that in branched forms the clots typical of thrombolites are to be found within the branches, although Aitken (1967) seems to have regarded the columns as clots. James and Gravestock (1990) used "calcimicrobe" (calcified microbial microfossil) to refer to filamentous and botryoidal fossils that are common in Cambrian reefs. These typically form dendrolite (Figure 9) and thrombolite (Figure 10) fabrics and include calcified cyanobacteria such as *Angusticellularia*, *Botomaella*, and *Girvanella*, and also *Epiphyton* and *Renalcis*, whose affinities are less certain. Calcified microbe thrombolites are widespread in shallow marine environments during the Neoproterozoic and early Palaeozoic.

**Microbialites, Stromatolites, and Thrombolites, Figure 9** Dendrolite. Middle Cambrian, Zhangxia Formation, near Jinan, Shandong, China

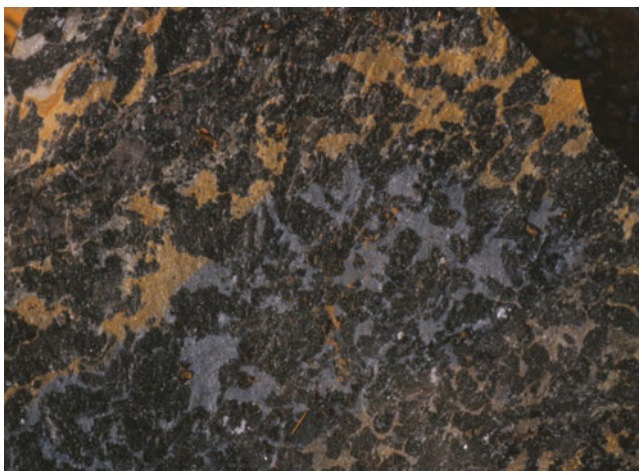

**Microbialites, Stromatolites, and Thrombolites, Figure 10** Thrombolite, early Cambrian, near Tiout, Anti-Atlas Mountains, Morocco. Width of view 8 cm.

(ii) *Coarse agglutinated thrombolites* are largely composed of fenestral microbially trapped sandy sediment within finer-grained microbially lithified matrix. They are closely associated with coarse agglutinated stromatolites (Figures 3 and 4) that Aitken (1967, p. 1171) described as "thrombolitic-stromatolites." They are only known in the late Neogene and their development appears to be linked to the rise of algal-cyanobacterial mats able to trap coarse sediment.

Coarse-grained thrombolites in the late Miocene of South-east Spain are closely associated with stromatolite fabrics in composite domes and columns up to 1.5 m high and 4 m across (Martín et al., 1993; Braga et al., 1995; Feldmann and McKenzie, 1997). They include oolitic examples in which clotted fabric is produced by irregular fenestrae up to 15 mm in size (Riding et al., 1991a, p. 123). Braga et al. (1995, Fig. 8, pp. 358–359) attributed the formation of these thrombolite fabrics to "a complex of irregular agglutination, microbial calcification, skeletal encrustation, and erosional processes."

Logan (1961) regarded Shark Bay columns as stromatolites but recognized that the lamination is often poor, describing some as "crudely laminated with laminae of 1–10 mm. in thickness" (p. 526, pl. 1, Fig. 4). Playford and Cockbain (1976, p. 403) observed that "Hamelin Pool stromatolites range from unlaminated (thrombolites) to finely laminated; most show only crudely developed lamination." Walter (1972, p. 64) attributed "the crude lamination of many Shark Bay stromatolites" to the thick irregular mats and coarse sediment. Logan et al. (1974, p. 154) related carbonate fabric to mat type, with thick irregular pustular mat dominated by *Entophysalis* in particular producing "unlaminated to poorly laminated" fenestral fabric, and Gebelein (1974) suggested that clotted fabric could reflect degradation of organic material. Similar Bahamian subtidal columns (Dravis, 1983) are coarse-grained and crudely laminated (Dill et al., 1986) and it has been suggested that abundant algae, including diatoms in these mats contribute to the coarse texture and poor lamination typical of both Shark Bay (Awramik and Riding, 1988) and Bahamian (Riding et al., 1991b) columns.

*Mesozoic-Cenozoic thrombolites*: Thrombolites are also common in the mid-late Jurassic (e.g., Leinfelder et al., 1993; Parcell, 2002; Kopaska-Merkel, 2003; Mancini et al., 2004), often in association with sponges and stromatolites in deeper water (e.g., Jansa et al., 1988; Leinfelder et al., 1994, p. 37; Dromart et al., 1994) and with corals in shallow-water (e.g., Bertling and Insalaco, 1998; Dupraz and Strasser, 1999; Olivier et al., 2003; Olivier et al., 2006; Helm and Schülke, 1998, 2006). They exhibit a variety of forms, including

arborescent and pendant that commonly occur as thick crusts on frame-building invertebrates, and are also closely associated with a variety of problematic encrusting organisms such as *Bacinella*, *Lithocodium,* and *Shamovella*/*Tubiphytes*, as well as annelids and foraminifers (Leinfelder et al., 1993, Fig. 6; Olivier et al., 2003, Fig. 4). Similar – but more often stromatolitic – crusts occur in late Neogene, including present-day, scleractinian reefs (Riding et al., 1991c; Montaggioni and Camoin, 1993; Leinfelder et al., 1993, pp. 222–224), and provide important clues to the formation of microbial carbonate microfabrics (Reitner, 1993; Reitner et al., 2000). In addition, the macrofabrics of these Mesozoic-Cenozoic examples broadly resemble those of early Palaeozoic calcified microbe thrombolites, but with significantly different skeletal components. Their microfabrics are fine-grained, with peloids and microclotted micrite (Olivier et al., 2006, Fig. 9), similar to those of many lithified microbial mat stromatolites.

*Tufa thrombolite and stromatolite* (Riding, 2000, pp. 191, 194) forms in calcifying lakes and streams as a result of cyanobacterial calcification that includes sheath impregnation and encrustation, together with calcification of associated microbes. It was comparisons with freshwater tufa that first led to recognition of links between stromatolites and cyanobacteria (Walcott, 1914; Roddy, 1915). These complex fabrics show considerable variety due to local differences in organisms and the extent of biocalcification and external encrustation. There are similarities between tufa stromatolites and hybrid crust stromatolites (Riding, 2008, p. 88) (Figure 4).

Kennard and James (1986, p. 498) noted that, although "poorly laminated and partially clotted microbial structures" occur on some present-day hypersaline marine shorelines (Laguna Mormona, Shark Bay) and in some lakes of various salinities (Great Salt Lake, Lake Clifton, Green Lake), in these examples "individual microbial clots are generally poorly defined" and "form an irregular, botryoidal-like, mesoscopic fabric that is unlike any of the fabrics observed by us in Lower Paleozoic thrombolites." However, Moore and Burne (1994, pp. 23) considered that thrombolites in brackish to normal marine Lake Clifton, Western Australia, do closely resemble some early Palaeozoic examples in mesoclot shape and "the interframework of infilled fenestrae" and they pointed out that in Lake Clifton filamentous cyanobacteria (*Scytonema*) are important in thrombolite formation. Moore and Burne (1994, p. 21) noted that fine laminae, initially present in the Lake Clifton structures, are synsedimentarily destroyed during mesoclot formation as carbonate precipitation continues, and also that the interframework fenestrae are intrinsic features "primarily related to the topography of the surface of the developing microbialite rather than to excavation of the structure by metazoan activity." Great Salt Lake "algal mounds," that consist of precipitated aragonitic framework and internal sediment (Halley, 1976, p. 439, Fig. 3), have a subcentimetric thrombolitic fabric. Ferris et al. (1997) suggested that thrombolitic fabrics in Kelly Lake, British Columbia, reflect a greater degree of calcification than in stromatolites.

*Post-depositional thrombolites* Aitken (1967, p. 1171) noted that thrombolite macroclots are prone to accentuation by recrystallization. This emphasizes a fundamental difference from stromatolites, whose laminae are essentially primary and not likely to be significantly enhanced by diagenesis. In contrast, clots could be significantly enhanced, e.g., by selective dolomitization, and in some cases secondarily produced, e.g., by bioturbation.

## Stromatolites and thrombolites through time

Microbialite types are generally long ranging. Nonetheless, they show some distinctive differences in time distribution (Figure 11). Marine sparry crusts and hybrid stromatolites are typically Precambrian, and fine-grained stromatolites and thrombolites mainly range Neoproterozoic to the present day. Wrinkle structures show the longest range, whereas lithified coarse-grained carbonate thrombolites and stromatolites are only known from the past 10 Ma or less.

### Archaean and Proterozoic

Stromatolites are relatively scarce in Archaean rocks until nearly the end of the eon. Their history begins with ~3.45 Ga coniform examples in the Pilbara region of Western Australia. These show fine continuous laminae (Lowe, 1980, 1983) and sparry microfabrics (Hofmann et al., 1999, Fig. 3). Their origins, and those of other Pilbara stromatolites, have been debated (e.g., Lowe, 1994, 1995; Buick et al., 1995), with recent studies supporting a biogenic origin (Hofmann et al., 1999, p. 1260–1261; Allwood et al., 2006, p. 717). Wrinkle and associated structures also suggest the presence of microbial mats in ~2,900 Ma siliclastic sediments of South Africa (Noffke et al., 2008), but these too are generally scarce. However, stromatolites are abundant in the ~2.55 Ga Campbellrand-Malmani carbonate platform of South Africa, locally forming elongate domes 10 m across and 40 m or more in length (Beukes, 1987, p. 9). In addition, these late Archaean carbonates contain distinctive "fenestrate microbialites" (Sumner and Grotzinger, 2004) consisting of millimetric to centimetric areas of light colored cement outlined by thin net-like layers (Figure 12). These have been interpreted as wispy convoluted microbial mats that were encrusted by calcite as they formed (Sumner, 1997a, b).

Large, often decametric, stromatolites are also conspicuous components of Proterozoic carbonate platforms (e.g., Grotzinger, 1986, p. 833; Petrov and Semikhatov, 2001, Fig. 6, p. 269). Where they are well preserved, they often show interlamination of sparry and micritic layers (e.g., Sami and James, 1996, p. 217). These dark-light layers that appear to represent alternations of lithified mat and abiogenic crust, are typical of "hybrid stromatolites" and are well seen in some *Conophyton* and *Baicalia* (Riding,

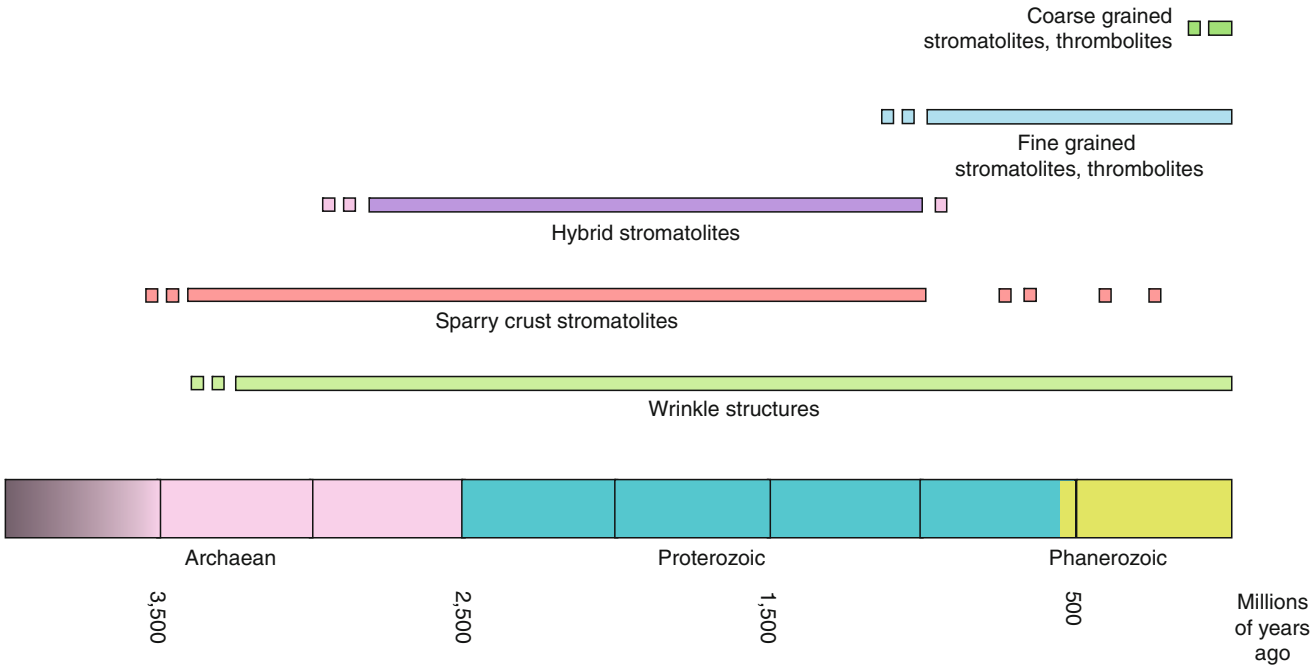


**Microbialites, Stromatolites, and Thrombolites, Figure 11** Approximate time distributions of major categories of marine microbialites. Coarse agglutinated mats are mainly Neogene. Fine-grained mats and thrombolites are mainly Neoproterozoic and Phanerozoic. Marine "sparry" and "hybrid" crusts are mainly Archaean and Proterozoic. Wrinkle structures range Archaean to present-day. For some possible controls, see Figure 14.

2008). Such incorporation of thin abiogenic sparry crusts appears to have contributed significantly to the size and relief of stromatolites throughout the Palaeo- and Mesoproterozoic. During the same period, extensive sheets of very small "microdigitate" stromatolites, typically <5 mm wide and <20 mm high (Hoffman, 1975, p. 262) were common in shallow peritidal environments (Figure 13). These "tufas" have been interpreted as essentially abiogenic (Grotzinger and Read, 1983).

An important control on Archaean-Proterozoic stromatolite formation was gradual decline in seawater carbonate saturation state (Grotzinger, 1989b; Grotzinger and Kasting, 1993). This progressively reduced stromatolite abundance (Grotzinger, 1990) and mediated a long-term trend from sparry crust to micritic carbonate sediments (Grotzinger and Kasting, 1993; Kah and Knoll, 1996). Transition to carbonate mud-dominated platforms ~1,400–1,300 Ma ago (Sherman et al., 2000) preceded the appearance of sheath-calcified cyanobacteria ~1,200 Ma ago (Kah and Riding, 2007). This significant transition, which led to Neoproterozoic development of calcimicrobial thrombolites (Aitken and Narbonne, 1989; Turner et al., 1993, 2000a, b), could reflect induction of $CO_2$-concentrating mechanisms (CCM) in cyanobacteria in response to fall in $CO_2$ levels below a threshold near ten times present-day levels (Riding, 2006) (Figure 14). CCMs are responses to reduced availability of inorganic carbon for photosynthesis, and in cyanobacteria include active bicarbonate uptake that locally increases sheath pH, promoting calcification (Merz, 1992). Calcified filaments, such as *Girvanella*, altered microbial carbonate fabrics, disrupting stromatolite layering and promoting thrombolitic macro-clotted fabric. In subtidal environments, Neoproterozoic stromatolites are commonly interlayed with thrombolites with filamentous, clotted, and spongy "cellular" fabrics (Aitken and Narbonne, 1989) comparable with those of Cambro-Ordovician thrombolitic bioherms (Turner et al., 1993; 1997, p. 441, 449; 2000a, Figs. 6e, 8h and i).

## Stromatolite decline

Stromatolites show long-term decline in abundance that may have commenced as early as the Palaeoproterozoic (Grotzinger, 1990) and is still observed in the Phanerozoic. Fischer (1965) suggested that decline since the Ordovician could reflect both reduction in carbonate saturation and competition by eukaryotes. Competition was subsequently emphasized when it appeared that marked late Proterozoic fall in stromatolite morphotypic diversity coincided with metazoan evolution (Awramik, 1971), but inception of decline prior to the appearance of metazoans implicates reduction in saturation state as the major influence (Grotzinger, 1990). It was also suggested that Cambrian thrombolites reflected disruption of stromatolites by burrowing organisms (Walter and Heys, 1985, pp. 150–151). However, Cambrian-Ordovician thrombolite fabrics are dominated by calcimicrobes that resist disruption (Kennard and James, 1986, p. 494) and

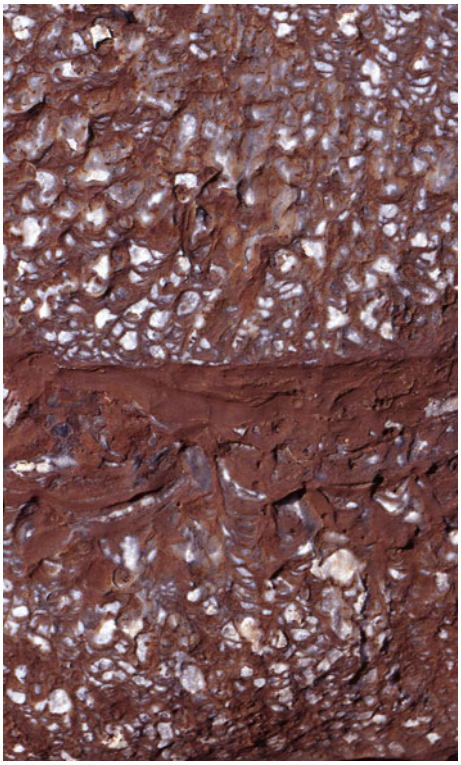

**Microbialites, Stromatolites, and Thrombolites, Figure 12** Fenestrate microbialite. Meshwork of large fenestrae (*white*) outlined by thin curved dark layers. Late Archaean Campbellrand-Malmani platform, South Africa. Width of field ~16 cm.

**Microbialites, Stromatolites, and Thrombolites, Figure 13** Microdigitate stromatolite, silicified after carbonate. Wumishan Formation, Mesoproterozoic, ~25 km north of Beijing, China. Width of view ~25 cm.

it has since been recognized that thrombolites appeared in the Neoproterozoic (Aitken and Narbonne, 1989), and possibly ~1.9 Ga in the Palaeoproterozoic (Kah and Grotzinger, 1992).

This leaves the question of the significance of trends in stromatolite diversity. Stromatolite shape reflects original synoptic relief, determined by accretion rate relative to adjacent sediment (Figure 15). Low relative accretion rate results in low relief that makes stromatolites more prone to lateral incursion by sediment, thereby fostering complex shapes such as digitate forms (Figure 16). In contrast, high relative accretion rate results in high relief and simple shapes, such as domes and cones. Consequently, although mid-Proterozoic increase in morphotypic diversity, e.g., in branched stromatolites, has been regarded as a proxy for abundance, it more likely reflects low synoptic relief due to reduced relative accretion rate. Paradoxically, therefore, increased diversity could be sign that stromatolite growth was in decline due to reduced microbial growth and/or reduction in synsedimentary lithification.

### Snowball Earth

The prolonged warm Mesoproterozoic interval (Jenkins, 2003) was followed by Neoproterozoic (Sturtian, ~0.7 Ga Ma, Walter et al., 2000; Marinoan, ~0.635 Ga, Bodiselitsch et al., 2005) glaciations. Lower temperature and $pCO_2$ levels would have decreased seawater saturation state, hindering microbial calcification generally. Cooling would also have favored diffusive entry of $CO_2$ into cells and therefore may have slowed CCM development, further reducing cyanobacterial calcification. Nonetheless, microbialites are locally conspicuous in Cap Carbonates that immediately follow glacial deposits (e.g., Hoffman and Schrag, 2002; Corsetti and Grotzinger, 2005). Cap Carbonates have been suggested to reflect precipitation from seawater highly saturated for carbonate minerals as a result of alkaline upwelling and enhanced terrestrial weathering (Grotzinger and Knoll, 1995; Hoffman and Schrag, 2002). In the ~600–700 Ma Noonday Dolomite of California, narrow laterally amalgamated stromatolites define tubes of intervening detrital sediment fill (Figure 17). The overall organization of some Cambro-Ordovician *Favosamaceria* thrombolites (Shapiro and Awramik, 2006) resembles these "tubestones" (Corsetti and Grotzinger, 2005, p. 360).

Following Neoproterozoic "snowball" glaciations, global warming and $O_2$ rise could have reactivated CCM development, and rising temperature, calcium (Brennan et al., 2004), and $pCO_2$ (Berner and Kothavala, 2001) levels would have increased seawater saturation state, stimulating microbial calcification (Riding, 2006). This favored microbialite resurgence, and dendrolites, thrombolites, and stromatolites all became widespread in the early Cambrian (Rowland and Shapiro, 2002) (Figure 18).

## Phanerozoic

### Secular distribution

Both reefal microbial carbonates (Kiessling, 2002, Fig. 16) and calcified cyanobacteria (Arp et al., 2001) decline in abundance during the Phanerozoic, but this trend shows marked fluctuations. They are common in the late Cambrian-early Ordovician and late Devonian-early Mississippian, and scarce during the Cenozoic.

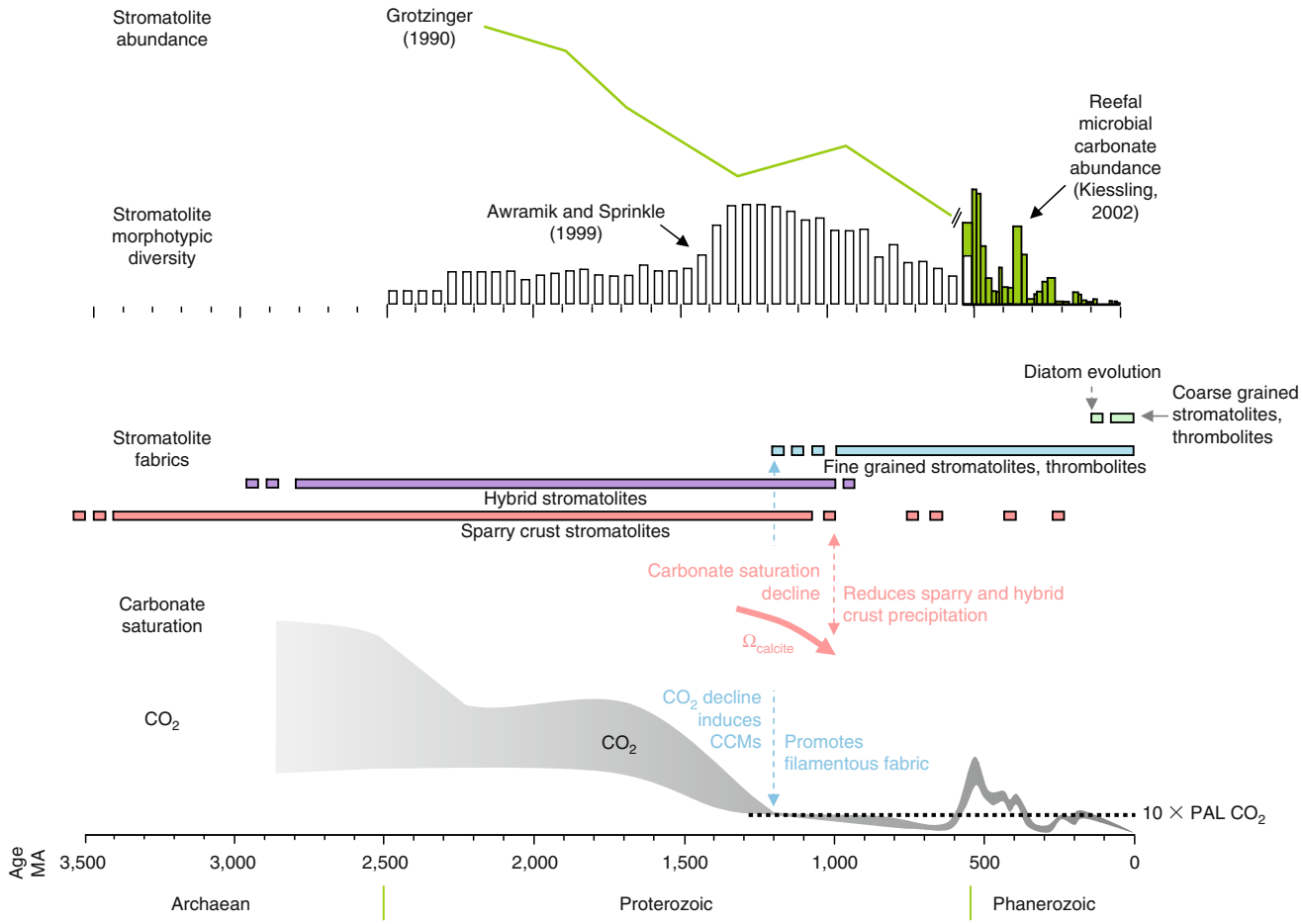


**Microbialites, Stromatolites, and Thrombolites, Figure 14** Some secular trends and possible controls on microbial carbonate developments. Proterozoic stromatolite abundance (Grotzinger, 1990) and morphotypic diversity (Awramik and Sprinkle, 1999), together with Phanerozoic reefal microbial carbonate abundance (Kiessling, 2002). These suggest overall long-term decline for at least the past 1,000 Ma. Reduction in both Sparry Crust and Hybrid stromatolites ~1,000 Ma ago may reflect decline in seawater carbonate saturation (Grotzinger, 1990). Stromatolite-like sparry crust occurs sporadically in the Phanerozoic, particularly in evaporite basins (Pope et al., 2000). Increase in thrombolites ~1,200–1,000 Ma ago could reflect development of cyanobacterial sheath calcification, reflecting inception of $CO_2$-concentrating mechanisms (CCMs) as $CO_2$ levels declined to ~10 times present atmospheric level (PAL) (Riding, 2006). Inferred Proterozoic $CO_2$ trend based on Sheldon (2006), Kah and Riding (2007), Hyde et al. (2000) and Ridgwell et al. (2003). Phanerozoic $CO_2$ trend from Berner and Kothavala (2001, Fig. 13). Threshold for CCMs (10 times PAL $CO_2$) based on Badger et al. (2002). Late Neogene inception of Coarse agglutinated stromatolites and thrombolite could in part reflect incorporation of diatoms into microbial mats and also generally low values of seawater carbonate saturation.

Fischer (1965) suggested that eukaryote competition and reduction in carbonate saturation state contributed to stromatolite decline from the Ordovician onward.

*Carbonate saturation*: Comparison with seawater saturation state for $CaCO_3$ minerals calculated from modeled seawater and $CO_2$ values shows broad positive correspondence with peaks of microbial/cyanobacterial carbonate abundance during much of the Palaeozoic and Mesozoic (Riding and Liang, 2005), supporting Fischer (1965). Lack of correspondence during the interval ~120–80 Ma ago (when calculated saturation ratio is high but microbial carbonate abundance was low) could reflect removal of carbonate deposition by pelagic plankton that significantly reduced actual saturation state.

*Competition*: The role of metazoan competition in late Proterozoic and early Palaeozoic stromatolite history is uncertain, and it is debatable whether metazoan grazing significantly affected stromatolite development (Pratt, 1982b) so long as carbonate saturation was high enough to ensure extensive early lithification of microbial mats. Nonetheless, it seems likely that from at least the mid-Ordovician onwards, overgrowth by skeletonized algae and invertebrates inhibited the formation of domical stromatolites and thrombolites. Subsumed within complex reef structures, microbial carbonates would instead have formed patchy and irregular crusts on and around skeletal organisms. Nonetheless, they were often important reef components (Kiessling, 2002, Fig. 16).

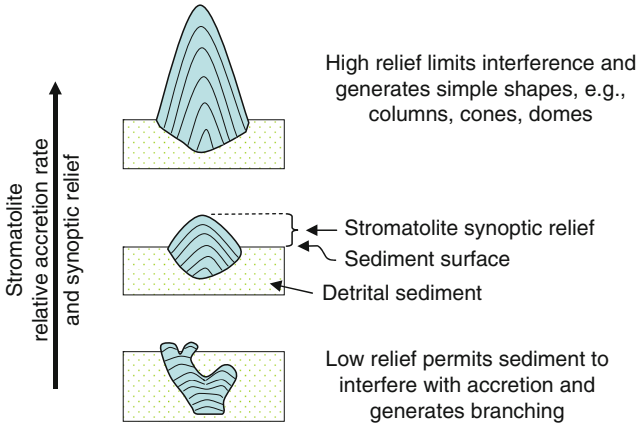


**Microbialites, Stromatolites, and Thrombolites, Figure 15** Hypothetical interpretation of the significance of stromatolite shape. Shape is determined by synoptic relief that in turn reflects accretion rate of the stromatolite surface relative to adjacent sediment. In this view, enhanced stromatolite accretion generates high relief and simple shapes, such as columns, cones, and domes. In contrast, relatively low stromatolite accretion results in low relief. As a result, the stromatolite surface is prone to overlap by adjacent sediment, generating branching and irregular margins.

**Microbialites, Stromatolites, and Thrombolites, Figure 16** *Gymnosolen*, digitate stromatolite, Dalien, China, ~1.0 Ga.

*Disaster biotas*: The concept of stromatolite decline resulting from algal-metazoan diversification (Fischer, 1965; Garrett, 1970; Awramik, 1971) has also given rise to that of stromatolite resurgence in the aftermaths of mass extinctions (Schubert and Bottjer, 1992, p. 885). In this view, if metazoans can competitively exclude microbial carbonates then temporary reduction in metazoan abundance and diversity in the immediate aftermaths of mass

**Microbialites, Stromatolites, and Thrombolites, Figure 17** Laterally amalgamated columnar stromatolites (light color) separated by slightly darker tubular fills of detrital sediment. Noonday Dolomite, late Neoproterozoic, Mesquite Mountains, California, USA.

extinctions should permit temporary increase in microbial carbonates. Schubert and Bottjer (1992, 1995) interpreted early Triassic stromatolites as "post-mass extinction disaster forms." However, whereas microbial carbonate reefal abundance also increased noticeably in the aftermath of late Devonian extinction, it did not increase following end-Ordovician, end-Triassic, and end-Cretaceous mass extinctions (Riding, 2006). Nonetheless, it is likely that in these situations, unconstrained by algal and invertebrate reef organisms, microbial mats were able to develop distinctive morphologies, and large domes, columns, and digitate structures have been reported, e.g., at the Permian-Triassic boundary in Sichuan, China (Kershaw et al., 1999).

*Thrombolites*: Flügel (2004, p. 378) suggested that thrombolite abundance also declined after the Cambrian, although they were still locally conspicuous, e.g., in the Silurian (Kahle, 2001), Devonian (Shapiro, 2000, p. 166), Mississippian (Webb, 1987, 2005), and near the Permian-Triassic transition (Kershaw et al., 1999; Ezaki et al., 2008). Thrombolites have been widely reported in the mid-late Jurassic (see Mesozoic-Cenozoic thrombolites, above), broadly coincident with the last major peak of abundance of calcified marine cyanobacteria (Arp et al., 2001, Fig. 3d).

*Evaporite stromatolites*: In addition to metazoan extinction, localized increase in carbonate saturation in evaporite basins will favor microbialite development. Pope et al. (2000, p. 1139) noted that isopachously laminated stromatolites, which they considered to be dominantly abiogenic, are well developed in association with major evaporite successions and cited examples in the Proterozoic and Phanerozoic, including the Silurian Michigan Basin of North America and the late Permian Zechstein Basin of northern Europe (Pope et al., 2000,

Figs. 7, 9). These conditions therefore marked temporary returns to conditions that promoted formation of the sparry and hybrid crusts typical of the Archaean and early Proterozoic.

## Neogene coarse-grained thrombolitic stromatolites

Well-known present-day examples of columns and domes occur in wave- and current-swept environments at Shark Bay (Logan, 1961) and the Bahamas (Dravis, 1983; Dill et al., 1986; Riding et al., 1991b; Reid et al., 2000). They accrete bioclastic and ooid sand, and have crudely layered (Logan, 1961) and thrombolitic (Aitken, 1967, p. 1171) fabrics. Several factors conspire in their formation: water movement, mat community, and seawater chemistry. High-energy grainy conditions facilitate trapping by lifting sand to the accreting mat surface, and simultaneously deter overgrowth by reefal encrusters (Dill et al., 1989, p. 10). At Shark Bay, seasonal hypersalinity also limits competitors. Together with rapid accretion this allows decimetric, and locally metric, columns to develop. Accretion is high because the mats are thick and soft, with abundant EPS (Decho et al., 2005). In addition to cyanobacteria, they contain diatoms and filamentous green algae that enhance trapping ability (Awramik and Riding, 1988; Riding et al., 1991b). The upper mat remains soft and sticky because it is largely uncalcified, and the early lithification necessary to support these large columns mainly occurs in, or below, the lower part of the mat. Microbial lithification by sulfate reduction (Visscher et al., 2000) is limited to very thin micritic crusts (Reid et al., 2000), cyanobacterial sheaths are uncalcified (Reid et al., 2000, p. 992), and calcification of algal filaments mainly occurs in cavities (Dravis, 1983; Whittle et al., 1993, p. 224). Formation of these coarse-grained thrombolitic stromatolites is therefore largely due to their thick, soft, EPS-rich mats. These in turn reflect a combination of Cenozoic circumstances: (i) seawater saturation state that is too low for cyanobacterial sheath impregnation, but permits early lithification and (ii) the presence of fast-growing microalgae, such as diatoms, which – from a geological standpoint – are relative newcomers to mat communities (Figure 14). Coarse-grained thrombolitic stromatolite domes and columns are well developed in the late Miocene of South-east Spain (Riding et al., 1991a; Braga et al., 1995; Feldmann and McKenzie, 1997) (Figure 19) but are not known in older rocks.

**Microbialites, Stromatolites, and Thrombolites, Figure 18** Late Cambrian (Trempealeauan) thrombolite overlain by stromatolite, Smoky Member, Nopah Fm, Dry Mountain, California, north-western Death Valley National Park, USA. Pen ~15 cm long.

**Microbialites, Stromatolites, and Thrombolites, Figure 19** Coarse-grained, oolitic, composite leiolite-stromatolite-thrombolite domes, late Miocene (Messinian), Joyazo, Almería, South-east Spain. Red pen, lower left, ~15 cm long.

## Summary

During the Archaean and much of the Proterozoic, both microbial mat growth and abiogenic precipitation were involved in stromatolite development that, locally, was particularly abundant from the latest Archaean to early Neoproterozoic (Grotzinger and Knoll, 1999). The combination of these biogenic and abiogenic factors was responsible for the rapid growth that enabled stromatolites, ranging from extensive small microdigitate sheets (Grotzinger and Read, 1983) to decametric domes (e.g., Hofmann, 1998, pl. 8a), to dominate carbonate platforms for 1,500 million years. Well-preserved stromatolites with dark-light lamination (Sami and James, 1996; Petrov and Semikhatov, 2001) suggest that lithified mat growth alternated with abiogenic sparry crust precipitation on a millimetric scale to form inter-layered hybrid crust stromatolites (Riding, 2008).

Decline in sparry crusts and hybrid stromatolites ~1,000 Ma ago probably largely reflects reduction in seawater saturation (Grotzinger, 1990). This change also broadly coincided with the inception of cyanobacterial sheath-calcification in the Mesoproterozoic. This important development may reflect induction of $CO_2$-concentrating mechanisms (CCM) to assist photosynthetic carbon uptake as $CO_2$ levels declined (Riding, 2006). It transformed microbialite fabrics, and calcified microbe thrombolites and stromatolites with filamentous fabrics were conspicuous in shallow subtidal environments until the early Ordovician. Subsequently, stromatolites and thrombolites were widely subsumed within algal-invertebrate reefs. In these closely packed habitats, they lacked space to develop classic dome and column morphologies, and instead mainly formed reefal crusts and irregular masses. Only where competitors were environmentally excluded, or absent (as in mass extinction aftermaths), did microbial domes briefly develop extensively.

Both competition and declining carbonate saturation limited the abundance of marine microbialites from the Ordovician onwards (Fischer, 1965), and they are much less widespread and abundant in the Cenozoic than in the Palaeozoic. But microbialite communities have the ability to reinvent themselves. Diatoms together with other microalgae have significantly enhanced mat trapping ability. In environments where reefal overgrowth is limited, and coarse grains abundant, these soft mats can create large coarse-grained columns, as at Shark Bay and Lee Stocking Island. Internally these have distinctive crudely layered thrombolitic stromatolite fabrics (Aitken, 1967); in external shape, they closely resemble some Palaeoproterozoic stromatolites.

Microbialites have changed significantly during their extraordinarily long history in shape, size, fabrics, and abundance. They have responded to microbial evolution, to environmental changes that have affected both carbonate sedimentation and microbial metabolism, and to the evolution of other organisms. To add to this complexity, whereas stromatolites are essentially lithified microbial mats, they may be intimately associated with abiogenic crusts. Microbialites archive important geobiological changes in atmospheric composition, seawater chemistry, mat evolution, and biotic interaction. Their study continues to offer many challenges and opportunities.

## Bibliography


Aitken, J. D., 1967. Classification and environmental significance of cryptalgal limestones and dolomites, with illustrations from the Cambrian and Ordovician of southwestern Alberta. *Journal of Sedimentary Petrology*, **37**, 1163–1178.

Aitken, J. D., and Narbonne, G. M., 1989. Two occurrences of Precambrian thrombolites from the Mackenzie Mountains, northwestern Canada. *Palaios*, **4**, 384–388.

Allwood, A. C., Walter, M. R., Kamber, B. S., Marshall, C. P., and Burch, I. W., 2006. Stromatolite reef from the Early Archaean era of Australia. *Nature*, **441**, 714–718.

Armella, C., 1994. Thrombolitic-stromatolitic cycles of the Cambro-Ordovician boundary sequence, Precordillera Oriental Basin, western Argentina. In Bertrand-Sarfati, J., and Monty, C. (eds.), *Phanerozoic Stromatolites II*. Dordrecht: Kluwer, pp. 421–441.

Arp, G., Reimer, A., and Reitner, J., 2001. Photosynthesis-induced biofilm calcification and calcium concentrations in Phanerozoic oceans. *Science*, **292**, 1701–1704.

Awramik, S. M., 1971. Precambrian columnar stromatolite diversity: reflection of metazoan appearance. *Science*, **174**, 825–827.

Awramik, S. M., and Margulis, L., 1974. *Stromatolite Newsletter*, **2**, 5.

Awramik, S. M., and Riding, R., 1988. Role of algal eukaryotes in subtidal columnar stromatolite formation. *Proceedings National Academy of Science USA*, **85**, 1327–1329.

Awramik, S. M., and Sprinkle, J., 1999. Proterozoic stromatolites: the first marine evolutionary biota. *Historical Biology*, **13**, 241–253.

Badger, M. R., Hanson, D., and Price, G. D., 2002. Evolution and diversity of $CO_2$ concentrating mechanisms in cyanobacteria. *Functional Plant Biology*, **29**, 161–173.

Berner, R. A., and Kothavala, Z., 2001. GEOCARB III. A revised model of atmospheric $CO_2$ over Phanerozoic time. *American Journal of Science*, **301**, 182–204.

Bertling, M., and Insalaco, E., 1998. Late Jurassic coral/microbial reefs from the northern Paris Basin - facies, palaeoecology and palaeobiogeography. *Palaeogeography, Palaeoclimatology, Palaeoecology*, **139**, 139–175.

Bertrand-Sarfati, J., 1976. An attempt to classify Late Precambrian stromatolite microstructure. In Walter, M. R. (ed.), *Stromatolites*. Amsterdam: Elsevier, pp. 251–259.

Bertrand-Sarfati, J., 1994. *Siliciclastic*-carbonate *stromatolite* domes in the Early Carboniferous of the Ajjers Basin (eastern Sahara, Algeria). In Bertrand-Sarfati, J., and Monty, C. (eds), *Phanerozoic stromatolites II*. Dordrecht: Kluwer, pp. 395–419.

Beukes, N. J., 1987. Facies relations, depositional environments and diagenesis in a major early Proterozoic stromatolitic carbonate platform to basinal sequence, Campbellrand Subgroup, Transvaal Supergroup, Southern Africa. *Sedimentary Geology*, **54**, 1–46.

Black, M., 1933. The algal sedimentation of Andros Island Bahamas. *Philosophical transactions of the Royal Society of London. Series B, Biological Sciences*, **222**, 165–192.

Bodiselitsch, B., Koeberl, C., Master, S., and Reimold, W. U., 2005. Estimating duration of Neoproterozoic snowball glaciations from Ir anomalies. *Science*, **308**, 239–242.

Braga, J., and Martín, J. M., 2000. Subaqueous siliciclastic stromatolites a case history from Late Miocene beach deposits in the Sorbas Basin, SE Spain. In Riding, R., and Awramik, S. M. (eds), *Microbial sediments*, Berlin: Springer, pp. 226–232.

Braga, J. C., Martín, J. M., and Riding, R., 1995. Controls on microbial dome fabric development along a carbonate-siliciclastic shelf-basin transect, Miocene, S.E. Spain. *Palaios*, **10**, 347–361.

Brennan, S. T., Lowenstein, T. K., and Horita, J., 2004. Seawater chemistry and the advent of biocalcification. *Geology*, **32**, 473–476.

Bucher, W., 1918. On oölites and spherulites. *Journal of Geology*, **26**, 593–609.

Buick, R., Groves, D. I., and Dunlop, J. S. R., 1995. Abiological origin of described stromatolites older than 3.2 Ga: comment and reply. *Geology*, **23**, 191.

Burne, R. V., and Moore, L., 1987. Microbialites; organosedimentary deposits of benthic microbial communities. *Palaios*, **2**, 241–254.

Cameron, B., Cameron, D., and Jones, J. R., 1985. Modern algal mats in intertidal and supratidal quartz sands, northeastern Massachusetts, USA. In Curren H. A. (ed.), *Biogenic Structures: Their Use in Interpreting Depositional Environments*. Tulsa, OK: Society of Economic Paleontologists and Mineralogists. SEPM special publication, 35, pp. 211–235.

Corsetti, F. A., and Grotzinger, J. P., 2005. Origin and significance of tube structures in Neoproterozoic post-glacial cap carbonates: Example from Noonday Dolomite, Death Valley, United States. *Palaios*, **20**, 348–362.

Davis, R. A., 1968. Algal stromatolites composed of quartz sandstone. *Journal of Sedimentary Petrology*, **38**, 953–955.

Decho, A. W., Visscher, P. T., and Reid, R. P., 2005. Production and cycling of natural microbial exopolymers (EPS) within a marine stromatolite. Palaeogeography, P*alaeoclimatology, Palaeoecology*, **219**, 71–86.

Dill, R. F., Kendall, C. G. St. C., and Shinn, E. A., 1989. Giant subtidal stromatolites and related sedimentary features. Field Trip Guidebook T373, 28th International Geological Congress, Washington, DC: American Geophysical Union, 33 pp.

Dill, R. F., Shinn, E. A., Jones, A. T., Kelly, K., and Steinen, R. P., 1986. Giant subtidal stromatolites forming in normal salinity waters. *Nature*, **324**, 55–58.

Draganits, E., and Noffke, N., 2004. Siliciclastic stromatolites and other microbially induced sedimentary structures in an Early Devonian barrier-island environment (Muth Formation, NW Himalayas). *Journal of Sedimentary Research*, **74**, 191–202.

Dravis, J. L., 1983. Hardened subtidal stromatolites, Bahamas. *Science*, **219**, 385–386.

Dromart, G., Gaillard, C., and Jansa, L. F., 1994. Deep-marine microbial structures in the Upper Jurassic of western Tethys. In Bertrand-Sarfati, J., and Monty, C. (eds), *Phanerozoic Stromatolites II*. Dordrecht: Kluwer, pp. 295–318.

Dupraz, C., and Strasser, A., 1999. Microbialites and microencrusters in shallow coral bioherms (Middle to Late Oxfordian, Swiss Jura mountains). *Facies*, **4**, 101–129.

Ezaki, Y., Liu, J., Nagano, T., and Adachi, N., 2008. Geobiological aspects of the earliest Triassic microbialites along the southern periphery of the tropical Yangtze Platform: initiation and cessation of a microbial regime. *Palaios*, **23**, 356–369.

Feldmann, M., and McKenzie, J. A., 1997. Messinian stromatolite-thrombolite associations, Santa Pola, SE Spain: an analogue for the Palaeozoic? *Sedimentology*, **44**, 893–914.

Feldmann, M., and McKenzie, J. A., 1998. Stromatolite-thrombolite associations in a modern environment, Lee Stocking Island, Bahamas. *Palaios*, **13**, 201–212.

Ferris, F. G., Thompson, J. B., and Beveridge, T. J., 1997. Modern freshwater microbialites from Kelly Lake, British Columbia, Canada. *Palaios*, **12**, 213–219.

Fischer, A. G., 1965. Fossils, early life, and atmospheric history. *Proceedings of the National Academy of Sciences*, **53**, 1205–1215.

Flügel, E., 2004. *Microfacies of Carbonate Rocks. Analysis, Interpretation and Application*. Berlin: Springer, xx + 976 pp.

Garrett, P., 1970. Phanerozoic stromatolites: noncompetitive ecologic restriction by grazing and burrowing animals. *Science*, **169**, 171–173.

Gebelein, C. D., 1974. Biological control of stromatolite microstructurc: implications for Precambrian time stratigraphy. *American Journal of Science*, **274**, 575–598.

Gerdes, G., Krumbein, W. E., and Noffke, N., 2000. Evaporite microbial sediments. In R. Riding, R., and Awramik, S. M. (eds), *Microbial Sediments*. Berlin: Springer, pp. 196–208.

Ginsburg, R. N., 1991. Controversies about stromatolites: vices and virtues. In Muller, D. W., McKenzie, J. A., and Weissert, H. (eds.), *Controversies in Modern Geology; Evolution of Geological Theories in Sedimentology, Earth History and Tectonics*, London: Academic Press, pp. 25–36.

Ginsburg, R. N., Isham, L. B., Bein, S. J., and Kuperberg, J., 1954. Laminated algal sediments of South Florida and their recognition in the fossil record. *Marine Laboratory, University of Miami, Coral Gables, Florida*, Unpublished Report, 54–20, 33 pp.

Grotzinger, J. P., 1986. Cyclicity and paleoenvironmental dynamics, Rocknest platform, northwest Canada. *Geological Society of America Bulletin*, **97**, 1208–1231.

Grotzinger J. P., 1989a. Introduction to Precambrian reefs. In Geldsetzer, H. H. J., James, N. P., and Tebbutt, G. E. (eds.), *Reefs, Canada and Adjacent Areas. Canadian Society of Petroleum Geologists Memoir* 13, pp. 9–12.

Grotzinger, J. P., 1989b. Facies and evolution of Precambrian carbonate depositional systems: emergence of the modern platform archetype. In Crevello, P. D., Wilson, J. L., Sarg, J. F., and Read, J. F. (eds.), *Controls on Carbonate Platform and Basin Development*. Tulsa, OK: Society of Economic Paleontologists and Mineralogists. SEPM special publication 44, pp. 79–106.

Grotzinger, J. P., 1990. Geochemical model for Proterozoic stromatolite decline. *American Journal of Science*, **290-A**, 80–103.

Grotzinger, J. P., and James, N. P., 2000. Precambrian carbonates: evolution of understanding. In Grotzinger, J. P., and James, N. P. (eds.), *Carbonate Sedimentation and Diagenesis in the Evolving Precambrian World.* Tulsa, OK: Society of Economic Paleontologists and Mineralogists. SEPM special publication, 67, pp. 3–20.

Grotzinger, J. P., and Kasting, J. F., 1993. New constraints on Precambrian ocean composition. *Journal of Geology*, **101**, 235–243.

Grotzinger, J. P., and Knoll, A. H., 1995. Anomalous carbonate precipitates: is the Precambrian the key to the Permian? *Palaios*, **10**, 578–596.

Grotzinger, J. P., and Knoll, A. H., 1999. Stromatolites in Precambrian carbonates: evolutionary mileposts or environmental dipsticks? *Annual Reviews of Earth and Planetary Sciences*, **27**, 313–358.

Grotzinger, J. P., and Read, J. F., 1983. Evidence for primary aragonite precipitation, lower Proterozoic (1.9-Ga) Rocknest Dolomite, Wopmay Orogen, Northwest Canada. *Geology*, **11**, 710–713.

Grotzinger, J. P., and Rothman, D. R., 1996. An abiotic model for stromatolite morphogenesis. *Nature*, **383**, 423–425.

Gürich, G., 1906. Les spongiostromides du Viséen de la Province de Namur. Musée Royal d'Histoire Naturelle de Belgique, *Mémoires*, **3**(4), 1–55, 13 pls.

Hagadorn, J. W., and Bottjer, D. J., 1997. Wrinkle structures: microbially mediated sedimentary structures common in subtidal siliciclastic settings at the Proterozoic-Phanerozoic transition. *Geology*, **25**, 1047–1050.

Hall, J., 1883. *Cryptozoön*, n.g.; *Cryptozoön proliferum*, nsp. New York State Museum of Natural History, 36th Annual Report of the Trustees, plate 6.

Halley, R. B., 1976. Textural variation within Great Salt Lake algal mounds. In Walter, M. R. (ed.), *Stromatolites, Developments in Sedimentology*, 20, Amsterdam: Elsevier, pp. 435–445.

Häntzschel, W., and Reineck, H.-E., 1968. Fazies-Untersuchungen im Hettangium von Helmstedt (Niedersachsen). *Mitteilungen aus dem Geologischen Staatsinstitut in Hamburg*, **37**, 5–39.

Harwood, G., 1990. 'Sandstone stromatolites' – an example of algal-trapping of sand grains from the Permian Yates Formation, New Mexico, U.S.A. Nottingham, England: 13th International Sedimentological Congress, Abstracts-Posters, p. 97.

Helm, C., and Schülke, I., 1998. A coral-microbialite patch reef from the late Jurassic (*florigemma*-Bank, Oxfordian) of NW Germany (Süntel Mountains). *Facies*, **39**, 75–104.

Helm, C., and Schülke, I., 2006. Patch reef development in the *florigemma*-Bank Member (Oxfordian) from the Deister Mts (NW Germany): a type example for Late Jurassic coral thrombolite thickets. *Facies*, **52**, 441–467.

Hoffman, P. F., 1975. Shoaling-upward shale-to-dolomite cycles in the Rocknest Formation (lower Proterozoic), Northwest Territories, Canada. In Ginsburg, R. N. (ed.), *Tidal Deposits*. New York: Springer, pp. 257–265.

Hoffman, P. F., and Schrag, D. P., 2002. The snowball Earth hypothesis: testing the limits of global change. *Terra Nova*, **14**, 129–155.

Hofmann, H. J., 1969. Attributes of stromatolites. *Geological Survey of Canada Paper 69–39*, 58 pp.

Hofmann, H. J., 1973. Stromatolites: characteristics and utility. *Earth Science Reviews*, **9**, 339–373.

Hofmann, H. A., 1998. Synopsis of Precambrian fossil occurrences in North America. In Lucas, S. B., and St-Onge, M. R. (co-ords), *Geology of Canada*, no. 7, pp. 271–376.

Hofmann, H. J., Grey, K., Hickman, A. H., and Thorpe, R. I., 1999. Origin of 3.45 Ga coniform stromatolites in Warrawoona Group, Western Australia. *Geological Society of America Bulletin*, **111**, 1256–1262.

Horodyski, R. J., 1982. Impressions of algal mats from the Middle Proterozoic Belt Supergroup, northwestern Montana, USA. *Sedimentology*, **29**, 285–289.

Hyde, W. T., Crowley, T. J., Baum, S. K., and Peltier, W. R., 2000. Neoproterozoic 'snowball Earth' simulations with a coupled climate/ice-sheet model. *Nature*, **405**, 425–429.

Jackson, M. J., 1989. Lower Proterozoic Cowles Lake foredeep reef, N.W.T., Canada. In Geldsetzer, H. H. J., James, N. P., and Tebbutt, G. E. (eds.), *Reefs, Canada and Adjacent Area.* Calgary: Canadian Society of Petroleum Geologists, Memoir 13, 64–71.

James, N. P., and Gravestock, D. I., 1990. Lower Cambrian shelf and shelf margin build-ups, Flinders Ranges, South Australia. *Sedimentology*, **37**, 455–480.

Jansa L. F., Pratt, B. R., and Dromart, G., 1988. Deep water thrombolite mounds from the Upper Jurassic of offshore Nova Scotia. In Geldsetzer, H. H. J., James, N. P., and Tebbutt, G. E. (eds.), *Reefs, Canada and adjacent areas*. Calgary: Canadian Society of Petroleum Geologists Memoir 13, 725–735.

Jenkins, G. S., 2003. GCM greenhouse and high-obliquity solutions for early Proterozoic glaciation and middle Proterozoic warmth. *Journal of Geophysical Research*, **108**, D3, 4118, doi:10.1029/2001JD001582, 2003.

Kah, L. C., and Grotzinger, J. P., 1992. Early Proterozoic (1.9 Ga) thrombolites of the Rocknest Formation, Northwest Territories, Canada. *Palaios*, **7**, 305–315.

Kah, L. C., and Knoll, A. H., 1996. Microbenthic distribution of Proterozoic tidal flats: environmental and taphonomic considerations. *Geology*, **24**, 79–82.

Kah, L. C., and Riding, R., 2007. Mesoproterozoic carbon dioxide levels inferred from calcified cyanobacteria. *Geology*, **35**, 799–802.

Kahle, C. F., 2001. Biosedimentology of a Silurian thrombolite reef with meter-scale growth framework cavities. *Journal of Sedimentary Research*, **71**, 410–422.

Kalkowsky, E., 1908. Oolith und Stromatolith im norddeutschen Buntsandstein. Zeitschrift Deutschen geol. *Gesellschaft*, **60**, 68–125, pls 4–11.

Kennard, J. M., 1994. Thrombolites and stromatolites within shalecarbonate cycles, Middle–Late Cambrian Shannon Formation, Amadeus Basin, central Australia. In Bertrand-Sarfati, J., and Monty, C. (eds.), *Phanerozoic Stromatolites II*. Dordrecht: Kluwer, pp. 443–471.

Kennard, J. M., and James, N. P., 1986. Thrombolites and stromatolites; two distinct types of microbial structures. *Palaios*, **1**, 492–503.

Kershaw, S., Zhang, T., and Lan, G., 1999. A microbialite crust at the Permian-Triassic boundary in south China, and its palaeoenvironmental significance. *Palaeogeography, Palaeoclimatology, Palaeoecology*, **146**, 1–18.

Kiessling, W., 2002. Secular variations in the Phanerozoic reef ecosystem. In Kiessling, W., Flügel, E., and Golonka, J. (eds.), *Phanerozoic Reef Patterns.* Tulsa, OK: Society of Economic Paleontologists and Mineralogists. SEPM special publication, 72, pp. 625–690.

Kopaska-Merkel, D. C., 2003. "Reefs" as exploration targets in the Smackover Formation. *Gulf Coast Association of Geological Sciences Transactions*, **53**, 411–421.

Krumbein, W. E., 1983. Stromatolites - the challenge of a term in space and time. *Precambrian Research*, **20**, 493–531.

Leinfelder, R. R., Nose, M., Schmid, D. U., and Werner, W., 1993. Microbial. crusts of the Late Jurassic: composition, palaeoecological significance and importance in reef construction. *Facies*, **29**, 195–229.

Leinfelder, R. R., Krautter, M., Laternser, R., Nose, M., Schmid, D. U., Schweigert, G., Werner, W., Keupp, H., Brugger, H., Herrmann, R., Rehfeld-Kiefer, U., Schroeder, J. H., Reinhold, C., Koch, R., Zeiss, A., Schweizer, V., Christmann, H., Menges, G., and Luterbacher, H., 1994. The origin of Jurassic reefs: current research developments and results. *Facies*, **31**, 1–56.

Logan, B. W., 1961. *Cryptozoon* and associated stromatolites from the Recent, Shark Bay, Western Australia. *Journal of Geology*, **69**, 517–533.

Logan, B. W., Rezak, R., and Ginsburg, R. N., 1964. Classification and environmental significance of algal stromatolites. *Journal of Geology*, **72**, 68–83.

Logan, B. W., Hoffman, P., and Gebelein, C. D., 1974. Algal mats, cryptalgal fabrics, and structures, Hamelin Pool, Western Australia. *American Association of Petroleum Geologists, Memoir*, **22**, 140–194.

Lowe, D. R., 1980. Stromatolites 3,400–3,500 Myr old from the Archean of Western Australia. *Nature*, **284**, 441–443.

Lowe, D. R., 1983. Restricted shallow-water sedimentation of early Archean stromatolitic and avaporitic strata of the Strelley Pool Chert, Pilbara Block, Western Australia. *Precambrian Research*, **19**, 239–283.

Lowe, D. R., 1994. Abiological origin of described stromatolites older than 3.2 Ga. *Geology*, **22**, 387–390.

Lowe, D. R., 1995. Abiological origin of described stromatolites older than 3.2 Ga: comment and reply. *Geology*, **23**, 191–192.

Mancini, E. A., Llinas, J. C., Parcell, W. C., Aurell, M., Badenas, B., Leinfielder, R. R., and Benson, D. J., 2004. Upper Jurassic thrombolite reservoir play, northern Gulf of Mexico. *AAPG Bulletin*, **88**, 1573–1602.

Martín, J. M., Braga, J. C., and Riding, R., 1993. Siliciclastic stromatolites and thrombolites, late Miocene, S.E. Spain. *Journal of Sedimentary Petrology*, **63**, 131–139.

McLoughlin, N., Wilson, L. A., and Brasier, M. D., 2008. Growth of synthetic stromatolites and wrinkle structures in the absence of

microbes – implications for the early fossil record. *Geobiology*, **6**, 95–105.
Merz, M. U. E., 1992. The biology of carbonate precipitation by cyanobacteria. *Facies*, **26**, 81–102.
Montaggioni, L. F., and Camoin, G. F., 1993. Stromatolites associated with coralgal communities in Holocene high-energy reefs. *Geology*, **21**, 149–152.
Monty, C. L. V., 1976. The origin and development of cryptalgal fabrics. In Walter, M. R. (ed.), *Stromatolites, Developments in Sedimentology* 20, Amsterdam: Elsevier, pp. 193–249.
Moore, L. S., and Burne, R. V., 1994. The modern thrombolites of Lake Clifton, western Australia. In Bertrand Sarfati, J., and Monty, C. L. (eds.), *Phanerozoic Stromatolites II*. Dordrecht: Kluwer Academic Publishers, pp. 3–29.
Noffke, N., Beukes, N., and Hazen, R., 2006. Microbially induced sedimentary structures in the 2.9 Ga old Brixton Formation, Witwatersrand Supergroup, South Africa. *Precambrian Research*, **146**, 35–44.
Noffke, N., Beukes, N., Bower, D., Hazen, R. M., and Swift, D. J. P., 2008. An actualistic perspective into Archean worlds - (cyano-) bacterially induced sedimentary structures in the siliciclastic Nhlazatse Section, 2.9 Ga Pongola Supergroup, South Africa. *Geobiology*, **6**, 5–20.
Noffke, N., Gerdes, G., Klenke, T., and Krumbein, W. E., 1996. Microbially induced sedimentary structures – examples from modern sediments of siliciclastic tidal flats. *Zentralblatt für Geologie und Paläontologie, Teil 1, 1995, Heft*, 1/2, 307–316.
Olivier, N., Hantzpergue, P., Gaillard, C., Pittet, B., Leinfelder, R. R., Schmid, D. U., and Werner, W., 2003. Microbialite morphology, structure and growth: a model of the Upper Jurassic reefs of the Chay Peninsula (Western France). *Palaeogeography, Palaeoclimatology, Palaeoecology*, **193**, 383–404.
Olivier, N., Lathuilière, B., and Thiry-Bastien, P., 2006. Growth models of Bajocian coral-microbialite reefs of Chargey-lès-Port (eastern France): palaeoenvironmental considerations. *Facies*, **52**, 113–127.
Parcell, W. C., 2002. Sequence stratigraphic controls on the development of microbial fabrics and growth forms - implication for reservoir quality distribution in the Upper Jurassic (Oxfordian) Smackover Formation, Eastern Gulf Coast, USA. *Carbonates and Evaporites*, **17**, 166–181.
Petrov, P. Yu., and Semikhatov, M. A., 2001. Sequence organization and growth patterns of late Mesoproterozoic stromatolite reefs: an example from the Burovaya Formation, Turukhansk Uplift, Siberia. *Precambrian Research*, **111**, 257–281.
Pia, J., 1927. Thallophyta. In Hirmer, M. (ed.), *Handbuch der Paläobotanik* 1, Munich: Oldenbourg, pp. 31–136.
Playford, P. E., and Cockbain, A. E., 1976. Modern algal stromatolites at Hamelin Pool, a hypersaline barred basin in Shark Bay, Western Australia. In Walter, M. R. (ed.), *Stromatolites*. Amsterdam: Elsevier, pp. 389–411.
Pope, M. C., Grotzinger, J. P., and Schreiber, B. C., 2000. Evaporitic subtidal stromatolities produced by in situ precipitation: textures, facies associations, and temporal significance. *Journal of Sedimentary Research*, **70**, 1139–1151.
Porada, H., Ghergut, J., and Bouougri, E. H., 2008. Kinneyia-type wrinkle structures – critical review and model of formation. *Palaios*, **23**, 65–77.
Pratt, B. R., 1982a. Stromatolitic framework of carbonate mudmounds. *Journal of Sedimentary Research*, **52**, 1203–1227.
Pratt, B. R., 1982b. Stromatolite decline – a reconsideration. *Geology*, **10**, 512–515.
Pratt, B. R., and James, N. P., 1982. Cryptalgal-metazoan bioherms of early Ordovician age in the St. George Group, western Newfoundland. *Sedimentology*, **29**, 543–569.
Reid, R. P., Visscher, P. T., Decho, A. W., Stolz, J. F., Bebout, B. M., Dupraz, C., Macintyre, I. G., Paerl, H. W., Pinckney, J. L., Prufert-Bebout, L., Steppe, T. F., and DesMarais, D. J., 2000. The role of microbes in accretion, lamination and early lithification of modern marine stromatolites. *Nature*, **406**, 989–992.
Reis, O. M., 1908. Kalkowsky: Ueber Oölith und Stromatolith im norddeutschen Buntsandstein. *Neues Jahrbuch für Mineralogie, Geologie und Paläontologie*, **2**, 114–138.
Reitner, J., 1993. Modern cryptic microbialite/metazoan facies from Lizard Island (Great Barrier Reef, Australia); formation and concepts. *Facies*, **29**, 3–39.
Reitner, J., Thiel, V., Zankl, H., Michaelis, W., Wörheide, G., and Gautret, P., 2000. Organic and biogeochemical patterns in cryptic microbialites. In Riding, R. E., and Awramik, S. M. (eds.), *Microbial Sediments*, Berlin: Springer, pp. 149–160.
Ridgwell, A. J., Kennedy, M. J., and Caldeira, K., 2003. Carbonate deposition, climate stability, and Neoproterozoic ice ages. *Science*, **302**, 859–862.
Riding, R., 1977. Skeletal stromatolites. In Flügel, E. (ed.), *Fossil Algae, Recent Results and Developments*, Berlin: Springer-Verlag, pp. 57–60.
Riding, R., 1991. Classification of microbial carbonates. In Riding, R., (ed.), *Calcareous algae and stromatolites*. Berlin: Springer-Verlag, pp. 21–51.
Riding, R., 1999. The term stromatolite: towards an essential definition. *Lethaia*, **32**, 321–330.
Riding, R., 2000. Microbial carbonates: the geological record of calcified bacterial-algal mats and biofilms. *Sedimentology*, **47** (Suppl. 1), 179–214.
Riding, R., 2006. Cyanobacterial calcification, carbon dioxide concentrating mechanisms, and Proterozoic-Cambrian changes in atmospheric composition. *Geobiology*, **4**, 299–316.
Riding, R., 2008. Abiogenic, microbial and hybrid authigenic carbonate crusts: components of Precambrian stromatolites. *Geologia Croatica*, **61**(2–3), 73–103.
Riding, R., and Liang, L., 2005. Geobiology of microbial carbonates: metazoan and seawater saturation state influences on secular trends during the Phanerozoic. *Palaeogeography, Palaeoclimatology, Palaeoecology*, **219**, 101–115.
Riding, R., Braga, J. C., and Martín, J. M., 1991a. Oolite stromatolites and thrombolites, Miocene, Spain: analogues of Recent giant Bahamian examples. *Sedimentary Geology*, **71**, 121–127.
Riding, R., Awramik, S. M., Winsborough, B. M., Griffin, K. M., and Dill, R. F., 1991b. Bahamian giant stromatolites: microbial composition of surface mats. *Geological Magazine*, **128**, 227–234.
Riding, R., Martín, J. M., and Braga, J. C., 1991c. Coral stromatolite reef framework, Upper Miocene, Almería, Spain. *Sedimentology*, **38**, 799–818.
Roddy, H. J., 1915. Concretions in streams formed by the agency of blue-green algae and related plants. *Proceedings American Philosophical Society*, **54**, 246–258.
Rowland, S. M., and Shapiro, R. S., 2002. Reef patterns and environmental influences in the Cambrian and earliest Ordovician. In Kiessling, W., Flügel, E., and Golonka, J. (eds.), *Phanerozoic Reef Patterns.* Tulsa, OK: Society of Economic Paleontologists and Mineralogists. SEPM special publication, 72, pp. 95–128.
Sami, T. T., and James, N. P., 1996. Synsedimentary cements as Paleoproterozoic platform building blocks, Pethei Group, northwestern Canada. *Journal of Sedimentary Research*, **66**, 209–222.
Schopf, J. W., and Klein, C., 1992. Glossary of technical terms. In Schopf, J. W., and Klein, C. (eds.), *The Proterozoic Biosphere: A Multidisciplinary Study.* Cambridge, UK: Cambridge University Press, pp. 1189–1204.
Schubert, J. K., and Bottjer, D. J., 1992. Early Triassic stromatolites as post-mass extinction disaster forms. *Geology*, **20**, 883–886.

Semikhatov, M. A., Gebelein, C. D., Cloud, P., Awramik, S. M., and Benmore, W. C., 1979. Stromatolite morphogenesis - progress and problems. *Canadian Journal of Earth Science*, **16**, 992–1015.
Serebryakov, S. N., (1976) Biotic and abiotic factors controlling the morphology of Riphean stromatolites. In Walter, M. R. (ed.), *Stromatolites, Developments in Sedimentology* 20, Amsterdam: Elsevier, pp. 321–336.
Shapiro, R. S., 2000. A comment on the systematic confusion of thrombolites. *Palaios*, **15**, 166–169.
Shapiro, R. S., and Awramik, S. M., 2006. *Favosamaceria cooperi* new group and form: a widely dispersed, time-restricted thrombolite. *Journal of Paleontology*, **80**, 411–422.
Sheldon, N. D., 2006. Precambrian paleosols and atmospheric $CO_2$ levels. *Precambrian Research*, **147**, 148–155.
Sherman, A. G., James, N. P., and Narbonne, G. M., 2000. Sedimentology of a late Mesoproterozoic muddy carbonate ramp, northern Baffin Island, Arctic Canada. In Grotzinger, J. P., and James, N. P. (eds.), *Carbonate Sedimentation and Diagenesis in the Evolving Precambrian World*. Tulsa, OK: Society of Economic Paleontologists and Mineralogists. SEPM special publication, 67, pp. 275–294.
Stal, L. J., van Gemerden, H., and Krumbein, W. E., 1985. Structure and development of a benthic marine microbial mat. *FEMS Microbiology Ecology*, **31**, 111–125.
Steele, J. H., 1825. A description of the Oolitic Formation lately discovered in the county of Saratoga, and state of New-York. *American Journal of Science*, **9**, 16–19, part of pl. 2.
Sumner, D. Y., 1997a. Carbonate precipitation and oxygen stratification in late Archean seawater as deduced from facies and stratigraphy of the Gamohaan and Frisco formations, Transvaal Supergroup, South Africa. *American Journal of Science*, **297**, 455–487.
Sumner, D. Y., 1997b. Late Archean calcite-microbe interactions: two morphologically distinct microbial communities that affected calcite nucleation differently. *Palaios*, **12**, 302–318.
Sumner, D. Y., and Grotzinger, J. P., 2004. Implications for Neoarchaean ocean chemistry from primary carbonate mineralogy of the Campbellrand-Malmani platform, South Africa. *Sedimentology*, **51**, 1–27.
Turner, E. C., Narbonne, G. M., and James, N. P., 1993. Neoproterozoic reef microstructures from the Little Dal Group, northwestern Canada. *Geology*, **21**, 259–262.
Turner, E. C., James, N. P., and Narbonne, G. M., 1997. Growth dynamics of Neoproterozoic calcimicrobial reefs, Mackenzie mountains, northwest Canada. *Journal of Sedimentary Research*, **67**, 437–450.
Turner, E. C., Narbonne, G. M., and James, N. P., 2000a. Framework composition of early Neoproterozoic calcimicrobial reefs and associated microbialites, Mackenzie Mountains, N.W.T., Canada. In Grotzinger, J. P., and James, N. P. (eds.), *Carbonate Sedimentation and Diagenesis in the Evolving Precambrian World*. Tulsa, OK: Society of Economic Paleontologists and Mineralogists. SEPM special publication, 67, pp. 179–205.
Turner, E. C., James, N. P., and Narbonne, G. M., 2000b. Taphonomic control on microstructure in early Neoproterozoic reefal stromatolites and thrombolites. *Palaios*, **15**, 87–111.
Visscher, P. T., Reid, R. P., and Bebout, B. M., 2000. Microscale observations of sulfate reduction: correlation of microbial activity with lithified micritic laminae in modern marine stromatolites. *Geology*, **28**, 919–922.
Walcott, C. D., 1914. Cambrian geology and paleontology III: Precambrian Algonkian algal flora. *Smithsonian Miscellaneous Collection*, **64**, 77–156.
Walter, M. R., 1972. Stromatolites and the biostratigraphy of the Australian Precambrian and Cambrian. *Special Papers in Palaeontology*, **11**, 190 pp, 33 pls.
Walter, M. R., and Heys, G. R., 1985. Links between the rise of the Metazoa and the decline of stromatolites. *Precambrian Research*, **29**, 149–174.
Walter, M. R., Veevers, J. J., Calver, C. R., Gorjan, P., and Hill, A. C., 2000. Dating the 840–544 Ma Neoproterozoic interval by isotopes of strontium, carbon, and sulfur in seawater, and some interpretative models. *Precambrian Research*, **100**, 371–433.
Webb, G. E., 1987. Late Mississippian thrombolite bioherms from the Pitkin Formation of northern Arkansas. *Geological Society of America, Bulletin*, **99**, 686–698.
Webb, G. E., 2005. Quantitative analysis and paleoecology of earliest Mississippian microbial reefs, lowermost Gudman formation, Queensland, Australia: not just post-disaster phenomena. *Journal of Sedimentary Research*, **75**, 875–894.
Whittle, G. L., Kendall, C. G. St. C., Dill, R. F., and Rouch, L., 1993. Carbonate cement fabrics displayed: a traverse across the margin of the Bahama Platform near Lee Stocking Island in the Exuma Cays. *Marine Geology*, **110**, 213–243.

## Cross-references

Biofilms
Calcified Cyanobacteria
Cap Carbonates
Microbial Biomineralization
Microbial Communities, Structure, and Function
Microbial Mats
Microbialites, Modern
Organomineralization
Snowball Earth

# MICROBIAL-METAL BINDING

Kurt O. Konhauser, David A. Fowle
University of Alberta, Edmonton, Alberta, Canada

## Definition

The accumulation of metal cations to microbes, largely through adsorptive processes to the outer cellular surfaces.

## Overview

All bacteria have low isoelectric points (below pH 2 in most cases), and consequently, they interact with soluble metal cations and have them intimately associated with their surfaces (Harden and Harris, 1953). Considering their ubiquity in the near-surface environment and their characteristically large surface area-to-volume ratios, bacteria can have a significant influence on metal mobility and speciation in these settings.

Some bound metals (e.g., Ca and Mg) serve the purpose of stabilizing the negative charges of the anionic functional groups, and thus are relatively "fixed" into place, while other metals are much more exchangeable and provide a temporary positive charge to counter the negative charge induced by the deprotonation of the cell's surface functional groups (Carstensen and Marquis, 1968). The strength of the metal–microbial bond is quantified by the surface complexation/binding constant ($K_M$), where M refers to the specific metal of interest. The greater its surface complex formation constant, the less likely

a metal cation will be desorbed into solution. Metal cation sorption is also directly affected by pH, which dictates metal partitioning (or speciation) between solid and soluble phases, and hence, controls its mobility, reactivity, and toxicity in aquatic environments. Of particular importance here is the hydrolysis constant, which measures the tendency of proton release from the hydration sphere of the cation. Figure 1 depicts a generalized adsorption edge curve for a metal binding to a bacterial surface. As pH increases, the cell wall deprotontates and adsorption of the positively charged metal cation increases, but in some instances, adsorption may actually decrease at high pH values as metal hydrolysis is enhanced.

Much of our understanding about how bacteria bind metals stems from the pioneering work of Terry Beveridge on metal accumulation by the Gram-positive bacterium, *Bacillus subtilis* (Beveridge and Murray, 1976). His research demonstrated that it was the carboxyl groups within the peptidoglycan that were the most electronegative sites, and that the bulk of the binding capacity was associated with the cell wall. In similar studies with Gram-negative cells, such as *Escherichia coli*, it was demonstrated that they did not bind as much metal from solution as did their Gram-positive counterparts, a pattern stemming simply from the smaller amounts of peptidoglycan associated with the *E. coli* cell walls (Beveridge and Koval, 1981). Many Gram-positive and Gram-negative bacteria also produce extracellular polymers (EPS), and due to their hydrated nature, dissolved metals can freely diffuse throughout the structure, binding to the anionic carboxyl groups of uronic acids and the neutrally charged hydroxy groups of sugars (Geesey and Jang, 1989). By possessing a large and reactive surface area, it is thus not unexpected that a number of studies have also documented that encapsulated bacteria bind more metals than nonencapsulated varieties (Rudd et al., 1983). Indeed, species producing EPS can tolerate higher metal concentrations than those that do not, and it has been shown that the proportion of encapsulated bacteria increases in metal-polluted sediment, whereas mutants that cannot produce capsules die off (Aislabie and Loutit, 1986).

Irrespective of the bacteria studied, what was repeatedly observed was that considerable variations in metal immobilization could be displayed by a single species. In some instances, cell walls were diffusely stained (Figure 2), while at other times so much metal was fixed to the cell surface that it formed a distinct mineral phase (Figure 3). This led Beveridge and Murray (1976) to originally propose a two-step mechanism for the metal adsorption process; the first step in time is an electrostatic interaction between the metal cations and the anionic sites in the cell wall/EPS. This interaction then acts as a nucleation site for the deposition of more metal cations (and anions) from solution, potentially leading to biomineralization. The size of the deposit depends on a number of variables, including the concentration of ions and the amount of time through which the reactions proceed. If sufficient time exists, then the mineral product grows in size within the intermolecular spaces until it is physically constrained by the organic polymers. The end result is a bacterial wall/EPS that contains copious amounts of metal, often approaching the mass of the bacterial cell itself (Beveridge, 1984).

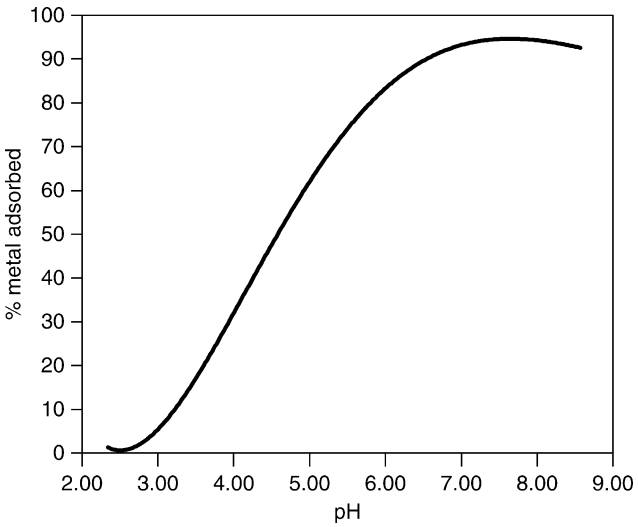


**Microbial-Metal Binding, Figure 1** Generic adsorption curve for a metal cation binding to a bacterial surface. Metal adsorption increases as pH increases and cell wall functional groups deprotonate.

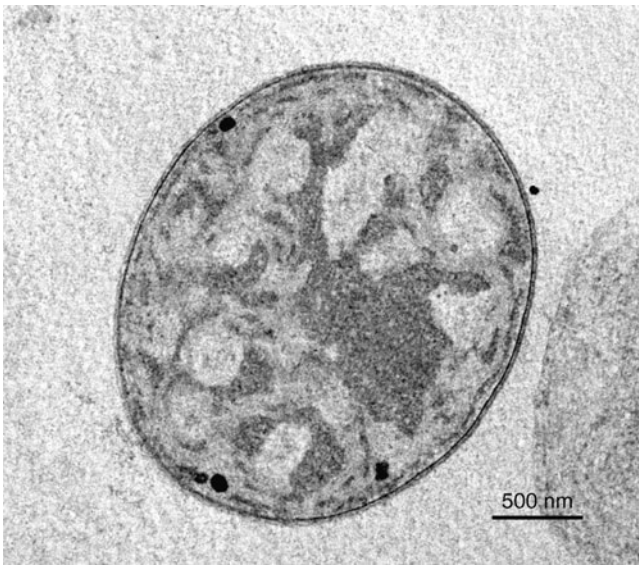


**Microbial-Metal Binding, Figure 2** Transmission electron micrograph (TEM) of the lab-cultured cyanobacterium *Anabena* sp. that was stained with uranium acetate and lead citrate to reveal cell ultrastructure. Note the dark staining of the cell wall and some of the cytoplasmic constituents.

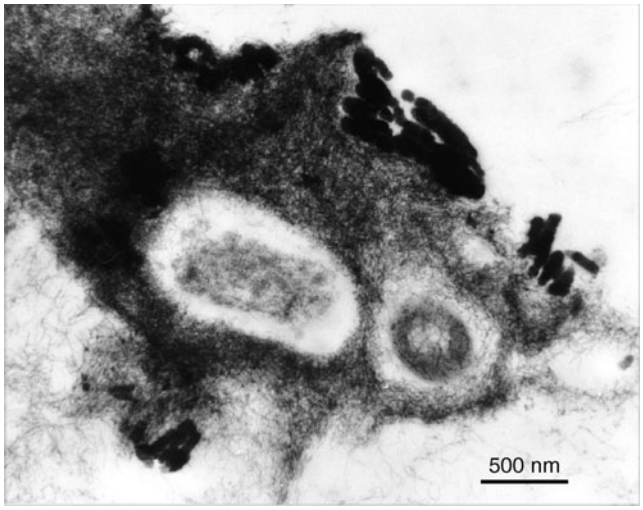


**Microbial-Metal Binding, Figure 3** TEM image of two unidentified bacteria surrounded by iron-stained extracellular polymers. The dark grains at the top right are ferric hydroxide, $Fe(OH)_3$. These cells grew naturally in Fe-rich hydrothermal fluids at the Lysuholl hot spring in Iceland. From Konhauser (2007).

Although binding of cations to a microbial surface is largely an electrostatic phenomenon, the structural and compositional complexity of the wall or EPS, as well as the unique physicochemical properties of each element, adds a level of complexity to the overall process. In other words, protons and each different cation should be capable of interacting in a distinctive way with surface ligands, such that a cell's surface will display varying affinities for binding different cations. Moreover, in natural systems, a multitude of cations (and anions) exist that should compete with one another for complex formation. This realization has led to a number of metal binding studies that have compared the relative affinities of protons and various cations for the anionic ligands on the cell surfaces of different microorganisms, by techniques that involve displacing one by another. Those studies have highlighted two very important points, the first being that metals and protons compete for the same surface sites, and as solution pH decreases, the functional groups become protonated, displacing loosely bound metal cations (Fowle and Fein, 2000). The second finding is that microbial–metal interactions are largely abiotic, nonspecific, and reliant upon thermodynamics (Warren and Haack, 2001). Some of the most important factors that influence metal binding to cells are (1) the ionic potential of the solution, (2) cell wall/EPS ligand spacing and their stereochemistry, (3) the ligand composition, and (4) the balance between the initial electrostatic attractions between a soluble metal cation and the organic ligands, and the subsequent covalent forces that arise from electron sharing across a metal cation–ligand molecular orbital (Williams, 1981). These properties are largely understood, and given sufficient information about the environment in which a microorganism is growing, it is possible to extrapolate and predict metal binding patterns on a cell surface.

In the past decade, metal binding experiments have begun to emphasize the stability constants for metal–organic ligand interactions and elucidate how metal binding correlates with cell surface reactivity during changes in solution chemistry. Moreover, unlike many of the early biosorption studies that were carried out in supersaturated conditions with respect to the metal of interest, more recent studies have focused on describing metal–microbe interactions at more realistic undersaturated conditions. The goal for much of this research is to develop geochemical speciation models that describe how microorganisms interact with metals and mineral surfaces under varying geochemical conditions, thus enabling their use in reactive transport models (Fein, 2000 for review). The reactions can be quantified using two different approaches: (1) bulk partitioning relationships or (2) surface complexation models (SCM). In the first instance, partitioning models, such as $K_d$, Freundlich and Langmuir isotherms, can easily be applied to complex systems because they do not require a detailed understanding of the nature of the surfaces or the adsorption/desorption mechanisms involved. However, they are system-specific, meaning that the results from a set of experiments can be inapplicable to different systems. In contrast, the SCM takes into account the effects of changing pH, solution composition and ionic strength, the acid–base properties of surface functional groups, competitive sorption with other solutes, and solid-phase reactivity and mineralogy. It then draws upon that information to extrapolate to conditions beyond those tested in the laboratory. However, in order to utilize these models in more complex settings, more detailed understanding is required of not only surface and aqueous speciation but also the adsorption and desorption mechanisms.

New experimental techniques are helping to elucidate both the mechanisms and stoichiometry of metal–microbe interactions. Spectroscopic data provide more direct evidence of the metal coordination environment than traditional SCM and partitioning models. For example, metal binding onto *B. subtilis* has been examined by X-ray absorption spectroscopy (XAS) and provided estimates of metal:functional group stoichiometry (Boyanov et al., 2003; Kelly et al., 2002). Mechanisms of metal binding have been directly probed via time-resolved laser-induced fluorescence spectroscopy (TRLFS) and have shown that some metals preferentially bond to one functionality in the cell wall (Panak et al., 2000), while others are less specific (Texier et al., 2000; Markai et al., 2003). A notable recent advance in constraining the thermodynamics of metal–microbe adsorption reactions was the combination of calorimetric data with SCM to generate site-specific enthalpies and entropies of metal adsorption onto the cell wall of *B. subtilis*. This work indicated that heavy metals bind to the cell wall via inner sphere complexation (e.g., no interlayer water molecules) with multiple anionic

oxygen ligands. Stoichiometry and temperature dependence of the metal–bacteria adsorption reactions can also be extracted using this approach (Gorman-Lewis et al., 2006).

## Summary

Microbial–metal adsorption includes the electrostatic and chemical association of metals with the organic functional groups of microbial cell surfaces. This can be considered a passive process driven by the electronegativity of the microbial cell wall/EPS and the Gibbs free energy of the adsorption reactions. These adsorption reactions seem to be dominated by binding of cations to the oxygen containing moieties on the cell surface. Future advances in elucidating the mechanisms of metal adsorption to microbes will come from combining novel analytical techniques, such as colorimetry and spectroscopy, with bulk partitioning studies and site-specific adsorption models.

## Bibliography


Aislabie, J., and Loutit, M. W., 1986. Accumulation of Cr(III) by bacteria isolated from polluted sediment. *Marine Environmental Research*, **20**, 221–232.

Beveridge, T. J., 1984. Mechanisms of the binding of metallic ions to bacterial walls and the possible impact on microbial ecology. In Reddy, C. A., and Klug, M. J. (eds.), *Current Perspectives in Microbial Ecology*. Washington, DC: American Society for Microbiology, pp. 601–607.

Beveridge, T. J., and Koval, S. F., 1981. Binding of metals to cell envelopes of *Escherichia coli* K-12. *Applied and Environmental Microbiology*, **42**, 325–335.

Beveridge, T. J., and Murray, R. G. E., 1976. Uptake and retention of metals by cell walls of *Bacillus subtilis*. *Journal of Bacteriology*, **127**, 1502–1518.

Boyanov, M. I., Kelly, S. D., Kemner, K. M., Bunker, B. A., Fein, J. B., and Fowle, D. A., 2003. Adsorption of cadmium to *Bacillus subtilis* bacterial cell walls: a pH dependent X-ray absorption fine structure spectroscopy study. *Geochimica et Cosmochimica Acta*, **67**, 3299–3311.

Carstensen, E. L., and Marquis, R. E., 1968. Passive electrical properties of microorganisms. III. Conductivity of isolated bacterial cell walls. *Biophysics Journal*, **8**, 536–548.

Fein, J. B., 2000. Quantifying the effects of bacteria on adsorption reactions in water-rock systems. *Chemical Geology*, **169**, 265–280.

Fowle, D. A., and Fein, J. B., 2000. Experimental measurements of the reversibility of metal-bacteria adsorption reactions. *Chemical Geology*, **168**, 27–36.

Geesey, G. G., and Jang, L., 1989. Interactions between metal ions and capsular polymers. In Beveridge, T. J., and Doyle, R. J. (eds.), *Metal Ions and Bacteria*. New York: John Wiley, pp. 325–357.

Gorman-Lewis, D., Fein, J. B., and Jensen, M. P., 2006. Enthalpies and entropies of proton and cadmium adsorption onto *Bacillus subtilis* bacterial cells from calorimetric measurements. *Geochimica et Cosmochimica Acta*, **70**, 4862–4873.

Harden, V. P., and Harris, J. O., 1953. The isoelectric point of bacterial cells. *Journal of Bacteriology*, **65**, 198–202.

Kelly, S. D., Boyanov, M. I., Fein, J. B., Fowle, D. A., Yee, N., and Kemner, K. M., 2002. X-ray absorption fine structure determination of pH-dependent U-bacterial cell wall interactions. *Geochimica et Cosmochimica Acta*, **66**, 3855–3871.

Markai, S., Andrés, Y., Montavon, G., and Grambow, B., 2003. Study of the interaction between europium (III) and *Bacillus subtilis*: fixation sites, biosorption modelling and reversibility. *Journal of Interface and Colloid Science*, **243**, 73–80.

Panak, P., Raff, J., Selenska-Pobell, S., Geipel, G., Bernhard, G., and Nitsche, H., 2000. *Radiochimica Acta*, **88**, 71–76.

Rudd, T., Sterritt, R. M., and Lester, J. N., 1983. Mass balance of heavy metal uptake by encapsulated cultures of *Klebsiella aerogenes*. *Microbial Ecology*, **9**, 261–272.

Texier, A. C., Andrés, Y., Illemassene, M., and Le Cloirec, P., 2000. Characterization of lanthanide ions binding sites in the cell wall of *Pseudomonas aeruginosa*. *Environmental Science and Technology*, **34**, 610–615.

Warren, L. A., and Haack, E. A., 2001. Biogeochemical controls on metal behaviour in freshwater environments. *Earth-Science Reviews*, **54**, 261–320.

Williams, R. J. P., 1981. Physico-chemical aspects of inorganic element transfer through membranes. *Philosophical Transactions of the Royal Society of London*, **B294**, 57–74.


## Cross-references


Carbonates
Clay Authigenesis, Bacterial
Dolomite, Microbial
Metalloenzymes
Microbial Biomineralization
Microbial Surface Reactivity
Nanocrystals, Microbially Induced
Organomineralization


# MICROBIOCORROSION


Aline Tribollet[1], Stjepko Golubic[2], Gudrun Radtke[3], Joachim Reitner[4]
[1]Institut de Recherche pour le Développement, Nouméa, Nouvelle-Calédonie, France
[2]Boston University, Boston, MA, USA
[3]Hessisches Landesamt für Umwelt und Geologie, Wiesbaden, Germany
[4]University of Göttingen, Göttingen, Germany


## Definition

Destruction of rocks and minerals by biological activities has been termed bioerosion (Neumann, 1966). It includes mechanical as well as chemical effects, that is, bioabrasion and biocorrosion (Schneider, 1976; Golubic and Schneider, 1979). However, both the processes often co-occur; they are functionally interconnected and mutually supportive. Biocorrosion can result from the activity of macro- or microorganisms and, thus, is called macrobiocorrosion and microbiocorrosion. Microbiocorrosion can also be closely associated with microbial rock formation and consolidation in stromatolitic structures (Reid et al., 2000; Macintyre et al., 2000; Garcia-Pichel et al., 2004; Dupraz and Visscher, 2005). In fact, the oldest known fossils of microboring organisms were located in lithified horizons of silicified stromatolites (Zhang and Golubic, 1987).

## Bibliography

Dupraz, C., and Visscher, P. T., 2005. Microbial lithification in marine stromatolites and hypersaline mats. *Trends in Microbiology*, **13**, 429–338.

Garcia-Pichel, F., Al-Horani, F., Ludwig, R., Farmer, J., and Wade, B., 2004. Balance between calcification and bioerosion in modern stromatolites. *Geobiology*, **2**, 49–57.

Golubic, S., and Schneider, J., 1979. Carbonate dissolution. In Trudinger, P. A., and Swaine, D. J. (eds.), *Biogeochemical Cycling of Mineral-Forming Elements*. Amsterdam: Elsevier, pp. 107–129.

Macintyre, I. G., Prufert-Bebout, L., and Reid, R. P., 2000. The role of endolithic cyanobacteria in the formation of lithified laminae in Bahamian stromatolites. *Sedimentology*, **47**, 915–921.

Neumann, A. C., 1966. Observations on coastal erosion in Bermuda and measurements of the boring rate of the sponge Cliona lampa. *Limnology and Oceanography*, **11**, 92–108.

Reid, R. P., Visscher, P. T., Decho, A. W., Stolz, J. F., Bebout, B. M., Dupraz, C. P., Macintyre, I. G., Paerl, H. W., Pinckney, J. L., Prufert-Bebout, L., Steppe, T. F., and DesMarais, D. J., 2000. The role of microbes in accretion, lamination and early lithification of modern marine stromatolites. *Nature*, **406**, 989–992.

Schneider, J., 1976. Biological and inorganic factors in the destruction of limestone coasts. *Contributions to Sedimentology*, **6**, 1–112.

Zhang, Y., and Golubic, S., 1987. Endolithic microfossils (cyanophyta) from early Proterozoic stromatolites, Hebei, China. *Acta Micropaleont Sinica*, **4**, 1–12.

# MICROSENSORS FOR SEDIMENTS, MICROBIAL MATS, AND BIOFILMS

Dirk de Beer
Max Planck Institute for Marine Microbiology, Bremen, Germany

## Synonyms

Amperometry; Diagenesis; Diffusion-reaction; Microelectrode; Microenvironment; Potentiometry

## Definition

Microsensors are needle-shaped sensors (Figure 1) that can be inserted in biologically active matrices, such as sediments, to measure directly concentrations of certain compounds.

## Introduction

In sediments, microbial mats, and biofilms steep gradients of substrates and products develop, due to high metabolic activities and mass transfer limitations (see Chapters *Biofilms*; *Microbial Mats*; *Sediment Diagenesis – Biologically Controlled*). Stratifications of microenvironments develop that determine the existence and activity of microbial consortia. For example, in active biofilms oxygen can penetrate less than 50 μm (de Beer et al., 1994c; de Beer et al., 1993), in sediments oxygen penetrates typically less than 2 mm (de Beer, 2001; Jørgensen and Revsbech, 1985; Meyers et al., 1987; Revsbech, 1983; Sorensen et al., 1981; Sweerts and de Beer, 1989). Below the oxic zone anaerobic microbial processes can occur, such as denitrification and sulfate reduction (see Chapter *Sulfur Cycle*), that determine the element cycling (the coupled degradative and chemolithotrophic processes) in the system as a whole. Stratifications on such a small scale cannot be studied by more classical techniques such as pore-water extraction and chemical analyzes. Extraction is impossible on such small scales, as it is highly destructive for the system and concentrations will have changed during the extraction procedure. To study such stratified systems we need microsensors that are minimally invasive and directly measure the concentrations without disturbing the system in which we measure. Moreover, as the system is not disturbed by microsensor analyses, we can perform sequences of measurements and, for example, study how the system responds to environmental changes. Microsensor measurements have enormously enhanced the insight in the vertical distribution of microbial processes in sediments. Microsensors were originally developed for physiological studies in animal and plant tissues, and even for intracellular measurements (Ammann, 1986; Hinke, 1969; Thomas, 1978), but soon applied in environmental studies (Bungay et al., 1969). They became an established technique for ecological studies by the developing work of Revsbech, who made them more robust and invented a large diversity of sensors (Kühl and Revsbech, 2000; Revsbech and Jørgensen, 1986).

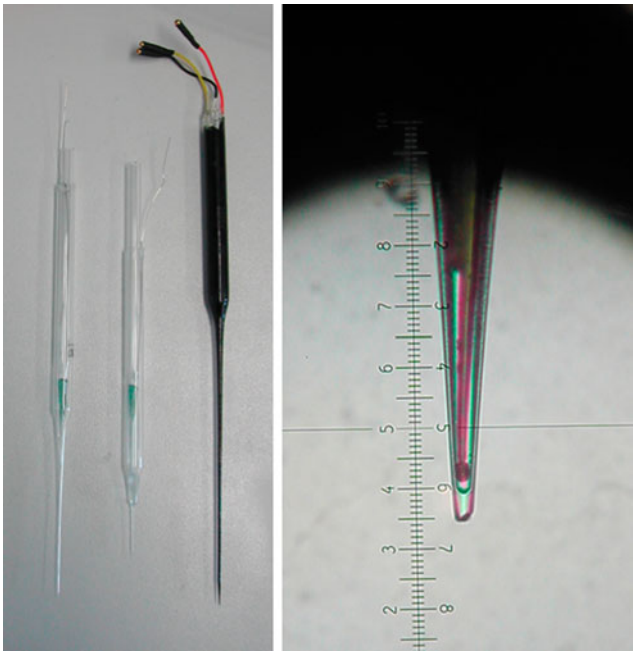

**Microsensors for Sediments, Microbial Mats, and Biofilms, Figure 1** *Left panel*, microsensors for oxygen (*left sensor*), for pH (*middle*), and for $H_2S$ (*right sensor*). The *right panel* zooms further in on the tip of an oxygen sensor, showing the gold-plated electrode behind a silicon membrane, the ticks on the ruler are 1 μm.

## Principle

The microsensors most commonly used for environmental studies are of the electrochemical principle, i.e., the compound to be measured induces a current (amperometric) or a potential (potentiometric) proportional to the concentration of the solute. The sensors are commonly made of glass, as this is easy to pull to fine tips, is inert and has excellent isolation properties. It involves the pulling of micropipettes in flames and electrical coils to exactly the desired geometry, thickness, and tip opening, followed by inserting the actual electrodes into these capillaries (Figure 1). The electrodes are mostly platinum wires, etched to micron thickness, and coated with a thin insulating glass layer. The making of microsensors is a fine art. For detailed descriptions of sensor preparation and electrochemical principles the reader is referred to various manuals and reviews (Gieseke and de Beer, 2004; Kühl and Revsbech, 2000; Revsbech and Jørgensen, 1986; Thomas, 1978).

The amperometric sensors consume the compound they measure, but since microsensors are so small this effect can be ignored. The tip diameter of some types can be less than 1 µm, but for most studies ranges between 3 and 15 µm are common, so the sensors are of similar size as the microbes studied. The size of the sensor must be carefully chosen. Small sensors respond faster and disturb the local microenvironment less, but are more fragile than larger sensors. The size of the sensor is a compromise between robustness and spatial resolution desired. For soft and extremely active biofilms microsensors of 1–3 µm are ideal; for measurements in coarse sand, tip diameters of 300 µm are used. Also for such big sensors, the actual sensing surface is ca 1 µm, the size is determined by the thick glass wall (Table 1).

## Essential equipment

Microsensors can be used in the laboratory and in the field. They can function also under high pressure, and can provide direct data from deep sea environments. Typical applications are measurements of concentration profiles and concentration changes upon a perturbation at a defined location. Microsensors are always positioned by micromanipulators mounted on a stable, heavy stand. The micromanipulator is preferably motorized, and controlled by a computer that is also used for data-acquisition. One can determine the exact position of the sensor to the surface of the studied object, with help of a dissection microscope. For in situ use all electronic components must be packed in water-sealed pressure housings. The most reliable in situ profiler consists of a single cylinder with amplifiers and computer for data storage and motor control. The sensors are mounted on special plugs directly on the cylinder, which can be moved vertically along a rail in steps of 12.5 µm (or multiples of this) by an external motor, according to a preprogrammed protocol. It is powered by a battery and can operate up to 72 h, at a depth of up to 6,300 m.

## Applications

Microsensors have been intensively used in studies on sediments, biofilms, and microbial mats (Kühl and Revsbech, 2000). The microscale distribution of substrates is a function of both mass transfer and local conversion rates, so if we have two of the phenomena quantified

**Microsensors for Sediments, Microbial Mats, and Biofilms, Table 1** Overview of microsensors suitable for environmental studies

| Compound measured | Main interferences | Tip size (µm) | Reference |
|---|---|---|---|
| *Amperometric* | | | |
| $O_2$ | $H_2S$ | 3 | Revsbech and Ward (1983) |
| $N_2O$ | $H_2S$, methanethiol | 3 | Andersen et al. (2001) |
| $H_2S$ | | 8 | Jeroschewski et al. (1996) |
| Glucose | $H_2O_2$ | 15 | Cronenberg et al. (1991) |
| $NO_3^-$ | $N_2O$, $NO_2^-$, $H_2S$ | 20 | Larsen et al. (1996, 1997) |
| $NO_2^-$ | $N_2O$, $H_2S$ | 20 | Nielsen et al. (2002) |
| $H_2O_2$ | | 5 | Cronenberg et al. (1991) |
| $HClO^-$ | | 10 | de Beer et al. (1994a) |
| $H_2$ | | 3 | Ebert and Brune (1997) |
| $CH_4$ | | 10 | Damgaard and Revsbech (1997) |
| NO | $H_2S$, methanethiol | 30 | Schreiber et al. (2008) |
| *Potentiometric* | | | |
| pH | – | 1 | de Beer et al. (1997b); Thomas, (1978) |
| $CO_3^{2-}$# | $Cl^-$ | 15 | Meyerhoff et al. (1987) |
| $NO_3^-$# | $Cl^-$ | 1 | de Beer and Sweerts (1989) |
| $NO_2^-$# | $Cl^-$ | 15 | de Beer et al. (1997b) |
| $Ca^{2+}$ | $H_2S$, $Mg^{2+}$ | 1 | de Beer et al. (2000); Tsien and Rink (1981) |
| $CO_2$ | $H_2S$ | 3 | de Beer et al. (1997a) |
| $NH_4^+$# | $K^+$, $Na^+$ | 1 | de Beer and Van den Heuvel (1988) |
| $S^{2-}$ | – | 6 | Revsbech et al. (1983) |

The sensors marked with # are only suitable for freshwater studies, the others can be used in all salinities

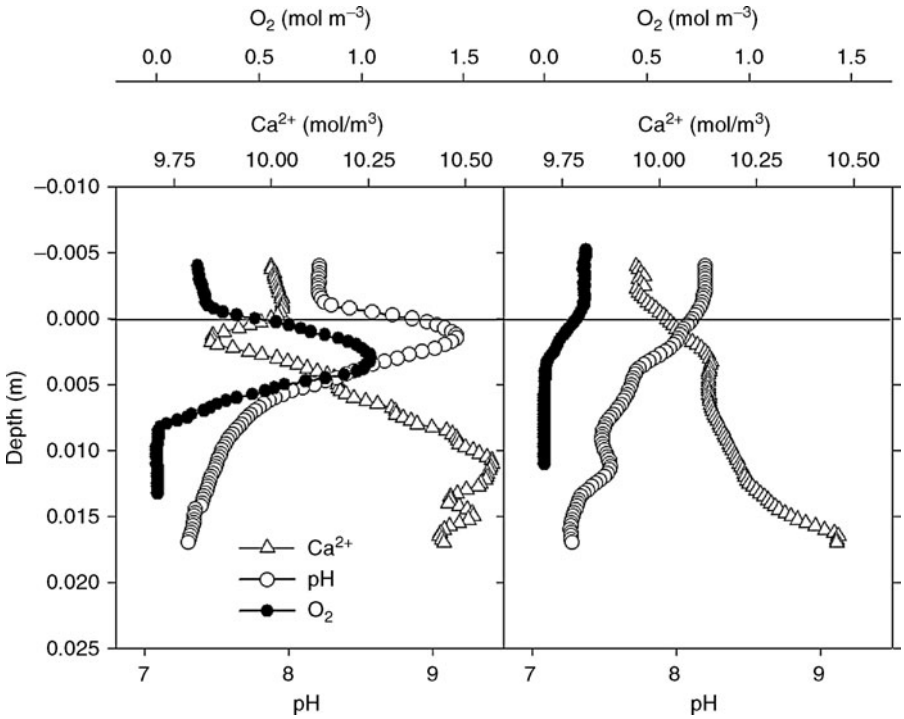


**Microsensors for Sediments, Microbial Mats, and Biofilms, Figure 2** Microprofiles of $O_2$, pH and $Ca^{2+}$ in calcareous sediments from a coral reef (Heron Island Australia). The effect of photosynthesis is demonstrated.

we can calculate the third: from the microprofiles and mass transfer we can determine the distribution of microbial activity (Berg et al., 1998; Gieseke and de Beer, 2004; Revsbech et al., 1986), and from the microprofiles and the local conversion rates we can determine the mass transfer rates (de Beer et al., 2006; de Beer et al., 2004). The latter possibility is rather rarely considered, but the most direct way to determine advection and areal conversion rates in advection-dominated sediments.

Calcification is for geology a highly relevant (micro) biological process (see Chapters *Microbial Biomineralization*; *Stromatolites*). The large background calcium concentrations of ca 8–10 mM make it difficult to determine calcification rates from a mass balance. With microsensors it is possible to measure micromolar concentration changes in seawater, in time or over distance, and thus to study the relation between (de)calcification and metabolic activities (*photosynthesis* and respiration). In Figure 2 the effect of light on coral reef sediments (Heron Island, Great Barrier Reef) is demonstrated: by photosynthesis the oxygen concentration peaks in the photic zone, due to $CO_2$ fixation the pH shifts up and calcium carbonate precipitates (concentration minimum). In the dark (right panel) calcium diffuses out of the sediment. The photic layer in which these processes occur is less than 5 mm thick.

Microsensors are extensively used to study photosynthesis in microbial mats (Hoehler et al., 2002; Polerecky et al., 2007; Revsbech et al., 1983; Wieland and Kuehl, 2000; Wieland et al., 2005) (see Chapter *Hypersaline Environments*), (de Beer and Schramm, 1999; de Beer et al., 1994b; Santegoeds et al., 1998; Schramm et al., 1996, 1999), in sediments (Revsbech, 1983; Sweerts, 1990; Sweerts and de Beer, 1989; Sweerts et al., 1990). Using diver-operated microprofilers well-controlled in situ measurements are possible (Weber et al., 2007; Ziebis et al., 1998). However, the most exciting applications are autonomous deployments on sites too remote or too harsh for human guidance: (1) direct in situ measurements during tidal cycles give insight in transport processes in permeable intertidal flats (de Beer et al., 2004; Røy et al., 2007; Werner et al., 2006a,b), (2) the in situ measurements in the deep sea supply physiological data communities associated with gas hydrates and high pressure volcanism (de Beer et al., 2006; Glud et al., 1993, 1994; Wenzhöfer et al., 2001a,b; Wenzhöfer and Glud, 2002). It is thinkable that some sort of microsensors will be used in future exploration of other planets.

## Summary

Microsensors can measure the microenvironment of dense and highly active microbial communities on the scale of microbes. Microsensors are used in field studies and in controlled laboratory experiments. As the sensors are very small they do not disturb the structure or the

pore-water chemistry, allowing precise, rapid, and online measurements of steady-state microprofiles, or concentration dynamics upon a perturbation. Both types of measurements are useful for high spatial resolution studies on the distribution of microbial activities, and on studies on mass transfer phenomena.

## Bibliography


Ammann, D., 1986. *Ion-Selective Microelectrodes: Principles, Design and Applications*. Berlin: Springer.

Andersen, K., Kjær, T., and Revsbech, N. P., 2001. An oxygen insensitive microsensor for nitrous oxide. *Sensors and Actuators*, **81**, 42–48.

Berg, P., Risgaard-Pedersen, N., and Rysgaard, S., 1998. Interpretation of measured concentration profiles in sediment pore water. *Limnology and Oceanography*, **43**, 1500–1510.

Bungay, H. R., Whalen, W. J., and Sanders, W. M., 1969. Microprobe techniques for determining diffusivities and respiration rates in microbial slimes. *Biotechnology and Bioengineering*, **11**, 765–772.

Cronenberg, C. C. H., Van Groen, H., de Beer, D., and Van den Heuvel, J. C., 1991. Oxygen-independent glucose microsensor based on glucose oxidase. *Analytica Chimica Acta*, **242**, 275–278.

Damgaard, L. R., and Revsbech, N. P., 1997. A microscale biosensor for methane containing methanotrophic bacteria and an internal oxygen reservoir. *Analytical Chemistry*, **69**, 2262–2267.

de Beer, D., 2001. Microsensor studies of oxygen, carbon and nitrogen cycles in lake sediments and microbial mats. In Taillefert, M., and Rozan, T. F. (eds.), *Environmental Electrochemistry: Analyses of Trace Element Biogeochemistry*. New York: Oxford University Press, pp. 227–246.

de Beer, D., and Schramm, A., 1999. Micro-environments and mass transfer phenomena in biofilms studied with microsensors. *Water Science and Technology*, **39**, 173–178.

de Beer, D., and Sweerts, J. P. R. A., 1989. Measurements of nitrate gradients with an ion-selective microelectrode. *Analytica Chimica Acta*, **219**, 351–356.

de Beer, D., and Van den Heuvel, J. C., 1988. Response of ammonium-selective microelectrodes based on the neutral carrier nonactin. *Talanta*, **35**, 728–730.

de Beer, D., van den Heuvel, J. C., and Ottengraf, S. P. P., 1993. Microelectrode measurements of the activity distribution in nitrifying bacterial aggregates. *Applied and Environmental Microbiology*, **59**, 573–579.

de Beer, D., Srinivasan, R., and Stewart, P. S., 1994a. Direct measurement of chlorine penetration into biofilms during disinfection. *Applied and Environmental Microbiology*, **60**, 4339–4344.

de Beer, D., Stoodley, P., and Lewandowski, Z., 1994b. Liquid flow in heterogeneous biofilms. *Biotechnology and Bioengineering*, **44**, 636–641.

de Beer, D., Stoodley, P., Roe, F., and Lewandowski, Z., 1994c. Effect of biofilm structures on oxygen distribution and mass transfer. *Biotechnology and Bioengineering*, **43**, 1131–1138.

de Beer, D., Glud, A., Epping, E., and Kühl, M., 1997a. A fast responding $CO_2$ micro-electrode for profiling sediments, microbial mats and biofilms. *Limnology and Oceanography*, **42**, 1590–1600.

de Beer, D., Schramm, A., Santegoeds, C. M., and Kühl, M., 1997b. A nitrite microsensor for profiling environmental biofilms. *Applied and Environmental Microbiology*, **63**, 973–977.

de Beer, D., Kühl, M., Stambler, N., and Vaki, L., 2000. A microsensor study of light enhanced $Ca^{2+}$ uptake and photosynthesis in the reef-building hermatypic coral *Favia* sp. *Marine Ecology. Progress Series*, **194**, 75–85.

de Beer, D., Wenzhöfer, F., Ferdelman, T. G., Boehme, S., Huettel, M., van Beusekom, J., Boettcher, M., Musat, N., and Dubilier, N., 2004. Transport and mineralization rates in North Sea sandy intertidal sediments (Sylt-Rømø Basin, Waddensea). *Limnology and Oceanography*, **50**, 113–127.

de Beer, D., Sauter, E., Niemann, H., Kaul, N., Foucher, J. P., Witte, U., Schlüter, M., and Boetius, A., 2006. In situ fluxes and zonation of microbial activity in surface sediments of the Håkon Mosby Mud Volcano. *Limnology and Oceanography*, **51**, 1315–1331.

Ebert, A., and Brune, A., 1997. Hydrogen concentration profiles at the oxicanoxic interface: A microsensor study of the hindgut of the wood-feeding lower termite Reticulitermes flavipes (Kollar). *Applied and Environmental Microbiology*, **63**, 4039–4046.

Gieseke, A., and de Beer, D., 2004. Use of microelectrodes to measure in situ microbial activities in biofilms, sediments, and microbial mats. In Akkermans, A. D. L., and van Elsas, D. (eds.), *Molecular Microbial Ecology Manual*. Dordrecht: Kluwer, pp. 1581–1612.

Glud, R. N., Gundersen, J. K., Revsbech, N. P., and Jørgensen, B. B., 1993. In situ measurements of total and diffusive oxygen uptake of sediments. *Trends in Microbial Ecology*, 427–430.

Glud, R. N., Gundersen, J. K., Jörgensen, B. B., Revsbech, N. P., and Schulz, H. D., 1994. Diffusive and total oxygen uptake of deep-sea sediments in the eastern South Atlantic Ocean: in situ and laboratory measurements. *Deep-Sea Research*, 41, 1767–1788.

Hinke, J., 1969. Glass microelectrodes for the study of binding and compartmentalisation of intracellular ions. In Lavallee, M., Schanne, O. F., and Herbert, N. C. (eds.), *Glass Microelectrodes*. New York: Wiley, pp. 349–375.

Hoehler, T. M., Albert, D. B., Alperin, M. J., Bebout, B., Martens, C. S., and Des Marais, D., 2002. Comparative ecology of H2 cycling in sedimentary and phototrophic ecosystems. *Antonie van Leeuwenhoek*, **81**, 575–585.

Jeroschewski, P., Steukart, C., and Kühl, M., 1996. An amperometric microsensor for the determination of $H_2S$ in aquatic environments. *Analytical Chemistry*, **68**, 4351–4357.

Jørgensen, B. B., and Revsbech, N. P., 1985. Diffusive boundary layers and the oxygen uptake of sediments and detritus. *Limnology and Oceanography*, **30**, 111–122.

Kühl, M., and Revsbech, N. P., 2000. Biogeochemical microsensors for boundary layer studies. In Boudreau, B., and Jørgensen, B. B. (eds.), *The Benthic Boundary Layer*. New York: Oxford University Press, pp. 180–210.

Larsen, L. H., Revsbech, N., and Binnerup, S. J., 1996. A microsensor for nitrate based on immobilized denitrifying bacteria. *Applied and Environmental Microbiology*, **62**, 148–1251.

Larsen, L. H., Kjaer, T., and Revsbech, N. P., 1997. A microscale $NO_3^-$ biosensor for environmental applications. *Analytical Chemistry*, **69**, 3527–3531.

Meyerhoff, M. E., Pretch, E., Welti, D. H., and Simon, W., 1987. Role of trifluoroacetophenone solvents and quaternary ammonium salts in carbonate-selective liquid membrane electrodes. *Analytical Chemistry*, **59**, 144–150.

Meyers, M. B., Fossing, H., and Powell, E. N., 1987. Microdistribution of interstitial meiofauna, oxygen and sulfide gradients, and the tubes of macro-fauna. *Marine Ecology. Progress Series*, **35**, 223–241.

Nielsen, M., Revsbech, N. P., Larsen, L. H., and Lynngaard-Jensen, A., 2002. On-line determination of nitrite in wastewater treatment by use of a biosensor. *Water Science and Technology*, **45**, 69–75.

Polerecky, L., Bachar, A., Schoon, R., Grinstein, M., Jørgensen, B. B., de Beer, D., and Jonkers, H., 2007. Contribution of Chloroflexus respiration to oxygen cycling in a hypersaline

microbial mat from Lake Chiprana, Spain. *Environmental Microbiology*, **9**, 2007–2024.
Revsbech, N. P., 1983. In situ measurement of oxygen profiles of sediments by use of oxygen microelectrodes. In Gnaigner, E., and Forstner, H. (eds.), *Polarographic Oxygen Sensors: Aquatic and Physiological Applications*. Berlin: Springer, pp. 265–273.
Revsbech, N. P., and Jørgensen, B. B., 1986. Microelectrodes: their use in microbial ecology. *Advances in Microbial Ecology*, **9**, 293–352.
Revsbech, N. P., and Ward, D. M., 1983. Oxygen microelectrode that is insensitive to medium chemical composition: use in an acid microbial mat dominated by *Cyanidium caldarum*. *Applied and Environmental Microbiology*, **45**, 755–759.
Revsbech, N. P., Jørgensen, B. B., Blackburn, T. H., and Cohen, Y., 1983. Microelectrode studies of the photosynthesis and $O_2$, $H_2S$ and pH profiles of a microbial mat. *Limnology and Oceanography*, **28**, 1062–1074.
Revsbech, N. P., Madsen, B., and Jørgensen, B. B., 1986. Oxygen production and consumption in sediments determined at high spatial resolution by computer simulation of oxygen microelectrode data. *Limnology and Oceanography*, **31**, 293–304.
Røy, H., Lee, J. S., Jansen, S., and de Beer, D., 2007. Tide-driven deep pore-water flow in intertidal sand flats. *Limnology and Oceanography*, **53**, 1521–1530.
Santegoeds, C. M., Ferdelman, T. G., Muyzer, G., and de Beer, D., 1998. Structural and functional dynamics of sulfate-reducing populations in bacterial biofilms. *Applied and Environmental Microbiology*, **64**, 3731–3739.
Schramm, A., Larsen, L. H., Revsbech, N. P., Ramsing, N. B., Amann, R., and Schleifer, K. H., 1996. Structure and function of a nitrifying biofilm as determined by in situ hybridization and the use of microelectrodes. *Applied and Environmental Microbiology*, **62**, 4641–4647.
Schramm, A., de Beer, D., van den Heuvel, J. C., Ottengraf, S. P. P., and Amann, R., 1999. Microscale distribution of populations and activities of *Nitrosospira* and *Nitrospira* spp. along a macroscale gradient in a nitryífying bioreactor: quantification by in situ hybridisation and the use of microsensors. *Applied and Environmental Microbiology*, **65**, 3690–3696.
Schreiber, F., Polerecky, L., and de Beer, D., 2008. Nitric oxide microsensor for high spatial resolution measurements in biofilms and sediments. *Analytical Chemistry*, **80**, 1152–1158.
Sorensen, J., Jørgensen, B. B., and Revsbech, N. P., 1981. A comparison of oxygen, nitrate, and sulfate respiration in coastal marine sediments. *Microbial Ecology*, **5**, 105–115.
Sweerts, J.-P. R. A., 1990. Oxygen consumption processes, mineralization and nitrogen cycling at the sediment-water interface of North temperate lakes, University of Amsterdam, 136 pp.
Sweerts, J.-P. R. A., and de Beer, D., 1989. Microelectrode measurements of nitrate gradients in the littoral and profundal sediments of a meso-eutrophic lake (lake Vechten, The Netherlands). *Applied and Environmental Microbiology*, **55**, 754–757.
Sweerts, J.-P. R. A., de Beer, D., Nielsen, L. P., Verdouw, H., van den Heuvel, J. C., Cohen, Y., and Cappenberg, T. E., 1990. Denitrification by sulphur oxidizing *Beggiatoa* spp. mats on freshwater sediments. *Nature*, **344**, 762–763.
Thomas, R. C., 1978. *Ion-Sensitive Intracellular Microelectrodes, How to Make and Use Them*. New York: Academic.
Tsien, R. Y., and Rink, T. J., 1981. $Ca^{2+}$-selective electrodes: a novel PVC-gelled neutral carrier mixture compared with other currently available sensors. *Journal of Neuroscience Methods*, **4**, 73–86.
Weber, M., Faerber, P., Meyer, V., Lott, C., Eickert, G., Fabricius, K. E., and de Beer, D., 2007. In situ applications of a new diver-operated motorized microsensor profiler. *Environmental Science and Technology*, **41**, 6210–6215.
Wenzhöfer, F., and Glud, R. N., 2002. Benthic carbon mineralization in the Atlantic: a synthesis based on in situ data from the last decade. *Deep-sea Research I*, **49**, 1255–1279.
Wenzhöfer, F., Adler, M., Kohls, O., Hensen, C., Strotmann, B., Boehme, S., and Schulz, H. D., 2001a. Calcite dissolution driven by benthic mineralization in the deep-sea: in situ measurements of $Ca^{2+}$, pH, $pCO_2$ and $O_2$. *Geochimica et Cosmochimica Acta*, **65**, 2677–2690.
Wenzhöfer, F., Holby, O., and Kohls, O., 2001b. Deep penetrating oxygen profiles measured in situ by oxygen optodes. *Deep-sea Research I*, **48**, 1741–1755.
Werner, U., Billerbeck, M., Polerecky, L., Franke, U., Huettel, M., van Beusekom, J. E. E., and de Beer, D., 2006a. Spatial and temporal patterns of mineralization rates and oxygen distribution in a permeable intertidal sand flat (Sylt, Germany). *Limnology and Oceanography*, **51**, 2549–2563.
Werner, U., Bird, P., Wild, C., Ferdelman, T. G., Polerecky, L., Eickert, G., Jonstone, R., Hoegh-Guldberg, O., and de Beer, D., 2006b. Spatial patterns of aerobic and anaerobic mineralization rates and oxygen penetration dynamics in coral reef sediments (Heron Island, Australia). *Marine Ecology. Progress Series*, **309**, 93–105.
Wieland, A., and Kuehl, M., 2000. Irradiance and temperature regulation of oxygenic photosynthesis and $O_2$ consumption in a hypersaline cyanobacterial mat (Solar Lake, Egypt). *Marine Biology*, **137**, 71–85.
Wieland, A., Zopfi, J., Benthien, M., and Kühl, M., 2005. Biogeochemistry of an iron-rich hypersaline microbial mat (Camargue, France). *Microbial Ecology*, **49**, 34–49.
Ziebis, W., Pillen, T., and Unger, B., 1998. A diver observatory for in situ studies in sublittoral sediments. *Journal of the Society for Underwater Technology*, **23**, 63–69.

## Cross-references

Biofilms
Biofilms and Fossilization
Cyanobacteria
Deep Biosphere of the Oceanic Deep Sea
Hypersaline Environments
Microbial Biomineralization
Microbial Mats
Microbialites, Modern
Photosynthesis
Sediment Diagenesis – Biologically Controlled
Sulfur Cycle

# MOLAR-TOOTH STRUCTURE

Brian R. Pratt
University of Saskatchewan, Saskatoon, SK, Canada

## Definition

Molar-tooth structure is a synsedimentary, combined deformation and early diagenetic feature occurring in calcareous strata of mainly Precambrian age. It consists of arrays of closely spaced, sharply defined, upright veins, and subordinate horizontal sheets and spheroids composed of calcite microspar. Veins are vertically to obliquely oriented, discontinuous, typically strongly squashed or crumpled, and often brecciated.

## Geological age

Molar-tooth structure (MTS) was first named in 1885 from its appearance on limestone bedding planes in the Mesoproterozoic Purcell Supergroup (= Belt Supergroup in USA.) along the border between southwestern Canada and adjacent northwestern Montana. Almost all occurrences are in Mesoproterozoic to late Neoproterozoic (Ediacaran) strata, representing a 1 billion-year time span from about 1,600 to 600 Ma, but there are several examples noted from the Paleoproterozoic and one from the Neoarchean (James et al., 1998; Pratt, 1998b; Shields, 2002; Meng and Ge, 2002). Importantly, a few Phanerozoic cases have also been reported (Figure 1c; Pratt, 1982; Rossetti, 2000).

## Geobiological implications

Organisms and organic matter have been alleged to be implicated in MTS formation in various ways. Its rarity after the Neoproterozoic has been ascribed generally to substrate modification by animals. However, the drastic reduction of MTS occurrences took place before the known appearance of infaunal invertebrates and, instead, Shields (2002) saw the decline as due to changes in the chemistry of seawater, especially a decrease in $CaCO_3$ saturation caused by a drop in atmospheric $pCO_2$. There may have been an evolutionary control on the shape and mineralogy of lime mud, leading to the precipitation of granular lime mud which was thus prone to fluidization (Pratt, 1998b, 2001). Pratt (1998b) postulated that the rheology of carbonate sediment altered with the changing nature of organic matter and the microbiota brought about by the "Cambrian explosion." Biomarkers in late Neoproterozoic examples represent cyanobacterial, anaerobic bacterial, and eukaryotic algal precursors in the sediment (Kuang et al., 2004). According to some interpretations, MTS was originally void space created by $CO_2$ generated by the biodegradation of organic matter

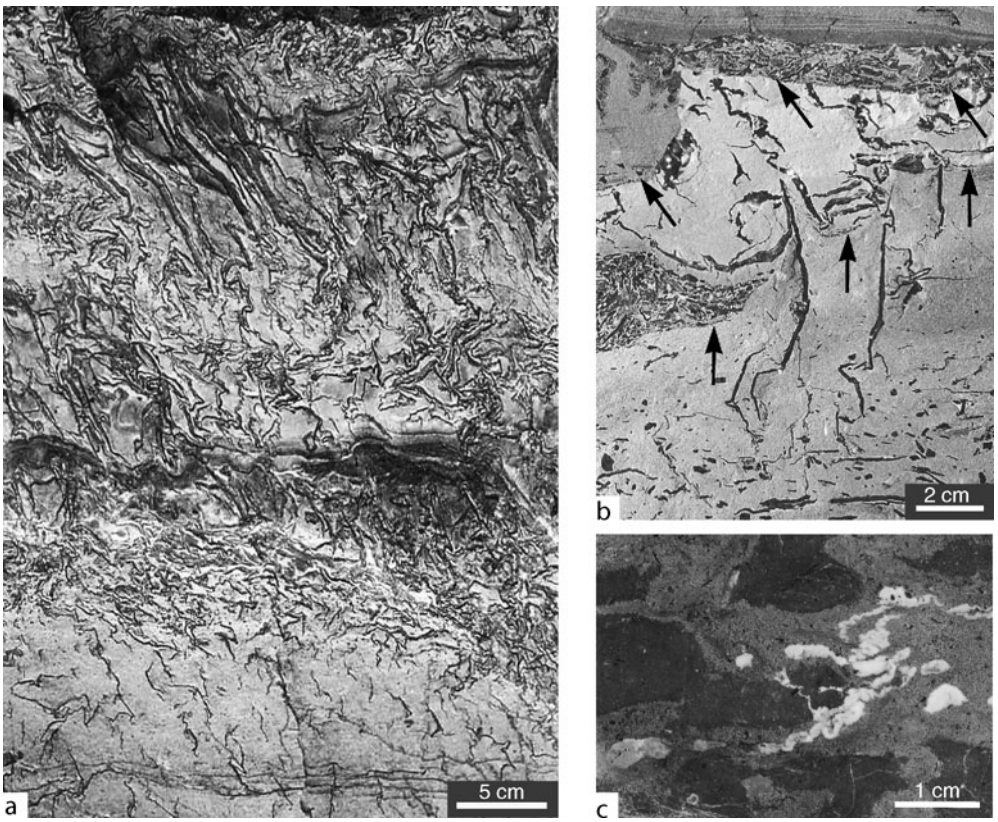


**Molar-tooth Structure, Figure 1** (**a**) Lime mudstone riddled with molar-tooth structure (MTS) veins (dark): initially sparse and upright, passing upward to dense and strongly oblique, thence, in the upper two thirds, to upright but markedly crumpled and tilted. George Formation, Muskwa Group (~1.6 Ga), northern British Columbia. (**b**) Mudstone with three generations of MTS and erosion surfaces. First-generation veins in lower part are fragmented and reworked while second-generation veins are upright. Lowest erosion surface (vertical arrows) is cuspate around upright veins, with vein fragments collected in gutter at left. Overlying mudstone contains third-generation veins that are variably oriented. Second erosion surface (oblique arrows) truncates veins; vein fragments are collected in gutter at left and on horizontal surface at right. Overlying cross-laminated grainstone contains a fourth generation of rare upright veins. George Formation. (**c**) Wackestone (dolomitic areas light gray) with crumpled veins (whitish). Coronach Member, Herald Formation Red River Group (late Ordovician), 14-26-6-11W2 (2,565.5 m), southern Saskatchewan (see El Taki and Pratt, 2009).

(Furniss et al., 1998; Pollock et al., 2006) or by $CO_2$-clathrate destabilization (Marshall and Anglin, 2004). James et al. (1998) suggested that a surface microbial mat sealed the sediment. If not physicochemical, precipitation of $CaCO_3$ crystals in the veins (Pollock et al., 2006) or as sediment grains before being fluidized (Pratt, 1998b, 2001) may have been triggered by dissolved organic molecules, nucleated on organic particles, or induced by photosynthesis.

## Shape

MTS occurs mostly in both clean and argillaceous subtidal lime mudstones (Figures 1a–c, 2a and b), but a few are in shales (Figure 2c). Individual vein arrays crosscut up to ~0.5 m of sedimentary bedding; locally, they can comprise more than 50% of the host rock. Veins are discontinuous, range from fairly uniform to variable in width up to ~5 mm along their length, and typically exhibit tapered terminations. Although more or less straight to gently curved in some beds, mostly veins are strongly squashed or crumpled. The whole array may be tilted in one direction. On bedding planes, veins describe variably continuous subparallel, crisscrossing, or irregularly reticulate lines. The upper and lower surfaces of horizontal veins match, indicating that they are dilatational sheet cracks. Crudely spheroidal blobs are up to ~1 cm across. Two crosscutting episodes of vein formation are common, and they typically show differing degrees of deformation. In some argillaceous and silty units, as many as four consecutive phases of vein generation can be delineated, with each containing progressively less calcite and more terrigenous particles, and consequently appearing less and less distinct from the matrix.

The matrix usually shows soft-sediment deformation especially in the form of small-scale folding. Typically, the matrix along with the enclosed MTS was deformed plastically together. Veins may be dislocated and the segments shingled in both vertical and horizontal directions, but they are also often stretched, boudinaged, or smeared. In many cases, a subsequent event caused the still plastic matrix to be deformed around veins that had become stiff due to calcite cementation, which also resulted in brecciation of the veins. After consolidation of the matrix, a further phase of deformation caused small mode I cracks in the veins but little displacement. These features are evidence for variably directed compressional, tensile and shear stresses that were imposed often repeatedly during the separate rheological evolution of both components.

Seafloor erosion affected many beds with MTS. The more resistant veins commonly protruded above the substrate, and vein segments and fragments were winnowed out and concentrated into interbedded intraclastic grainstones (Figures 1b and 2b). In a so far unique case, cross-lamination in vein fills indicates that they were exhumed and reworked by waves before cementation (Bishop and Sumner, 2006).

## Composition

Locally MTS consists of micrite. However, in most cases it is composed of interlocking, equant, inclusion-free microspar crystals 7–15 μm across (Figure 3a). Backscattered electron microscopy and cathode-luminescence reveal that in some examples these crystals consist of

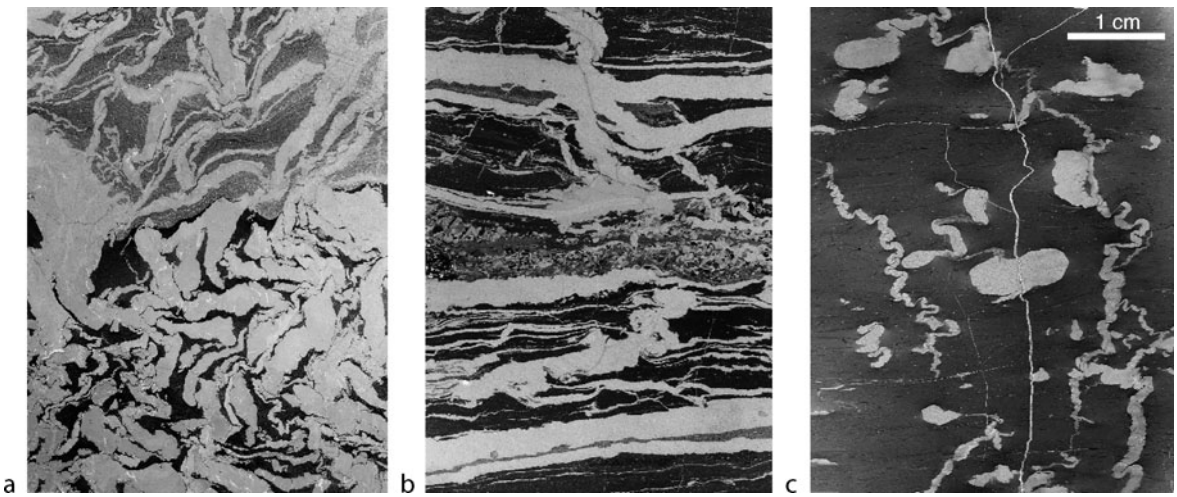


**Molar-tooth Structure, Figure 2** Thin section photomicrographs of molar-tooth structure (MTS) (light gray); scale bar same for all. (**a**) $C_{org}$-rich mudstone with densely packed squashed and broken veins, overlain by distorted, laminated mudstone with tilted and crumpled upright and subhorizontal veins. George Formation. (**b**) Dolomitic mudstone with two crosscutting generations of horizontal and squashed upright veins. In middle, grainstone lamina (composed of micrite peloids and grains of MTS) is crossed by veins and part of its interparticle porosity is filled with microspar. I-5 unit, Atar Group (~1.1 Ga), Mauritania. (**c**) Slightly calcareous shale with spheroidal and crumpled upright veins. (Vertical crack in center is an artifact.) Chamberlain Formation, Belt Supergroup (1.45 Ga), central Montana.

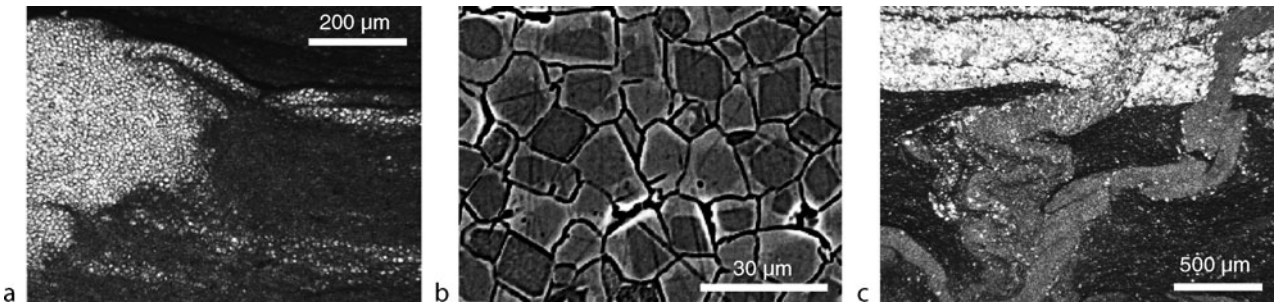


**Molar-tooth Structure, Figure 3** (**a**) Thin section photomicrograph of calcite microspar in pod-shaped molar-tooth structure (MTS) and smeared, variably distinct, horizontal veins, and stringers; isolated microspar grains are also dispersed in shale matrix. Chamberlain Formation. (**b**) Back-scattered electron photomicrograph showing microspar mosaic with euhedral mud-sized cores (dark gray). Cores are rhombs and less commonly multifaceted crystals. Monteville Formation, Transvaal Supergroup (~2.6 Ga), South Africa (see Bishop and Sumner, 2006, fig. 9C; photograph courtesy of J. W. Bishop). (**c**) Thin section photomicrograph of squashed and shingled veins crossing argillaceous lime mudstone overlain by sandstone. Veins contain quartz silt and very fine-grained sand (whitish grains near the sandstone and sourced from it; those elsewhere are authigenic quartz crystals). Helena Formation, Belt Supergroup, northwestern Montana.

well-sorted rhombs and multifaceted euhedra with calcite cement overgrowths (Figure 3b; Pollock et al., 2006; Bishop and Sumner, 2006). These cores may be the original mud particles or a product of synsedimentary recrystallization. Similar grains occur in the matrix mudstone or shale. Microspar in MTS is typically uniform in size but locally there is variation that describes crude wall-parallel lamination; indistinct shear veins or cracks can be detected in some examples. In some units the MTS is recrystallized to pseudospar.

Where veins penetrate interbedded siltstone or sandstone layers the microspar may contain silt or fine sand plus minor amounts of clay (Figure 3c; Pratt, 1998b, 1999; Bishop and Sumner, 2006). MTS may grade into dikelets and thin sills of injected silt and sand of the kind that have been termed "syneresis" cracks (Pratt, 1998a; cf. Tanner, 1998; Shi et al., 2009).

The calcite in MTS exhibits $\delta^{13}C_{PDB}$ values in the range of about −1.5‰ to 3.5‰, which are similar to those in co-occurring sedimentary carbonate particles (Frank and Lyons, 1998; Pratt, 1998b; Marshall and Anglin, 2004; Bishop et al., 2006; Kuang et al., 2007).

## Formation

For more than a century, the enigmatic nature of MTS was tolerated but largely ignored. Because fragments of MTS comprise sedimentary particles, it was eventually recognized as having formed intrastratally just below the sediment–water interface. Some geologists presumed MTS to be a fossil algal or microbial object. Later it was accepted as a deformation feature involving substantial shrinkage of the host sediment – although not due to desiccation because there is no evidence for associated subaerial exposure.

Pore-lining cement fabrics are absent in MTS even though they are present in co-occurring grainstones. Nevertheless, it is still debated whether or not MTS was initially a system of cavities, in which case $CaCO_3$ precipitated later as tiny crystals inside them (Fairchild et al., 1997; Furniss et al., 1998; Pollock et al., 2006; Bishop and Sumner, 2006; Bishop et al., 2006). The presence in MTS of sand, silt, and clay impurities as suspended particles, clusters of grains, or seams is difficult to reconcile with this interpretation.

The possibility that MTS began as voids forced open by bubbles of $CO_2$ passively generated by the oxidation of organic matter in the sediments is unlikely because of the extreme amount of organic matter required, the shallow-water, oxidizing depositional setting, the linear to reticulate shape of vein arrays, the evidence for concomitant sand and silt injection, and the complex nature of the stresses demonstrated by accompanying physical deformation (Pratt, 1999). Because of the tropical sedimentary environment of host limestones, the involvement of $CO_2$-clathrates is implausible. In most units, the absence of closely associated high-energy features is further evidence against the possibility of void opening by wave-induced loading (Bishop et al., 2006).

Pratt (1998b) explained MTS as a seismically induced deformation feature of calcareous sediment possessing unique geotechnical properties for which modern analogues are lacking. By this model, cyclic loading during earthquakes caused elevated fluid pressure and loss of shear strength in the muddy sediment. During abrupt dewatering, veins, sheet cracks, and spheroidal pockets were jacked open by the injection of granular lime mud that was segregated from the sediment. Examples where more than 50% of limestones consist of MTS indicate that a substantial proportion of the lime mud was mobilized. However, shaly host rocks still contain poorly defined seams and residual disseminated calcite grains that did not find their way into veins. Incorporated sand and silt show that dewatering and injection were both downwardly and upwardly directed. Spheroids formed where dewatering was localized and fluids did not escape to the surface. All this caused a striking shrinkage of the matrix and compaction of upright veins. As shaking proceeded,

they were squeezed, sheared, and stretched in different directions. After cementation of the mud infill, subsequent events deformed the matrix again, generated more veins, and brecciated the first set of veins, until the sediment was too stiff to deform further. Indeed, in almost every case, distortion of MTS and the matrix testifies to differential rheologies and progressive evolution from liquefaction through plastic deformation to brittle failure, as would be expected if affected by repeated earthquakes during dewatering and early diagenesis. A similar seismic model has been invoked for sand and silt dykelets (syneresis cracks), except that synsedimentary cementation was not involved (Pratt, 1998a).

## Bibliography


Bishop, J. W., and Sumner, D. Y., 2006. Molar tooth structures of the Neoarchean Monteville Formation, Transvaal Supergroup, South Africa. I: constraints on microcrystalline $CaCO_3$ precipitation. *Sedimentology*, **53**, 1049–1058.

Bishop, J. W., Sumner, D. Y., and Huerta, N. J., 2006. Molar tooth structures of the Neoarchean Monteville Formation, Transvaal Supergroup, South Africa. II: a wave-induced fluid flow model. *Sedimentology*, **53**, 1069–1082.

El Taki, H., and Pratt, B. R., 2009. Synsedimentary deformation in laminated dolomites and evaporites of the Herald Formation (Red River Group): signature of Late Ordovician tectonic activity in southern Saskatchewan. In Summary of investigations 2009, Vol. 1. Saskatchewan Geological Survey, Saskatchewan Ministry of Energy and Resources, Miscellaneous Report 2009-4.1, Paper A-3, p. 10.

Fairchild, I. J., Einsele, G., and Song, T., 1997. Possible seismic origin of molar tooth structures in Neoproterozoic carbonate ramp deposits, North China. *Sedimentology*, **44**, 611–636.

Frank, T. D., and Lyons, T. W., 1998. "Molar-tooth" structures: a geochemical perspective on a Proterozoic enigma. *Geology*, **26**, 683–686.

Furniss, G., Rittel, J. F., and Winston, D., 1998. Gas bubble and expansion crack origin of "molar-tooth" calcite structures in the middle Proterozoic Belt Supergroup, Western Montana. *Journal of Sedimentary Research*, **68**, 104–114.

James, N. P., Narbonne, G. M., and Sherman, A. G., 1998. Molar-tooth carbonates: shallow subtidal facies of the mid- to late Proterozoic. *Journal of Sedimentary Research*, **68**, 716–722.

Kuang, H., Li, Y., Zeng, Y., Meng, X., and Ge, M., 2004. Biomarkers in the molar tooth (MT)-bearing limestones in the Jilin–Liaoning area of China. *Chinese Journal of Geochemistry*, **23**, 334–341.

Kuang, H., Liu, Y., Meng, X., and Ge, M., 2007. A study on the environmental conditions of the microsparite (molar-tooth) carbonates. *Chinese Journal of Geochemistry*, **26**, 28–34.

Marshall, D., and Anglin, C. D., 2004. $CO_2$-clathrate destabilization: a new model of formation for molar tooth structures. *Precambrian Research*, **129**, 325–341.

Meng, X., and Ge, M., 2002. The sedimentary features of Proterozoic microspar (molar-tooth) carbonates in China and their significance. *Episodes*, **25**, 185–195.

Pollock, M. D., Kah, L. C., and Bartley, J. K., 2006. Morphology of molar-tooth structures in Precambrian carbonates: influence of substrate rheology and implications for diagenesis. *Journal of Sedimentary Research*, **76**, 310–323.

Pratt, B. R., 1982. Limestone response to stress: pressure solution and dolomitization—discussion and examples of compaction in carbonate sediments. *Journal of Sedimentary Petrology*, **52**, 323–327.

Pratt, B. R., 1998a. Syneresis cracks: subaqueous shrinkage in argillaceous sediments caused by earthquake-induced dewatering. *Sedimentary Geology*, **117**, 1–10.

Pratt, B. R., 1998b. Molar-tooth structure in Proterozoic carbonate rocks: origin from synsedimentary earthquakes, and implications for the nature and evolution of basins and marine sediment. *Geological Society of America Bulletin*, **110**, 1028–1045.

Pratt, B. R., 1999. Gas bubble and expansion crack origin of "molar-tooth" calcite structures in the middle Proterozoic Belt Supergroup, western Montana—Discussion. *Journal of Sedimentary Research*, **68**, 1136–1140.

Pratt, B. R., 2001. Oceanography, bathymetry and syndepositional tectonics of a Precambrian intracratonic basin: integrating sediments, storms, earthquakes and tsunamics in the Belt Supergroup (Helena Formation, ca. 145 Ga), Western North America. *Sedimentary Geology*, **141–142**, 371–394.

Rossetti, D. F., 2000. Molar-tooth carbonates: shallow subtidal facies of the mid- to late Proterozoic—Discussion. *Journal of Sedimentary Research*, **70**, 1246–1248.

Shi, X. Y., Jiang, G. Q., Zhang, C. H., Gao, L. Z., and Liu, J., 2009. Sand veins and MISS from the Mesoproterozoic black shale (ca. 1.7 Ga) in North China: implications for methane degassing from microbial mats. *Science in China Series D: Earth Sciences*, **51**, 1525–1536.

Shields, G. A., 2002. 'Molar-tooth microspar': a chemical explanation for its disappearance ~750 Ma. *Terra Nova*, **14**, 108–113.

Tanner, P. W. G., 1998. Interstratal dewatering origin for polygonal patterns of sand-filled cracks: a case study of late Proterozoic metasediments of Islay, Scotland. *Sedimentology*, **45**, 71–89.


## Cross-references


Calcite Precipitation, Microbially Induced
Carbonate Environments
Carbonates
Deep Fluids
Microbialites, Modern


# MOONMILK


Joachim Reitner
University of Göttingen, Göttingen, Germany


## Synonyms

Bergmilch; Lac lunae; Lac montanum; Mannmilch; Mondmilch; Montmilch; Mundmilch

## Definition

Moonmilk is a carbonate deposit that occurs within various subterranean systems. Moonmilk has a white to gray color and, in contrast to rigid cave deposits (*speleothems*) such as stalactites and stalagmites, exhibits a soft, muddy texture of microcrystalline aggregates. These aggregates are mainly composed of calcite, and to a lesser extent of aragonite, monohydrocalcite, hydromagnesite, sulfates, and nitrates (Martínez-Arkarazo et al., 2007; Richter et al., 2008; Cañaveras et al., 2006; Borsato et al., 2000). The calcite shows an aragonite-like needle form ("lublinite"), which is normally associated

with soil bacteria. The crystal needles have a diameter of about 0.1 µm and a length of ca. 8–10 µm. The name "moonmilk – Mondmilch" is derived from the name of a cave, "Mondmilchloch," located at the Pilatus mountain (Emmental Alps, Switzerland) (Fischer, 1988).

## Geobiological implications

Moonmilk differs in many aspects from the traditional cave carbonates such as stalagmites and stalactites (Moore and Sullivan, 1997; Bögli, 1978). Its formation is strongly influenced by microbial activity, as suggested by the presence of microbial aggregates, biofilms, and/or fungal mycelia (Cañaveras et al., 1999, 2001, 2006; Borsato et al., 2000; Gadd, 2004; Burford et al., 2003). Moonmilk is a result of (1) microbially mediated weathering and *microbiocorrosion* of carbonate host rock under highly humid conditions and (2) microbially mediated reprecipitation of various carbonate minerals. After dissolution of the mineral components, the residue exhibits high amounts of organic remains. Besides many fungal and actinomycetes, the bacterium *Macromonas bipunctata* plays a major role in the formation of moonmilk. *M. bipunctata* is a lophotrichous, heterotrophic and strictly aerobic betaproteobacterium that has been classified as a colorless sulfur bacterium capable of oxidizing sulfide (Dubinia and Grabovich, 1984). Within *extracellular polymeric substances (EPS)* of *M. bipunctata* and further microbes, calcite seed nuclei are formed to precipitate "lublinite" moonmilk crystals. *M. bipunctata* was originally described as *Pseudomonas bipunctata* by Gicklhorn (1920) and renamed by Utermöhl and Koppe (1924).

## Bibliography


Bögli, A., 1978. *Karsthydrographie und physische Speläologie*. Springer, Berlin/Heidelberg/New York.

Borsato, A., Frisia, S., Jones, B., and Van den Borg, K., 2000. Calcite moonmilk: crystal morphology and environment of formation in caves in Italian alps. *Journal of Sedimentary Research*, **70**, 1179–1190.

Burford, E. P., Fomina, M., and Gadd, G., 2003. Fungal involvement in bioweathering and biotransformations of rocks and minerals. *Mineralogical Magazine*, **67**(6), 1172–1155.

Cañaveras, J. C., Hoyos, M., Sanchez-Moral, S., Sanz-Rubio, E., Bedoya, J., Soler, V., Groth, I., Schumann, P., Laiz, L., Gonzalez, I., and Saiz-Jimenez, C., 1999. Microbial communities associated with hydromagnesite and needle-fiber aragonite deposits in a Karstic cave (Altamira, Northern Spain). *Geomicrobiology Journal*, **16**, 9–25.

Cañaveras, J. C., Sanchez-Moral, S., Sloer, V., and Saiz-Jimenez, C., 2001. Microorganisms and microbially induced fabrics in cave walls. *Geomicrobiology Journal*, **18**, 223–240.

Cañaveras, J. C., Cuezva, S., Sanchez-Moral, S., Lario, J., Laiz, L., Gonzalez, J. M., and Saiz-Jimenez, C., 2006. On the origin of fiber calcite crystals in moonmilk deposits. *Naturwissenschaften*, **93**, 27–32.

Dubinia, G. A., and Grabovich, M. Y., 1984. Isolation, cultivation and characteristics of *Macromonas bipunctata*. *Mikrobiologiya*, **53**, 748–755.

Fischer, H., 1988. Etymologie von Mondmilch bzw. Mondmilchloch. *Zeitschrift der deutschen Geologischen Gesellschaft*, **139**, 155–159.

Gadd, G. M., 2004. Mycotransformation of organic and inorganic substrates. *Mycologist*, **18**, 60–70.

Gicklhorn, J., 1920. Über neue farblose Schwefelbakterien.- Zentralblatt für Bakteriologie, Parasitenkunde, Infektionskrankheiten und Hygiene, Abt.2, **50**, 415–427.

Martínez-Arkarazo, I., Angulo, M., Zuloaga, O., Usobiaga, A., and Madariaga, J. M., 2007. Spectroscopic characterisation of moonmilk deposits in Pozalagua tourist cave (Karrantza, Basque Country, North of Spain). *Spectrochimica Acta Part A*, **68**, 1058–1064.

Moore, G. W., and Sullivan, N., 1997. *Speleology: Caves and the Cave Environment*. Huntsville: National Speleological Society, p. 176.

Richter, D., Immenhauser, A., and Neuser, R. D., 2008. Electron backscatter diffraction documents randomly orientated c-axes in moonmilk calcite fibers: evidence for biologically induced precipitation. *Sedimentology*, **55**, 487–497.

Utermöhl, H., and Koppe, F., 1924. Genus Macromonas. In Koppe, F. (ed.), *Die Schlammflora der ostholsteinischen Seen und des Bodensees*; *Archiv für Hydrobiologie*, **14**, 619–672.


## Cross-references


Biofilms
Carbonate Environments
Carbonates
Karst Ecosystems
Microbial Mineralisation
Microbial Mats


# MUD MOUNDS


Marta Rodríguez-Martínez
Universidad de Alcalá, Alcalá de Henares, Madrid, Spain


## Synonyms

Biodetrital mound; Carbonate mounds; Carbonate mud mound; Lime mud mound; Microbial mound; Mudbank; Reef mound; Stromatactis mounds

## Definition

Mud mounds are biosedimentary buildups, part of the reef system and are dominated by fine-grained carbonates (up and more than 50% of rock volume), which form heterogeneous polygenetic matrix-supported fabrics (stromatolitic, thrombolitic, leiolitic, fenestral, laminar, reticulate, stromatactoid, etc.). These fabrics are composed of both allomicrites and automicrites (abiogenetic, biogenetically induced, and biogenetically controlled). Production and accretion mechanisms in mud mounds are varied and not always clear, but are associated with the activity of microbial benthic communities (in different degrees of participation). Metazoans, being important colonizers, can or cannot occur but never produce a primary skeletal framework. Mud mounds colonized the oceans from the Proterozoic times, and they grow up from deep aphotic basinal settings to shallow water platforms.

## Evolution of the term mud mound

Probably, the core of the Silurian Wabash buildup (Indiana, EEUU) was the first carbonate deposit referred to in the literature as a "carbonate mud mound" and was described as a mound of calcisiltite containing crinoid, bryozoan, ostracode bioclastics, and stromatactis, but essentially no stromatoporoids or corals (Textoris, 1966). The Silurian mud mound facies were compared by Textoris with similar buildups reported from other parts of the world (Devonian of Canada, Carboniferous of Europe and EEUU).

### When reefs turned mud mounds

In the 1960s, the lack of a recognizable skeletal framework in these buildups pointed out their differences with the "classical" reef idea. During some years, most works on mud mounds were focused on the study of their scarce fauna and few were mentions to the origin of the carbonate mud, paradoxically the main component. Wilson (1975) extended in his book the definition and denomination of "lime mud mound" to many other Phanerozoic buildups, which were seen as dominated by detrital, bioclastic micrites with minor organic boundstone and *perceived to accumulate both through hydrodynamic processes and in situ organic production*. Thus, during the 1970s, the origin of the matrix was explained by the baffling theory: the carbonate mud, externally produced, was baffled by metazoans (crinoids, bryozoans, sponges, etc.). The role of early submarine cementation was also taken into consideration to explain the stabilization of mud mound depositional slopes. Baffled micrites and subsequent cementation was the proposed origin; thus, mud mounds were compared with very different types of Holocene buildups: shallow-water seagrass mudbanks and deep-water coral lithoherms.

### When some mud mounds turned into microbial reefs

From the 1970s to the 1980s, some fabrics and textures present in the mud mounds were related with "cryptalgal" and other biosedimentary structures as stromatolites and thrombolites (Monty, 1976; Pratt, 1982). The mud mound matrix could be now bound, trapped, and precipitated by the activity of microorganisms ("blue-green algae" – cyanophytes and cyanobacteria).

From then, the source or origin of the carbonate mud, the matrix problem, will be the leitmotiv in the study of mud mounds. Bosence et al. (1985), from the recent carbonate mounds from Florida Keys, proposed three mud mound models based on the relation between the external and the internal sediment (carbonate mud) supplies in the mound: export, import, and self-sufficient models, respectively. From the 1970s and clearly in the 1990s, mud mounds began to be seen as "self-sufficient" mounds, and the role of microbial communities in their construction gained more importance (Tsien, 1985; Lees and Miller, 1985; Camoin and Maurin, 1988).

James and Bourque (1992) proposed a conceptual classification of reefs and "mounds," where mounds *are those structures which were built by smaller, commonly delicate and/or solitary elements in tranquil settings*. They differentiated three types of mounds: "microbial" mounds, "skeletal" mounds, and "mud" mounds. Microbial and skeletal mounds are grouped into "biogenic mounds" because they are organically controlled, whereas the term "mud mound" was restricted by the authors to those *formed by inorganic accumulation of mud with variable amounts of fossils*. The authors pointed out that *the division between biogenic mounds and mud mounds depends on the nature of the accumulation/construction controls, not on the percentage of fossils*.

One of the main outstanding questions concerning the mud mounds is related to the modes of formation of the carbonate mud matrix and their recognition. The increase in the number of studies on microbial carbonates and their formation and fabric classifications (Kennard and James, 1986; Burne and Moore, 1987; Riding, 1991) led to new horizons in the matrix problem. Fabrics and geochemical signatures from automicrites of recent cryptic microbialites and controls in their formation (Reitner, 1993) were found to be similar to those recorded in Cretaceous and Jurassic mud mounds (Neuweiler, 1993; Keupp et al., 1993; Reitner et al., 1995; Leinfelder and Keupp, 1995). Thus, modern automicrites began to be used as modern counterparts of some mud mound end products.

Some authors began to use the term mud mound in a descriptive nongenetic *way as carbonate buildup consisting of more than 50% of mud and/or peloidal mud* (Reitner and Neuweiler, 1995), having depositional relief, and forming part of a polygenetic and continuum spectrum ranging from "biodetrital" to "microbial" mud mounds (Bosence and Bridges, 1995). Pratt (1995) considered mud mounds as ecologic reefs because they posses "rigid frameworks" produced by both microbial activity and synsedimentary cementation.

Last formal definition of mud mound has been given by Riding (2002), *as carbonate mud-dominated (micrite and fine-silt) deposits with topographic relief and with few or no stromatolites, thrombolites, or in-place skeletons*. Riding added that the deposits *can be organic and/or inorganic in origin and it can be difficult to distinguish their origins*.

## General features

Mud mounds have varied external forms; the term mud mound is used here not in a morphological way due to the fact that not all of them are mounds or dome-shaped; they can be tabular-shaped and can occur as isolated massive bodies or as stacked or amalgamated bodies, spreading over kilometers. The biggest mud mound complex is the Waulsortian mudbank from Ireland.

They could develop as a high synsedimentary relief and show depositional dips from 10° up to 50°, can be or cannot be flanked by bioclastic limestones, and grow up from

basinal to platform settings. Mud mounds are composed mainly of fine-grained carbonate-matrix-supported fabrics, which are called, depending on the classification schemes followed, mudstones, wackestones, biomicrites, etc. These carbonate muds are texturally and genetically varied. The presence of cavities can be a characteristic feature in some mud mounds. Their macrobiota are diverse and can be important volumetrically in some mounds, although they never constitute a skeletal framework.

## Types of carbonate muds

Carbonate muds are formed by pure aphanitic micrites and/or mixture of silt-sized calcite particles (up to 62 μm) as peloids. Then, they can be texturally grouped into aphanitic and peloidal micrites. Both types occur separately, or there is grading between them; they also occur as neomorphosed microspars. Microstructurally, they appear as dense and/or clotted/grumelar/spongiostromic microfabrics, which constitute at mesoscale, stromatolitic, thrombolitic, fenestral, and/or cryptalgal/cryptomicrobial/leiolitic fabrics (summarized in Riding, 2000).

The carbonate muds can be classified in relation to the *locus* of their production. The muds externally produced and later imported into the mound are named allomicrites (Figure 1). They are stabilized at mound surface by mound biota (eukaryotes and prokaryotes) through baffling, trapping, and/or binding mechanisms and early cementation.

The in situ produced carbonate muds are named automicrites. They are formed through abiogenic, biologically induced, and biologically controlled mechanisms (summarized in Flügel, 2004). The biologically related mechanisms are known as nonenzymatically and enzymatically controlled carbonates. Mud mounds seem to be specially dominated by the nonenzymatically carbonate production of automicrites via nonliving substrates (organomineralization of the organic matter derived from decaying organisms) and/or via metabolic processes (by heterotrophic, chemolithotropic, and phototrophic bacterias and cyanobacterias). In the first case, the

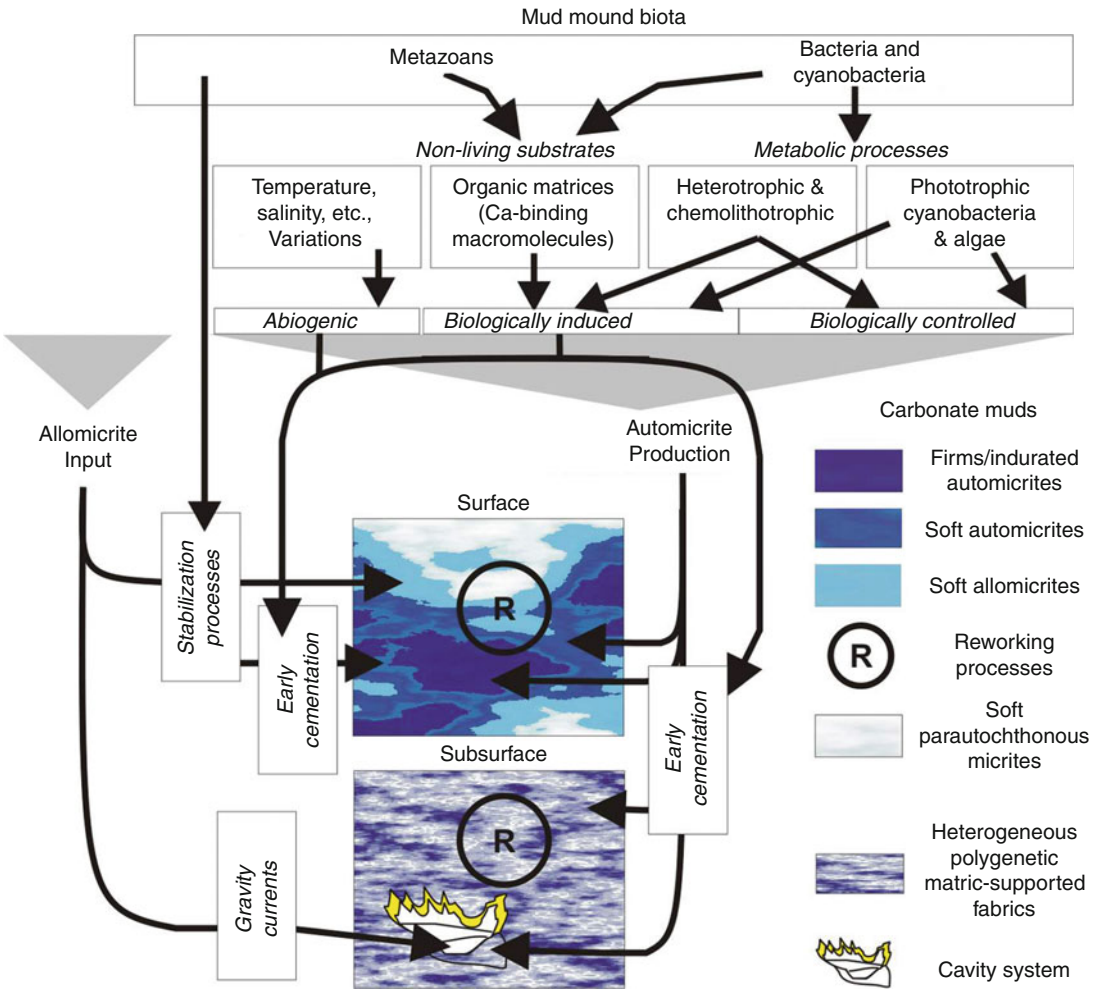


**Mud Mounds, Figure 1** Relationships between the mud mound biota and carbonate mud stabilization and production processes.

resulting automicrites are known as organomicrites. The automicrite production occurs at mound surface as well as at subsurface.

The mud mound system comprises both soft (allomicrites and automicrites) as well as firm/early indurated carbonate muds (automicrites), which can suffer from reworking processes (chemical, physical, and/or biological ones) resulting in parautochthonous muds. These secondary muds or the next successive generations of in situ muds, therefore, resemble a mixture of previous ones. This system should be analyzed as a continuous series of processes of automicrite production, allomicrite input, and internal reworking.

The filling of mound cavity system records many of the last mud mound synsedimentary episodes: (1) the entry of allomicrite by gravity or currents, (2) the colonization by cryptic biota, (3) production of automicrites, (4) reworking processes, and (5) the early marine cementation phases as well as burial-related phases.

So mud mounds have polygenetic carbonate mud-dominated fabrics resulting from automicrites production, allomicrites input, and recycling processes (Figure 1). But some microfabrics have been related at the same time with different types of biogenic as well as abiogenic processes, and discriminating between some processes and their products is not always possible.

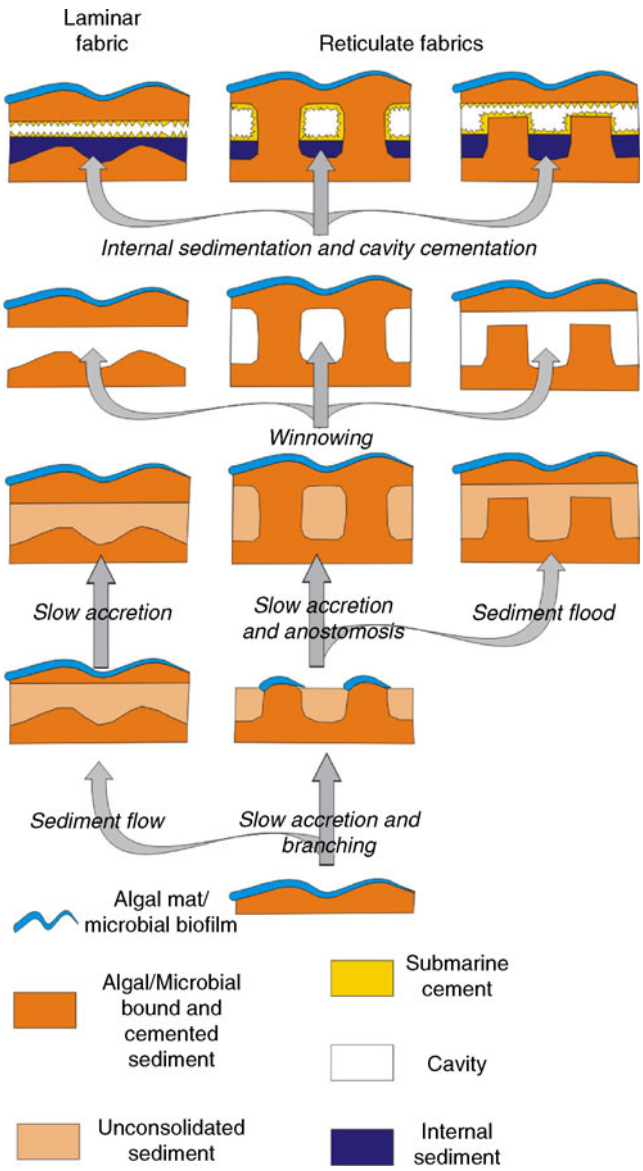


**Mud Mounds, Figure 2** Microbial mat-based model for accretion of mud mounds and development of cavities. (Modified from Pratt, 1982.)

## Biota

Dominant invertebrate macrofossils on mud mounds were suspension feeders as pelmatozoans, bryozans, and sponges – siliceous and calcareous types, although others such as brachiopods, molluscs, and arthropods could be sporadically important. Solitary and colonial corals occasionally occurred on mud mound records as well as calcareous algae, but they were much less common (not as colonizers of the shallow-water mud mound phases). Others such as benthic foraminifera and polychaete worms also occurred as part of the mud mound biota from the Carboniferous times. In general, the biota of mud mounds was mainly dominated by heterozoan assemblages.

In mud mounds, excluding the evident microbial fabrics (stromatolitic, thrombolitic and others), the main signal or product of microbial activity is hidden in the carbonate mud (biogenic automicrites) and in some authigenic mineralizations (iron pigments, Fe/Mn surfaces, framboidal pyrites, etc.). There is also direct evidence of calcified microbes (*Girvanella*, *Renalcis*, *Epiphyton*, *Bacinella*, *Rivularia*-like forms, etc.), and most of them have been interpreted as cyanobacterial fossils. Other evidence of microbial activity is the presence of unidentified filament-rich microfabrics, filaments and spherulites as moulds or casts, and peloids.

Sponge–bacterial assemblages have also played an important role in the initiation and first stages of many mud mound developments (early cementation of sponge tissues is related with the activity of symbiotic bacteria as well as the organomicrite production through the decaying of their tissues).

## Cavities

There is a wider spectrum of cavity types in mud mounds (stromatactis, zebra, irregular, and sheet-like shapes). Probably, the most famous are the stromatactis, with smooth, flat base and irregularly digitate roofs, matrix-supported in general, although some can be partially or totally sheltered by remains of fossils. Filled with centripetal marine fibrous cement crusts and varied internal sediments (allomicrites and automicrites), stromatactis were abundant in Paleozoic mud mounds, especially from the Ordovician–Mississippian interval.

The origin of stromatactis has been largely debated, and today it remains controversial. Several hypothesis has been used (summarized in Flügel, 2004, 194 p.), which can be groped in "organic" (recrystallized fossils, related with decaying organism, burrowing, etc.) and "inorganic" theories (dissolution, collapse, internal erosion between submarine crusts or bioclasts, dewatering and compaction of the muds, recrystallization, enlargement of preexisting cavities, presence of gas hydrates, etc.). In the organic cases, there are two models: the cryptalgal/microbial mat model and the sponge model.

The microbial mat model was initially proposed by Pratt (1982) to explain the mud mound accretion and its final observed fabrics (Figure 2). The fabrics and the resulting cavities were the result of the combination of three variables: (1) the distribution of the microbial mat, (2) the rate of sediment loading onto the mat, and (3) the degree of winnowing. The distribution of the microbial mat (laterally continuous or in patches) produces the resulting fabrics (laminar or reticulate, respectively). The winnowing of the unconsolidated sediment between the microbial bounds and cemented sediment produces the cavities.

In the sponge model (Bourque and Boulvain, 1993), the cavities are formed by the partial collapse of the sponge body as result of early diagenetic processes through four stages (Figure 3): (1) zone of the living community, (2) zone of sulphate reduction, (3) zone of oxidation of ferrous iron, and (4) zone of marine cementation. In the living surface, the mud is trapped by sponges and/or produced by microbial activity. Below the surface, the microbial decay of sponges occur; part of the sponge body and the mud are cemented, and other sponge parts are in collapsed state; the later internal erosion of the unconsolidated material produces the open cavities. A few meters

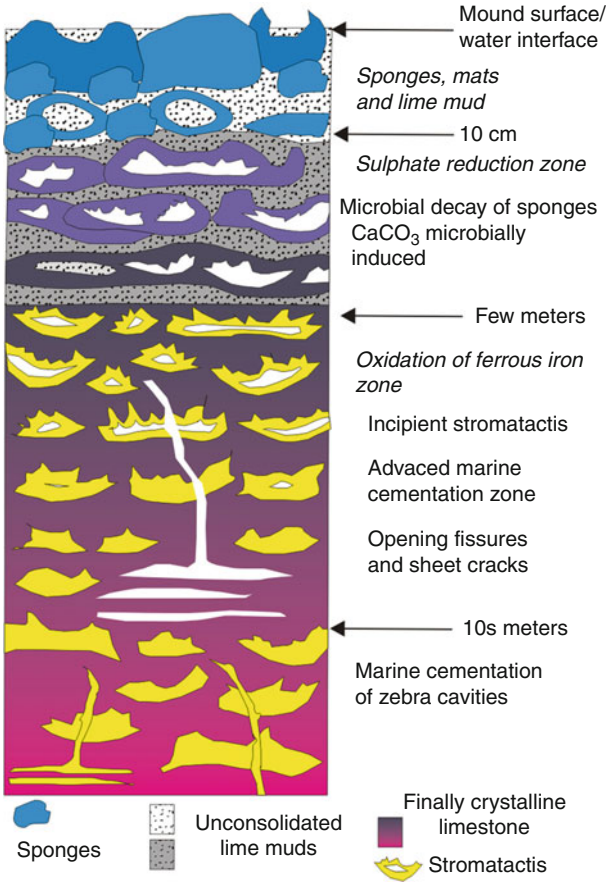


**Mud Mounds, Figure 3** Sponge model for the Paleozoic red stromatatics mounds. (Modified from Bourque and Boulvain, 1993.)

below, in the ferrous iron oxidation zone began the incipient marine cementation of these cavities forming the stromatactis.

## Types of mud mounds through the Phanerozoic record

The classification and distribution of mud mounds through the record depend on the "mud mound versus reef concept" of almost each researcher and thus remain controversial in several aspects. Mud mounds have existed from Proterozoic times and through the Phanerozoic record (see reviews by Monty, 1995; Pratt, 1995), and important growth episodes occurred in early Cambrian, late Devonian, and Mississippian times. Cambrian to Ordovician mud mounds (Figure 4) were characterized by different fabrics and assemblages (stromatolitic, thrombolitic, and massive fabrics with calcimicrobes, and cambrian archaeocyathid/sponge-calcimicrobial assemblages). From the Ordovician to the Mississippian, some of the carbonate mud-rich buildups, which typify this interval, have been regarded as the classical massive mud mounds with abundant stromatactis (Figure 4) as the 'red stromatactis mounds' (Recíf Rouges-type mound) and the Waulsortian mudbanks (Figure 5a and b). Clear microbilite-related fabrics (stromatolites and thrombolites) are extremely rare in classical mud mounds, although they show other nonskeletal reef frameworks (calcimicrobial and biocementstones *sensu*, Webb, 1996), as well as filaments and some characteristic features (clotted, peloidal micrites, and fenestral microfabrics). The parallel diversification of skeletal mound macro- and micro-biota produced more varied metazoan–microbialitic assemblages. One of the most persistent through the mud mound record is the sponge–microbialitic association, very common in Jurassic mud mounds as well as in the deeper initial stages of many Paleozoic mounds. Early Cretaceous is considered the last significant moment of organomineralic mud mound development (Neuweiler et al., 1999), although

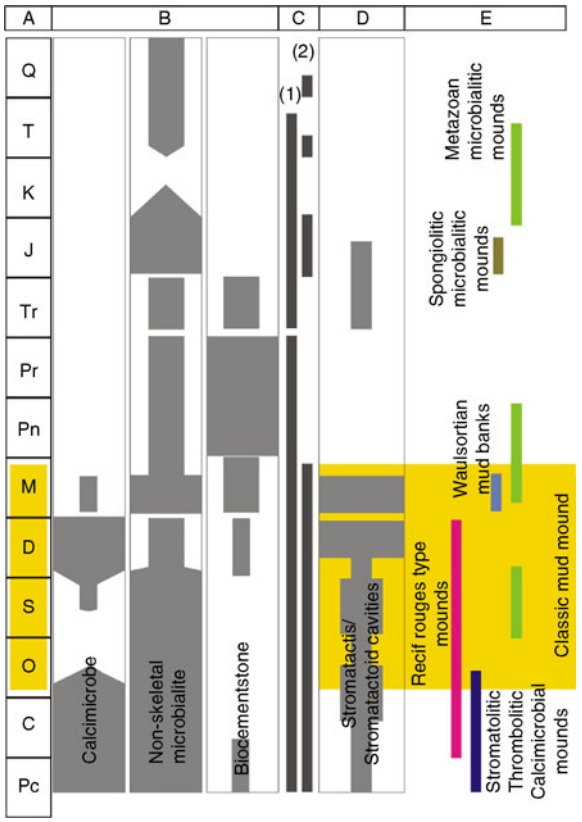


**Mud Mounds, Figure 4** Distribution of mud mounds through the geologic record. (A) Precambrian to Quaternary time divisions. (B) Distribution and relative importance of nonenzymatic reef frameworks (from Webb, 1996), characteristic also in mud mounds. (C) Distribution of (1) microbial and (2) biodetrital mud mounds. (Modified from Bosence and Bridges, 1995.) (D) Distribution of stromatactis and stromatactoid cavities, the size of the bar represents their relative importance in mud mounds. (E) Interval distribution of the main typologies of mud mounds.

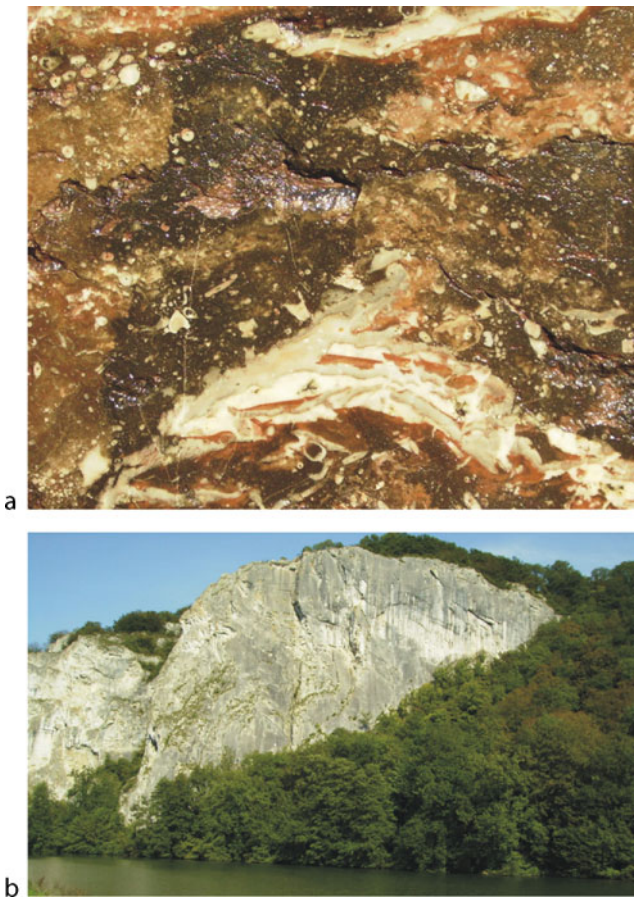


**Mud Mounds, Figure 5** Classical mud mounds. (**a**) Close view of a Devonian Recífs Rouges-type mound, Beauchateau Quarry, Belgium. (**b**) Carboniferous Waulsortian mudbank, Waulsort, Belgium.

other authors mentioned that the latest mud mounds are Miocene (Pratt, 2000).

## Ecological zonation models

The Récifs Rouges-type mounds and the Waulsortian mudbanks are probably the most famous and are well know as "classical mud mounds" (Figures 4 and 5) Devonian (Frasnian) mounds from Belgium show a shallowing upward succession from deep basal greenish-grey shales through their mud mound facies: red lime mudstones to wackestones with stromatactis, pink wackestones with millimeter stromatactis to crudely bedded grey wackestones to packstones, and bindstones, and their associated biota. Similar facies (red stromatactis mounds) and assemblages have been found in other mud mounds through the Paleozoic record (Bourque, 1997). The carboniferous Waulsortian mudbanks of Belgium show a four grain-type assemblages related with the growth of these mounds from deep subtidal, aphotic to photic conditions. A depth-related phase model was recognized by Lees and coworkers (summarized in Lees and Miller, 1995) and applied to Waulsortian mudbanks of Europe and North America. Bourque (1997) compared Recífs Rouges-type mounds from Silurian of Canada and Devonian of France and Belgium with carboniferous mounds from Algeria and the Waulsortian mudbanks model and established an ecological zonation model formed by four benthic communities zones (Figure 6): (1) the sponge zone, (2) the fenestellid–sponge zone, (3) the delicate skeletons–sponge zone, and (4) the delicate skeletons–microbial encrusters zone.

## Controlling factors

Today, many parameters about the initiation, accretion, and spread of many mud mounds seem to be enigmatic. However, some others begin to be more clear.

Locations of some mud mounds have been related with submarine cold seeps, vents, faults, halokinetic and argilokinetic settings, and local antecedent topographic irregularities, have been associated to nutrient-enriched areas (by endo-, down- and/or up-welling currents), and could be also related with stratified basin waters and fluctuating oxygen minimum zone. Many of them grew up into aphotic to disphotic depths (more than 200 m); however, they could reach and colonize the euphotic zone. Some grew at lower sedimentation rates and/or during sedimentary starvation during TST episodes, although this is not a general trend for all of them. Most of these factors are oceanographic and/or tectonically basin-related parameters and could co-occur together in many cases.

Those factors (biological and chemical parameters) associated with the carbonate mud precipitation related with eukaryotes and prokaryotes should be taken into consideration:

(a) Production of acidic organic macromolecules (AOM) and an increase in carbonate alkalinity via (1) bacterial heterotrophic pathways (ammonification and sulphate reduction), (2) carbonate, and (3) silicate weathering. AOM and high alkalinity favor the organomicrite production in microbialites and mud mounds (Reitner and Neuweiler, 1995).
(b) Extracellular polymeric substances (EPS)-biomineralization of microbial mats and biofilms.
(c) Calcification of cyanobacteria.

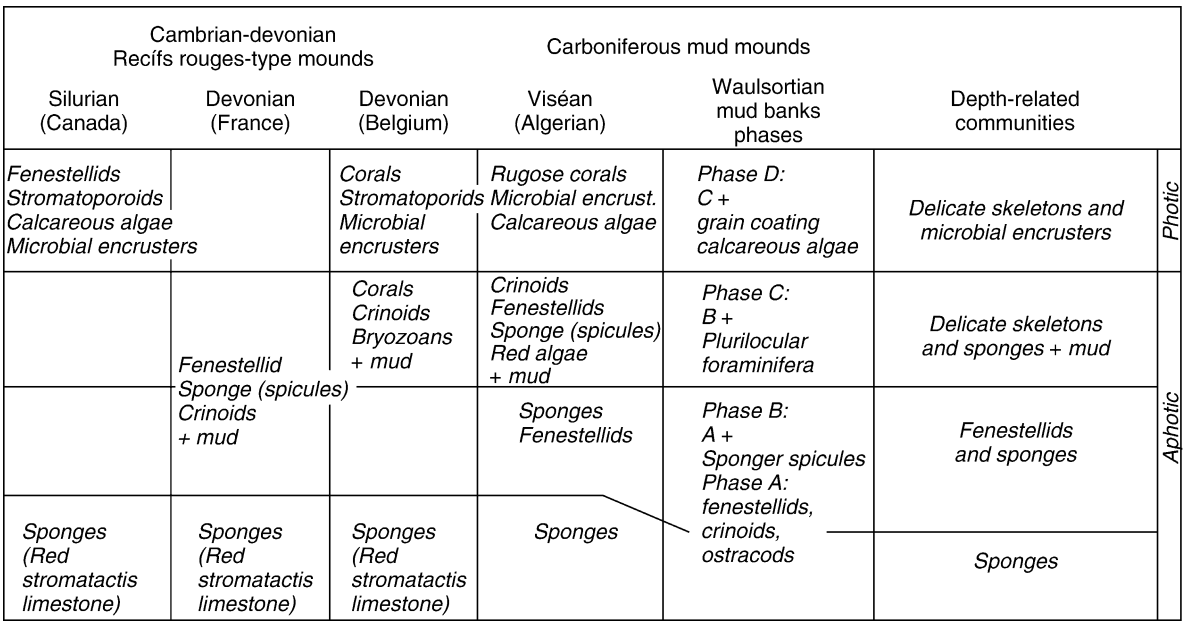


**Mud Mounds, Figure 6** Ecological zonation assemblages in some Paleozoic mud mounds. (Modified from Bourque, 1997.)

(d) $CO_2$ depletion of the medium through autotrophic pathways by methanogenic archaea, sulfurous and nonsulfurous purple and green photosynthetic bacteria, and cyanobacteria (Castanier et al., 2000).

## Conclusions

Mud mounds are considered mainly as nonenzymatic carbonate deposits that formed a polygenetic and very continuous record of buildups through the Phanerozoic and reached a maximum development during the Paleozoic times. They are of considerable importance not from an economic point of view (hydrocarbon reservoirs, major mineral host-rock and base deposits, ornamental rocks) alone. In fact, they represent an excellent record for the study and establishment of (1) the interactions between the marine microbial and nonmicrobial benthic communities (paleoecologic and paleoenvironmental parameters), (2) marine carbonate production models (mud mound factory), and (3) proxies in palaeoceanographic reconstructions (nonenzymatic carbonates are formed in equilibrium with ambient sea water).

Mud mounds are characterized by different modes of carbonate mud production (abiogenic, biologically induced, and biologically controlled automicrites) and sedimentation input (allomicrites). The key of mud mounds understanding lies behind here: to recognize and differentiate between the automicrite and allomicrite relationship and their contribution to the mud mound accretion.

## Bibliography


Bosence, D. W. J., and Bridges, P. H., 1995. A review of the origin and evolution of carbonate mud-mounds. In Monty, C. L. V., Bosence, D. W. J., Bridges, P. H., and Pratt B. R. (eds.), *Carbonate Mud-mounds: Their Origin and Evolution*. Oxford: Blackwell Science for the International Association of Sedimentologists, Special Publication, **23**, pp. 3–9.

Bosence, D. W. J., Rowlands, R. J., and Quine, M. L., 1985. Sedimentology and budget of a recent carbonate mound, Florida keys. *Sedimentology*, **32**, 317–343.

Bourque, P. A., 1997. Paleozoic finely crystalline carbonate mounds: cryptic communities, petrogenesis and ecological zonation. *Facies*, **36**, 250–253.

Bourque, P.-A., and Boulvain, F., 1993. A model for the origin and petrogenesis of the red stromatactis limestone of Paleozoic carbonate mounds. *Journal of Sedimentary Petrology*, **63**, 607–619.

Burne, R. V., and Moore, L. S., 1987. Microbialites: organosedimentary deposits of benthic microbial communities. *Palaios*, **2**(3), 241–254.

Camoin, G., and Maurin, A.-F., 1988. Roles of micro-organisms (bacteria, cyanobacteria) in the formation of mud mounds: examples from the Turonian strata of Jebels Bireno and Mrhila (Tunisia). *Compte Rendu des Académie des Sciences de París*, Série II, **307**, 401–407.

Castanier, S., Le Méteyer-Levrel, G., and Perthuisot, J. P., 2000. Bacterial roles in the precipitation of carbonate minerals. In Riding, R. E., and Awramik, S. M. (eds.), *Microbial Sediments*. Berlin: Springer, pp. 32–39.

Flügel, E., 2004. *Microfacies of Carbonate Rocks: Analysis, Interpretation and Application*. Berlin: Springer, 976 p.

James, N. P., and Bourque, P.-A., 1992. Reefs and mounds. In Walker, R. G., and James, N. P. (eds.), *Facies Models*: *Response to Sea Level Change*. St. John's, Newfoundland: Geological Association of Canada, pp. 323–347.

Kennard, J. M., and James, N. P., 1986. Thrombolites and stromatolites: two distinct types of microbial structures. *Palaios*, **1**(5), 492–503.

Keupp, H., Jenisch, A., Herrmann, R., Neuweiler, F., and Reitner, J., 1993. Microbial carbonate crusts – a key to the environmental analysis of fossil spongiolites? *Facies*, **29**, 41–54.

Lees, A., and Miller, J., 1985. Facies variation in Waulsortian buildups. Part 2. Mid-Dinantian buildups from Europe and North America. *Geological Journal*, **20**, 159–180.

Leinfelder, R. R., and Keupp, H., 1995. Part III Upper Jurassic mud mounds: allochthonous sedimentation versus autochthonous carbonate production. *Facies*, **32**, 17–26.

Monty, C. L. V., 1976. The origin and development of cryptalgal fabrics. In Walter, M. R. (ed.), *Stromatolites*: *Developments in Sedimentology*. Amsterdam: Elsevier, Vol. 20, pp. 193–249.

Monty, C. L. V., 1995. The rise and nature of carbonate mud-mounds: an introductory actualistic approach. In Monty, C. L. V., Bosence, D. W. J., Bridges, P. H., and Pratt, B. R. (eds.), *Carbonate Mud Mounds, Their Origin and Evolution*. International Association of Sedimentologists. Special publication, 23, pp. 11–48.

Neuweiler, F., 1993. Development of Albian microbialites and microbialites reefs at marginal platform areas of the Vasco-Cantabrian Basin (Soba Reef, Cantabria, N. Spain). *Facies*, **29**, 231–250.

Neuweiler, F., Gautret, P., Thiel, V., Langes, R., Michaelis, W., and Reitner, J., 1999. Petrology of lower cretaceous carbonate mud mounds (Albian, N. Spain): insights into organomineralic deposits of the geological record. *Sedimentology*, **46**, 837–859.

Pratt, B. R., 1982. Stromatolitic framework of carbonate mud-mounds. *Journal of Sedimetary Petrology*, **52**(4), 1203–1227.

Pratt, B. R., 1995. The origin, biota and evolution of deep water mud-mounds. In Monty, C. L. V., Bosence, D. W. J., Bridges, P. H., and Pratt, B. R. (eds.), *Carbonate Mud Mounds, Their Origin and Evolution*. Oxford: Blackwell Science for the International Association of Sedimentologists, Special Publication, **23**, pp. 49–123.

Pratt, B. R., 2000. Microbial contribution to reefal mud-mounds in ancient deep-water settings: evidence from Cambrian. In Riding, R. E., and Awramik, S. M. (eds.), *Microbial Sediments*. Berlin: Springer, pp. 282–287.

Reitner, J., 1993. Modern cryptic microbialite/metazoan rich-facies from Lizard Island (Great Barrier Reef, Australia) – formation and concepts. *Facies*, **29**, 3–40.

Reitner, J., and Neuweiler, F., 1995. Part I, mud mounds: recognizing a polygenetic spectrum of fine-grained carbonate buidups. *Facies*, **32**, 2–4.

Reitner, J., Neuweiler, F., and Gautret, P., 1995. Part II modern and fossil automicrites: implications for mud mounds genesis. *Facies*, **32**, 4–17.

Riding, R., 1991. Classification of microbial carbonates. In Riding, R. (ed.), *Calcareous Algae and Stromatolites*. Berlin: Springer, pp. 21–51.

Riding, R., 2000. Microbial carbonates: the geological record of calcified bacterial-algal mats and biofilms. *Sedimentology*, **47**, 179–214.

Riding, R., 2002. Structure and composition of organic reef and carbonate mud mounds: concepts and categories. *Earth-Science Reviews*, **58**, 163–231.

Textoris, D. A., 1966. Algal cap for a Niagaran (Silurian) carbonated mud mound of Indiana. *Journal of Sedimentary Petrology*, **36**(2), 455–461.

Tsien, H. H., 1985. Algal-bacterial origin of micrites in mud mounds. In Toomey, D. F., and Nitecki, M. H. (eds.), *Paleoalgology*. Berlin: Springer, pp. 290–296.
Webb, G. E., 1996. Was Phanerozoic reef history controlled by the distribution of non-enzymatically secreted reef carbonates (microbial carbonate and biologically induced cement)? Sedimentology, **43**, 947–971.
Wilson, J. L., 1975. *Carbonate Facies in Geologic History*. Berlin: Springer, 471 p.

## Cross-references

Bacteria
Biofilms
Calcite Precipitation, Microbially Induced
Cyanobacteria
Extracellular Polymeric Substances (EPS)
Microbial Communities, Structure, and Function
Microbial Mats
Microbialites, Modern
Reefs
Waulsortian Mud Mounds

## MUTUALISM

Mutualism is a form of a symbiosis, in which both organisms involved benefit. See entry "*Symbiosis*" for further reading.

## MYCORRHIZAE

A mycorrhiza (pl mycorrhizae, from the Greek "*mycos*" = fungus and "*rhiza*" = root) is a plant-fungal association that comprises the most widespread type of terrestrial symbiosis. See entry "*Symbiosis*" for further reading.